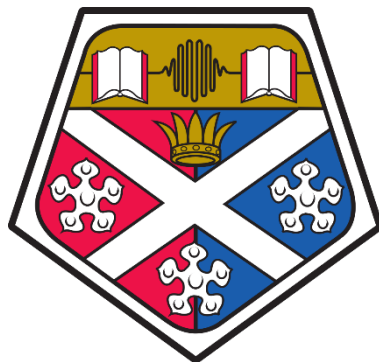University of Strathclyde

Department of Pure and Applied Chemistry

Oxidations with Endocyclic Peroxides and Their Derivatives

A thesis submitted to the University of Strathclyde in part fulfilment of regulations for the degree of Doctor of Philosophy in Chemistry.

Andrei Dragan

Supervised by Professor Nicholas C. O. Tomkinson

2016

Declaration

This thesis is the result of the author's original research. It has been composed by the author and has not previously been submitted for examination which has led to the award of a degree.

The copyright of this thesis belongs to the author under the terms of the United Kingdom Copyright Acts as qualified by University of Strathclyde Regulation 3.50. Due acknowledgement must always be made of the use of any material contained in, or derived from, this thesis.

Signed ....   Date ....

Abstract

This thesis describes two novel transformations (a method to synthesize alkylidene phthalides and a different approach toward the Baeyer-Villiger oxidation) and the development and mechanistic study of a metal-free oxidation of arenes.

Chapter 1 introduces the concept of alkene oxyamination. Synthesis of a series of hydroxylamine derivatives of endocyclic peroxides was undertaken, which were then reacted with nitrogen, sulfur and carbon nucleophiles. This led to the discovery of a new reaction that provides access to alkylidene phthalides, a class of compounds which exhibit interesting biological activity.

Chapter 2 describes the development of an alternative approach to the Baeyer-Villiger oxidation, through the reaction of hydrogen peroxide and a nitrile in the presence of a base.

Chapter 3 describes direct methods for the formation of new aromatic C–O bonds, followed by the presentation of an organic peroxide mediated approach. Herein, an examination of the mechanism of the reaction of a malonoyl peroxide with an arene is studied through Hammett analysis, isotope labeling experiments, EPR studies, DFT calculations and reactivity patterns.

Chapters 4 and 5 present the experimental procedures and analytical data relevant to the three reactions developed.

Chapter 6 contains a bibliography.

Acknowledgements

Table of Contents

Abbreviations

Below is a list of abbreviations that have been used throughout this report that might not be known to the reader.

Ac	Acetyl
acac	Acetylacetonate
APCI	Atmospheric pressure chemical ionization
appd	Apparent doublet
appt	Apparent triplet
appdd	Apparent doublet of doublets
apptd	Apparent triplet of doublets
appdq	Apparent doublet of quartets
appp	Apparent pentet
aq.	Aqueous
Ar	Aryl
ATR	Attenuated total reflectance
BHT	Butylated hydroxytoluene
Bn	Benzyl
Boc	*tert*-Butoxycarbonyl
BPO	Benzoyl peroxide
br	Broad
Bu	Butyl
BV	Baeyer-Villiger
Cbz	Carbobenzyloxy
CEO	2-Chloroethanol
CFL	Compact fluorescent light
CI	Chemical ionization

COSY	Correlation spectroscopy
CPCM	Conductor polarized continuum model
CSA	Camphorsulfonic acid
Cy	Cyclohexyl
d	Doublet
DABCO	1,4-Diazabicyclo[2.2.2]octane
dba	Dibenzylideneacetone
DBU	1,8-Diazabicyclo[5.4.0]undec-7-ene
DCE	1,2-Dichloroethane
dd	Doublet of doublets
ddd	Doublet of doublets of doublets
DFT	Density functional theory
dhept	Doublet of heptets
DHQ	Dihydroquinine
DHQD	Dihydroquinidine
DEAD	Diethyl azodicarboxylate
dec	Decomposed
DIAD	Diisopropyl azodicarboxylate
DIC	*N*,*N'*-Diisopropylcarbodiimide
DMAP	*N*,*N*-Dimethyl-4-aminopyridine
DMF	Dimethylformamide
DMSO	Dimethylsulfoxide
d.r.	Diastereomeric ratio
dtd	Doublet of triplets of doublets
EDTA	Ethylenediaminetetraacetic acid
ee	Enantiomeric excess
EI	Electron impact

EPR	Electron paramagnetic resonance
equiv	Equivalent(s)
ESI	Electrospray ionization
esp	$\alpha,\alpha,\alpha',\alpha'$-Tetramethyl-1,3-benzenedipropionate
Et	Ethyl
FT	Fourier transform
g	Gram(s)
h	Hour(s)
hept	Heptet
HFIP	1,1,1,3,3,3-Hexafluoroisopropanol
HMDS	Hexamethyldisilazane
HMPA	Hexamethylphosphoramide
HRMS	High resolution mass spectrometry
HSQC	Heteronuclear single quantum coherence
HT	Hydrotalcite
Hz	Hertz
IR	Infrared
IT	Ion trap
J	Joule
J	Coupling constant
k	Kilo
L	Ligand
LDA	Lithium diisopropylamide
lit.	Literature
LRMS	Low resolution mass spectrometry
LUMO	Lowest unoccupied molecular orbital
m	*meta*

m	Multiplet
M	Molar
m-CPBA	*meta*-Chloroperoxybenzoic acid
Me	Methyl
Mes	Mesityl
mg	Milligram(s)
MHz	Megahertz
min	Minute(s)
mL	Milliliters
mmol	Millimole(s)
m.p.	Melting point
Ms	Methanesulfonyl/Mesyl
MS	Mass spectrometry
MS (in reaction schemes)	Molecular sieves
MSD	Mass selective detector
n	*normal*
n.d.	*Not determined*
Naphth	Naphthyl
NBO	Natural bond orbital
NBP	n-Butyl phthalide
NBS	*N*-Bromosuccinimide
NCS	*N*-Chlorosuccinimide
NHC	*N*-Heterocyclic carbene
NIS	*N*-Iodosuccinimide
NMI	*N*-Methylimidazole
NMR	Nuclear magnetic resonance
NOE	Nuclear Overhauser effect

o	*ortho*
p	*para*
pent	Pentet
PFB	Perfluoro-*tert*-butanol
Ph	Phenyl
PHAL	Phthalazine
Phth	Phthalate
Piv	Pivalate
PMP	*para*-Methoxyphenyl
ppm	Parts per million
^{i}Pr	Isopropyl
^{n}Pr	n-Propyl
PYR	Pyrenyl
q	Quartet
RDS	Rate determining step
R_f	Retention factor
r.t.	Room temperature
s	Singlet
SCRF	Self-consistent reaction field
SDBS	Sodium dodecylbenzene sulfonate
SDS	Sodium dodecyl sulfate
SET	Single electron transfer
S_N2	Substitution, nucleophilic, bimolecular
t	Triplet
t appd	Triplet of apparent doublets
TBAF	Tetra-*n*-butylammonium fluoride
TBS	*tert*-Butyldimethylsilyl

TCE	2,2,2-Trichloroethanol
Tces	Trichloroethylsulfate
TEMPO	2,2,6,6-Tetramethylpiperidine-1-oxyl
Tf	Triflyl
TFA	Trifluoroacetic acid
TFE	2,2,2-Trifluoroethanol
THF	Tetrahydrofuran
TLC	Thin layer chromatography
Ts	Toluenesulfonyl/Tosyl
TS	Transition state
UHP	Urea hydrogen peroxide
vs	*versus*
wt%	Weight percent
z	Charge

Chapter 1: Synthesis of Alkylidene Phthalides

1.1 Introduction – *β*-Amino Alcohols

β-Amino alcohols represent an important class of functional group which are potent pharmacophores present in a number of pharmaceuticals (Figure 1). The common functionality of these compounds comprises of an amine and an alcohol group on vicinal carbons (highlighted). Methods for obtaining this class of compounds include: hydrolysis of aziridines[1] and ring opening of epoxides.[2] However, an attractive method for their preparation is the direct oxyamination of alkenes, with the Sharpless asymmetric oxyamination reaction being the most effective method developed to date.[3]
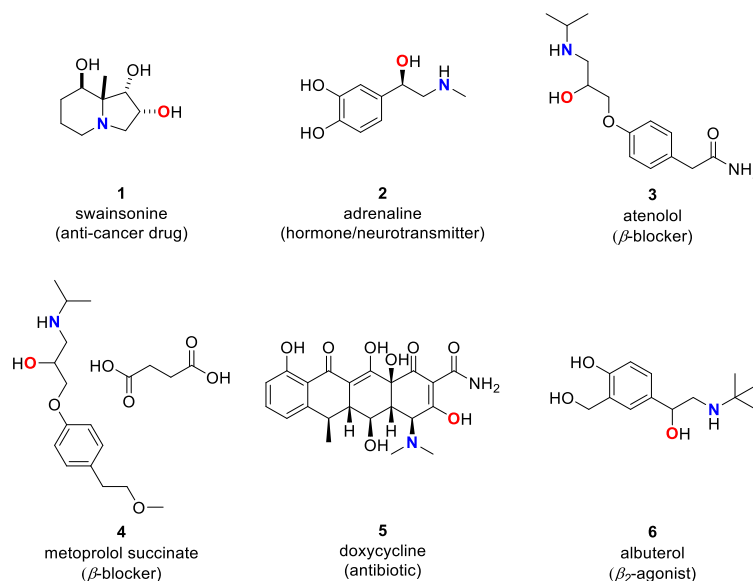
Figure 1: Biologically active compounds containing 1,2-amino alcohols

There are a number of methods to synthesize *β*-amino alcohols in the literature and these will be described in turn within this section. These methods include indirect methods such as nucleophilic ring opening of aziridines and epoxides and direct methods such as the oxyamination of alkenes. These will be presented in three parts: Sharpless oxyamination (Section 1.1.3.1), other metal-based methods for oxyamination (Section 1.1.3.2) and finally, metal-free processes (Section 1.1.3.3).

1.1.1 Ring Opening of Aziridines

Aziridines are heterocyclic three-membered rings containing two carbon atoms and a nitrogen atom. A common method for synthesizing β-amino alcohols is the hydrolysis of aziridines. Obtaining the corresponding *anti*-amino alcohol **8** can be achieved by heating an aziridine, such as **7**, under reflux conditions in water.[1a] This reaction was high yielding (99%) and provided the *anti*-diastereomer exclusively (Scheme 1).
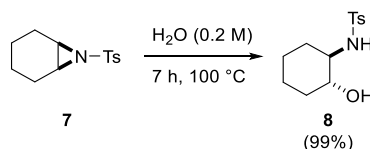
Scheme 1: Ring opening of aziridines

Ring opening of aziridines may be a simple and direct path to obtain β-amino alcohols, but it has its drawbacks. Regioselectivity can be a major issue, since water is a small molecule and addition can take place at either of the two carbon atoms on the aziridine ring, although this addition can be predicted through choice of substrate and reaction conditions. Furthermore, the products obtained are racemic and the only direct approach for obtaining enantioenriched amino alcohols such as **10** from aziridines (*e.g.* **9**) is the hydrolysis of chiral aziridines (Scheme 2).[4]
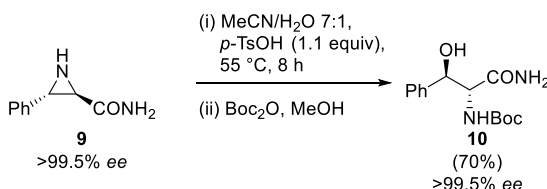
Scheme 2: Ring opening of chiral aziridines

1.1.1.1 Synthesis of Aziridines

A review by Degennaro *et al.* in 2014, summarizes methods for the stereoselective synthesis of aziridines and their application in organic synthesis.[5] Enantioselective syntheses of aziridines can be grouped into two main categories: nitrogen transfer to olefins and carbon transfer to imines. An example of each of these is shown in this section.

Chapter 1: Synthesis of Alkylidene Phthalides

In 2007, Córdova published an enantioselective organocatalytic process for the formation of aziridines (Scheme 3).[6] The reaction was catalyzed by a proline-derived organocatalyst **13** and involved the reaction of a hydroxylamine derivative **12** with α,β-unsaturated aldehyde **11** to afford aziridine **14** in good yield (62%). The reaction was highly enantioselective (99% *ee*) and diastereoselective (10:1 *d.r.*).
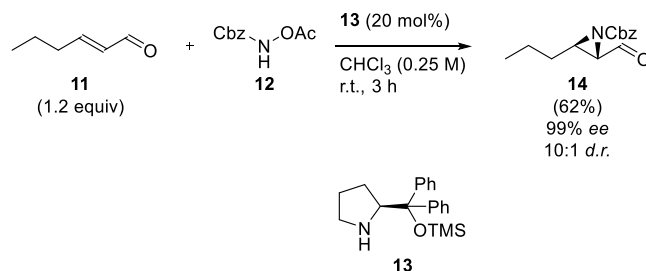
Scheme 3: Enantioselective synthesis of aziridines *via* nitrogen transfer

In 2013, Maruoka developed a method for the formation of aziridines *via* carbon transfer to imines (Scheme 4).[7] Aziridine **19** was synthesized in good yield from the corresponding imine **15** and excess *N*-phenyldiazoacetamide **16** using an *in situ* generated catalyst assembly between boronic acid **17** and diol **18**. The reaction showed excellent enantioselectivity (up to 98% *ee*) for most substrates and an excellent diastereoselectivity (up to >19:1 *d.r.*).
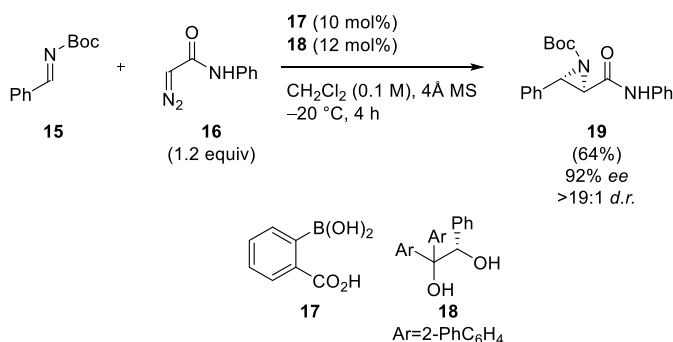
Scheme 4: Enantioselective synthesis of aziridines *via* carbon transfer

While many aziridines can be prepared in moderate to high yields with excellent stereoselectivity using methods such as those described above, or alternatives presented by Degennaro *et al.*,[5] there are some issues regarding the stereoselective synthesis of aziridines which remain, that include regioselectivity, stereoselectivity, stoichiometry and also catalyst synthesis.

1.1.2 Ring Opening of Epoxides

Epoxide aminolysis is a second method for the synthesis of *β*-amino alcohols. Similar to aziridine hydrolysis, an amine nucleophile such as **21** ring opens the epoxide in an S_N2 manner. Advantages to this method include good regioselectivity, as well as a broad substrate scope.[2] There are methods for the ring opening of epoxides (Scheme 5), which generate the product in excellent yield and stereoselectivity, as well as good regioselectivity. A drawback, however, is that a high catalyst loading is frequently required.[8]
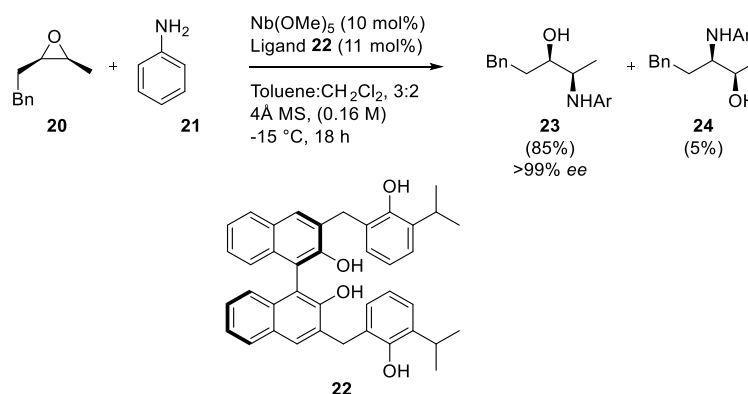
Scheme 5: Ring opening of epoxides

A more recent piece of work by Kureshi involved the use of a sulfinamide organocatalyst **27** (Scheme 6).[9] This method involved the treatment of a series of *meso*-epoxides, such as **25**, with anilines (e.g. **26**) to form the *β*-amino alcohol **28** in very high yield (up to 95%). The reaction provided the product with high enantiomeric excess of up to 99%, for most substrates. Metal-based methods for desymmetrizing *meso*-epoxides also exist, requiring a lower catalyst loading (3%) and providing very similar results in terms of yield and enantioselectivity.[10]
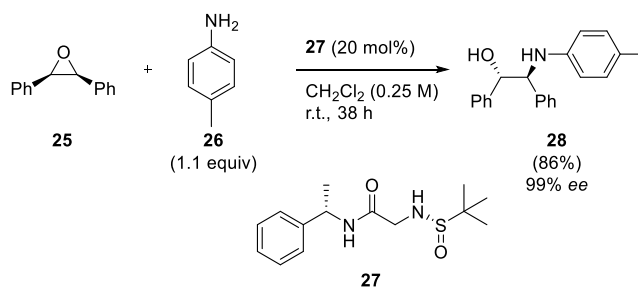
Scheme 6: Enantioselective organocatalytic ring opening of *meso*-epoxides

1.1.3 Oxyamination of Alkenes

The oxyamination of alkenes is a very powerful method for synthesizing β-amino alcohols. This functionalization can be easily applied to symmetrical alkenes; however, there is a regioselectivity issue for non-symmetrical alkenes. This is despite significant research being devoted to this challenge over the past three decades.

1.1.3.1 Sharpless Oxyamination

One of the first methods of producing β-amino alcohols from alkenes was discovered by Sharpless in 1975.[11] Its major limitation, however, was the stoichiometric use of osmium tetroxide which is known to be highly toxic.[12] One year later, a catalytic method was developed by Sharpless for alkene *cis*-oxyamination, using the trihydrate of chloramine-T **29** as a source of nitrogen (Scheme 7).[13] The catalyst loading was very low (1 mol%), but the reaction was not asymmetric.
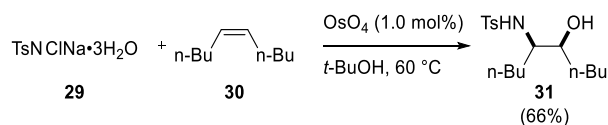
Scheme 7: First catalytic alkene oxyamination developed by Sharpless

Twenty years later (1996), Sharpless developed the first catalytic enantioselective method for alkene *cis*-oxyamination.[14] This method is a modification of the Sharpless asymmetric dihydroxylation.[15] The same source of nitrogen (chloramine-T **29**) was used and potassium osmate as oxidant. Chirality was induced by the addition of phthalazine (PHAL) adducts of cinchona alkaloids dihydroquinine (DHQ) and dihydroquinidine (DHQD), shown in Figure 2.
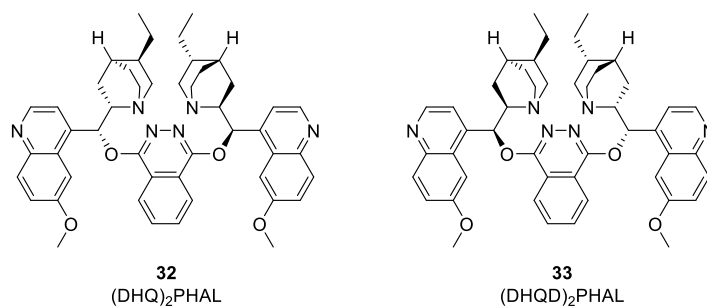
Figure 2: Chiral ligands used for Sharpless asymmetric oxyamination

The reactions are not sensitive to air or moisture, which means that there are no significant problems associated with the reaction setup. They also have the advantage of requiring only catalytic quantities of both metal and chiral agent, and reagents are commercially available. This was the first enantioselective method for this transformation, and the *ee*s obtained for the products were typically reasonable (around 70–80%, Scheme 8). Enantiopure products can be obtained, however, by crystallization of the amino alcohol products.
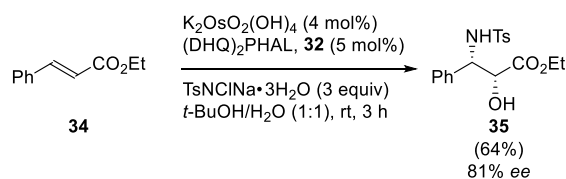
Scheme 8: Sharpless asymmetric oxyamination

In 1996, Sharpless published further work with emphasis on the regioselectivity of the reaction for non-symmetrical alkenes.[16] It was determined that changing the source of nitrogen from chloramine-T **29** to chloramine-M (MsNClNa) increased both the regioselectivity and enantioselectivity observed (Scheme 9).
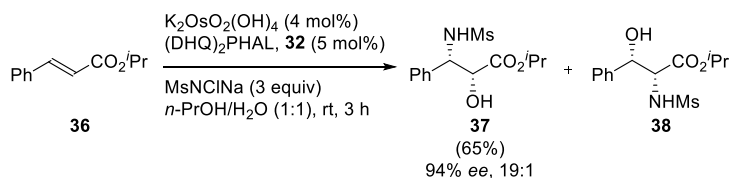
Scheme 9: Sharpless asymmetric oxyamination

1.1.3.1.1 Sharpless Asymmetric Oxyamination Mechanism

The first step of the proposed mechanism in this oxyamination process includes the formation of an imidotrioxoosmium(VIII) **41**, the active oxyamination species, by oxidizing OsO_3 **40** with chloramine (Scheme 10).
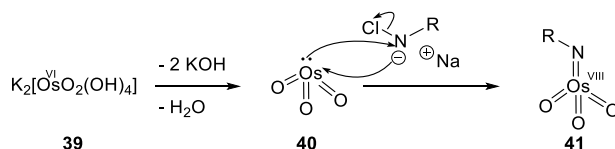
Scheme 10: Imidotrioxoosmium(VIII) **41** formation

Once the intermediate **41** is formed, the reaction is proposed to proceed *via* two catalytic cycles (Scheme 11).[16,17] Of these two, only the **primary cycle** would provide the desired product in high enantioselectivity. The **secondary cycle** would afford essentially no selectivity, as the addition of a second molecule of alkene **42** to intermediate **44** would displace the chiral ligand from the osmium, thus reducing the level of asymmetric induction.
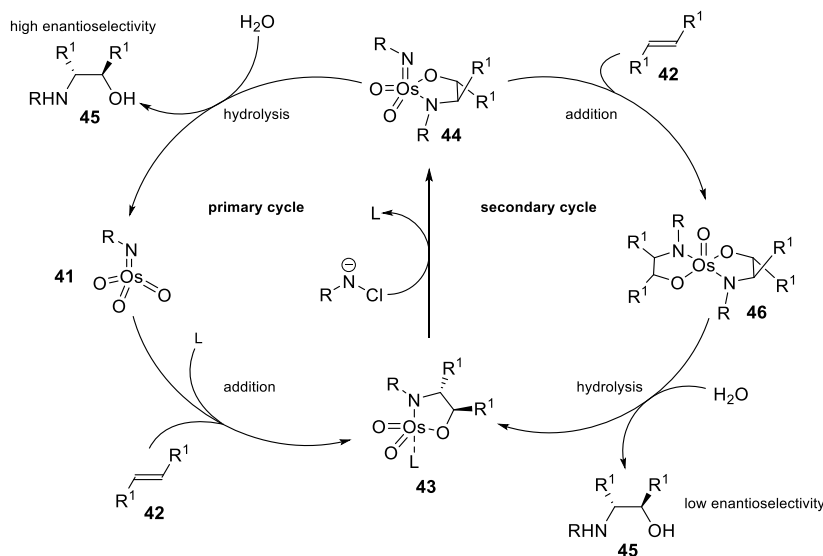
Scheme 11: Proposed catalytic cycles for Sharpless asymmetric oxyamination

Another mechanistic feature that is still questioned is the formation of intermediate **43** (Scheme 11). Two possible mechanisms for its formation have been postulated: one *via* a [3+2] cycloaddition and another *via* a [2+2] cycloaddition (Scheme 12). The former is considered to be favored, according to a computational study, but it has not been observed experimentally.[18]
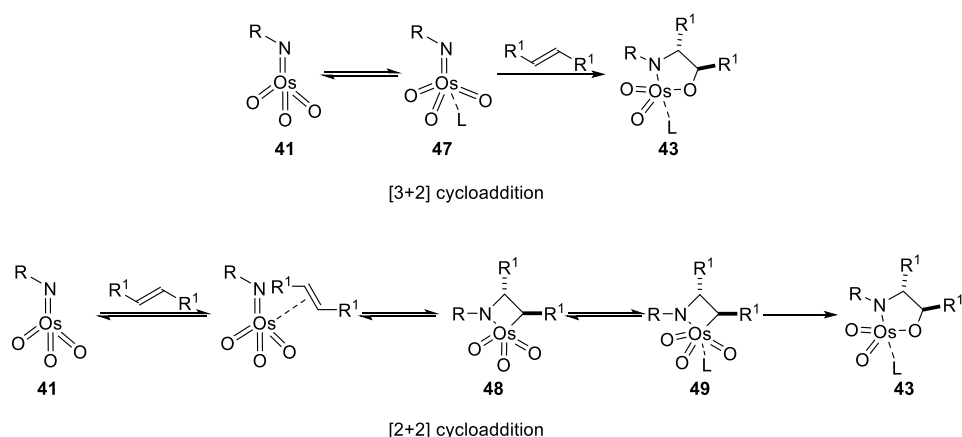
Scheme 12: Proposed cycloaddition of alkene to oxidant

1.1.3.1.2   Conclusions on Sharpless Asymmetric Oxyamination

There have been many developments of the Sharpless asymmetric oxyamination over the past decade and there are several reviews which cover these improvements in detail.[17,19] The range of substrates has increased, along with the possible sources of nitrogen. Therefore, a multitude of synthetic applications of this transformation have been documented and it is perhaps the most efficient method for oxyamination. Donohoe *et al.* have optimized a tethered process for alkene oxyamination that provides a pyrrolidine product **51** as a single diastereomer, using Sharpless' conditions (Scheme 13).[20]
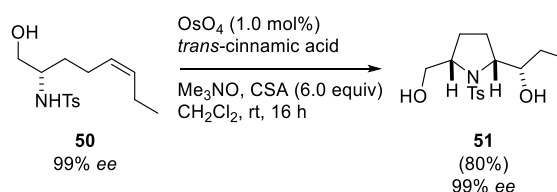
Scheme 13: Tethered oxyamination using OsO₄

Regardless of the variety of applications and the extension of the transformation to include more substrates, it must be noted that there is still room for improvement in substrate scope and, more importantly, regioselectivity. Additionally, osmium tetroxide is known to be highly toxic, therefore, other metal-based or metal-free methods have been developed to overcome this issue, and a number of alternative oxyamination procedures have been reported. These approaches will be described in the Sections 1.1.3.2 and 1.1.3.3.

1.1.3.2   Other Transition Metal-based Methods for Oxyamination

1.1.3.2.1   Rhodium

The use of rhodium(II) catalysts in the oxyamination of alkenes is one potential option to avoid the use of osmium. However, applications are mostly limited to intramolecular reactions, and no enantioselective procedure has been developed.[17] Dauban published a report in 2010, where oxyamination was achieved *via* an intermolecular process using rhodium, providing a single diastereomer **53** in high yield (Scheme 14).[21] Developments to the method were published by the same research group more recently, but the method is still not enantioselective.[22]
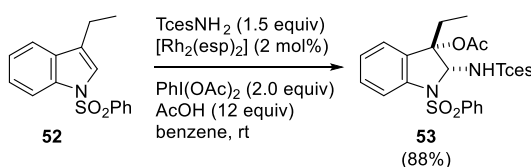
Scheme 14: Rhodium catalyzed oxyamination

1.1.3.2.2   Palladium

The first direct oxyamination of alkenes was published by Bäckvall in 1975 which involved the use of palladium acetate and lead acetate.[23] Besides the high toxicity of lead acetate, the functional group tolerance proved to be low.[17] More recently, Stahl introduced a highly regio- and diastereoselective method which, unlike the other approaches, provides the *syn*-product **56** (44%) as a single diastereomer (Scheme 15).[24]
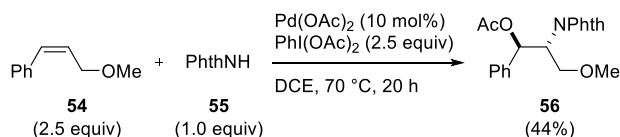
Scheme 15: Palladium catalyzed oxyamination

1.1.3.2.3 Platinum

For platinum mediated oxyamination, a study was published by Muñiz in 2009.[25] The reaction was performed under an oxygen atmosphere using copper(II) bromide as a co-catalyst, to provide the product **59** with very good diastereoselectivity (Scheme 16). Another isolated study by Verenikov in 2011 showed a platinum mediated oxyamination of ethylene under aerobic conditions.[26]
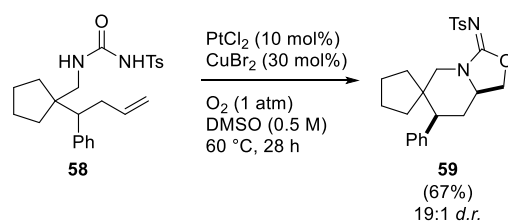
Scheme 16: Platinum catalyzed oxyamination

1.1.3.2.4 Copper

The use of copper in oxyamination reactions has been widely explored over the past decade.[17] Significant progress has been achieved within the Yoon laboratory, with the best result obtained shown in Scheme 17.[27] Treatment of styrene derivatives with oxaziridines such as **60** using a catalytic amount of a copper catalyst and a chiral ligand **61** led to a series of intermolecular oxyamination products such as **62**.
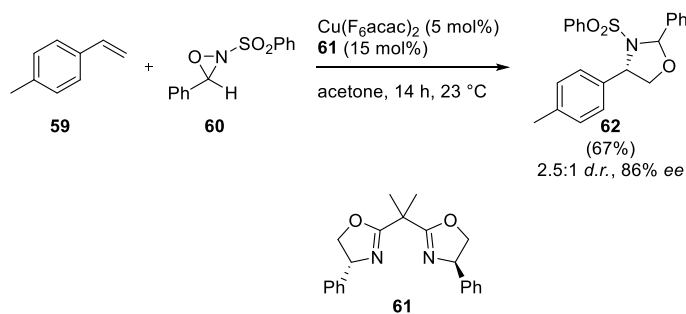
Scheme 17: Copper catalyzed oxyamination

The main advantage of this intermolecular copper catalyzed oxyamination was the enantioselectivity. The limitations involved poor diastereoselectivity (2.5:1 *d.r.*) and low substrate scope (terminal alkenes).

1.1.3.2.5   Iron

Building on the copper catalyzed oxyamination method, Yoon discovered that iron(II) provides much better diastereoselectivity (>10:1) for the functionalization of terminal alkenes.[28] Yoon extended this work to achieve an intermolecular enantioselective oxyamination (Scheme 18).[29] The oxyamination product **65** was generated by reacting the styrene derivative **59** and the oxaziridine **63** in the presence of an iron catalyst and a chiral ligand **64**. More recently, Xu published a highly diastereoselective method for the oxyamination of alkenes using tethered hydroxylamines, which was not limited to terminal alkenes.[30]
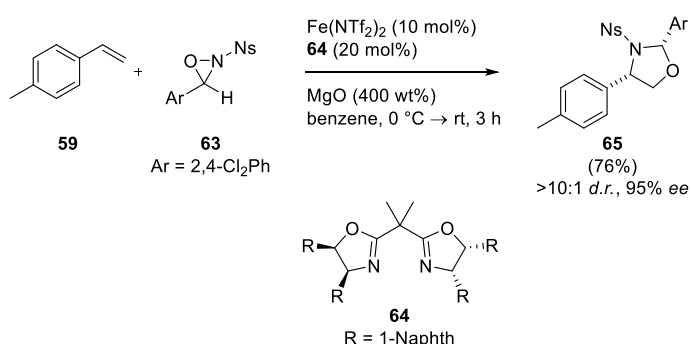
Scheme 18: Iron catalyzed oxyamination

1.1.3.2.6   Iridium

In 2015, Akita developed a photoredox catalyst based on iridium for the intermolecular oxyamination of alkenes (Scheme 19).[31] Alkenes such as styrene **66** were treated with a slight excess of amine **67** using only 1.0 mol% catalyst loading of iridium complex **68**. This afforded oxyamination products such as **69** in high yields. The reaction proceeded *via* a single electron transfer (SET) mechanism upon excitation of the iridium catalyst with blue light. The water present in the solvent mixture for this transformation acted as the oxygen source in the oxyamination process.
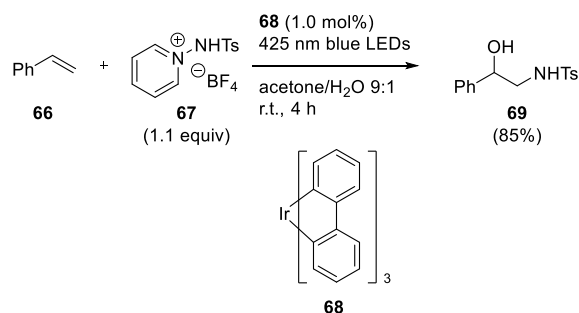
Scheme 19: Iridium/photoredox catalyzed oxyamination of alkenes

1.1.3.2.7 Conclusions on Transition Metal-based Oxyamination

Many methods involving transition metals have been developed to complement and augment Sharpless asymmetric oxyamination.[17] A few of these have shown great promise and address the need to replace the highly toxic and expensive osmium(VIII) required for the Sharpless procedure. However, there are still problems such as significant amounts of inorganic waste and the use of precious metals. Consequently, the most reliable transition metal-based method remains the Sharpless asymmetric oxyamination.

1.1.3.3 Metal-free Oxyamination

A potential way to overcome the problems encountered in transition metal-based oxyamination would be replacing the metal catalysts with organic molecules. Current methods for achieving this transformation will be discussed within this section.

1.1.3.3.1 Iodine

Of all of the metal-free approaches known, oxyamination using iodine-based reagents is the most common. These involve the use of iodine(0), iodine(III) or iodine(V).[17] Intramolecular oxyamination reactions using iodine are often high yielding and diastereoselective, but not enantioselective. To date, no direct intermolecular oxyamination has been published using iodine based reagents. However, many of the methods show great promise, such as the intramolecular oxyamination of alkene **70**, which affords **72** as a single diastereoisomer (Scheme 20).[32]
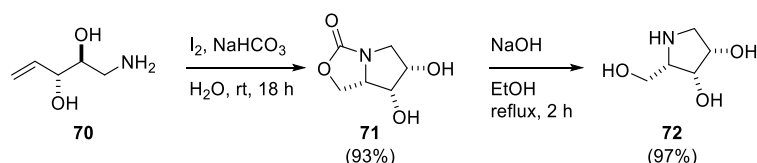
Scheme 20: Iodine(0) catalyzed oxyamination

1.1.3.3.2 Addition of Azides to Olefins

In 2005, Johnston reported an unusual method for the metal-free oxyamination of alkenes, which occurred with *anti*-selectivity.[33] This involved the reaction of an azide with an activated alkene, such as an *α,β*-unsaturated carbonyl compound, under acidic conditions. The reactions provided amino alcohols such as **75** in very high yields with good to excellent diastereoselectivity (>20:1 *d.r.*, Scheme 21). In this case, only the nitrogen source was external, as the oxygen was delivered in an intramolecular fashion.
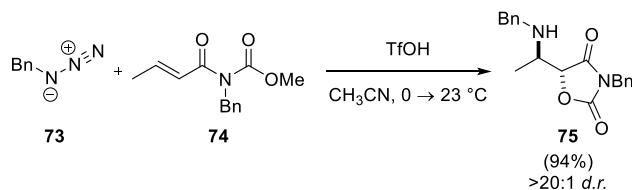
Scheme 21: Addition of azides to activated olefins

1.1.3.3.3   Vicinal Alcohols *via* Diels-Alder

An interesting method of obtaining amino alcohols was developed by Weinreb in 1984.[34] It involved a Diels-Alder reaction between a diene such as **76** and an *N*-sulfinyl dienophile such as **77**. The addition of a Grignard reagent to the Diels-Alder adduct **78** resulted in a [2,3] sigmatropic rearrangement, and a single diastereomer of the corresponding amino alcohol **80** was obtained after desulfurization of **79** with trimethylphosphite (Scheme 22). The disadvantage of this method is the limited substrate scope, which prevented further significant developments of this transformation.
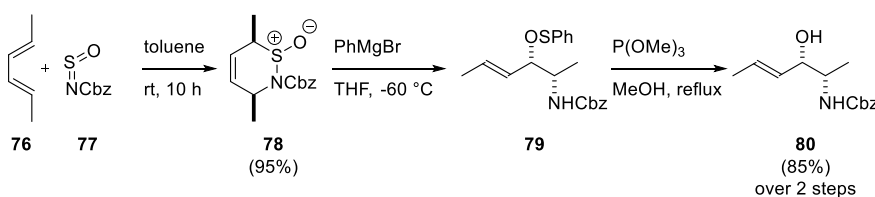
Scheme 22: Weinreb amino alcohol synthesis

1.1.3.3.4   Brønsted Acid Catalyzed Oxyamination

A novel method for achieving the metal-free oxyamination of alkenes was reported by Moriyama and Togo in 2012.[35] The method involved an intramolecular reaction that used Oxone® as the oxygen source and *p*-toluenesulfonic acid as the catalyst. The authors mentioned that the reaction mechanism involved an *in situ* epoxide formation, followed by epoxide opening by the tethered amine, to form the corresponding amino alcohol. The yields were good to excellent for the substrates reported, and the reaction was stereospecific for only three of the substrates described, including the alkene **81** (Scheme 23).
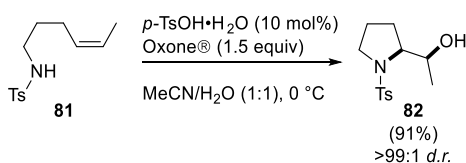
Scheme 23: Brønsted acid catalyzed oxyamination

1.1.3.3.5 Radical-induced Oxyamination

In 2012, Alexanian used *N*-aryl hydroxamic acids tethered to an olefin (e.g. **83**) and a radical trap (diisopropyl azodicarboxylate, DIAD) to form the corresponding oxyamination products (e.g. **84**) in good to excellent yields (up to 92%).[36] For cyclic substrates, excellent *anti*-diastereoselectivity was achieved (Scheme 24).
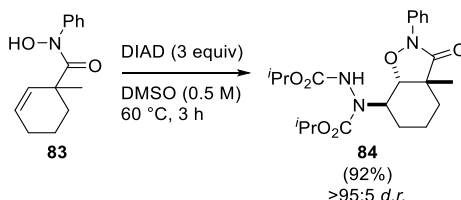
Scheme 24: Alexanian's radical induced oxyamination

In the same year, Han and coworkers reported a similar type of reaction, using oximes tethered to olefins and a different radical initiator/trap (diethyl azodicarboxylate, DEAD).[37] The conditions and products were very similar to Alexanian's work, providing excellent yields and diastereoselectivities for cyclic reactants (Scheme 25). However, there were a few drawbacks concerning these reactions such as their limitation to intramolecular cyclizations, which were not asymmetric.
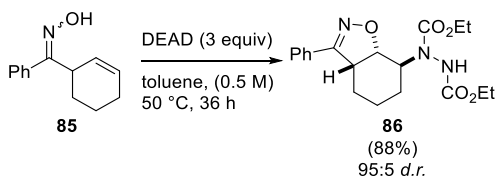
Scheme 25: Han's radical induced oxyamination

Another metal-free method involving radicals was published in 2015 by Studer and coworkers.[38] The method was very important as a metal-free process, particularly because it brought about an intermolecular reaction *via* an SET process (Scheme 26). Treatment of a series of alkenes (e.g. **87**) with excess *N*-fluoro-benzenesulfonimide **88** and excess TEMPONa for 6 h at room temperature provided the *trans*-oxyamination product (e.g. **89**) in moderate to good yields and excellent diastereoselectivity.
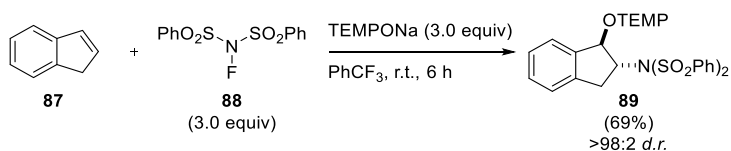
Scheme 26: Radical-induced intermolecular oxyamination of alkenes

1.1.3.3.6   Conclusions on Metal-free Oxyamination

Several methods for achieving the metal-free oxyamination of alkenes have been described. Their main advantage is that they do not use expensive or highly toxic metals such as osmium, and they generally do not require an inert atmosphere. Additionally, the amount of inorganic waste is minimized in comparison with the Sharpless asymmetric oxyamination. However, none of the metal-free approaches are asymmetric, and only one of these methods involved an intermolecular reaction. Hence, many opportunities exist before a synthetically useful metal-free procedure is achieved for this important transformation.

1.2 Previous Work

The idea to examine alkene oxyamination stemmed from previous work within the group on alkene dihydroxylation using malonoyl peroxides.[39] This metal-free method for *syn*-dihydroxylation of alkenes is shown in Scheme 27. The reaction employs malonoyl peroxide **90** to produce *syn*-diols in high yield (up to 93%) and diastereoselectivity (up to >50:1 *d.r.*). The amount of peroxide **90** required is stoichiometric, therefore the method is not catalytic. It has been established that fluorinated alcohols (TFE, HFIP, PFB) can be used as hydrogen bond donors to catalyze the reaction.[40]
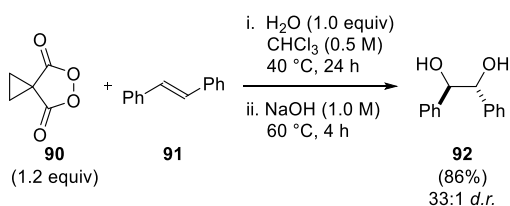
Scheme 27: *syn*-Dihydroxylation of alkenes using malonoyl peroxide **90**

The proposed mechanism of the metal-free alkene dihydroxylation reaction is shown in Scheme 28.[41] Alkene **93** reacts with malonoyl peroxide **90** *via* an ionic mechanism to provide zwitterionic species **94**, which ring closes to obtain dioxonium species **95** (major) or 7-membered ring **98** (minor). Dioxonium **95** is then hydrolyzed by a molecule of water to form ester **97** *via* dioxolane **96**. Hydrolysis of a mixture of **97** and **98** provides the corresponding *syn*-diol **99** together with the dicarboxylic acid **100**, which can be recycled to malonoyl peroxide **90**.
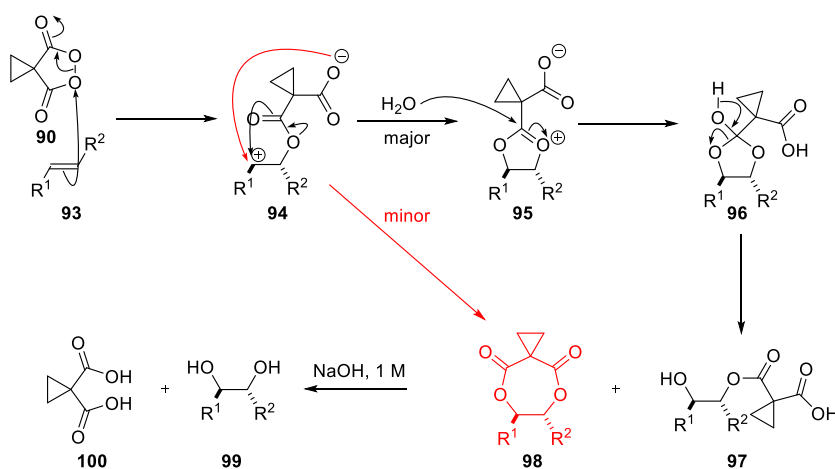
Scheme 28: Proposed mechanism for metal-free dihydroxylation of alkenes using malonoyl peroxide **90**

Based on the reactivity of malonoyl peroxide **90**, the question was whether a similar system could be developed for the oxyamination of alkenes. It was proposed that nitrogen-containing derivatives (**101**–**103**, Figure 3) of peroxide **90** could potentially be used as reagents in a novel oxyamination process.
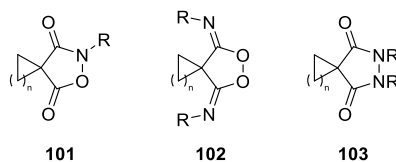
Figure 3: Proposed oxidants for the oxyamination of alkenes

The products shown below (Scheme 29) represent the potential *syn*-amino alcohol products by analogy to the proposed mechanism of the metal-free *syn*-dihydroxylation developed within the group. If successful, a major benefit of reagents **101**–**103** would be the discovery of an intermolecular metal-free oxyamination of alkenes through which the regiochemical outcome of the transformation could be controlled.
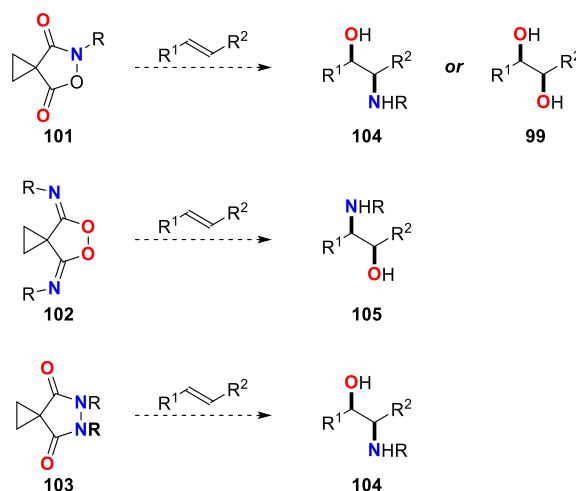
Scheme 29: Proposed oxyamination reactivity

It must be noted that for oxidant **101**, there is the possibility that the alkene nucleophile attacks the oxygen (red) instead of the nitrogen (blue), leading to the dihydroxylation products **99** (Scheme 28). This would not be an issue of concern, but rather a useful tool, since the –R group on the nitrogen has the potential to be functionalized to render the *syn*-dihydroxylation asymmetric. Furthermore, it would provide the corresponding diol

without the need for a peroxide, reagent which presents a concern due to the known sensitivity of peroxides to shock or heat.[39,42]

Oxidants **102** and **103** could potentially solve the regioselectivity issue of the oxyamination of alkenes. If the two oxidants are attacked by alkenes on the weak heteroatom–heteroatom bond, based on the proposed mechanism (Scheme 28), the expected oxyamination products **104** and **105** would be complementary to each other.

1.3   Results and Discussion – Oxyamination of Alkenes

1.3.1   Synthesis of Hydroxylamine-derived Oxidants

At first, hydroxylamine derivatives **101** were targeted. The reason behind having a cyclopropane ring attached to the oxidant is the malonoyl peroxide **90** precedent, where this peroxide proved to be more reactive in the dihydroxylation of alkenes than other derivatives such as phthaloyl peroxide **106**.[39]

90   **106**
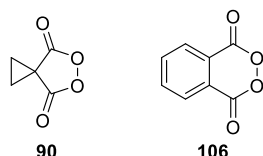
Figure 4: Peroxides used for the dihydroxylation of alkenes

The initial retrosynthetic pathway for **101** is shown below (Scheme 30). Compound **101** could be formed by treating diacid chloride **107** with hydroxylamine derivatives. The diacid chloride **107** could be made by reacting the corresponding diacid **100** with thionyl chloride.[43] Cyclopropyl malonic acid **100** is commercially available, but it can also be made easily from a cheaper, commercially available chemical, diethyl malonate **108**.[44]

101   **107**   **100**   **108**
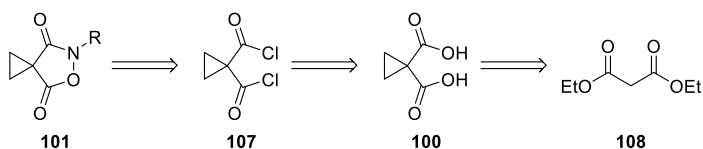
Scheme 30: Retrosynthesis of the first class of oxidants

The first step of the synthesis was a straightforward scalable procedure by Danishefsky (Scheme 31).[44] Diethyl malonate **108** and 1,2-dibromoethane were reacted in 50% aqueous sodium hydroxide using a phase transfer catalyst to afford malonic acid **100** in 78% yield.

BrCH₂CH₂Br (1.5 equiv)
Et₃BnNCl (1.0 equiv)
50% aq. NaOH (0.5 M)
rt, 2 h

108   **100**
                 (78%)
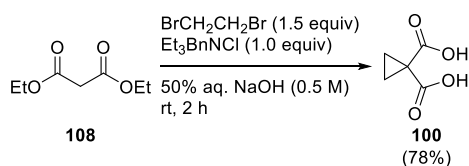
Scheme 31: Synthesis of cyclopropyl malonic acid

The next step was the formation of the corresponding diacyl chloride **107** (Scheme 32). Dicarboxylic acid **100** was treated with 12 equivalents of thionyl chloride under reflux conditions to afford **107** in 78% yield. This reaction proved amenable to scale up and diacyl chloride **107** was clean enough for further transformations upon simple removal of thionyl chloride *in vacuo*. Additionally, **107** proved stable over a time period of at least four months when stored at -18 °C, under an argon atmosphere and with the exclusion of moisture to avoid hydrolysis.
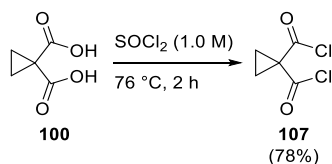
Scheme 32: Synthesis of diacid chloride **107**

Diacyl chloride **107** was treated with a series of *N*-substituted hydroxylamines **109**–**114** in an attempt to generate a family of cyclopropyl hydroxylamines **101** (Table 1). Conditions for the synthesis of *N*-Boc hydroxylamine derivative **115** were successful based on previous results obtained within the research group. These were then applied to hydroxylamines **110**-**114**.

Table 1: Formation of oxidants based on hydroxylamines **109**–**114**

Entry	Hydroxylamine	Product	Yield (%)	t (h)
1	**109**	**115**	73	4.5
2	**110**	**116**	25	3
3	NH$_2$OH•HCl **111**	**117**	0[a]	48
4	NH$_2$OH•H$_2$SO$_4$ **112**	**117**	0[a]	48
5	**113**	**118**	0[b]	48
6	**114**	**119**	0[a]	72

[a] No expected product observed by ^{1}H NMR spectroscopy; diacyl chloride **107** decomposed or monoacylated products were formed and their remaining acyl chloride was hydrolyzed during work-up, therefore these possible products could have been very soluble in water and easily lost.
[b] Only starting material observed by ^{1}H NMR spectroscopy.

Malonoyl hydroxylamines **115** and **116** were synthesized, but the main goal remained to synthesize compound **117** (Table 1, entries 3 and 4), since it had greater potential for functionalization on the nitrogen. Initial methods to synthesize **117** in one step from malonoyl diacyl chloride **107** failed. However, deprotection of **115** provided the target compound **117** in very high yield (97%, Scheme 33). This was an undesirable route since it involved four synthetic steps: formation of diacid **100**, conversion to the corresponding diacyl chloride **107**, reaction with *N*-Boc hydroxylamine **109**, followed by removal of the Boc group (39% yield over four steps).
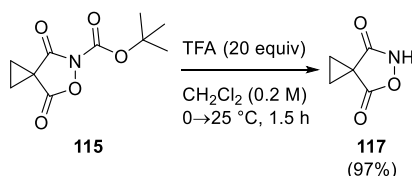
Scheme 33: Synthesis of **117**

An alternative route to malonoyl hydroxylamine **117** was reported by Zinner, who treated diethyl cyclopropane-1,1-dicarboxylate **120** with hydroxylamine in dioxane.[45] The reaction was reported with a low yield (31%) and in our hands did not provide the desired product **117** after several attempts to repeat the procedure. A paper describing the synthesis of hydroxylamines similar to **117** was reported by Richon *et al.* and their general method was adapted (Scheme 34).[46] An initial result using their exact conditions (1.5 equivalents of both hydroxylamine and sodium ethoxide) provided malonoyl hydroxylamine **117** in 21% yield and a simple increase in the equivalents of the reagents (2.5 equiv) led to full consumption of the starting material which made purification more facile. The method was not optimized further due to the low cost of the reaction components. The method involved two steps: synthesizing **120** (71%, from malonic acid),[47] and reacting it with hydroxylamine (29%, Scheme 34), with an overall yield of 21%. This approach for synthesizing malonoyl hydroxylamine **117** was lower yielding than the four-step method, but was preferred since it saved two synthetic steps.
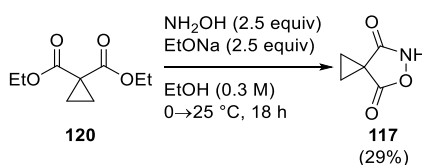
Scheme 34: Alternative synthesis of **117**

With two reliable routes to synthesize **117**, it was proposed that functionalizing the nitrogen of **117** with an electron withdrawing group would weaken the N–O bond. Unfortunately, the synthesis of **119** and **121** failed under the reaction conditions examined (Scheme 35), probably due to the poor nucleophilicity of the nitrogen atom of **117**.
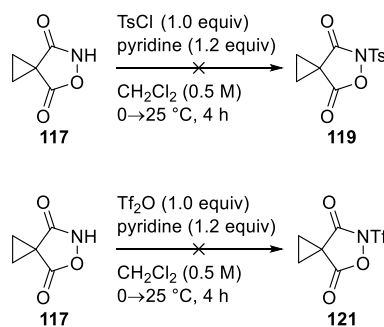
Scheme 35: Attempts to functionalize **117**

Despite the synthetic frustration, we had prepared three interesting hydroxylamine derivatives **115**, **116** and **117** and we sought to investigate their reactivity with alkene nucleophiles

1.3.2   Initial Oxyamination Attempts

The first oxyamination attempt was performed using malonoyl hydroxylamine derivatives **115–117** and *trans*-stilbene **91**. Employing the same reaction conditions to those developed for the *syn*-dihydroxylation of alkenes proved unsuccessful (Scheme 36). Nothing apart from starting materials was observed in the ^{1}H NMR spectrum of the crude reaction mixture prior to the hydrolytic step.
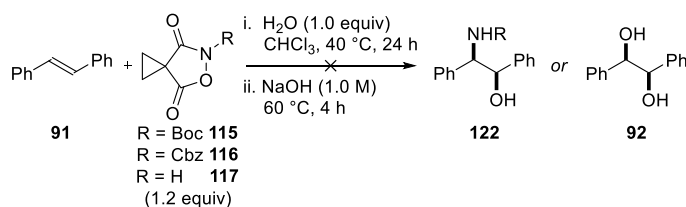
Scheme 36: Oxyamination attempts under *syn*-dihydroxylation conditions

Since the first set of reactions did not proceed as desired, harsher conditions were adopted *i.e.* higher temperature and the addition of a hydrogen bond donor, perfluoro-*tert*-butanol (PFB) as shown in Scheme 37. These conditions were employed since it was already known that for the metal-free *syn*-dihydroxylation method, perfluorinated alcohols accelerated the reaction.[40] The only change observed within these reactions was thermal loss of the -Boc group on malonoyl hydroxylamine reagent **115**. Reactions with **116** and **117** both returned unreacted starting materials.
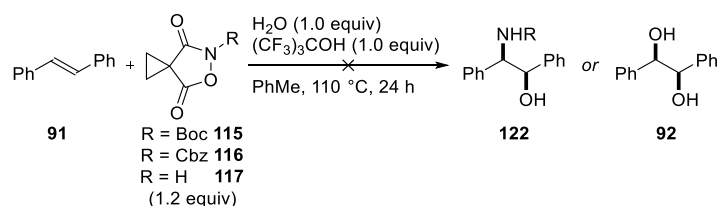
Scheme 37: Oxyamination attempts at higher temperature and in the presence of PFB

Given that *trans*-stilbene **91** was found to be inert to the reaction conditions examined, a more nucleophilic alkene was examined. 4-Methoxystyrene **123** was investigated under standard reaction conditions performing the reaction in CDCl₃ within an NMR tube (Scheme 38). Once again, no reaction occurred with any of the reagents examined (**115–117**).
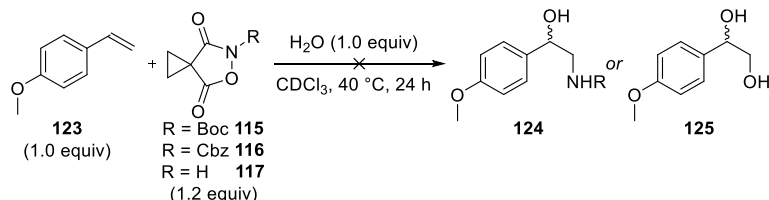
Scheme 38: Oxyamination attempts with 4-methoxystyrene **123**

In another attempt to obtain functionalization of alkenes using malonoyl hydroxylamines **115–117**, the same electron-rich nucleophilic alkene **123** was used, along with hydrogen bond donors which were expected to weaken the N–O bond. *N*-Cbz malonoyl hydroxylamine **116** was chosen as the reagent because it had been stable to date (high temperature, hydrogen bond donors) and it had three carbonyl groups around the N–O bond that could take part in hydrogen bond activation. The hydrogen bond donors examined in this study were ureas and thioureas **126–129**, selected due to their decreasing pK_a which it is envisaged would increase their hydrogen bond donor ability. No reaction occurred with each system examined, thus it was believed that the N–O bond was too strong to cleave with alkene nucleophiles under the conditions examined (Scheme 39).
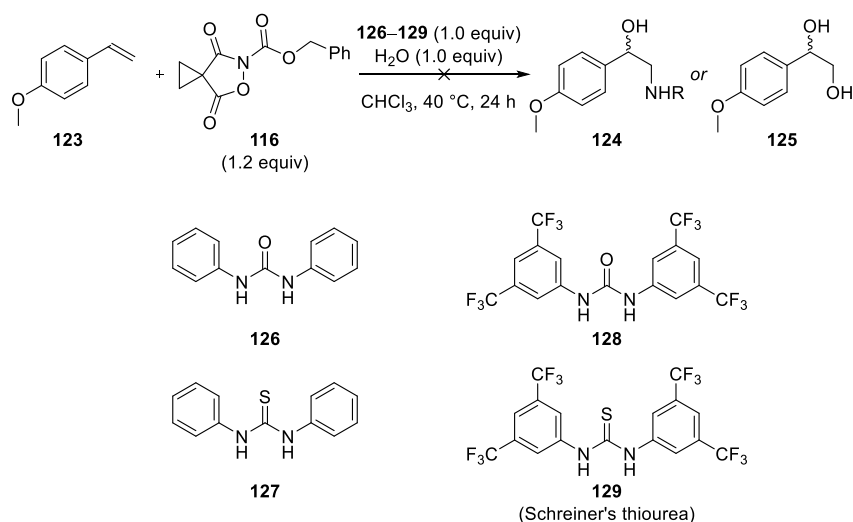
Scheme 39: Oxyamination attempts using hydrogen bond donors **126–129** as activators

1.3.3 Breaking the N–O Bond

Malonoyl hydroxylamines **115–117** had proven unreactive with alkenes, irrespective of whether a hydrogen bond donor was added to weaken the N–O bond. As a consequence, it was decided to try to break this bond using different nucleophiles.

First, thioanisole **130** was examined as a nucleophile (Scheme 40), since it was known in the research group that it reacted vigorously with malonoyl peroxide **90**.[48] It was expected that the reaction would form the corresponding sulfoxide **131** or sulfone **132**. Surprisingly, under the conditions examined with each of the hydroxylamine derivatives **115–117** no reaction was observed.
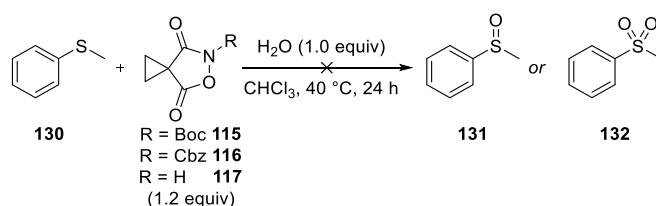
Scheme 40: Reactions with thioanisole **130**

Another attempt to bring about reaction was performed using morpholine **133** as the nucleophile (Scheme 41). Compound **117** was unreactive to morpholine, however for **134** and **135** the protecting group was transferred to the nitrogen of morpholine in moderate yield. It was expected that the N–O bond would be weak enough to break, but the outcome showed the C–N bond was weaker in the reaction examined.
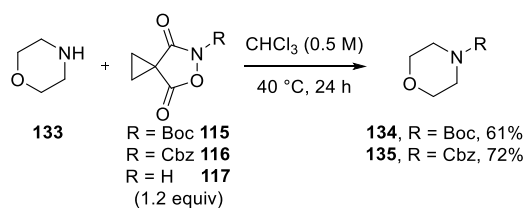
Scheme 41: Reactions with morpholine **133**

All of the results obtained from reacting these oxidants (**115**–**117**) with nitrogen and sulfur nucleophiles (thioanisole **130**, morpholine **133**) suggested that the N–O bond was, once again, too strong. This lack of reactivity could be explained by the bond energy difference (gas phase) between an O–O bond and N–O bond of 132 kJ/mol.[49] Thus, this class of compounds could not be used for the oxyamination of alkenes under the conditions examined. The only observed reactivity was exhibited by hydroxylamine derivatives **115** and **116**, involving protecting group transfer. As a consequence, our attention at this stage turned to investigating alternative oxidants.

1.3.4   An Alternative Oxidant

The N–O bond in compounds **115**–**117** proved unreactive to the nitrogen, sulfur and carbon nucleophiles examined. The next approach was to examine the synthesis of a more reactive imidoperoxide derivative **102** (Figure 5). A literature precedent by Payne *et al.* described the use of the highly reactive peroxy imidic acid **136** (Figure 5) within oxidation reactions.[50] This peroxy imidic acid intermediate was proposed to form *in situ*, by reacting a nitrile **137** with a source of hydrogen peroxide **138**, under basic conditions (Scheme 42). The reactivity of **136** was similar to that of *m*-chloroperoxybenzoic acid (*m*-CPBA) in performing epoxidations of alkenes. The main drawback of the method described by Payne was that the nitrile (acetonitrile or benzonitrile) was used as solvent, whereas we wanted to use our derivative as a stoichiometric reagent.
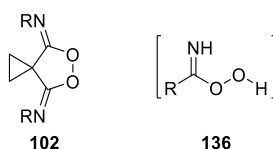
Figure 5: Alternative oxidant
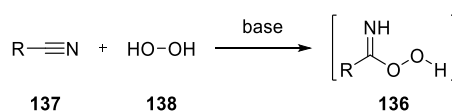
Scheme 42: Formation of generic peroxy imidic acid **136**

During the course of this investigation, an encouraging piece of work was published by Ji *et al.* in 2013.[51] This report described epoxidations of alkenes based on Payne's work which were performed using nitriles as reagents. A general reaction scheme is shown below (Scheme 43). Treatment of *trans*-stilbene **91** with urea hydrogen peroxide and benzonitrile using a mild base (potassium bicarbonate) as catalyst provided epoxide **139** in good yield (79%) and as a single diastereomer.
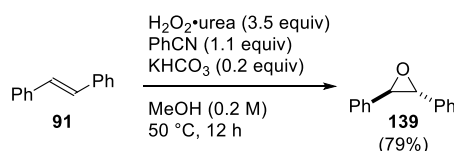
Scheme 43: Payne epoxidation

Because of this precedent, attempts were made to synthesize the simplest peroxide of the proposed class, spirocyclic imidoperoxide **140**. A retrosynthetic analysis is shown in Scheme 44. Imidoperoxide **140** could be synthesized by reacting cyclopropane-1,1-dicarbonitrile **142** under Payne's reaction conditions with a source of hydrogen peroxide. A peroxy imidic acid intermediate **141** is expected to form followed by ring closure to afford the target compound **140**. Dinitrile **142** could be synthesized from commercially available malononitrile **143**.
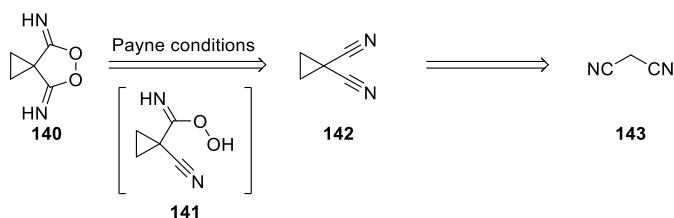
Scheme 44: Retrosynthesis of peroxide **140**

The first step of the synthesis was performed according to a literature procedure.[52] Malononitrile **143** was reacted with 1,2-dibromoethane in THF under reflux conditions in the presence of base (potassium carbonate) to afford dinitrile **142** in low yield (26%, Scheme 45). Despite the low yield, the method had the advantage that the product could be purified by distillation, thus the reaction could easily be performed on large scale. In addition, all of the reagents were commercially available, so it was not an issue to perform this low-yielding reaction on a multi-gram scale.
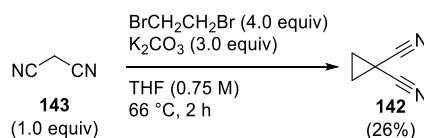
Scheme 45: Synthesis of dinitrile **142**

The next step was critical, as it involved potentially generating a new class of peroxide, thus all safety precautions for handling new peroxides were taken.[53]

At first, dinitrile **142** was reacted under standard Payne epoxidation conditions,[51] without an alkene present (Scheme 46). A peroxy imidic acid intermediate **141** could form and potentially ring close to give the proposed imidoperoxide **140**. Unfortunately, no material was recovered under the given conditions. This could suggest that the peroxide was formed *in situ* and it might have been too reactive/unstable, decomposing under the conditions examined. Under basic conditions, there was a possibility that the nitrogen of imidoperoxide **140** attacked another molecule of imidoperoxide **140** to form a peroxide species such as **144** (Scheme 47). This could be avoided under acidic conditions. Another explanation could be based on the known reactivity of malonoyl peroxide **90**, which was shown within the group to decompose in methanol.[48]
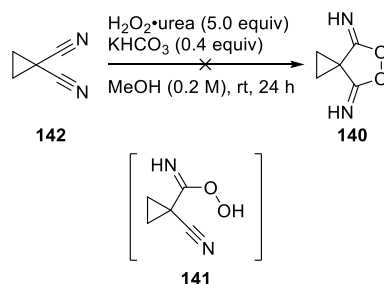
Scheme 46: Attempt to synthesize peroxide **140** using Payne's conditions
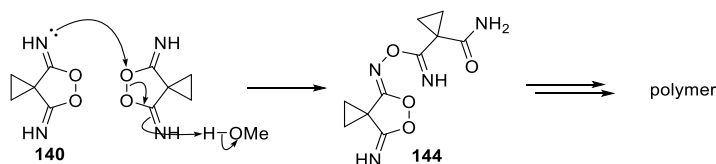
Scheme 47: Potential decomposition of imidoperoxide **140** under basic conditions

The reaction between dinitrile **142** and urea hydrogen peroxide was also examined under acidic conditions.[40] These conditions were the same as those used for the synthesis of malonoyl peroxide **90** (Scheme 48). Only compound **145** (34%) was isolated after work-up and flash chromatography (5% starting material still present). Interestingly, only one of the nitrile groups underwent a Radziszewski amidation,[54] whereas the other nitrile remained intact. Again, there is the possibility that the desired peroxide **140** was generated *in situ* followed by subsequent decomposition. In hindsight, there is also a possibility that imidoperoxide **140** formed and existed as a salt **146** under the acidic conditions examined (Figure 6).
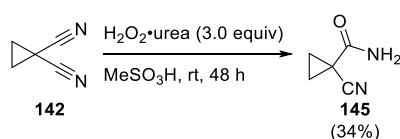
Scheme 48: Attempt to synthesize peroxide **140** under acidic conditions
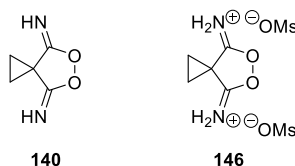
Figure 6: Imidoperoxide **140** and its corresponding methanesulfonate salt **146**

Having obtained these results, dinitrile **142** was treated with urea hydrogen peroxide under neutral conditions (Scheme 49). In this case, starting material **142** was recovered quantitatively.
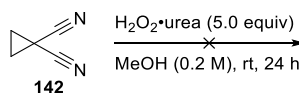
Scheme 49: Attempt to synthesize peroxide **140** under neutral conditions

After these failed attempts to generate peroxide **140**, replication of Li's work was examined to verify if the Payne system worked.[51] The reaction was performed as specified in the original paper using *trans*-stilbene **91** as the alkene and it provided the corresponding

epoxide **139** in moderate yield (44%, Scheme 50), whereas the reported yield was 79%. The result was encouraging, as it showed that a peroxy imidic acid could exist.
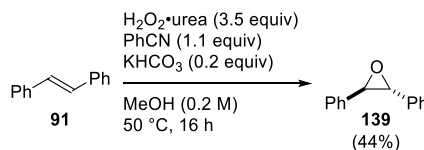
Scheme 50: Payne epoxidation of *trans*-stilbene **91**

The reaction was briefly optimized, using the specified reagents, to determine potential conditions for the formation of a peroxy imidic acid (Table 2). The reactions were all sampled after 24 h and performed at 50 °C. Reactions at 25 °C showed no product formation. The initial transformation showed a conversion of 48% after 24 h (entry 1) which verified the 44% yield obtained. Increasing the equivalents of nitrile had marginal effect on conversion (entries 2–4). Removing the base had a negative effect, some product still forming (10%, entry 5). Decreasing the amount of H_2O_2•urea or the concentration also reduced the conversion to epoxide **139** (entries 6 and 7). Increasing the concentration to 0.5 M had no effect (entry 8), but was preferred for potential detection of a peroxy imidic acid intermediate as solvent removal for sampling was more facile. Increasing the amount of H_2O_2•urea had a beneficial effect to the transformation, increasing the conversion to 62% (entry 9). Finally, having 6.0 equivalents of both H_2O_2•urea and benzonitrile boosted conversion to 85%, thus making these conditions appropriate for screening other nitriles.

Table 2: Optimizations for the Payne epoxidation
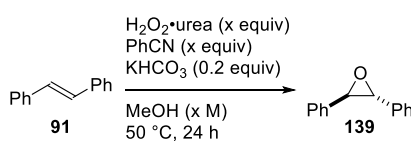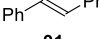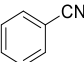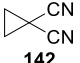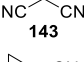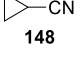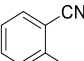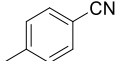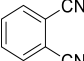
Entry	H_2O_2•urea (equiv)	KHCO₃ (equiv)	PhCN (equiv)	MeOH (M)	Conversion (%)[a]
1	3.5	0.2	1.1	0.2 M	48
2	3.5	0.2	2.0	0.2 M	46
3	3.5	0.2	4.0	0.2 M	52
4	3.5	0.2	6.0	0.2 M	54
5	3.5	–	2.0	0.2 M	10
6	1.0	0.2	2.0	0.2 M	4
7	3.5	0.2	2.0	0.1 M	11
8	3.5	0.2	2.0	0.5 M	51
9	6.0	0.2	2.0	0.5 M	62
10	6.0	0.2	6.0	0.5 M	85

[a] Conversion was monitored by ¹H NMR against an internal standard (1,4-dinitrobenzene).

The best conditions after the brief optimization (H_2O_2•urea (6 equiv), benzonitrile (6 equiv), potassium bicarbonate (0.2 equiv) in MeOH (0.5M)) were screened for a series of nitriles **142**, **143**, **147**–**152** within the epoxidation of stilbene (Table 3). Interestingly, there was no epoxide formation observed for dinitriles **142** and **143** (entries 2 and 3), but the two dinitriles were completely consumed under the reaction conditions. A reason for cyclopropane malononitrile **142** (entry 2) not having worked could be that it formed the desired peroxide **140** (Figure 7), which might have been very unstable. For malononitrile **143** (entry 3), one reason could be that it was deprotonated by the base under the reaction conditions. It could have also formed a five-membered ring peroxide **153** (Figure 7) which might have been unstable. The formation of epoxide **139** when using cyclopropane carbonitrile **148** (entry 4) suggested that it was possible that a cyclic peroxide such as **140** formed when using dinitrile **142**. Tolunitriles **150** and **151** (entries 6 and 7) suggested a marginal steric effect on the reaction, *i.e.* when the methyl group was *ortho* to the cyano group, the reaction was slightly less efficient.

Table 3: Payne epoxidation nitrile screening

Entry	Nitrile	Conversion (%)[a]
1	**147**	85
2[b]	**142**	<5%
3	**143**	<5%
4	**148**	79
5	MeCN **149**	53
6	**150**	51
7	**151**	61
8[c]	**152**	23

[a] Conversion determined by ^{1}H NMR spectroscopy using 1,4-dinitrobenzene as internal standard.
[b] 1.0 equiv dinitrile used.
[c] 3.0 equiv dinitrile used.
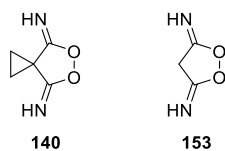
Figure 7: Potential peroxides generated *in situ*

Reactions under Payne epoxidation conditions without *trans*-stilbene **91** were carried out using tolunitriles **150** and **151** in an attempt to observe peroxy imidic acid intermediates such as **154** and **155** (Figure 8). The reactions were monitored by ^{1}H NMR spectroscopy, knowing the chemical shifts for the singlets corresponding to the methyl groups on the nitrile starting materials (2.52 ppm for nitrile **150** and 2.42 ppm for nitrile **151**). New signals were observed in both cases: one new singlet at 2.43 ppm when using nitrile **150** and one new singlet at 2.40 ppm when using nitrile **151**. These new singlets observed in the ^{1}H NMR spectrum of the reaction mixture belonged to the corresponding amides **156** and **157** (Figure 9).[55]
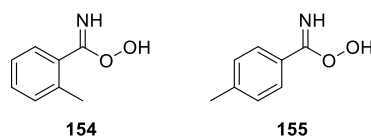
Figure 8: Proposed peroxy imidic acid intermediates corresponding to nitriles **154** and **155**
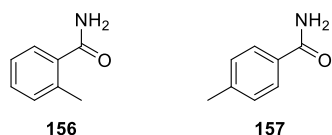
Figure 9: Amides from the hydrolysis nitriles **156** and **157**

An interesting substrate was phthalonitrile **152**, because it was able to convert *trans*-stilbene **91** to its corresponding epoxide **139** (23%, Table 3, entry 8). It is a dinitrile that could potentially ring close upon formation of a Payne intermediate **158** (Figure 10), and peroxide **159** could be an interesting reagent, provided that it could be generated or even isolated.
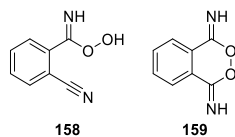
Figure 10: Phthalonitrile peroxide **159**, and peroxy imidic acid intermediate **158**

No intermediates were observed within the Payne epoxidation reactions performed, and no isolated intermediates have been reported in the literature despite the high number of citations (>200) of the original papers.[50] There is one theoretical study which analyzes the energy levels of postulated peroxy imidic acid intermediates such as **136** (Figure 11).[56] An experimental study by Vacque *et al.* using attenuated total reflectance (ATR) coupled with Fourier transform infrared (FTIR) and Fourier transform Raman spectroscopy (FT Raman) suggested the existence of a peroxy imidic acid intermediate, which was not isolated.[57] All other studies assume that a peroxy imidic acid intermediate such as **136** is formed *in situ*. Thus, additional experiments were performed to further support the existence of such an intermediate.
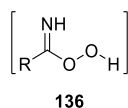
Figure 11: Postulated Payne epoxidation intermediate

Assuming that an intermediate such as **136** reacts in a similar manner to *m*-chloroperoxybenzoic acid (*m*-CPBA), it was believed that a Baeyer-Villiger oxidation could occur if Payne's conditions were applied to a ketone.[58,59] Cyclohexanone **160** was reacted under the optimized Payne epoxidation conditions and the corresponding lactone **161** was observed in the ^{1}H NMR spectrum of the crude reaction mixture (Scheme 51). This observation was encouraging as it suggested that it was possible to have a peroxy imidic acid intermediate. Furthermore, control reactions without base, nitrile or urea hydrogen peroxide were performed using the conditions below and no lactone **161** was observed by ^{1}H NMR spectroscopy. Given the fact that this was a novel and simple Baeyer-Villiger reaction, a project was started in order to further optimize the conditions (See Chapter 2, page 71).
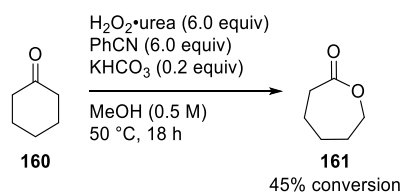
Scheme 51: Baeyer-Villiger oxidation using Payne epoxidation conditions

Further support for an intermediate similar to *m*-CPBA was the observed stereoselectivity. When reacting *E*-stilbene **91** under Payne conditions, the corresponding *trans*-epoxide **139** was formed (77%). This was confirmed by performing an *m*-CPBA epoxidation with the same alkene. To further support this concept, *Z*-stilbene **162** was reacted under the Payne epoxidation conditions developed (Scheme 52). A standard *m*-CPBA epoxidation of the alkene was also performed to confirm the formation of the *meso*-epoxide **25**.
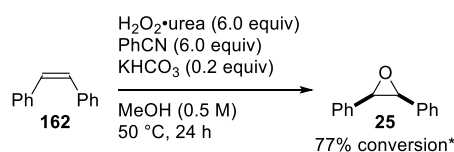
Scheme 52: Payne epoxidation of *Z*-stilbene.
* Conversion determined using 1,4-dinitrobenzene as internal standard.

1.4 Alternative Hydroxylamine Derivatives and Synthesis of Alkylidene Phthalides

Previous attempts to cleave the N–O bond of compounds **115–117** using a series of nucleophiles including alkenes (Section 1.3.2), sulfides (Section 1.3.3) and nitrogen-based nucleophiles (Section 1.3.3) were unsuccessful (Figure 12). For this reason, stronger nucleophiles such as *in situ* generated enolates were considered.
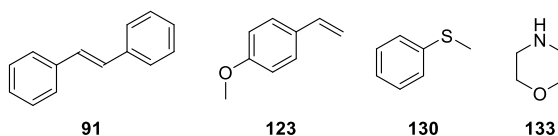
Figure 12: Nucleophiles examined

1.4.1 Literature Precedents

Cleavage of the heteroatom–heteroatom σ-bond of hydroxylamine derivatives **163** with enolate nucleophiles **164** or enamines could generate either α-oxygenation products such as **165** or α-amination products **166** (Scheme 53). This could happen *via* nucleophilic attack on the oxygen (N–O bond) or on the nitrogen of the hydroxylamine bond. A series of literature precedents involving reactions of enolates/enamines with peroxides or compounds bearing an N–O bond (resulting in cleavage of the sigma bond connecting the two heteroatoms) will be shown in the next sections.
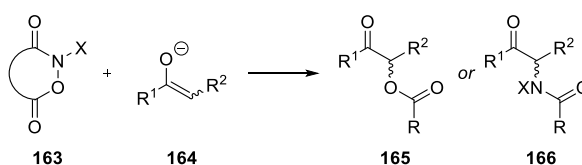
Scheme 53: Proposed α-oxygenation/α-amination reaction using enolate nucleophiles

1.4.1.1 Organocatalyzed *α*-Oxygenation of Ketones

There are a number of organocatalyzed processes for *α*-oxygenation of ketones using benzoyl peroxide **167** as an electrophile.[60] Each of these was proposed to involve the formation of an enamine nucleophile *in situ* which facilitates functionalization in the *α*-position of the carbonyl carbon. One example by List *et al.* made use of cinchona alkaloid organocatalyst **168** and benzoyl peroxide (BPO) **167** as the oxygen source to provide *α*-oxygenation products such as **169** (Scheme 54). The reaction was highly enantioselective, with *ee*s >90%. It is noteworthy that BHT was added as a radical inhibitor, to prevent unwanted benzoyl radical related side reactions.
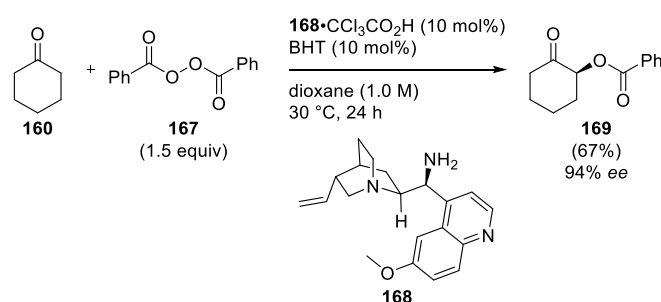
Scheme 54: Organocatalyzed *α*-oxygenation of cyclohexanone using BPO **167** as the electrophile

1.4.1.2 *α*-Oxygenation of Ketones using Chiral Oxaziridines

In 1990, Davis developed a sequential method for the enantioselective *α*-oxygenation of ketones using chiral oxaziridines (Scheme 55).[61] The method involved *in situ* formation of an enolate using NaHMDS, followed by treatment with chiral oxaziridine **171** (excess) to provide the desired products **172** in high yields and excellent enantioselectivity. While this method is not catalytic, and enantioselectivity is induced by the oxaziridine **171**, it was of particular interest to us as the reaction involved the cleavage of an N–O bond.
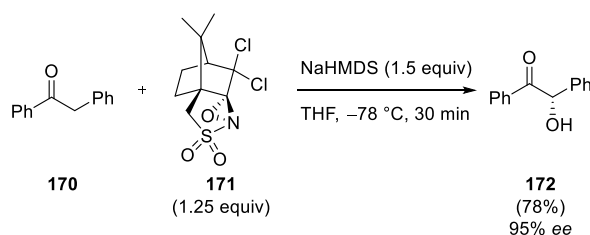
Scheme 55: Chiral oxaziridine mediated *α*-oxygenation of ketones

1.4.1.3   Enantioselective *α*-Amination of Aldehydes using Imidazolidinone Catalysts

MacMillan in 2013, published a method for the direct *α*-amination of aldehydes (Scheme 56).[62] The method used *O*-sulfonyl hydroxylamines such as **174** as a nitrogen source and excess aldehyde (e.g. **173**) in the presence of imidazolidinone catalyst **176** and 2,6-lutidine **175** under a compact fluorescent light (CFL) to provide the target compounds (e.g. **177**) in moderate to good yields and very high enantioselectivities (>89%). This transformation proved versatile as it can be applied to a series of different aldehydes and *O*-sulfonyl hydroxylamines.
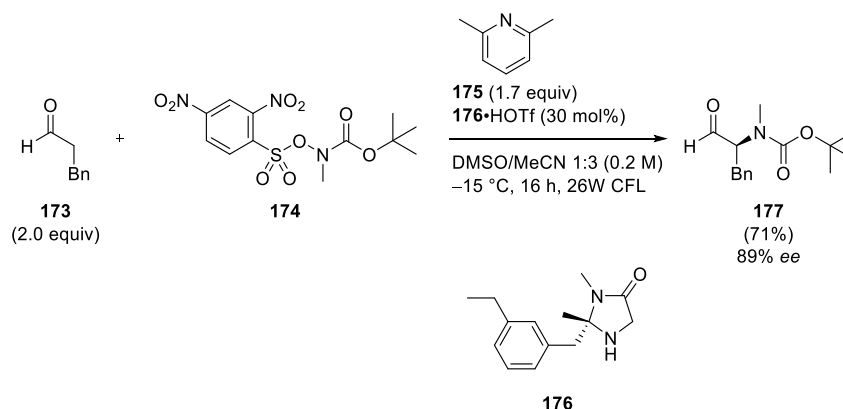
Scheme 56: Organocatalyzed photoredox *α*-amination of aldehydes

1.4.1.4   *α*-Amination of Ketones using Oxaziridines

Another method for the *α*-amination of ketones involving the cleavage of an N–O bond was discovered by Collet in 1993.[63] The method was rendered enantioselective by Enders in 1998, using chiral auxiliary **178** (Scheme 57).[64] Treatment of an *in situ* formed enolate of ketone **178** with oxaziridine **179** provided the *α*-amination product **181** in low yield with good diastereoselectivity. The poor yield was attributed to the formation of an undesired aldol product **182** (Figure 13), a byproduct which was generally formed in a 1:1 ratio with the target compound. This unwanted product was also observed more recently by Armstrong *et al.* and, unfortunately, the side reaction that led to its formation could not be suppressed.[65]
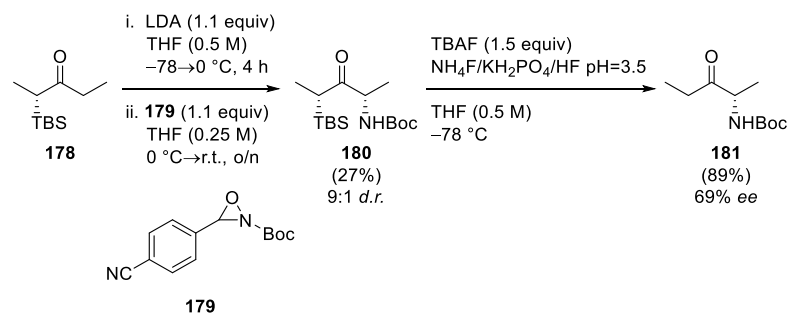
Scheme 57: Oxaziridine mediated α-amination of prochiral ketones
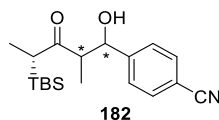
Figure 13: Undesired aldol product **182**

1.4.2 Initial Result

To probe the possibility of using enolates as nucleophiles, two more hydroxylamine derivatives **183** and **184** were synthesized, which are derivatives of phthaloyl peroxide **106** which is a known reagent for the dihydroxylation of alkenes (Figure 14).[66]
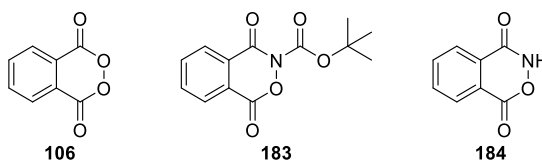
Figure 14: Phthaloyl peroxide **106** and phthaloyl hydroxylamines **183** and **184**

The synthesis of the two hydroxylamine derivatives **183** and **184** shown above had already been established within our research group (Scheme 58). These had already been unsuccessfully examined for the oxyamination of alkenes by a previous group member.[48] Commercially available phthaloyl chloride **185** was treated with *N*-Boc-hydroxylamine **109** in the presence of triethylamine in CH$_2$Cl$_2$ for 6 h to afford phthaloyl hydroxylamine **183** in low to moderate yields (32–56%). The low yield did not prove problematic as all reagents were inexpensive, the product was easily purified by trituration followed by two filtrations, and reactions were performed on a multi-gram scale. Phthaloyl hydroxylamine **184** was generated in good yield (80%) by treatment of **183** with an excess of TFA in CH$_2$Cl$_2$.
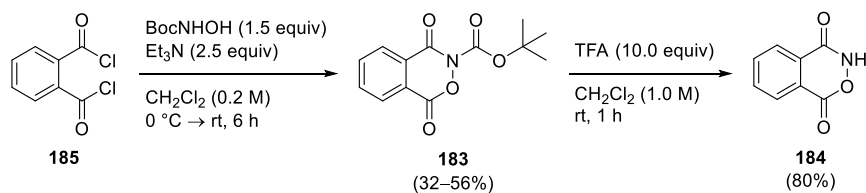
Scheme 58: Synthesis of phthaloyl hydroxylamines **183** and **184**

After preparing these two additional hydroxylamine derivatives, 5 different electrophiles **115**-**117**, **183** and **184** were available for testing in a reaction with enolates (Figure 15).
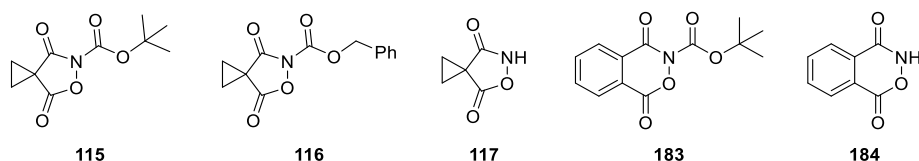
Figure 15: Synthesized hydroxylamine derivatives

After discovering the encouraging precedent in the literature using enolates or enamine nucleophiles for α-oxygenation or α-amination of ketones, the next step was to react an enolate with one of the hydroxylamine derivatives prepared. Phthaloyl hydroxylamine **183** was chosen as a first electrophile, because of its scalable synthesis from commercially available starting materials. The reaction conditions examined were similar to those used by Vidal *et al.* for the α-amination of ketones using oxaziridines.[63b] The *in situ* generated enolate was reacted with an equimolar amount of phthaloyl hydroxylamine **183** to afford an unexpected compound, alkylidene phthalide **187**, in 38% yield. Compound **187** was isolated as a single diastereomer after column chromatography and its structure was determined by comparison of its ^{1}H NMR to a previous report of this molecule.[67] Within the same report, the minor diastereomer (*Z*) was reported and by comparing the ^{1}H NMR spectrum of the crude reaction mixture to the literature, it was determined that a *E*/*Z* ratio of 4:1 was obtained in the transformation shown in Scheme 59. This intriguing result meant that the attack of the nucleophile did not occur as intended/predicted, on the nitrogen atom or on the oxygen atom of the weak hydroxylamine bond, but rather on one of the carbonyl carbons of the reagent.
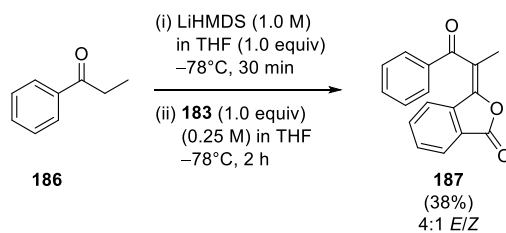
Scheme 59: Reaction of phthaloyl hydroxylamine **183** with enolates (initial result)

A mechanism for this initial result is proposed below (Scheme 60). First, propiophenone enolate **188** (known to be exclusively *cis* when using LiHMDS in THF at –78 °C)[68] attacks the ester moiety of phthaloyl hydroxylamine **183** to form anionic intermediate **189**. This intermediate then allows the formation of another enolate **190** which can cyclize by attacking the less electrophilic amide and eliminating the anion of *N*-Boc hydroxylamine **109** to form propiophenone alkylidene phthalide **187**.
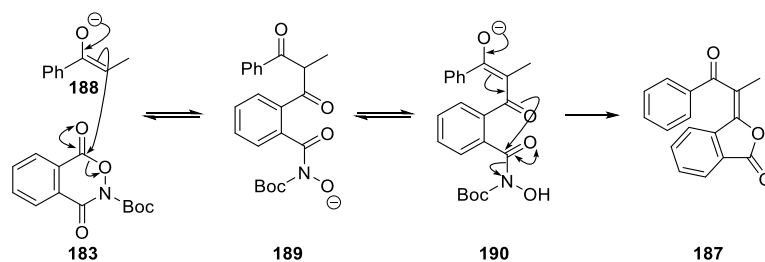
Scheme 60: Proposed mechanism for the formation of alkylidene phthalide **187**

In an attempt to further explain this unexpected result, the LUMO of phthaloyl hydroxylamine **183** was simulated using Gaussian software (Figure 16).[69] The π* orbitals across the carbonyls of the compound can be clearly observed in the simulation, and no σ* orbital was generated across the N–O bond for the LUMO. This case was very different when comparing with malonoyl peroxide **90**, which is an effective reagent for the dihydroxylation of alkenes, and was shown to react with nucleophiles *via* the peroxide oxygen atoms.[41,131] For the LUMO of malonoyl peroxide **90**, the σ* orbital of the O–O bond is shown in Figure 16. Since nucleophilic attack occurs by introducing electron density into the LUMO, the simulated LUMO of phthaloyl hydroxylamine **183** helped explain why, in this case, the attack took place on the carbonyl carbon of the reagent.
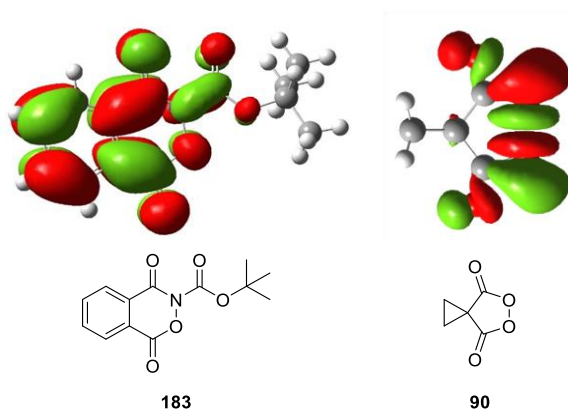
Figure 16: LUMOs of phthaloyl hydroxylamine **183** and malonoyl peroxide **90**

1.4.3 Alkylidene Phthalides

After this initial result, it was of interest to find out more about alkylidene phthalides as a class of compounds to establish the synthetic use of the transformation. An extensive review by Mal in 2014 covered the synthetic applications of phthalides as well as their biological properties.[70] A selection of the phthalides discussed in the review (both naturally occurring and synthetic) exhibiting biological activity are shown below (Figure 17). Due to the very high number of synthetic methods for obtaining phthalides, the methodologies discussed will be restricted to the formation of alkylidene/arylidene phthalides.

NBP **191**
3-butylisobenzofuran-1(3*H*)-one
antiviral/antibacterial

192
Noscapine
antitussive

193
Epicoccone
antioxidant

194
(*Z*)-butylidene phthalide
sedative

195
Typhaphthalide
venereal diseases/diarrhoea

196
Vermistatin
antibiotic/antifungal
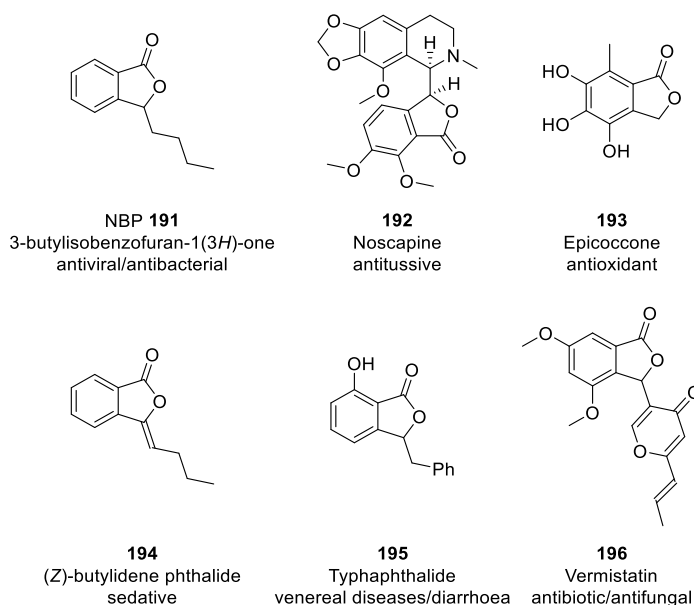
Figure 17: Examples of phthalides possessing biological activity

1.4.3.1   Palladium Catalyzed Heteroannulation of Acetylenes

A transition metal-based method for generating alkylidene phthalides was published by Kundu in 1993 (Scheme 61).[71] Reaction of 2-iodobenzoic acid **197** with two equivalents of an alkyne (e.g. **198**) under basic conditions in the presence of a palladium catalyst and copper iodide as a co-catalyst at 60 °C in DMF led to the formation of a series of alkylidene phthalides, such as **199**. The transformation was remarkable as it provided the *Z*-isomer of the alkylidene phthalide exclusively.
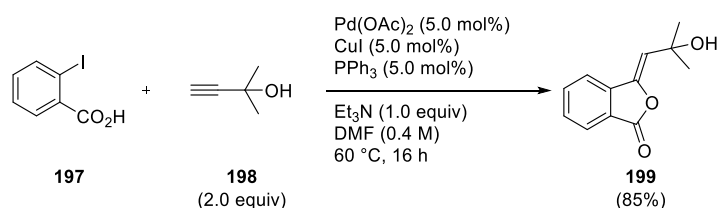
Scheme 61: Alkylidene phthalide synthesis *via* heteroannulation of acetylenes

This method was even more remarkable as it involved a one-pot Sonogashira coupling followed by cyclization, avoiding a multi-step process. Cyclizations of preformed alkynes with a carboxylic acid functionality in the *ortho* position under basic conditions are also known in the literature.[72] Terada's method, for example, was applied to a series of substrates to generate alkylidene phthalides (Scheme 62).[72b] Treatment of a series of alkynes such as **200** with a catalytic amount of DBU in MeCN under reflux conditions provided the corresponding *Z*-arylidene phthalide **201** in very high yields. Like in the case above, the *Z*-stereochemistry could be explained *via* a 5-*exo-dig* cyclization of carboxylate **202** assisted by the conjugate acid of DBU.
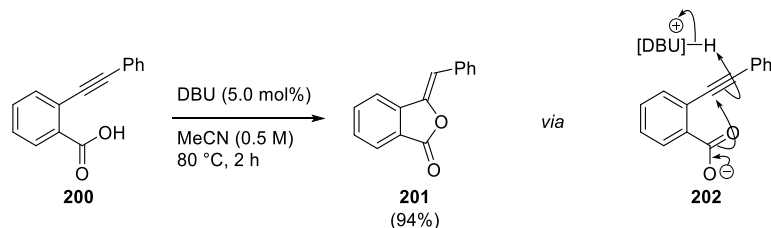
Scheme 62: DBU catalyzed arylidene phthalide synthesis

1.4.3.2   Palladium Catalyzed Stille Coupling

Abarbri *et al.* developed a palladium catalyzed cross-coupling reaction of stannanes with vinyl or aryl iodides (Scheme 63).[73] The method was applied to a series of phthalides which involved treatment of an aryl/vinyl iodide (e.g. **204**) with excess stannane (e.g. **203**) in the presence of PdCl$_2$(MeCN)$_2$ at room temperature to provide a series of arylidene phthalides in moderate to good yields. The transformation mainly provided *E*-arylidene phthalides, such as **205**, retaining the stereochemistry of the initial stannanes. One exception is shown below, in which iodobenzene **206** was used as a reactant, leading to *Z*-selectivity for this class of compound, which the authors explained through the thermodynamic stability of the *Z*-isomer.
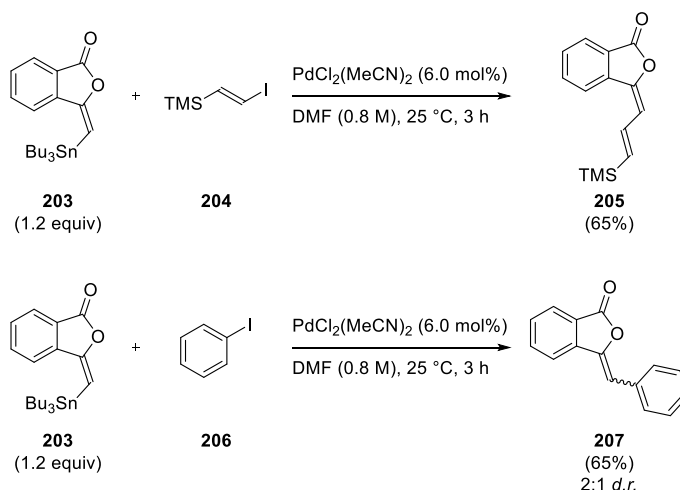
Scheme 63: Alkylidene phthalide synthesis *via* cross-coupling reaction

1.4.3.3   Copper(II) Chloride Mediated Cyclization

In 2011, Miyata published a paper on an intramolecular cyclization/halogenation reaction of Weinreb amides and alkynes (Scheme 64).[74] A series of arenes, such as **208**, were reacted to provide the *E*-alkylidene phthalides (e.g. **209**) in good yields. The reactions proceeded *via* a *5-exo-dig* cyclization similar to that shown in Scheme 62.
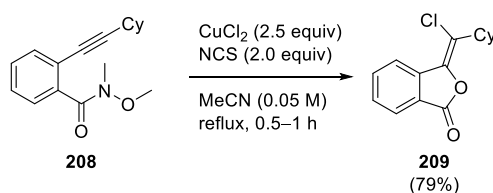
Scheme 64: CuCl$_2$/NCS mediated intramolecular cyclization/halogenation

1.4.3.4 NHC Catalyzed Oxidative Cyclization

Another intramolecular cyclization to give alkylidene phthalides was published in 2011 by Youn.[75] This versatile transformation was applied to a broad range of substrates such as **210** in the presence of a catalytic amount of *N*-heterocyclic carbene (NHC) precursor **211** and DBU to afford a series of alkylidene phthalides such as **201**. However, while the method had a broad substrate scope, its disadvantage was that the phthalide products were inseparable from the isocoumarin isomers that were also formed (e.g. **212**).
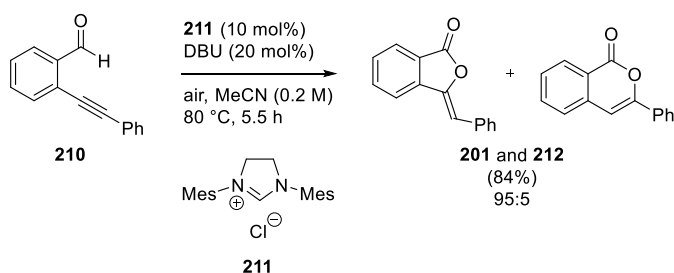
Scheme 65: NHC catalyzed oxidative cyclization

1.4.3.5 Organocadmium Addition–Dehydration Protocol for the Synthesis of Phthalide Derivatives

Hu in 2007, published a two-step process for the synthesis of alkylidene phthalides (Scheme 66).[76] Treatment of phthalic anhydride **213** with an *in situ* generated dialkyl cadmium species (e.g. **214**) in Et$_2$O followed by acidic work-up formed intermediate **215**. This intermediate was then dehydrated to provide a series of *Z*-alkylidene phthalides, such as **216**. The method was successfully applied to a series of dialkyl cadmium species.
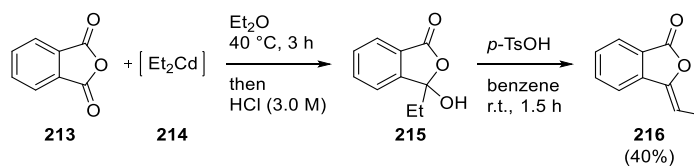
Scheme 66: Organocadmium addition–dehydration for the synthesis of alkylidene phthalides

1.4.3.6 Condensation of Arylacetic Acids with Phthalic Anhydride

In 2006, Alcamí published a report on the anti-HIV activity of a multitude of arylidene phthalides.[77] Arylidene phthalides such as **218** have shown antiviral activity and were prepared by reacting arylacetic acids **217** with phthalic anhydride **213** (which also served as the solvent) under basic conditions (AcONa). This condensation reaction has been established in the literature for more than 50 years as a method for the synthesis of arylidene phthalides.[78]
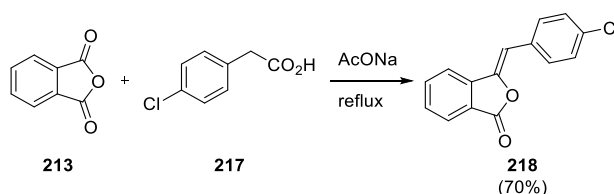
Scheme 67: Condensation of arylacetic acids with phthalic anhydride **213**

1.4.3.7 Microwave Mediated Condensation

In 2007, Safari published work on a microwave assisted synthesis of arylidene phthalides (Scheme 68).[79] The method involved treatment of a series of methylated quinolines (e.g. **219**) with various phthalic anhydrides (e.g. **213**) in acetic anhydride using microwave irradiation to afford quinoline phthalides such as **220** in very high yields. Major benefits of the process include very quick reaction times (< 3 min) and exclusive selectivity for the *E*-isomer. The stereochemistry was assigned only based on a deshielded vinylic proton in the ¹H NMR spectrum and comparison with the existing literature.
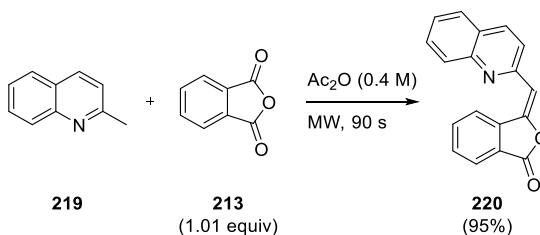
Scheme 68: Microwave mediated condensation for generation of quinoline phthalides

1.4.3.8 Wittig Olefination

A simple procedure for obtaining alkylidene phthalides was published by Abell *et al.* in 1988 (Scheme 69).[80] Phthalic anhydride **213** was treated with Wittig reagent **221** in CH_2Cl_2 at room temperature for 8 hours to form alkylidene phthalide **222** in good yield and diastereoselectivity. A similar method was also used in the synthesis of natural product sporotricale methylether **223** (Figure 18), a metabolite of the fungus *Sporotrichum laxum*, using a Horner-Wadsworth-Emmons reaction instead of a Wittig reaction.[81]
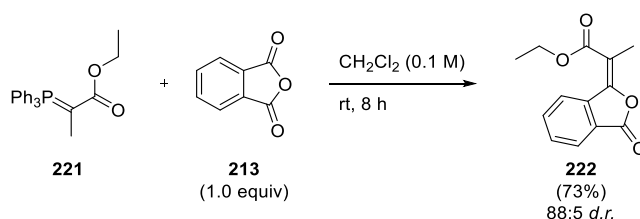
Scheme 69: Alkylidene phthalide synthesis *via* Wittig olefination
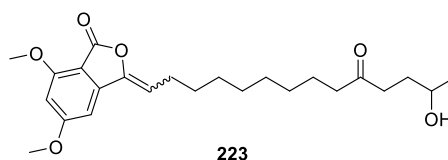
Figure 18: Sporotricale methylether **223**

1.4.3.9 Palladium Catalyzed Carbonylative Cyclization

In 2006, Coelho *et al.* developed an intramolecular cyclization method for synthesizing alkylidene phthalides (Scheme 70).[82] The first step of the transformation was a base-catalyzed Baylis-Hillman reaction between aromatic aldehyde **224** and ethyl acrylate **225** to generate compound **227** in very high yield (92%). The second step was a one-pot carbonylation/cyclization reaction catalyzed by $Pd_2(dba)_3$ under basic conditions, followed by sealing the reaction vessel under two atmospheres of carbon monoxide, to afford the desired alkylidene phthalide **222** in excellent yield and good diastereoselectivity.
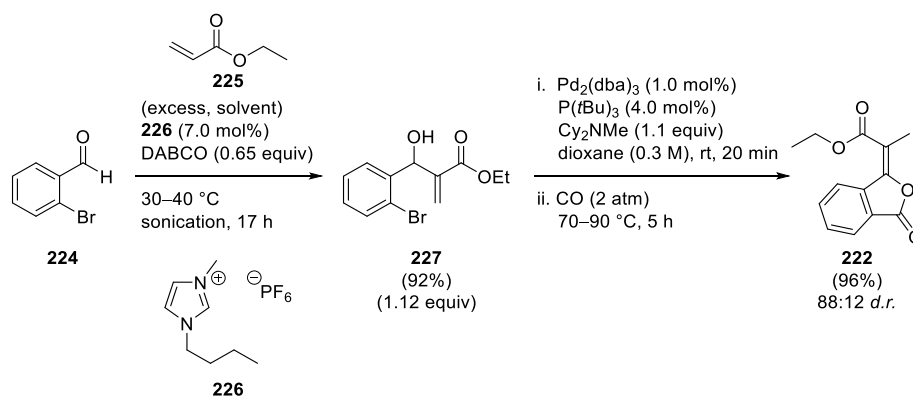
Scheme 70: Pd catalyzed carbonylative cyclization of Baylis-Hillman adducts

1.4.3.10 Baylis-Hillman Reaction

Another approach involving a Baylis-Hillman reaction was described by Kim in 2003 (Scheme 71).[83] This method is similar to the one described above, with the cyclization occurring in one step due to the presence of the carboxylic acid moiety in the starting material **228**. Treatment of **228** with ethyl vinyl ketone **229** under basic conditions in hot acetonitrile afforded alkylidene phthalides, such as **230**, in good yield, providing the *E*-isomer for most products or a mixture of isomers with moderate diastereoselectivity for two examples (1.4:1 *d.r.*).
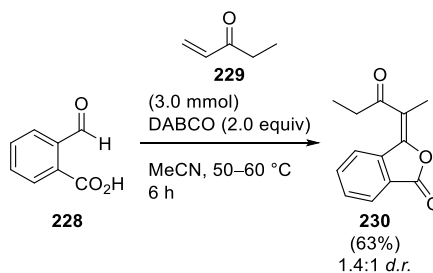
Scheme 71: Alkylidene phthalides *via* Baylis-Hillman reaction

1.4.3.11 Photochemistry

A photochemical method for the preparation of alkylidene phthalides was developed by Kato *et al.* in 1978 (Scheme 72).[84] In this case, epoxide **231** was irradiated using a 400 W lamp to obtain a mixture of arylidene phthalides **232** and **233** in low yield. The method was only used on this substrate to generate the phthalides and despite the fact that both isomers were isolated, no diastereomeric ratio of the crude reaction mixture was reported.
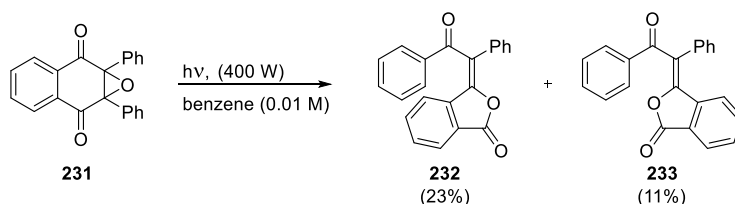
Scheme 72: Photochemically induced synthesis of arylidene phthalides **232** and **233**

Recently, Mor *et al.* developed a photochemical method which provided access to a series of alkylidene phthalides (Scheme 73).[67] The synthesis was a two-step process: first, polyketone **234** was methylated using iodomethane under basic conditions to obtain **235**, which was then irradiated using a 450 W lamp in benzene for 3 h to provide alkylidene phthalide **187** in excellent yield in a 1:1 diastereomeric ratio. The diastereomeric ratio for this transformation was not an issue as the two isomers were separable by column chromatography.
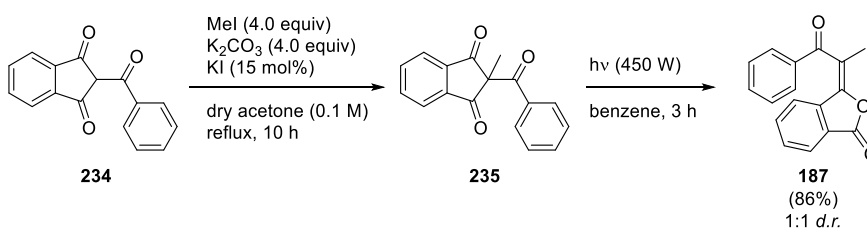
Scheme 73: Photochemically assisted synthesis of alkylidene phthalides

1.4.3.12 Enamine Mediated Synthesis

In 1965, Helmers published a method for the synthesis of cyclohexanone phthalide **239** through use of an enamine nucleophile (Scheme 74).[85] The enamine of cyclohexanone and morpholine **236** was reacted with phthaloyl chloride **185** under basic conditions to form intermediate **237** which subsequently cyclized to provide enamine product **238**. This enamine was then hydrolyzed under acidic conditions to afford a single product, alkylidene phthalide **239**.
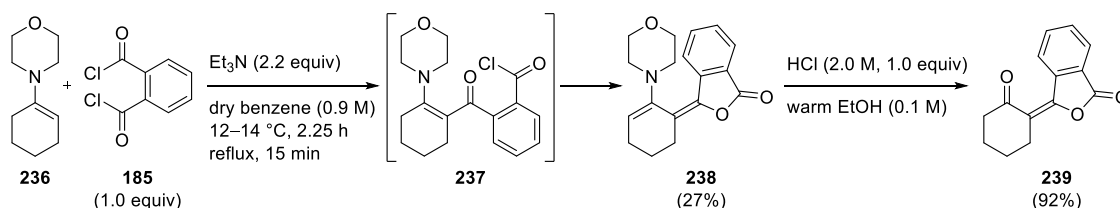
Scheme 74: Enamine mediated synthesis of alkylidene phthalide **239**

1.4.3.13 Conclusions on Alkylidene Phthalide Precedents

In Section 1.4.3, phthalides were introduced as an important class of compounds with different types of bioactivity and applications in synthesis.[70] Because of the interesting result obtained when reacting the enolate of propiophenone **186** with phthaloyl hydroxylamine **183** presented in Section 1.4.2, which generated alkylidene phthalide **187** (Scheme 75), it was of interest to find alternative syntheses for this class of compounds. These have been described in the previous sections and they included various methods involving metal catalysts, organocatalysts, photochemical reactions or more traditional methods such as Wittig reactions, dehydrations and enamine mediated transformations. From these, it was noted that our method using phthaloyl hydroxylamine **183** was novel and unique, and it provided moderate selectivity toward the *trans*-alkylidene phthalide **187**. Thus, we elected to optimize the transformation and to identify whether other electrophiles reacted in a similar manner.
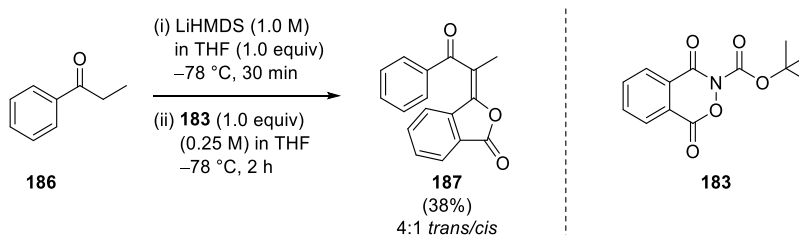
Scheme 75: Reaction of phthaloyl hydroxylamine **183** with enolates (initial result)

1.4.4 Optimizations

The ketone used for optimizations was 4'-methylpropiophenone **240** since it was less volatile than propiophenone **186**, which helped with reaction monitoring. Furthermore, the expected *E* and *Z*-products from the reaction with phthaloyl hydroxylamine **183** had been reported in the literature.[67] The first reaction involved treatment of 4'-methylpropiophenone **240** under the same conditions as propiophenone **186** (Scheme 75) to check conversion to the expected products and to obtain an isolated yield (Table 4, entry 1, 23% yield of alkylidene phthalide **241**). The result was encouraging, particularly as it was possible to identify all relevant signals in the ^{1}H NMR of the crude reaction mixture, obtaining a 30% overall conversion and a *E/Z* ratio of 5:1. The isolated yield of the major isomer **241** was within reasonable error of the observed conversion (23% yield, 25% conversion to major isomer **241**), while the minor isomer was not isolated.

Next, the equivalents of LiHMDS used were increased (entries 2–4); the best conversion was achieved when using 2.0 equivalents of base (entry 3, 79%). This result was consistent with the second deprotonation step suggested in the mechanism outlined in Scheme 60. An isolated yield of 62% for the major isomer **241** under these conditions confirmed that the ^{1}H NMR spectroscopic monitoring was a reliable method for following reaction progress (67% conversion to major product **241**).

Warming up the reaction to room temperature by removing the cooling bath after addition of the electrophile resulted in a decrease in conversion and *d.r.* (entry 4, 45%, *E/Z* 4.5:1), which suggested that there was a possible decomposition of reactive intermediates at higher temperatures, or that the process was reversible when allowing it to warm to room temperature. When leaving the reaction to run longer, a decrease in conversion was once again observed, perhaps due to decomposition of product after prolonged exposure to the basic reaction conditions (entry 5, 54%). Increasing the amount of phthaloyl hydroxylamine **183** to 2.0 equivalents returned a close to full conversion (entry 6, 95%). An isolated yield of the major isomer of 83% confirmed these reaction conditions to be optimal.

Table 4: Optimizations for the alkylidene phthalide methodology
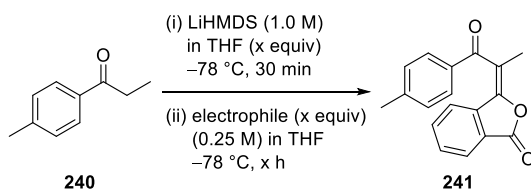
Entry	LiHMDS equiv	Electrophile (equiv, reaction time)	Conversion[a]	E/Z
1	1.0	**183** (1.0, 1 h)	30% (23%)	5:1
2	1.5	**183** (1.0, 1 h)	34%	5.5:1
3	2.0	**183** (1.0, 1 h)	79% (62%)	6:1
4	2.0	**183** (1.0, 1 h)[b]	45%	4.5:1
5	2.0	**183** (1.0, 5 h)	54%	6:1
6	2.0	**183** (2.0, 1 h)	95% (83 %)	5.5:1
7	2.0	**185** (2.0, 1 h)	n.d., (<5%)[c]	n.d.
8	2.0	**213** (2.0, 1 h)	not detected	n.d.
9	2.0	**242** (2.0, 1 h)	not detected	n.d.
10	2.0	**243** (2.0, 1 h)	not detected[d]	n.d.

[a] Conversion determined from the ^{1}H NMR spectrum of crude reaction mixture; isolated yield of major isomer shown in parantheses.
[b] Reaction allowed to warm up to room temperature after addition of **183** after which it was stirred for 1 h.
[c] Target compound could be observed but was not isolated by chromatography, <5% yield, purity n.d.
[d] Compound **244** was isolated in 49% yield (Scheme 76).

After optimizing the reaction between 4'-methylpropiophenone **240** and phthaloyl hydroxylamine **183** to generate alkylidene phthalide **241**, other electrophiles were also examined. First, phthaloyl chloride **185** was used as an electrophile under the optimized conditions, as it had been used previously as an electrophile to generate alkylidene phthalide **239** in the reaction with enamine **236** (Section 1.4.3.12).[85] Some of the major isomer **241** was observed in the ^{1}H NMR of the crude reaction mixture, but it was <5% conversion and it was not isolated (Table 4, entry 7). Other commercially available electrophiles such as phthalic anhydride **213** and *N*-methylphthalimide **242** were also used, but no product was detected by ^{1}H NMR analysis (entries 8 and 9).
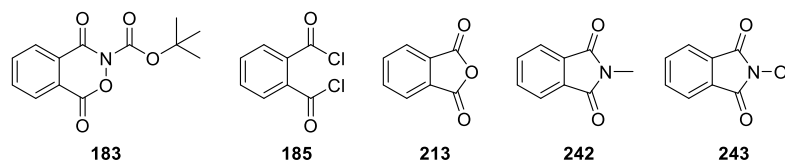
Figure 19: Electrophiles examined in the reaction with the enolate of **240**

An interesting result was obtained when using another custom made electrophile, *N*-methoxyphthalimide **243** (Table 4, entry 10). The usual alkylidene phthalide **241** was not observed, however another kind of product, diketone **244** (Scheme 76), was isolated in moderate yield (49%). Its structure was identified by a combination of techniques (NMR, IR, HRMS): the ^{1}H NMR spectrum showed an expected broad signal at 7.03 ppm which belonged to the amide, while H^a was a quartet coupled to the protons of the methyl group; the IR spectrum confirmed the presence of three carbonyl groups along with an N–H stretch (3339 cm^{-1}), while the ^{13}C NMR and HRMS were consistent with this structure. This suggested that the *in situ* generated enolate attacked one of the carbonyl carbons and broke the amide bond of *N*-methoxyphthalimide **243**, but once it formed intermediate **245**, the anion of *O*-methylhydroxylamine **246** was likely not a very good leaving group and diketone **244** was generated upon protonation and tautomerization of **245**. Another possibility was that *O*-methylhydroxylamine **246** was nucleophilic enough to ring open the alkylidene phthalide product **241** reversing the process, shifting the equilibrium toward intermediate **245**.
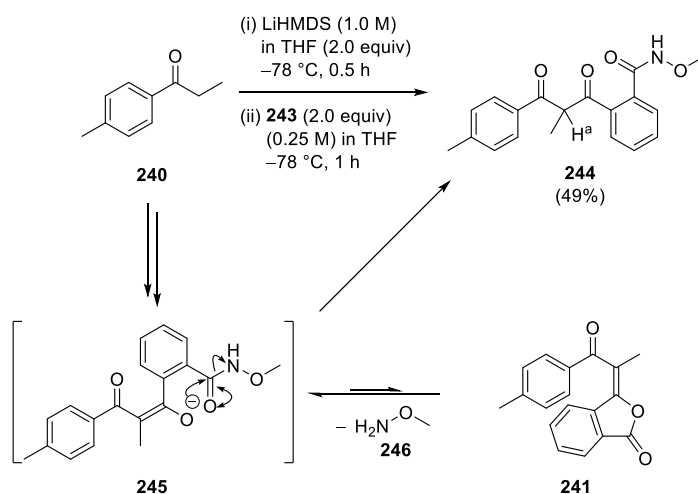
Scheme 76: Reaction between 4'-methylpropiophenone **240** and *N*-methoxyphthalimide **243**

After these findings during the optimization of this transformation, it was concluded that phthaloyl hydroxylamine **183** was a novel reagent in the synthesis of alkylidene phthalides from enolates. Furthermore, the reaction was optimized to provide alkylidene phthalide **241** in very high yield, maintaining a moderate diastereoselectivity.

1.4.5   Substrate Scope

After optimizing the alkylidene phthalide formation using 4'-methylpropiophenone **240**, the next step was to extend the scope of the reaction to different ketones (Table 5, page 58). In the postulated mechanism shown (Scheme 60, page 41), there are two possible configurations of the intermediate enolate formed, each of which exist in two resonance forms and can adopt two conformations prior to cyclization, which can provide access to the two isomers of the alkylidene phthalide (Scheme 77). Enolates **247**–**250** would lead to the *Z*-isomer **245**, while enolates **251**–**254** would form the *E*-isomer **246**. If the reaction were directed by steric factors, then having the aromatic ring of the ketone (Ar) pointing away from the bulk of the phthalide ring would be favorable, meaning that either enolates **247**–**250** would be preferred, leading to the *Z*-product **245**, or **253** and **254**, leading to the *E*-product **246**. A minimized dipole would have the oxygen atom of the starting ketone (blue) pointing away from the other heteroatoms of the molecule, and perhaps even on the opposite side of the new double bond (*i.e.* **251** and **252**), thus leading to *E*-product **246**. Another reason why enolates **251** and **252** could be favored is the possibility of a π-π interaction between the aromatic ring labeled Ar and the aromatic ring of the phthalide.[86] Given the possible conformations of the intermediates **251** and **252**, this proposed interaction could be either T-shaped (with the two aromatic rings perpendicular to each other) or parallel-displaced.[86a,87]
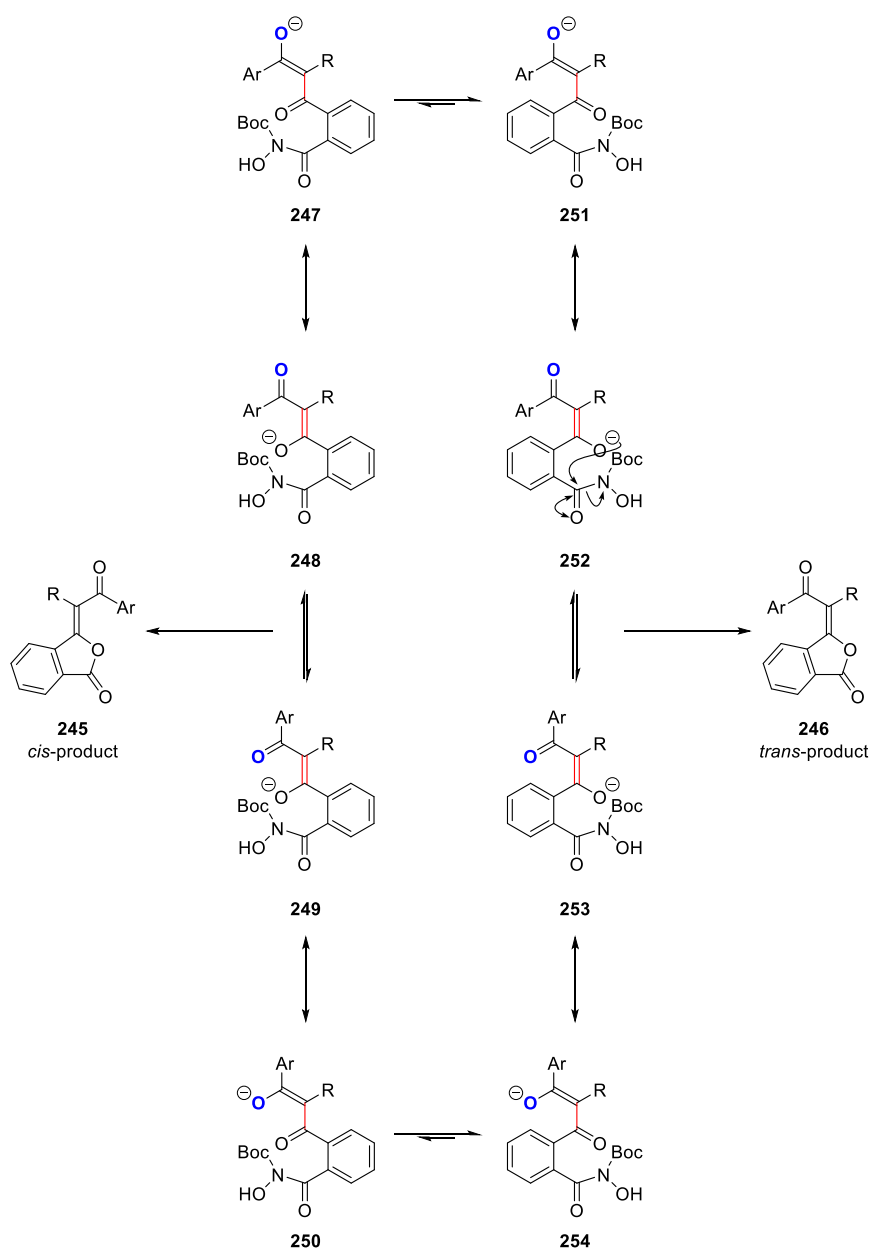
Scheme 77: Proposed cyclization of second enolate for the formation of alkylidene phthalides

In Section 1.4.4, the synthesis of alkylidene phthalide **241** was optimized to obtain the product in good yield and diastereoselectivity (83% yield, 5.5:1 *d.r.*, Table 5, entry 1). The diastereomeric ratio was determined by comparing the ^{1}H NMR spectrum of the reaction mixture to data from the literature,[67] and analysis of the ^{1}H NMR spectra used during the optimizations (Section 1.4.4). The identified singlets of the two methyl groups of the *trans*-isomer **241** (major) were 2.43 and 2.31 ppm (2.44 and 2.32 according to Mor),[67] while the singlets belonging to the minor isomer were 2.45 and 2.41 ppm (2.44 and 2.42 in the literature).[67] Furthermore, the *E*-diastereomer was less polar by silica gel chromatography for all of the substrates examined, a trend also observed by Mor.[67] The structure of *E*-alkylidene phthalide **241** was also confirmed by X-ray crystallography (Figure 20).
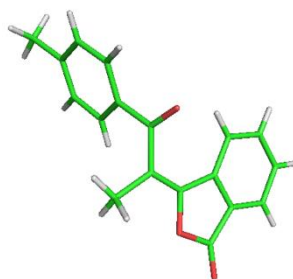
Figure 20: X-ray crystal structure of **241**

Two additional methylpropiophenones, 3'-methylpropiophenone and 2'-methylpropiophenone provided the *trans*-alkylidene phthalides **258** and **259** in moderate yield with erosion in diastereoselectivity relative to **241** (47% yield and 4:1 *d.r.* for **258**, 58% yield and 3.5:1 *d.r.* for **259**). This erosion in diastereoselectivity could be attributed to sterics in the proposed reactive enolate for the cyclization. This observation was based on the fact that having a methyl group in the *meta* position of the aromatic ring of the starting ketone would potentially disrupt a π-π stacking interaction in the proposed model more than a methyl group in the *para* position, and to a lesser extent than a methyl substituent in the *ortho* position.

When reacting a ketone without a substituent on the aromatic ring (*i.e.* propiophenone **186**), a slight erosion in stereoselectivity with little compromise in yield relative to 4'-methylpropiophenone **240** was observed (4.5:1 *d.r.*, Table 5, entry 4). This small difference could be attributed to the presence of an electron donating group (methyl) in the case of 4'-methylpropiophenone, which would potentially favor the conformations **251**–**252** of the enolate intermediate, thus diminishing free rotation about the highlighted bond (Scheme 77). This theory is also supported by the marginally higher *d.r.* for compound **260** bearing a methoxy group (6:1, entry 5) and the lower *d.r.* for alkylidene phthalide **261** (3:1, entry 6), which has an electron withdrawing –Br atom. The assignment of the stereochemical outcome for phthalides **187** and **260** was determined by comparing the ^{1}H NMR spectra of the reaction mixtures to literature values.[67] The diastereomeric ratio of alkylidene phthalide **261** was determined by analogy to the observed polarity trend (*E*-isomer less polar) and was unequivocally confirmed through an X-ray crystal structure (Figure 21), as well as isolation and X-ray crystallography of the minor isomer **298** from this transformation (Section 1.4.6.3).
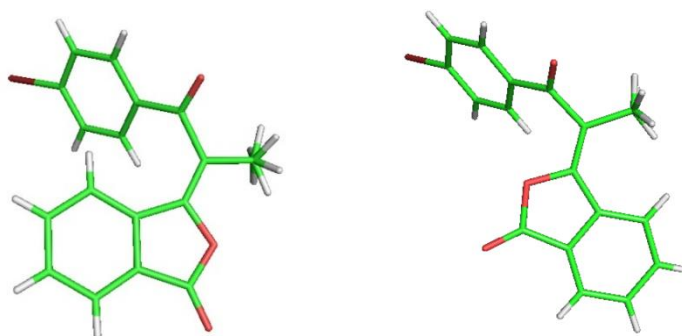
Figure 21: X-ray crystal structures of **261** (left) and **298** (right)

Alkylidene phthalide **232**, whose –R^2 group was a phenyl, was successfully synthesized in a moderate yield and diastereoselectivity (39%, 3:1 *d.r.*, entry 7). The lower yield and change in *d.r.* could be attributed to having a more sterically demanding starting ketone. Alkylidene phthalide **262** was isolated in a 47% yield and showed no significant change in selectivity in comparison with other products (5:1 *d.r.*, entry 8).

Table 5: Substrate scope

1.	2.	3.
241 (83%)[a]	**258** (47%)[a]	**259** (58%)[a]
E/Z 5.5:1[b]	*E/Z 4:1*[b]	*E/Z 3.5:1*[b]
4.	5.	6.
187 (76%)[a]	**260** (56%)[a]	**261** (41%)[a]
E/Z 4.5:1	*E/Z 6:1*	*E/Z 3:1*[b]
7.	8.	9.
232 (39%)[a]	**262** (47%)[a]	**263** (19%)[a]
E/Z 3:1[b]	*E/Z 5:1*[b]	*E/Z n.d.*
10.	11.	12.
264 (44%)[a]	**264** (43%)[a]	**264** (28%)[a]
E/Z 1:6[b]	*E/Z 1:1*[b,c]	*E/Z 1:3*[b,d]
13.	14.	15.
239 (63%)[a]	**265** (80%)[a]	**222** (77%)[a]
E/Z n.d.	*E/Z n.d.*	*E/Z 6.5:1*[b]
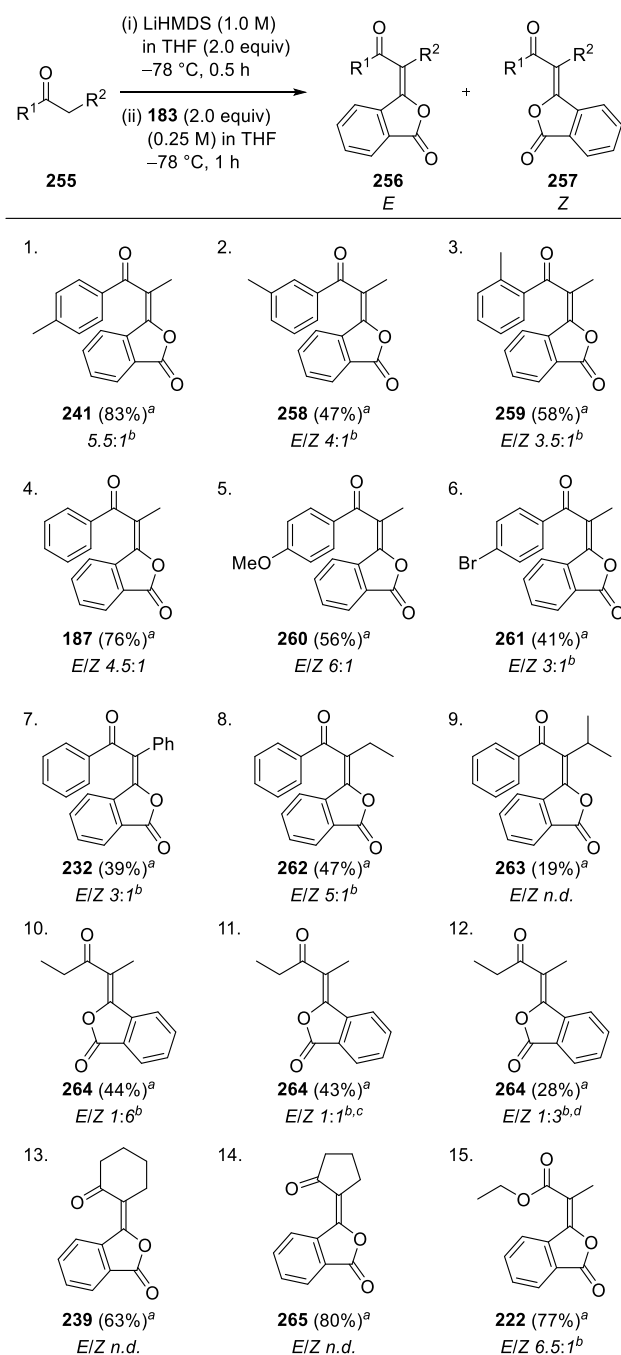
[a] Isolated yield of major isomer (shown).
[b] Ratio determined by ^{1}H NMR spectroscopy of crude reaction mixture.
[c] 23% *v/v* HMPA in THF used as solvent.
[d] Toluene used as solvent.

A very interesting substrate was isovalerophenone **266**, which provided alkylidene phthalide **263** in a low yield (19%, Scheme 78). While the *E/Z* ratio could not be determined by examination of the ^{1}H NMR of the crude reaction mixture, the lower yield could be

attributed to the steric requirements of the isopropyl substituent. However, it was even more interesting that it provided novel compound **267** (12%), which was identified *via* a combination of NMR techniques (^{1}H, ^{13}C, COSY, HSQC) along with HRMS data, to be the α-oxygenation product **267**. This result was rather unexpected considering that such a product was not observed for the other ketones. Its formation could be attributed to the increased steric requirements of the reacting carbon of the enolate, resulting in attack of the enolate carbon of the oxygen of phthaloyl hydroxylamine **183**.
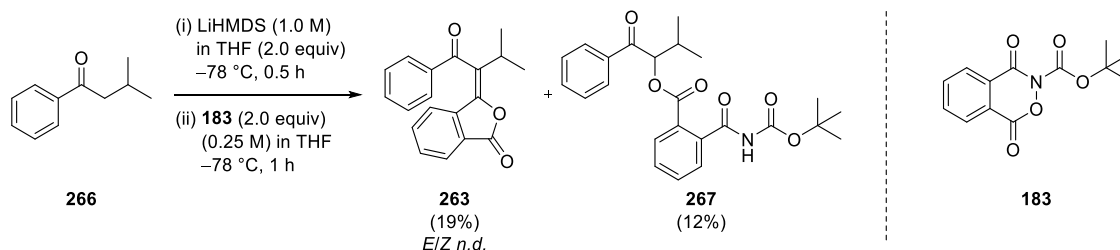
Scheme 78: Formation of a novel α-oxygenation product **267**

Another interesting substrate was 3-pentanone (Table 5, entries 10–12). Under standard reaction conditions, it showed a very intriguing reversal of diastereoselectivity (*E/Z* 1:6, entry 10), which was confirmed by X-Ray crystallography of the major diastereomer **264** (Figure 22). The reasoning behind this observed result could be based on steric hindrance, with enolates **268** and **271** being less hindered than enolates **272** and **275**, thus shifting the equilibrium toward enolates **268**–**271** shown in Scheme 79.
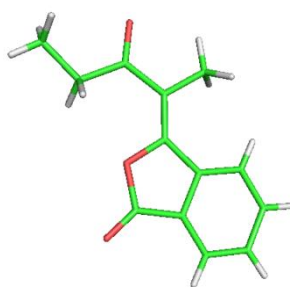
Figure 22: X-ray crystal structure of **264**

Changing the reaction solvent to toluene provided the product **264** with a *E/Z* ratio of 1:3 (entry 12), rendering the transformation less selective and less efficient (23% yield) than when using THF as a solvent. Addition of HMPA as a co-solvent altered this ratio even more significantly, resulting in a 1:1 *d.r.* (entry 11). It is known that enolate configuration plays an important role in nucleophilic addition to carbonyl groups such as the classical aldol reaction, where the stereochemistry of the product obtained is generally related to the enolate

geometry (*e.g.* Z-enolates providing *syn*-products).[88] The enolate configuration can be altered by using a different solvent medium or base, resulting in a change of stereochemical outcome in the product.[88c,89] There is a possibility that the favored models in this case would be **270** and **271**, similar to the Crimmins aldol reaction;[90] analogous to the literature precedents,[88c,89] and considering the results in Table 5 (entries 10–12), the stereochemical integrity of the enolate could have been altered by changing the reaction medium, although we have not unequivocally defined how we arrived at the products **264** and **230**.
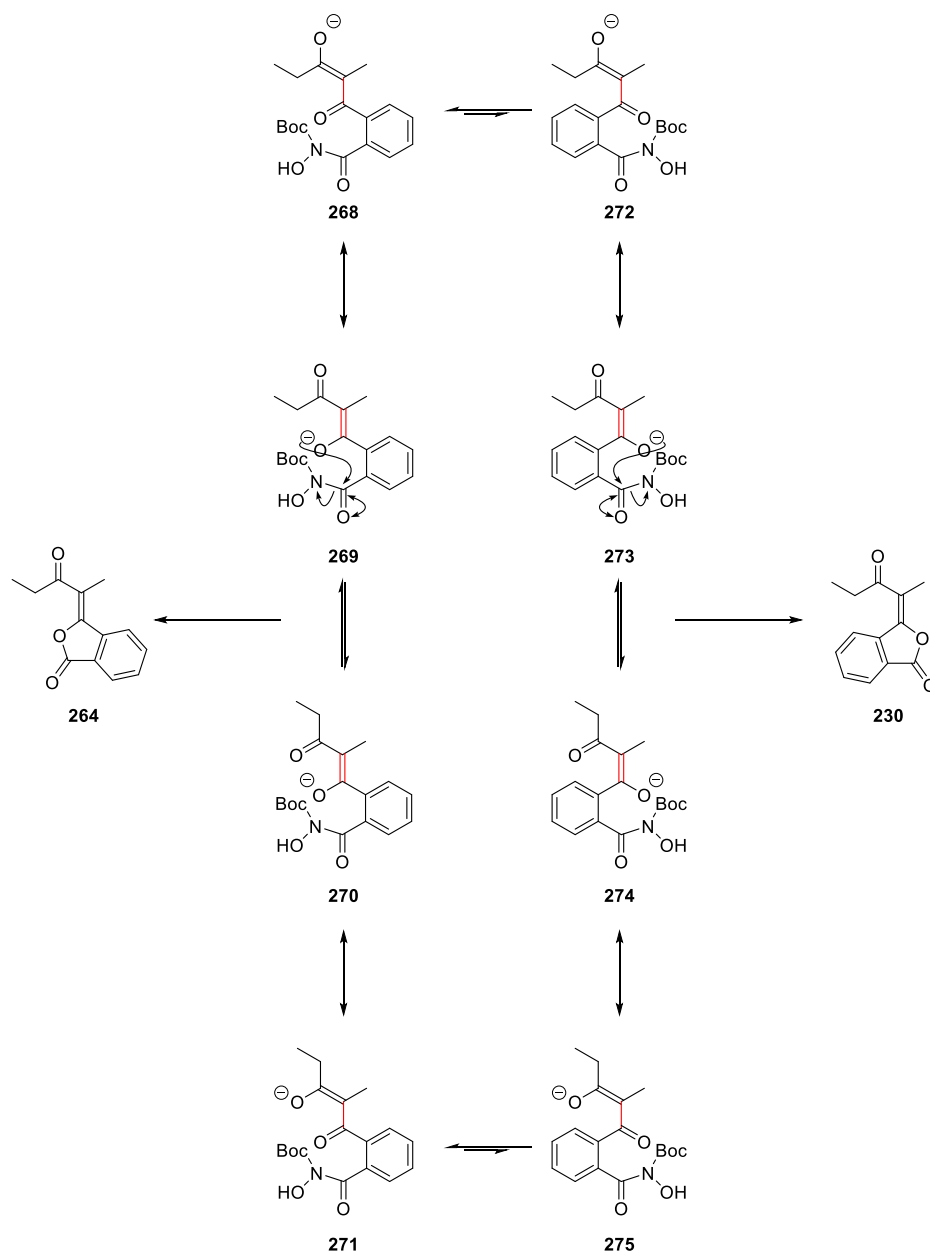
Scheme 79: Proposed mechanistic pathway for the formation of alkylidene phthalides **264** and **230**

Based on the behavior of 3-pentanone under the optimized reaction conditions, one would have predicted that reaction of ethyl propionate would result in the *cis*-isomer **276** as the major product (Table 5, entry 15). However, the product had the opposite diastereoselectivity, with the *trans*-isomer **222** predominating (*trans*:*cis* 6.5:1). If the proposed mechanism shown in Scheme 80 is correct, then it suggests that enolates **281**–**284** represent the preferred conformation of the intermediates.
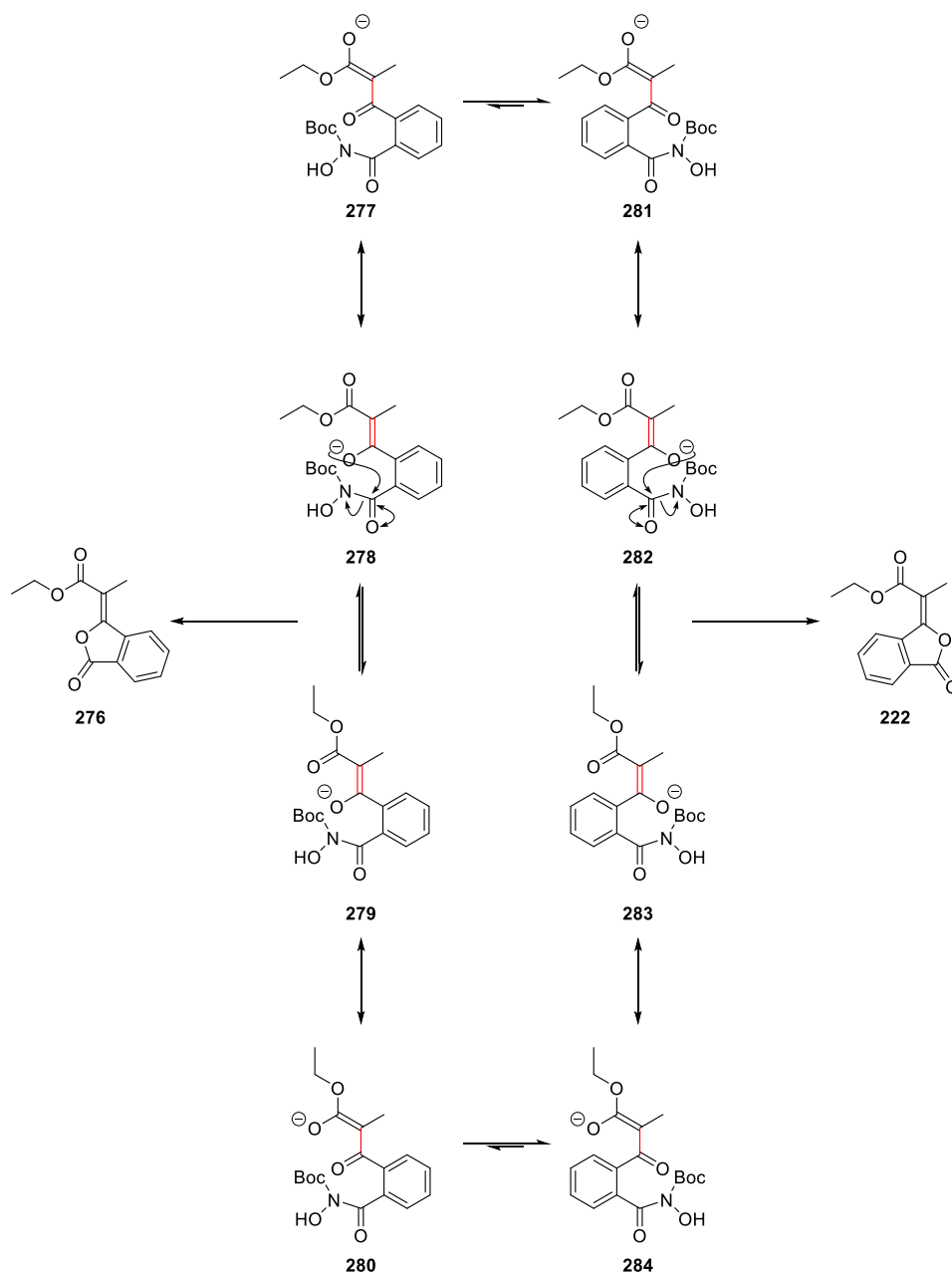
Scheme 80: Proposed mechanistic pathway for the formation of alkylidene phthalides **276** and **222**

Alkylidene phthalides **239** and **265** were identified as single products from the cyclic ketones cyclopentanone and cyclohexanone. As the *cis*-isomers of these products had not been reported in the literature, a *d.r.* could not be determined (Table 5, entries 13 and 14). No nOe signal was observed between the aliphatic ring protons and the aromatic ring protons for both alkylidene phthalides. This was consistent with the X-ray crystal structure of **265** which was the *trans*-isomer (Figure 23). By analogy, alkylidene phthalide **239** was also assigned as the *trans*-isomer. A mechanism is proposed in Scheme 81, whereby enolates **288** and **289** react preferentially to **286** and **287** due to a reduced steric interaction between the cyclopentanone ring and the aromatic ring, based on the isolated yields of the alkylidene phthalide **265** (80%).
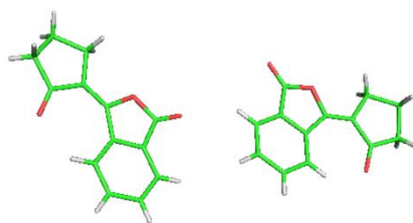
Figure 23: X-ray crystal structure of **265** (dimer)
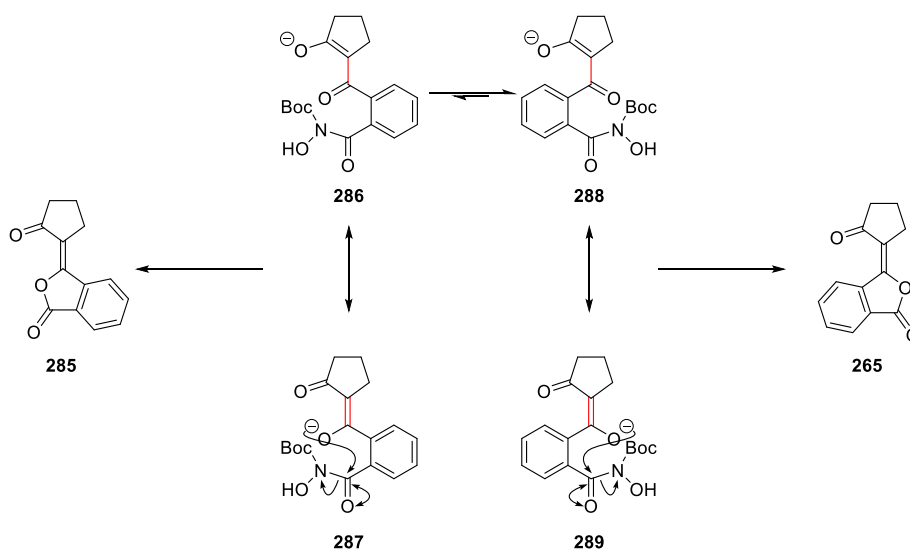
Scheme 81: Proposed mechanistic pathway for the formation of alkylidene phthalide **265**

Overall, the transformation was synthetically useful, providing access to a range of alkylidene phthalides in moderate to good diastereomeric ratios (with the *trans*-isomer preferred in the majority of cases). Furthermore, it provided a preliminary result toward a novel *α*-oxygenation process when using phthaloyl hydroxylamine **183** with a more sterically demanding nucleophile.

1.4.6 Reactions of Alkylidene Phthalides

Having developed a method for the formation of alkylidene phthalides using phthaloyl hydroxylamine **183**, it was of interest to find ways of functionalizing these compounds to understand their reactivity.

1.4.6.1 Reaction with Methylamine

First, it was of interest to react an alkylidene phthalide with a nucleophile. Methylamine was chosen as it was a small, non-sterically demanding molecule and a good nucleophile. It was expected that methylamine would open the phthalide of **241** to form diketone **290** (Scheme 82).
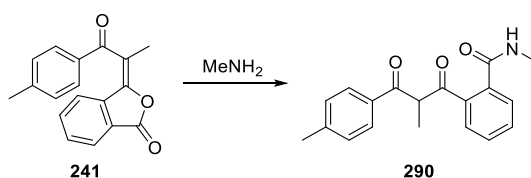
Scheme 82: Expected reaction of alkylidene phthalide **241** with methylamine

Reaction of **241** with a large excess of methylamine (80 equiv) led to *N,N'*-dimethylphthalamide **291** in 95% isolated yield (Scheme 83). It is expected that this transformation proceeded *via* diketone **290** which reacted again with methylamine to eliminate 4'-methylpropiophenone **186** (initial ketone), which was observed in the ^{1}H NMR spectrum of the crude reaction mixture.
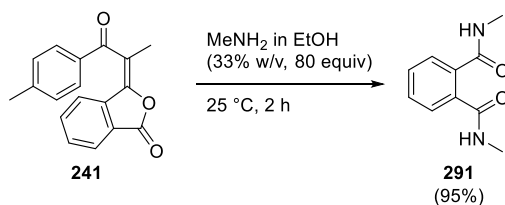
Scheme 83: Reaction of alkylidene phthalide **241** with methylamine

1.4.6.2   Epoxidations

Another reaction examined was the epoxidation of alkylidene phthalides, as it would generate two vicinal tetra-substituted sp[3] carbons. The first trial using *m*-CPBA was performed on alkylidene phthalide **241** (Scheme 84).[91] No product formed and >90% of the starting material was recovered upon work-up.
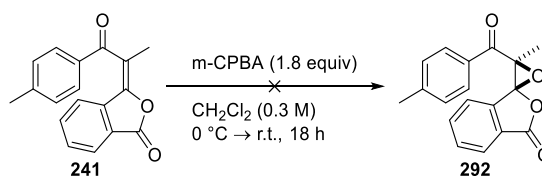
Scheme 84: Attempted epoxidation of alkylidene phthalide **241**

There was a possibility that alkylidene phthalide **241** was not reactive enough toward epoxidation with an electrophilic oxidant. However, it is known that allylic alcohols readily formed epoxides, with high H-bond directed stereocontrol.[92] A known transformation to selectively reduce α,β-unsaturated carbonyls to the corresponding allylic alcohol is the Luche reduction.[93] The reaction uses $NaBH_4$ in the presence of cerium chloride. Based on a recent literature protocol, a Luche reduction was carried out using alkylidene phthalide **241** (Scheme 85).[94] The product was formed in a low isolated yield (4%); however, the ^{1}H NMR spectrum of the crude reaction mixture was rather clean, with the main two components being alkylidene phthalide **241** and the Luche reduction product **293**.
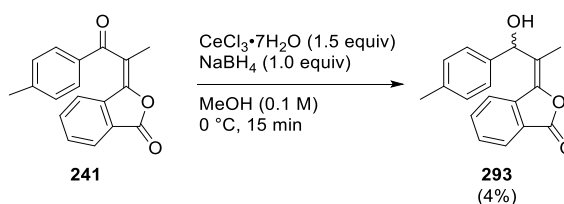
Scheme 85: Luche reduction of alkylidene phthalide **241** – initial result

After this initial result, a quick optimization of the reaction was performed (Table 6). Using 2.0 equivalents of the Luche reduction reagents provided a conversion of 40% after 15 min (entry 1), and no improvement in conversion was observed after allowing the reaction to run for a longer period. Increasing the equivalents of $CeCl_3 \cdot 7H_2O$ reduced the conversion to 24% (entry 3), while increasing the amount of sodium borohydride showed complete

consumption of the starting material and the Luche product was isolated in an excellent yield (95%, entry 4).

Table 6: Optimizations of Luche reduction
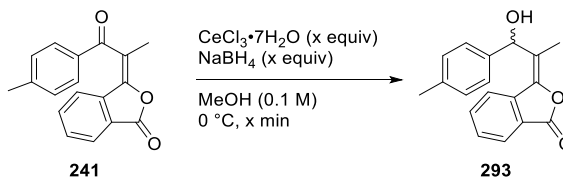
Entry	CeCl₃•7H₂O (equiv)	NaBH₄ (equiv)	Time (min)	Conversion (%)[a]
1	2.0	2.0	15	40
2	2.0	2.0	90	38
3	4.0	2.0	15	24
4	2.0	4.0	15	99 (95%)[b]

[a] Conversion determined by ^{1}H NMR spectroscopy.

[b] Isolated yield in parantheses.

The reaction was then performed on 1.0 mmol of the alkylidene phthalide **241** (five times the scale used for optimizations) and the Luche product **293** was obtained in a moderate yield of 60–70% (Scheme 86).
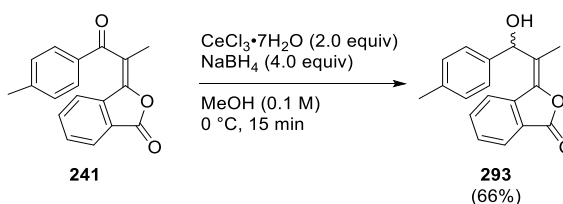
Scheme 86: Scale-up of Luche reduction

The next step was to perform an epoxidation on allylic alcohol **293**. It was known from Davies' paper that for acyclic allylic alcohols, the epoxide should form on the opposite face of the hydroxyl group.[92] An *m*-CPBA epoxidation using the conditions outlined in Scheme 87 was examined with allylic alcohol **293**, and epoxide **294** was isolated in good to excellent yields. This meant that a highly diastereoselective method to generate two vicinal tetra-substituted sp^3 carbons was found. At this stage, the structure of the epoxide could not be determined unequivocally, and any crystals grown of the product were not of sufficient quality to obtain an X-ray structure.
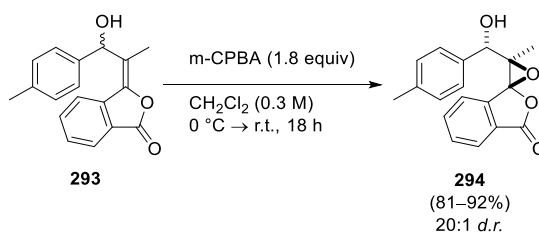
Scheme 87: *m*-CPBA epoxidation of allylic alcohol **293**

The hydroxyl group of epoxide **294** was acetylated using acetic anhydride (Scheme 88).[95] Epoxide **294** was treated with a slight excess of acetic anhydride and triethylamine using a catalytic amount of DMAP to afford epoxy acetate **295** in excellent yield (95%), as a single diastereomer. The relative configuration of the product was confirmed by X-ray crystallography (Figure 24).
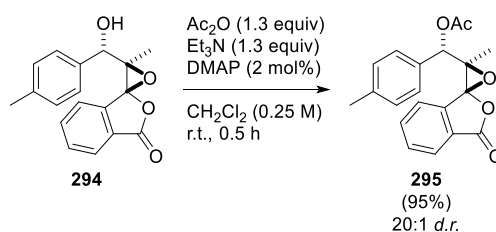
Scheme 88: Acetylation of hydroxyl group of epoxide **294**
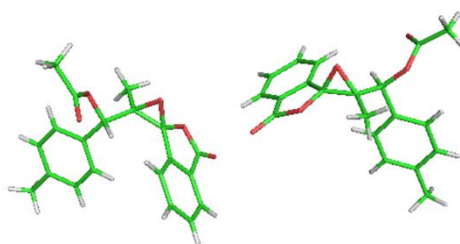
Figure 24: X-ray crystal structure of epoxide **294**

Based on Davies' work using allylic alcohols, it was known that protecting the free hydroxyl group with an acetate group could change the stereoselectivity of the epoxidation.[92] Thus, allylic alcohol **293** was acetylated under standard reaction conditions to afford **296** in good yield (Scheme 89).
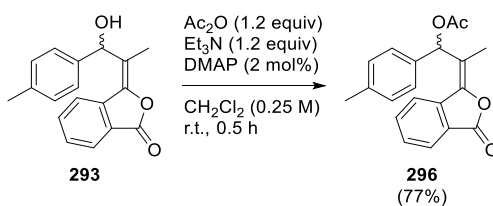
Scheme 89: Acetylation of allylic alcohol **293**

An *m*-CPBA epoxidation of alkene **296** was attempted using the conditions developed for the reaction of **293** (Scheme 90). Unfortunately, no product formation was observed by TLC after 5 h and >90% of the starting material was recovered. As a result, it was likely that alkene **296** was too sterically encumbered to allow epoxidation.
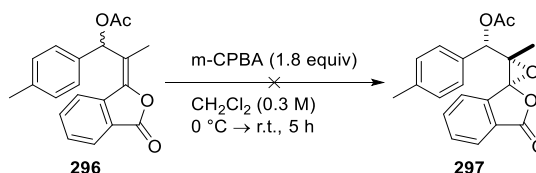
Scheme 90: Attempted epoxidation of alkene **296**

1.4.6.3 Alkylidene Phthalides under Acidic Conditions

All of the alkylidene phthalides were synthesized under strongly basic conditions, thus it was of interest to understand how they behaved under acidic conditions. A first attempt was made stirring alkylidene phthalide **241** in 1 M HCl (aq., Scheme 91). The compound was stirred as a suspension in HCl at 25 and 50 °C for one hour after which it was extracted with EtOAc to recover >95% of the starting material. Therefore, treatment with HCl under these conditions had minimal effect on the integrity of alkylidene phthalide **241**.
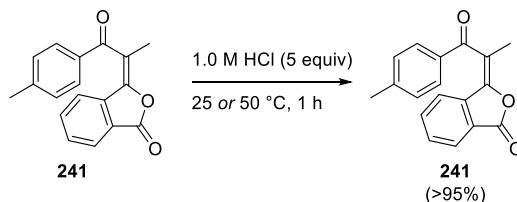
Scheme 91: Treatment of alkylidene phthalide **241** with 1.0 M HCl

In 2001, it was observed by Kundu that treatment of alkylidene phthalides with concentrated H_2SO_4 led to isomerization of the alkene double bond.[96] Thus, the conditions reported by Kundu were applied to alkylidene phthalide **261**. Treatment of alkene **261** with concentrated sulfuric acid provided a clean 1:3 mixture of the *E*- and *Z*-isomers **261** and **298**. The two isomers were separated and pure *Z*-alkylidene phthalide **298** was isolated in 65% yield. It is important to note that the 1:3 *E*/*Z* mixture represents the thermodynamic equilibrium under these conditions, the same ratio of 1:3 being observed after stirring *Z*-**298** in sulfuric acid for 18 h.
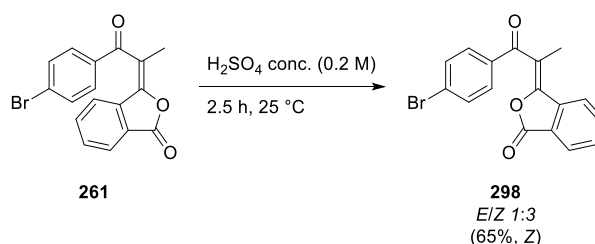
This method showed some potential for obtaining both diastereomers of the alkylidene phthalide products.

1.5   Conclusions

A series of hydroxylamine-based oxidants **115**–**117**, **183** and **184** (Figure 25), were synthesized and were reacted with several nucleophiles including alkenes, sulfides, amines and enolates. Alkenes and sulfides were unreactive under the conditions employed, amines transferred the –Boc or –Cbz groups, whereas enolates provided access to alkylidene phthalides as class of compounds.
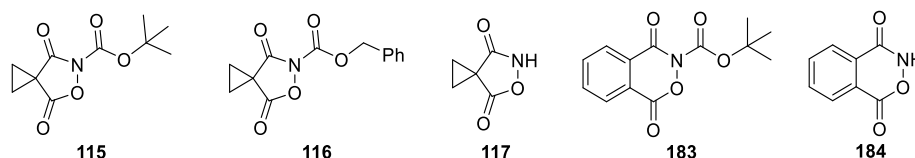
Figure 25: Hydroxylamine-based oxidants

Phthaloyl hydroxylamine **183** was effective for the synthesis of alkylidene phthalides **256** (Scheme 92). Phthalides are known to be highly appealing compounds due to their unique biological activity. Therefore, a novel transformation which provides access to this class of compounds could be of use.[70] The alkylidene phthalides generated (**256**) were isolated in yields ranging from 19–83% and with up to 6.5:1 diastereoselectivity. Furthermore, based on a single case, an α-oxygenation product could provide the pathway for other types of functionalization using these compounds. It was also shown that the alkylidene phthalides prepared could be isomerized under acidic conditions, providing access to both isomers of the compound. The selectivity observed in the transformation can also be altered by changing the polarity of the reaction medium.
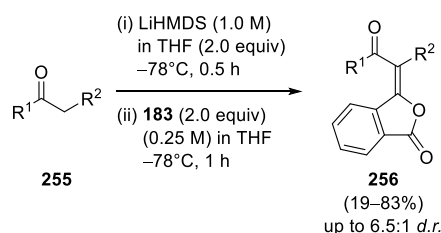
Scheme 92: General scheme for the synthesis of alkylidene phthalides **256**

Chapter 2: Baeyer-Villiger Oxidation under Payne Epoxidation Conditions

2.1 Introduction

The Baeyer-Villiger (BV) oxidation is a well-known transformation discovered in 1899 by Adolf von Baeyer and Victor Villiger.[58] It involves the insertion of an oxygen atom between a carbonyl carbon and a carbon in the α-position through the reaction of an aldehyde or ketone with a peroxy acid or a reactive peroxide (Scheme 93). A typical mechanism for the reaction using a generic peracid **300** as oxidant is shown in Scheme 94. First, the ketone **299** is attacked by the peracid **300** to form zwitterionic species **303**, which undergoes a proton transfer leading to Criegee intermediate **304**. This intermediate then undergoes rearrangement, to form the corresponding ester **301** and a carboxylic acid coproduct **302**.[59] The reaction exhibits a predictable regiochemistry, with typical migrating group (R^M) aptitudes, based on carbocation stability: tertiary alkyl > secondary alkyl > benzyl > phenyl > primary alkyl > methyl.[59,97] The reaction is also known to be stereoselective, occurring with retention of the migrating group stereoconfiguration.[59]
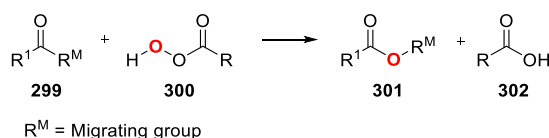
Scheme 93: Generic BV oxidation
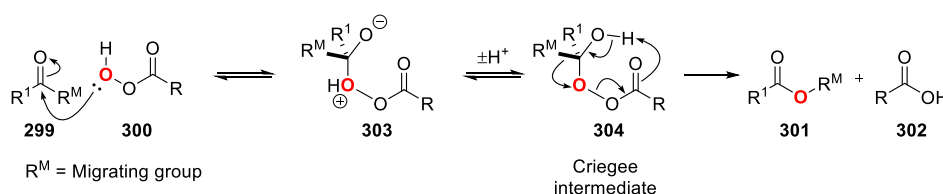
Scheme 94: Typical BV mechanism involving a peracid

Since its discovery, the reaction has become a reliable transformation in organic synthesis.[59,98] The reaction is reliant upon a source of peroxide, *m*-CPBA being one of the most commonly used reagents for this transformation.[99] However, according to Sheldon, it is desirable to use hydrogen peroxide as the oxidant due to its low cost, particular ease of handling, its high oxygen content and generation of water as a byproduct.[59] Hydrogen peroxide is also commercially available as an aqueous solution, an anhydrous urea complex (commonly known as H_2O_2•urea or UHP),[100] and as a sodium percarbonate salt amongst others.[101] Nevertheless, even though hydrogen peroxide has a number of applications in organic synthesis, it requires activation, or a highly reactive ketone in order for it to participate in the BV reaction.[59]

2.2 Methods for Activation in the Hydrogen Peroxide Mediated BV Reaction

There are multiple methods for catalyzing BV oxidations with H_2O_2. These activators (catalysts) can either activate the substrate (ketone) by lowering its LUMO, or they can activate the nucleophile (hydrogen peroxide) by forming a more reactive peroxide/peracid species *in situ*. These methods are presented in the following sections and they include metals, enzymes and organocatalysts.

2.2.1 Tin (Sn) Zeolites

One very efficient method for the BV oxidation using H_2O_2 as oxidant, published by Corma in 2001, involved the use of Sn-zeolite beta (composition: 1.0 SiO_2 : 0.0083 SnO_2 : 0.54 $[Et_4N]^+[OH]^-$: 7.5 H_2O : 0.54 HF) as catalyst (Scheme 95).[102] The method was very important as it showed enzyme-like selectivity toward BV reactions *versus* epoxidations, in spite of the low regioselectivity (2:1 regioisomeric ratio). This feature was achieved by ketone coordination to the Lewis acid center of the zeolite. Within the same research group, a mechanistic study on the transformation making use of ^{18}O isotopic labeling experiments have provided strong evidence toward ketone activation: the ^{18}O label was introduced at the carbonyl oxygen atom and it remained unchanged, suggesting a Criegee intermediate was present in the reaction mechanism.[103]
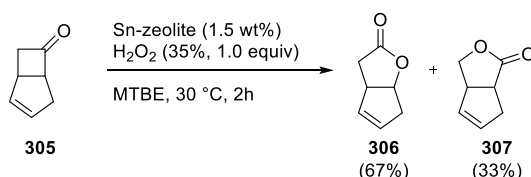
Scheme 95: BV oxidation using Sn-zeolite beta as catalyst

Relying on the benefits of this work (enzyme-like selectivity, high abundance of Sn), several other follow-up articles using surface based catalysts containing Sn have been published for this transformation.[104]

2.2.2 Selenium

Recently, Yu and coworkers have shown that organoselenium catalysts can form a highly reactive peroxide species **310** in combination with aqueous H_2O_2 (30 wt%) for the BV oxidation of α,β-unsaturated ketones (Scheme 96).[105] The reaction proceeds with retention of the *E*-configuration of the alkene to afford a series of vinyl ester products such as **309** in very good yields (up to 85%). Furthermore, the catalyst can be recycled with little compromise in yield for the transformation after a 2nd and 3rd run (79% and 77% yield, respectively).
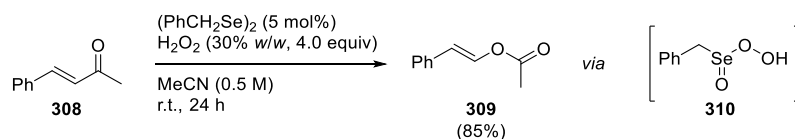
Scheme 96: BV oxidation using dibenzyl diselenide as catalyst

2.2.3 Rhenium

Another novel method for the BV oxidation published by Martins in 2013,[106] makes use of water-soluble oxorhenium complexes, such as **313**, as catalysts (Scheme 97). The reaction employs a remarkably low catalyst loading (0.001 mol%), but it exhibits low regioselectivity with mediocre conversions for a series of cyclic and acyclic ketones.
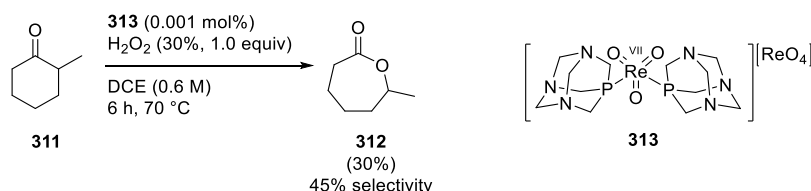
Scheme 97: BV oxidation using Re complexes as catalysts

2.2.4 Lithium and Calcium Borates

In 2012, Ishihara developed a method using lithium or calcium perfluorophenyl borates for selective BV oxidation with aqueous H_2O_2 as the oxidant (Scheme 98).[107] The method involves treatment of a series of ketones such as **305** with aqueous H_2O_2 (30 wt%) at room temperature using a catalytic amount of a lithium (or calcium) borate and oxalic acid as a co-catalyst. The reaction exhibited excellent selectivity and the catalyst mimics enzyme-like selectivity by forming the desired lactones **306** and **307** without potential epoxidation

products. Moreover, while this transformation is similar in terms of chemoselectivity to Corma's method involving Sn zeolites, it shows better regioselectivity (83:13 *versus* 67:33).[102]
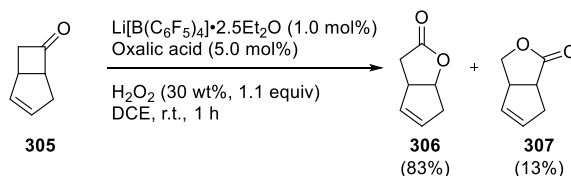
Scheme 98: BV oxidation using lithium borates

2.2.5 Platinum

Platinum has been used as a catalyst for BV oxidations for more than two decades.[108] However, perhaps the biggest breakthrough in Pt-catalyzed BV oxidations came in 1994 when Strukul *et al.* published an enantioselective method for prochiral ketones using chiral Pt complexes.[109] The *ee*s observed were up to 58%), but they have improved (up to 89% for 4-*tert*-butylcyclohexanone **314**) in more recent years (Scheme 99).[110] Yields were substrate dependent, with cyclobutanones performing better than cyclohexanones due to a relief of ring strain that makes the reaction favored. The transformation is applicable to a broad range of ketones and it involves the use of a chiral Pt-phosphine catalyst **316**, a surfactant (sodium dodecyl sulfate, SDS) and 1.3 equivalents of H_2O_2 (35 wt%, aqueous).
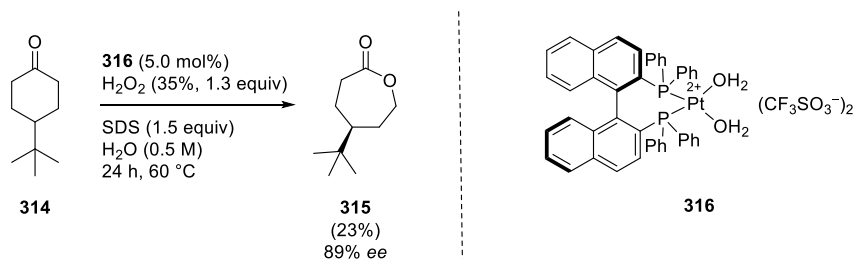
Scheme 99: Enantioselective BV oxidation using Pt complexes

2.2.6 Palladium

Another enantioselective method for the BV oxidation was published by Malkov in 2008.[111] The method was applied to a series of 3-substituted cyclobutanones such as **317**, providing the desired lactone products **319** in high yields (generally >90%) and excellent enantioselectivities (up to 81% *ee*) *via meso*-desymmetrization of the starting ketones

(Scheme 100). The active catalyst was generated *in situ* by premixing the palladium source with the ligand **318** and additive AgSbF$_6$ to form an active complex such as [ligand **318**][Pd(SbF$_6$)$_2$]. While the method is excellent for the substrates described, the only potential disadvantage is that its applicability was only shown for 3-substituted cyclobutanones.
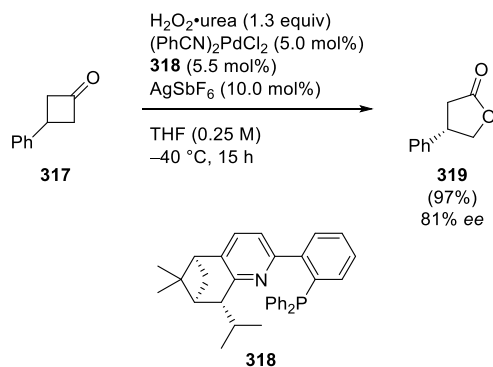
Scheme 100: Enantioselective BV oxidation using Pd complexes

2.2.7 Zirconium

A report by Katsuki showed that Zr(salen) complex **320** can catalyze the BV oxidation of prochiral ketones to provide the lactone products with excellent enantioselectivity (Scheme 101).[112] The method was only applied to five different ketones, resulting in highly enantioenriched lactone products (81–94% *ee*), and involved the use of urea hydrogen peroxide (UHP) as an oxidant.
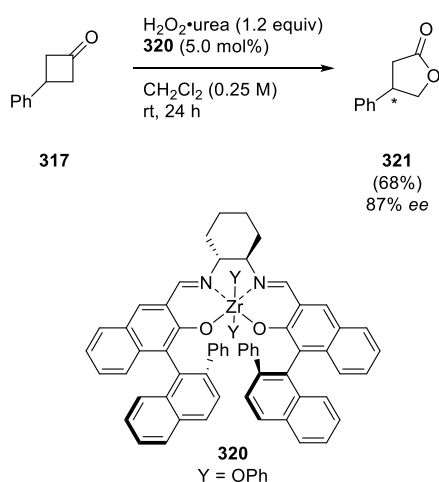
Scheme 101: Zr(salen) catalyzed enantioselective BV oxidation

Zr catalyst **320** was further examined by the same research group on racemic ketones to form a series of lactones with unexpected regioselectivity, given that the BV oxidation occurred mainly on the least substituted carbon (Scheme 102).[113] The method was highly enantioselective (up to 99% *ee*), preferentially converting one enantiomer of the starting ketone **305** to **306** and the opposite enantiomer to lactone **307**. Furthermore, the method was chemoselective toward BV oxidation *versus* epoxidation.
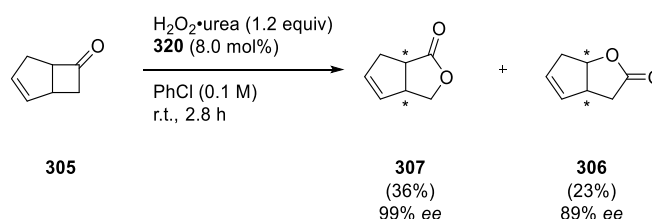
Scheme 102: Zr(salen) catalyzed BV oxidation of racemic ketones

2.2.8   Enzymes and Ionic Liquids

A green, metal-free method for activating urea hydrogen peroxide using enzyme Novozym-435 (25 mg for 0.5 mmol of substrate) was published by Olivo in 2007 (Scheme 103).[114] The procedure involved treatment of a series of cyclohexanone derivatives such as **322** with peracetic acid **324**, generated *in situ via* a lipase-mediated perhydrolysis of ethyl acetate, to form a series of lactones such as **323**. The method showed exclusive chemoselectivity toward ketones, regioselectively forming the lactone on the most hindered side of the ketone, but had very long reaction times (1–26 days).
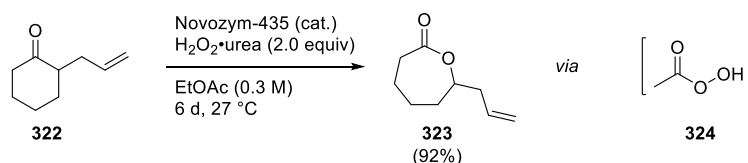
Scheme 103: Novozym-435 catalyzed BV oxidation

While the method described above was slow, a more recent piece of work by Arends has shown a way to improve reaction times for the transformation.[115] The method used the same enzyme at the same loading, but used a different source of hydrogen peroxide (H_2O_2 50%, aqueous) and a different reaction medium, ionic liquid (IL) **326**. The reaction proceeded *via* a similar peracid **328** which was generated *in situ*, but the reaction times were significantly lower (5 h).
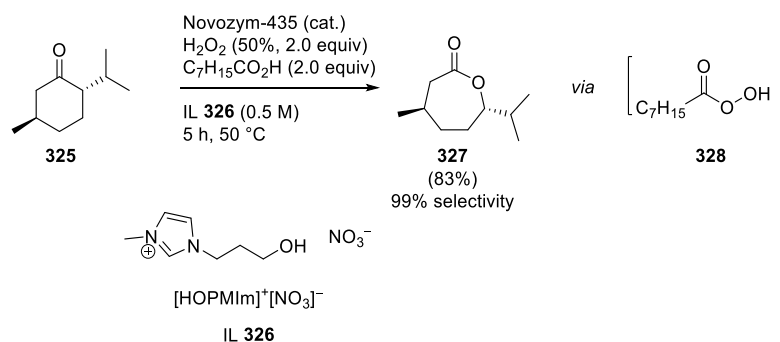
Scheme 104: Novozym-435/ionic liquid mediated BV oxidation

2.2.9 Carboxylic Acids

In 2008, Miller found a method for activating hydrogen peroxide using carboxylic acids (Scheme 105).[116] The method involved the *in situ* formation of a peracid **331** which reacted with ketone **329** to form the desired lactone **330** in very high yield (up to 96%). Furthermore, a peptide based catalyst **333** led to preliminary results for an enantioselective process (Scheme 106). However, there was room for improvement because of the high catalyst loading and the very large molar equivalents of H_2O_2 and additive (DIC).
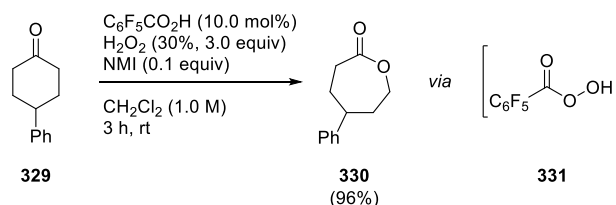
Scheme 105: Carboxylic acid mediated BV oxidation
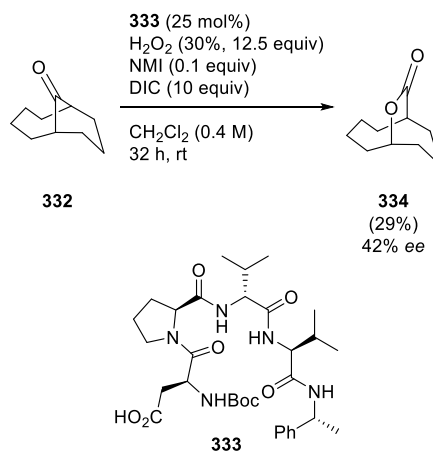
Scheme 106: Enantioselective BV oxidation catalyzed by peptides

Based on their initial result, Miller *et al.* in 2014, developed an enantioselective method for the BV oxidation of cyclic ketones bearing amide, urea and sulfonamide groups (Scheme 107).[117] The catalyst **336**, used for the activation of hydrogen peroxide, was similar to **333**, and the reaction proceeded under mild conditions, by selective BV oxidation of one enantiomer of ketone **335**. The transformation was regioselective, the main product **338** being formed with high enantioselectivity (94% *ee*, 43% conversion).
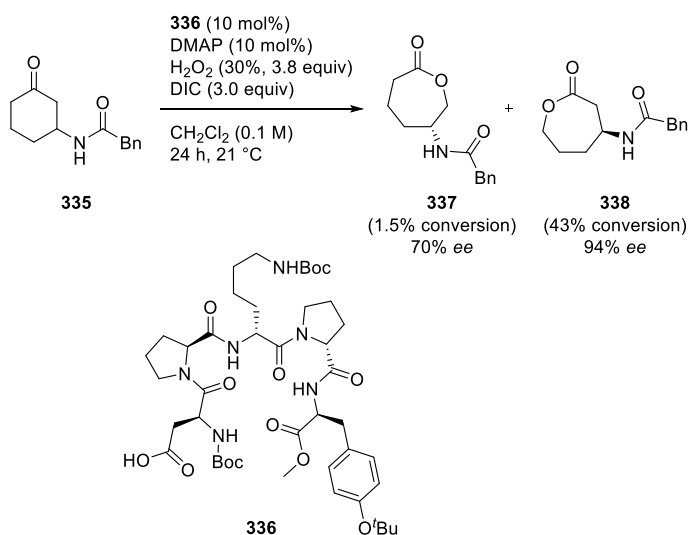
Scheme 107: Peptide catalyzed enantioselective BV oxidation of functionalized cyclic ketones

2.2.10 Phosphoric Acids

In 2008, Ding published a method in which chiral phosphoric acids were used as catalysts for the enantioselective BV oxidation of 3-substituted cyclobutanones with aqueous H_2O_2.[118] The optimal reaction conditions used 10 mol% of an H_8-binol-derived phosphoric acid **339** in the reaction of ketones, such as **317**, with 1.5 equiv aqueous H_2O_2 (30%). The reactions had excellent yields (generally, 99%) and proceded with very good enantioselectivity (up to 93% *ee*), the only limitation of the transformation being the exclusive applicability to cyclobutanone substrates.
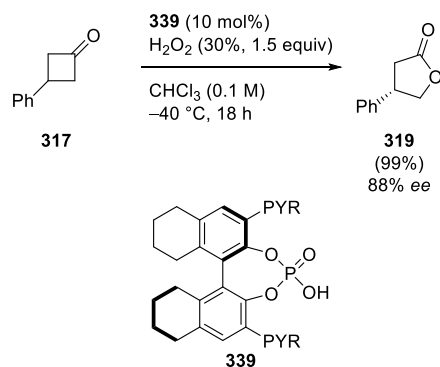
Scheme 108: Enantioselective BV oxidation catalyzed by chiral phosphoric acids

2.2.11 Flavins and Bisflavins

Another metal-free method for the activation of H_2O_2 was discovered by Furstoss in 1996.[119] The method made use of flavin **340** as a hydrogen peroxide activator to form active peroxide species **341** (Scheme 109). This active species then reacted with a series of cyclic ketones such as **305** to form the desired lactones in high yields. Moreover, this catalyst showed chemoselectivity toward BV oxidation over epoxidation.
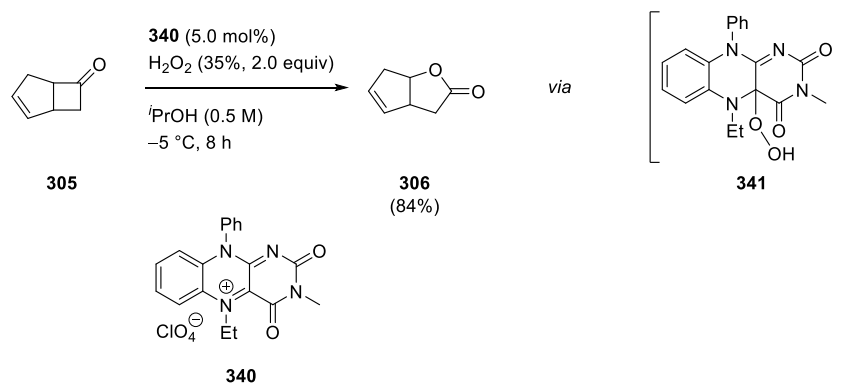
Scheme 109: Flavin catalyzed BV oxidation

Furstoss suggested that their catalytic method for the BV oxidation could be the starting point of an enantioselective transformation.[119] This was achieved by Murahashi *et al.* in 2002 by synthesizing bisflavin **342** and using it as an organocatalyst for the BV oxidation of cyclobutanones, such as **317** (Scheme 110).[120] A generic example is shown below with cyclobutanone derivative **317** being treated with aqueous H_2O_2 (30%). The reaction was the first metal-free enantioselective BV oxidation, achieving moderate yields (up to 67%) and enantioselectivity (up to 74%), while also having long reaction times (6 days).
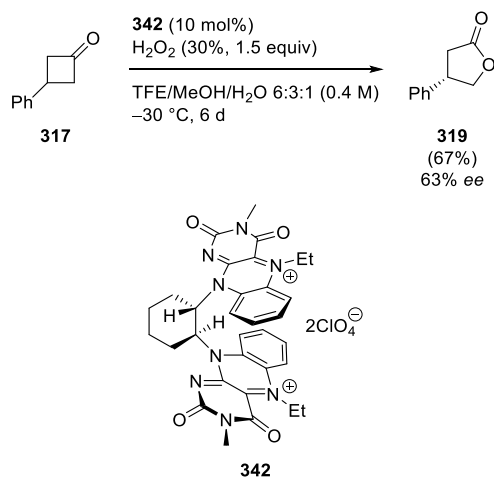
Scheme 110: Enantioselective BV oxidation using bisflavins as organocatalysts

2.2.12 Conclusions on H_2O_2 Mediated BV Oxidation using Catalysts

The Baeyer-Villiger oxidation is a well established organic transformations in the literature which converts a ketone to the corresponding ester or lactone. In the development of such transformations, one should aim toward an atom efficient, safe and "green" oxidant.[59] Hydrogen peroxide (H_2O_2) matches these criteria and, for that reason, extensive studies have been performed to identify methods of activating either the carbonyl substrate (Lewis acids and Brønsted acids) or the peroxide. Some of these methods have been discussed in the previous sections. Furthermore, these catalysts can not only perform the BV oxidation successfully, but they have also shown interesting features such as chemoselectivity, improved regioselectivity, enantioselectivity, or enzyme-like levels of selectivity. Ideally, one would use a relatively cheap, commercially available catalyst/activator to promote the BV reaction such as a hydrogen bond donor, or would form a peracid *in situ*.

2.3 Payne Epoxidation

The Payne epoxidation was introduced in Section 1.3.4 in an attempt to generate a class of imidoperoxides **102** (Figure 26).[50] Payne's method was used for the epoxidation of alkenes *via* an *in situ* generated peroxy imidic acid **136**. While the original method involved the use of benzonitrile or acetonitrile as a solvent, Ji *et al.* showed that the nitrile could be used as a reagent instead of the solvent (Section 1.3.4).[51]
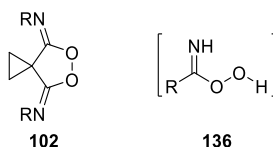
Figure 26: Generic imido peroxide **102** and peroxy imidic acid **136**

2.3.1 Applications of Peroxy Imidic Acids

Peroxy imidic acids are well-known in the literature since their original discovery. Interestingly, despite the extensive chemistry developed involving the intermediacy of these species, they have never been isolated. Along with Ji's methodology on the epoxidation of a series of alkenes, this section will present additional applications of peroxy imidic acids in synthesis.

In 2013, Sugai used Payne epoxidation in total synthesis.[121] The epoxidation was used as one of the synthetic steps toward a precursor of natural product laninamivir **345** (Scheme 111). The procedure used acetonitrile as a solvent and a large excess of aqueous H_2O_2 (16 equiv) under basic conditions, to provide the *cis*-epoxidation product **344**. It must be mentioned that the obtained ratio between the all-*cis* and the *trans*,*cis*,*trans*-products was 2:1, but the minor diastereomer could not be separated from the alkene starting material **343**.
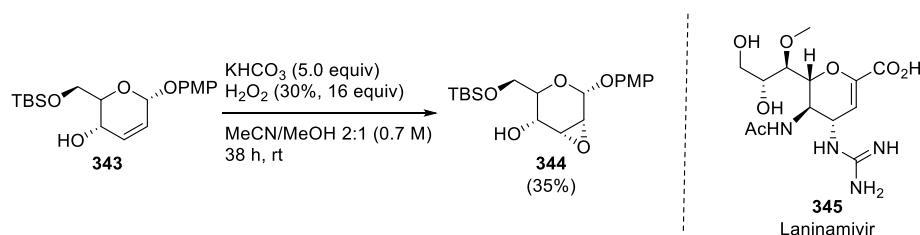
Scheme 111: Application of Payne epoxidation in total synthesis

In 1998, Frank observed a very interesting stereoselectivity when using Payne's conditions to epoxidize terpinen-4-ol **346** (Scheme 112).[122] The reaction involved treatment of terpinen-4-ol **346** with a slight excess of aqueous H_2O_2 using $KHCO_3$ as base and MeCN as a reagent to provide epoxide **347** in excellent yield. The transformation could be performed on a kilogram scale, retaining the enantiomeric excess of the starting material. More impressive was the resulting diastereoselectivity, which the author attributed to the directing capability of the free hydroxyl group of alkene **346** through hydrogen bonding (Figure 27, transition state **TS1**).
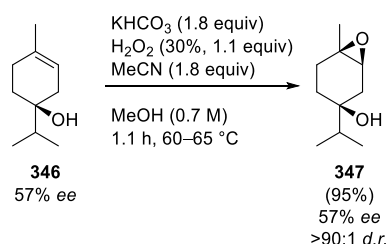
Scheme 112: Highly diastereoselective Payne epoxidation of terpinen-4-ol **346**
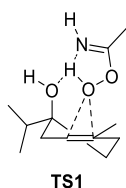
Figure 27: Proposed transition state **TS1** for the –OH directed Payne epoxidation of terpinen-4-ol **346**

Payne's epoxidation conditions have been used for enantioselective Shi epoxidations of olefins.[123] The reaction employed a Payne type oxidant using a base (K_2CO_3), acetonitrile and aqueous hydrogen peroxide in comparison with the original peroxide source, oxone®.[124] The catalyst **349** is a ketone used to generate a chiral dioxirane **351** *in situ*, which was suggested as the active agent for epoxidation. Treatment of a series of alkenes such as **348** provided the desired product **350** in moderate to high yields (61–93%) and excellent enantioselectivity (82–96% *ee*).
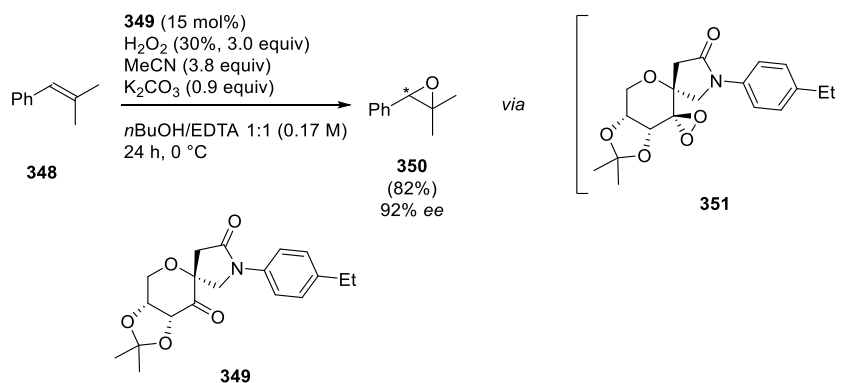
Scheme 113: Shi epoxidation using Payne's conditions

A Payne-type system for the asymmetric oxidation of *N*-sulfonyl imines has been recently developed by Ooi for the enantioselective formation of oxaziridines (Scheme 114).[125] The reaction made use of a chiral super-base organocatalyst **353** (labeled as P* in the catalytic cycle), which can deprotonate hydrogen peroxide, facilitating its reaction with trichloroacetonitrile (Cl₃CCN) to form peroxy imidate **355**. The peroxy imidate **355** was the postulated reactive species that attacked the *Re*-face of the imine, the stereochemistry being induced by the chiral counterion (protonated base), to form intermediate **356**. This intermediate then cyclized to form oxaziridine **354**, releasing the imidate anion **357** which, *via* protonation, formed the coproduct trichloroacetamide **358** and regenerated the active catalyst **353**.
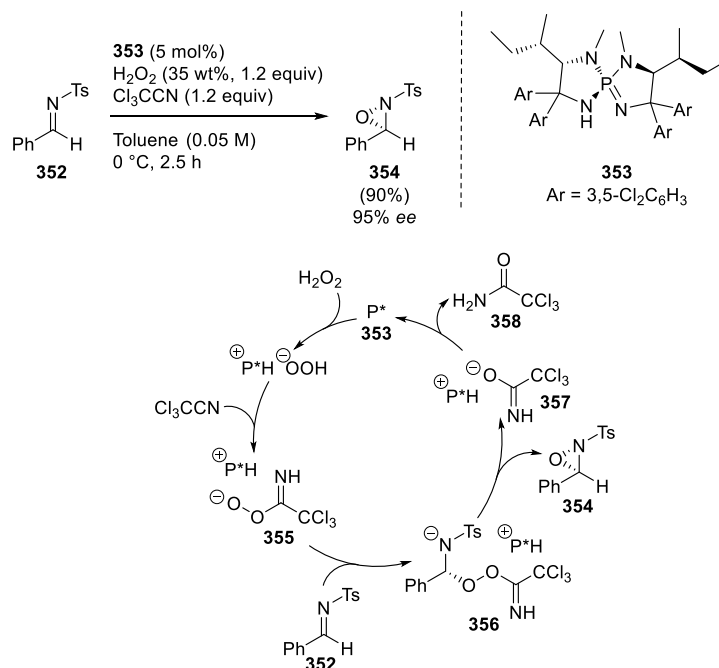
Scheme 114: Organocatalytic formation of oxaziridines using a Payne-type system

2.3.2   BV Oxidation using Payne Epoxidation Conditions

In 2006, Ruiz was the first to use Payne's system with H_2O_2/nitriles for a Baeyer-Villiger oxidation of cyclohexanone.[126] Therein, a series of hydrotalcites (HTs), which are surface based catalysts, were examined and it was determined that HT-Sn2 ($Mg_{0.650}Al_{0.325}Sn_{0.025}(OH)_2(CO_3)_{0.115} \cdot 0.65 H_2O$) was the most efficient. The reaction was performed using excess aqueous H_2O_2 and excess PhCN (which also served as solvent). The method was extended afterward to a series of substrates for the BV oxidation, showing the synthetic applicability of these Mg/Al hydrotalcites as catalysts.[127]
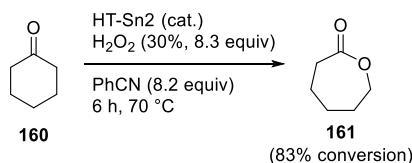
Scheme 115: Payne-type BV oxidation of cyclohexanone **160** using HT-Sn2 as catalyst

After this initial finding, another method for the BV oxidation using $Mg(OH)_2$ and MgO catalysts was developed within the same research group (Scheme 116).[128] The catalysts were obtained by calcination in the air at a very high temperature of 600 °C. The most reactive of

these catalysts was obtained by precipitation from $Mg(NO_3)_2 \cdot 6H_2O$ over a Na_2CO_3 solution kept at pH 10 with KOH (1 M). The reactions were examined using cyclohexanone **160** as a substrate, excess hydrogen peroxide, excess PhCN, a surfactant (SDBS, sodium dodecylbenzene sulfonate) and an unspecified volume of solvent. Moreover, the authors suggested that the addition of MeOH helped the transformation by increasing the miscibility of the aqueous and organic phases.
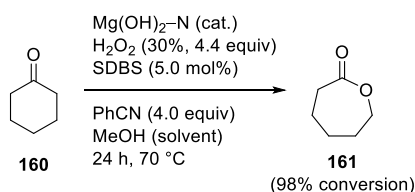
Scheme 116: $Mg(OH)_2$–N/DBS catalyzed BV oxidation using Payne type conditions

A mechanism for the transformation was proposed (Scheme 117). In the first step, H_2O_2 is deprotonated by the catalyst to form a hydroperoxy anion that adds to benzonitrile to form the active peroxy imidic acid **360**. In the second step, cyclohexanone is activated by the surface of the catalyst, facilitating the nucleophilic attack of peroxy imidic acid **360** to form the Criegee intermediate **361**. This intermediate then rearranges to form ε-caprolactone **161** and the coproduct, benzamide **362**.
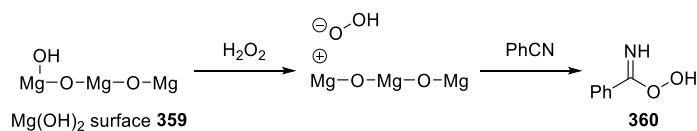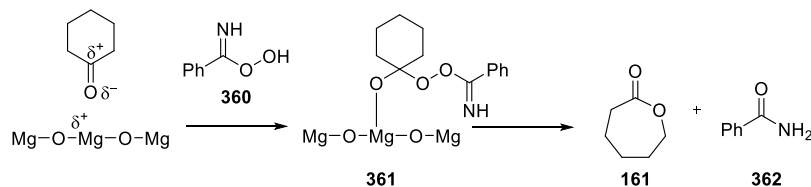
Scheme 117: Proposed mechanism for the $Mg(OH)_2$ mediated BV oxidation

The same group gained further insight into the transformation by using a different Mg/Al HT ($Mg_{0.80}Al_{0.20}(OH)_2(CO_3)_{0.10} \cdot_{0.72} H_2O$) **363** as catalyst and SDBS as a surfactant (Scheme 118).[129] The reaction also required 2.0 equivalents of H_2O_2 and excess benzonitrile (which acted as solvent), providing a range of lactones from their corresponding ketones. Another important fact is that the reaction could be performed in an organic solvent such as MeOH, albeit the best performance was shown in benzonitrile.
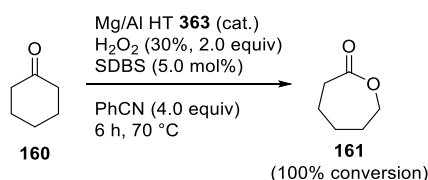
Scheme 118: Mg/Al HT **363** catalyzed BV oxidation using a Payne-type system

All of the results obtained by Ruiz have shown that a BV oxidation using Payne epoxidation conditions is achievable.[126,127,128,129] These novel methods made use of surface-based catalysts, which require specialized conditions and knowledge for their synthesis. In addition, the reaction generally used benzonitrile as a solvent. Thus, it was encouraging to pursue a BV oxidation project starting from our observed conditions to establish if Payne methodology could also be applied to a homogeneous BV oxidation (Section 1.3.4).

2.4   Optimizations

Based on the initial result in MeOH (Scheme 119) and on the encouraging results from Ji and Ruiz, our initial aim was to optimize the reaction conditions.[51,126,127,128,129] Our starting point involved treating cyclohexanone **160** with a catalytic amount of KHCO$_3$ (0.2 equiv) as base, H$_2$O$_2$•urea (6.0 equiv) as a source of hydrogen peroxide and benzonitrile (6.0 equiv), in MeOH (0.5 M) to afford ε-caprolactone **161** in 38% conversion by ^{1}H NMR spectroscopy. Most of these optimizations were performed by Ms. Tyne Bradley (Table 7).[130]
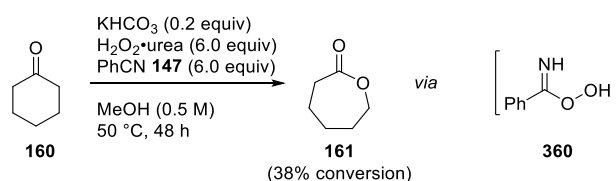
Scheme 119: Initial result for the BV oxidation using Payne epoxidation conditions (Tyne Bradley)

The initial result in MeOH was repeated in CD$_3$OD to facilitate ^{1}H NMR monitoring of the reaction. Pleasingly, 38% conversion was noted after 48 h, the same as the initial result (Table 7, entry 1). This was encouraging because it meant the optimizations that followed could be performed in CD$_3$OD. Increasing (30%, Table 7, entry 2) or decreasing (33%, Table 7, entry 3) the reaction concentration showed lower conversion under the conditions examined. The temperature was varied and, as expected, performing the reaction at 25 °C provided a lower conversion (14%, entry 4) and only a slight increase was observed by performing the raction at reflux (44%, entry 5). Decreasing the equivalents of H$_2$O$_2$•urea had a negative effect on the transformation (25% conversion, entry 6), while the addition of 10 equivalents of the oxidant improved conversion (47%, entry 7). While this large excess showed a better conversion, the nitrile was consumed to afford benzamide **362** via a Radziszewski reaction.[54,130] Changing the hydrogen peroxide source to aqueous H$_2$O$_2$ (30%) resulted in a decrease in conversion after 48 h (31%, entry 8). Decreasing the amount of benzonitrile (entries 9 and 10) or introducing an electron donating group (entry 11) or an electron withdrawing group (entry 12) on the aromatic ring of the nitrile structure all had a negative effect on conversion.

Table 7: Optimizations for the BV oxidation
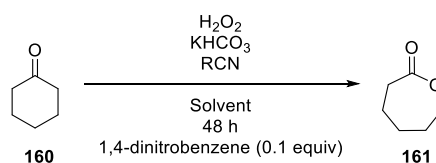
Entry	H_2O_2 source (equiv)	$KHCO_3$ (equiv)	Nitrile (equiv)	Solvent (M)	T (°C)	Conversion (%)[a]
1[e]	H_2O_2•urea (6.0)	0.2	PhCN (6.0)	CD_3OD (0.5 M)	50	38
2[e]	H_2O_2•urea (6.0)	0.2	PhCN (6.0)	CD_3OD (1.0 M)	50	30
3	H_2O_2•urea (6.0)	0.2	PhCN (6.0)	CD_3OD (0.2 M)	50	33
4[e]	H_2O_2•urea (6.0)	0.2	PhCN (6.0)	CD_3OD (0.5 M)	25	14
5[e]	H_2O_2•urea (6.0)	0.2	PhCN (6.0)	CD_3OD (0.5 M)	65	44
6[e]	H_2O_2•urea (3.0)	0.2	PhCN (6.0)	CD_3OD (0.5 M)	50	25
7[e]	H_2O_2•urea (10.0)	0.2	PhCN (6.0)	CD_3OD (0.5 M)	50	47
8[e]	H_2O_2 30% in H_2O (6.0)	0.2	PhCN (6.0)	CD_3OD (0.5 M)	50	31
9[e]	H_2O_2•urea (6.0)	0.2	PhCN (3.0)	CD_3OD (0.5 M)	50	21
10[e]	H_2O_2•urea (6.0)	0.2	PhCN (1.1)	CD_3OD (0.5 M)	50	10
11[e]	H_2O_2•urea (6.0)	0.2	4-MeO-C_6H_4CN (6.0)	CD_3OD (0.5 M)	50	26
12[e]	H_2O_2•urea (6.0)	0.2	4-NO_2-C_6H_4CN (6.0)	CD_3OD (0.5 M)	50	19
13[e]	H_2O_2•urea (6.0)	0.2	PhCN (6.0)	HFIP (0.5 M)	50	42
14[e]	H_2O_2•urea (6.0)	0.2	4-MeO-C_6H_4CN (6.0)	HFIP (0.5 M)	50	34
15[e]	H_2O_2•urea (6.0)	0.2	4-NO_2-C_6H_4CN (6.0)	HFIP (0.5 M)	50	60
16[e]	H_2O_2•urea (6.0)	0.2	4-NO_2-C_6H_4CN (2.0)	HFIP (0.5 M)	50	59
17[e]	H_2O_2•urea (6.0)	0.2	3,5-$(NO_2)_2$-C_6H_3CN (4.0)	HFIP (0.5 M)	50	74
18[e]	H_2O_2•urea (10.0)	0.2	PhCN (6.0)	HFIP (0.5 M)	50	39
19[e]	H_2O_2•urea (6.0)	0.2	PhCN (6.0)	PFB (0.5 M)	50	4
20[e]	**H_2O_2•urea (6.0)**	**0.2**	**PhCN (6.0)**	**TFE (0.5 M)**	**50**	**76 (70%)[b]**
21	H_2O_2•urea (6.0)	0.5	PhCN (6.0)	TFE (0.5)	50	84[c,d]
22	H_2O_2•urea (6.0)	0.1	PhCN (6.0)	TFE (0.5)	50	37
23[e]	H_2O_2•urea (6.0)	0.2	p-NO_2-C_6H_4CN (4.0)	TFE (0.5 M)	50	66
24[e]	H_2O_2•urea (6.0)	0.2	Cl_3CCN (6.0)	TFE (0.5 M)	50	58[c,d]

[a] Conversion was monitored by ^{1}H NMR spectroscopy against an internal standard (1,4-dinitrobenzene).
[b] Isolated yield after aqueous work-up and purification by column chromatography in parantheses.
[c] Reaction monitored over 24 h.
[d] Product decomposition observed.
[e] Performed by Tyne Bradley.[130]

Thorough examination of the crude reaction mixtures showed that a small amount (5–10%) of the ε-caprolactone **161** underwent solvolysis during the course of the reaction (methanolysis, Scheme 120). The methyl ester of the lactone, methyl 6-hydroxyhexanoate **364** was observed in the ^{1}H NMR of the crude reaction mixture. This likely occurred due to the nucleophilicity of methanol and the high temperature of the reactions (50 °C).
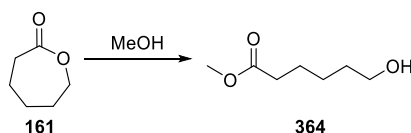
Scheme 120: Methanolysis of ε-caprolactone

Considering the observed methanolysis, fluorinated alcohols were examined, because of their lower nucleophilicity, which we hoped would reduce this undesired side-reaction. Moreover, fluorinated alcohols are known in the literature for the activation of peroxides.[131,132] An interesting piece of work was published by Neumann in 2000, in which aqueous H_2O_2 (60%) was activated by fluorinated alcohols and used as an oxidant for epoxidations and some BV oxidations (Scheme 121).[133] In spite of the literature precedent, the BV oxidation was attempted under the standard Payne conditions using HFIP (1,1,1,3,3,3-hexafluoroisopropanol) as a solvent, providing marginal improvement in conversion (42%, Table 7, entry 13). Control reactions were then performed in HFIP using H_2O_2•urea (6.0 equiv) in the absence of the Payne reagents ($KHCO_3$, benzonitrile, or both).[130] The results were surprising, with <5% of ε-caprolactone **161** observed by ^{1}H NMR spectroscopy, even though cyclohexanone **160** was being consumed against the internal standard.
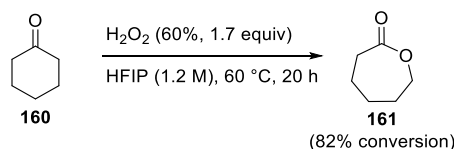
Scheme 121: BV oxidation using H_2O_2 (60%) and HFIP reported by Neumann[133]

Changing the nitrile in the reaction at this stage showed a decrease in conversion to ε-caprolactone **161** when using 4-MeO-benzonitrile (34%, entry 14), and an exciting increase when 4-NO_2-benzonitrile was used (60%, entry 15). Unfortunately, this increase in conversion was also complemented by consumption of cyclohexanone **160** against the internal standard (1,4-dinitrobenzene). To try and counteract this unwanted consumption of starting material, the amount of nitrile was decreased to 2.0 equivalents and the conversion was maintained (59%, entry 16). However, there was only 7% of the cyclohexanone **160** remaining after 48 h. Therefore, using 4-NO_2-benzonitrile was not an option under these

reaction conditions. A benzonitrile derivative with two electron withdrawing groups (3,5-dinitrobenzonitrile) was also examined and exhibited the best conversion to the lactone of all nitriles examined (74%, entry 17), but no cyclohexanone **160** was left in the reaction mixture. In an attempt to improve conversion using benzonitrile, a larger excess of $H_2O_2 \cdot$urea was used, but no significant change was observed (39%, entry 18).

Replacing HFIP with a perfluorinated alcohol, PFB (perfluoro-*tert*-butanol) was expected to enhance the conversion given the fact that it is a better hydrogen bond donor, but only 4% lactone **161** was observed at 48 h and this solvent was not examined further (Table 7, entry 19). TFE (2,2,2-trifluoroethanol) was then examined and it provided a significantly better conversion than the other fluorinated solvents examined (76%, entry 20). This was the solvent that provided the best conversion when using $H_2O_2 \cdot$urea (6.0 equiv), benzonitrile (6.0 equiv) and $KHCO_3$ (0.2 equiv). In an attempt to improve conversion, 0.5 equivalents of base were used (entry 21), but in spite of an improved conversion of 84%, the lactone product **161** started to decompose, which was an undesirable feature. Decreasing the amount of base (0.1 equiv) significantly affected the conversion (37%, entry 22), thus 0.2 equivalents were adopted in our standard conditions. Based on the results obtained when using HFIP as solvent, 4-NO_2-benzonitrile was also examined as a nitrile source, but a lower conversion was obtained (66%, entry 23). The reason why fewer equivalents of the nitrile bearing an electron withdrawing group were used in this experiment was the low solubility of this particular nitrile. In another attempt to increase conversion, trichloroacetonitrile was used, but in spite of the 58% conversion at 24 h (entry 24), all of the cyclohexanone **160** had been consumed at this point.

With all of the reaction optimizations performed, it was concluded that the optimum reaction conditions involved using 0.2 equivalents of $KHCO_3$ as base, 6.0 equivalents of $H_2O_2 \cdot$urea and benzonitrile with TFE (0.5 M) as solvent (Scheme 122). The reaction was scaled up to 4.0 mmol and an isolated yield of 70% was obtained when using cyclohexanone **160** as a substrate.
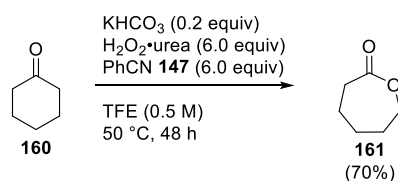
Scheme 122: Optimum BV oxidation conditions using a Payne-type system

2.5 Substrate Scope

After optimizing the reaction, a series of substrates were reacted under these conditions in order to determine the versatility of the BV oxidation developed (Table 8). The reaction provided lactones of a series of cyclohexanone derivatives in good to excellent yields (Table 8, entries 1–9). The C_2 symmetric cyclohexanone derivatives **160**, **365**, **314**, **329** and **377** each provided a single product in very good yields (entries 1–4 and 12, 70–83%). α-Substituted cyclohexanones displayed the expected regioselectivity features of the BV reaction, with the more substituted carbon preferentially migrating (entries 5–7). Another important characteristic of the BV oxidation observed when using (–)-menthone **325** was the retention of stereochemistry of the migrating carbon atom (entry 9). The stereochemistry of the product was determined by comparing its optical rotation (–20.56°) to that of the enantiomerically pure compound (–19.7°).[134] When changing the ring size of the ketone, a decrease in reactivity was observed for cyclopentanone **373** (30% after 72 h, entry 10), which is consistent with observations in the literature.[135] An increase in reactivity and an excellent yield was obtained in the case of cyclobutanone **375** (85% after 18 h, entry 11). This could be attributed to the relief of ring strain, which makes the reaction more favorable. The reaction was sluggish when applied to acyclic ketones such as pinacolone **379** (49% conversion after 7 days, entry 13). The latter is a limitation of the transformation, which will be discussed in Section 2.5.1.

Table 8: Substrate scope for the Baeyer-Villiger oxidation

Entry	Ketone	Product (major)	Time (h)	Yield[a] (%)	Selectivity[b]	Entry	Ketone	Product (major)	Time (h)	Yield[a] (%)	Selectivity[b]
1	**160**	**161**	48	70	-	8	**371**	**372**	72	36	-
2	**365**	**366**	48	82	-	9	**325**	**327**	72	51	*n.d.*
3	**314**	**315**	48	81	-	10	**373**	**374**	72	30	-
4	**329**	**330**	72	83	-	11	**375**	**376**	18	85	-
5	**311**	**312**	48	91	7:1	12	**377**	**378**	24	82	-
6	**367**	**368**	72	83	15:1	13	**379**	**380**	144	49[c,d]	*n.d.*
7	**369**	**370**	42	90	20:1						

[a] Isolated yield.
[b] Ratio between regioisomeric products (major isomer shown), determined by ^{1}H NMR spectroscopy of the crude reaction mixture.
[c] Conversion to single product monitored by ^{1}H NMR against an internal standard (1,4-dinitrobenzene).
[d] Average of two runs.

2.5.1 Limitations

As observed in the previous section, a few ketones were sluggish under the BV oxidation conditions adopted. A series of substrates were examined to test these findings and their conversions are reported in Table 9. First, it was noted from the substrate scope that decreasing ring size from cyclohexanone **160** to cyclopentanone **373** only provided lactone **374** in 30% yield under the optimized reaction conditions (Table 8, entry 10). 1-Indanone **382** and 2-indanone **383** only showed low conversions of up to 7% (Table 9, entries 1 and 2); this significant decrease in conversion could be attributed to the presence of the aromatic ring. This negative effect of an aromatic ring attached *via* two carbon atoms to a cyclic ketone was confirmed when using 1-tetralone **384** as it showed a significant decrease in conversion against other cyclohexanone derivatives (23% after 6 days, entry 3). The reason behind this might be connected to the required electronic effects behind the BV oxidation at the Criegee intermediate **381** stage of the reaction mechanism.[136] There is a possibility that the aromatic rings distort the cyclic ketone in such a way that the alignment between the migrating group (R_M) and the peroxide O–O bond (red) is not antiperiplanar, meaning that the σ orbital of R_M and the σ* orbital of the peroxide are not ideally overlapped for migration (primary electronic effect) such as in conformer **381A**; another possible interaction that could be altered by this distortion is the secondary electronic effect, *i.e.* the highlighted lone pair (non-bonding orbital) of the hydroxyl oxygen is not optimally overlapped with the σ* orbital of R_M (antiperiplanar alignment in conformer **381B**).[136,137]
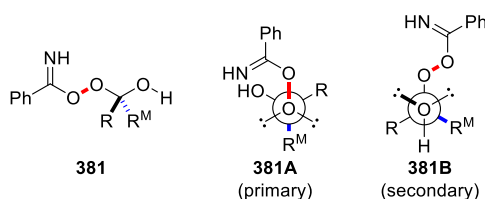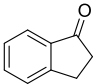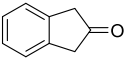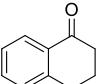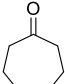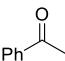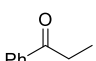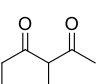
Figure 28: Primary and secondary electronic effects in the Criegee intermediate **381**

Increasing the ring size to a 7-membered ring (cycloheptanone **385**) provided nearly no conversion (<5%, entry 4), which was in accordance with previous literature findings.[135] Furthermore, it was noted that the transformation did not perform in a similar fashion for acyclic ketones (Table 8, entry 13), thus, it was unsurprising that acetophenone **386** and propiophenone **186** only provided 10–11% conversion after four days under the BV reaction conditions (Table 9, entries 5 and 6). Having shown that the reaction worked selectively for

cyclic ketones, diketone **387** was tested to probe this selectivity (entry 7). Unfortunately, the conversion was <5%, with no starting material being consumed. This could be attributed to the acidic proton in the α-position to the carbonyl carbons that would be deprotonated under the reaction conditions, preventing BV oxidation.

Table 9: Limitations of the BV oxidation

Entry	Ketone	Time (d)	Conversion[a] (%)
1	**382**	2	<5
2	**383**	2	7
3	**384**	6	23
4	**385**	4	<5
5	**386**	4	10
6	**186**	4	11
7	**387**	6	<5

[a] Conversion to product(s) measured against internal standard (1,4-dinitrobenzene).

2.6   Proposed Mechanism

A mechanism for the BV oxidation is proposed based on the Payne epoxidation.[50] The first step of the mechanism is the formation of peroxy imidic acid intermediate **360** (Scheme 123). The formation of the intermediate can occur in a two-step process: first, the base deprotonates H_2O_2, after which the peroxy anion adds to the nitrile carbon to form peroxy imidic acid **360**. This intermediate is known to be short lived as it has never been isolated, but has shown remarkable reactivity, comparable to that of *m*-CPBA.
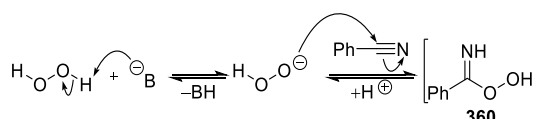
Scheme 123: Formation of peroxy imidic acid **360** using benzonitrile

The second part of the proposed mechanism is based on the peracid mediated BV oxidation described in Section 2.1 (Scheme 124). Peroxy imidic acid **360** adds to ketone **301** to form zwitterionic species **388**, which leads to Criegee intermediate **381** upon proton transfer. The resulting intermediate undergoes a typical BV rearrangement to form the observed ester **301** together with benzamide **362** as a coproduct.
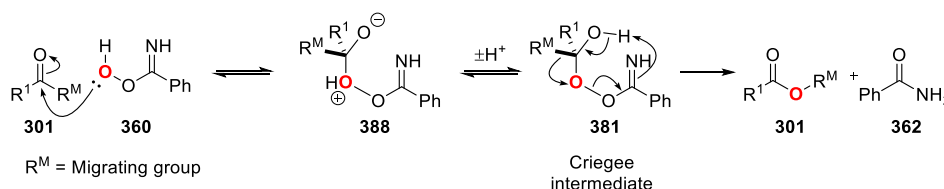
Scheme 124: BV oxidation using peroxy imidic acid **360**

2.7   Conclusions

In conclusion, a novel BV oxidation using Payne epoxidation conditions has been developed. The reaction uses H_2O_2•urea as a source of peroxide, which is activated by a catalytic amount of base ($KHCO_3$) and a nitrile (benzonitrile **147**) in a fluorinated alcohol. The active oxidant is believed to be a peroxy imidic acid **360**. The reaction provides moderate to good yields of the lactone products, with the expected regioselectivity and retention of configuration of the migrating carbon atom. This BV oxidation uses a 6-fold excess of two reagents and its synthetic applicability would be limited, in comparison with established methods such as the *m*-CPBA mediated transformation.[99] However, considering the enantioselective Payne-type epoxidation reaction using *in situ* formed peroxy imidic acids,[125] these results could serve as an excellent starting point for potential asymmetric BV oxidations.
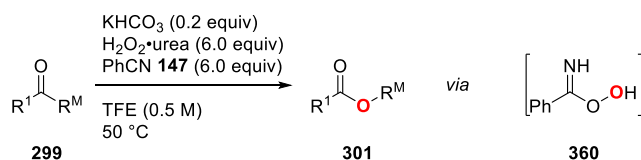
Scheme 125: General BV oxidation using Payne conditions

Chapter 3: Arene Oxidation

3.1   Introduction – Phenols

Phenols are an important class of compound which are well known antioxidants.[138] They are present in products consumed by people in everyday life, such as fruit, chocolate, alcoholic beverages (wine and whiskey), coffee and tea. Phenol functionalities are also present in some of the most prescribed drugs on the market (Figure 29). These exist as the free phenol (**389**–**392**) or the aryl ether (**393** and **394**).
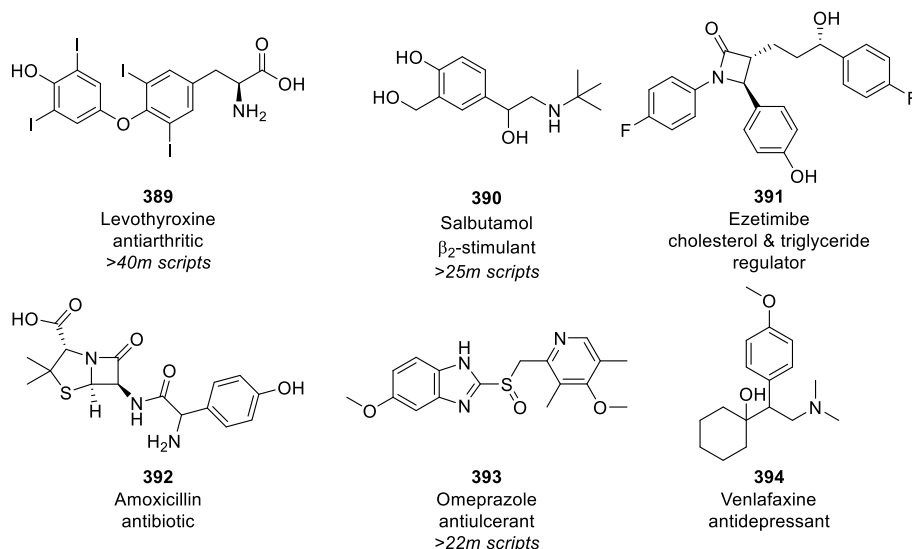
Figure 29: Phenols and phenolic ethers in pharmaceutical drugs

3.1.1   Synthesis of Phenols *via* Arene Oxidation

There are many methods in the literature for the oxidation of arenes and the synthesis of phenols.[139] Herein, methods for the direct oxygenation of arenes will be described. Methods include the use of peroxides and strong acids, radical functionalization, and transition metal catalyzed oxygenation. Despite the importance of this functional group, many of the methods reported have poor selectivity or they require a directing group, thus limiting the substrate scope for the transformation.

3.1.1.1 Hydroxyl Cations

Methods for generating phenols *via* hydroxyl cations have been known in the literature for more than 50 years. Derbyshire and Waters first oxidized mesitylene **395** using hydrogen peroxide under strongly acidic conditions (Scheme 126).[140] Mesitol **396** was formed as a major product, with minimal over-oxidation due to the methyl groups present in *ortho* and *para* positions to the hydroxyl group. According to the authors, this was very different to benzene, which decomposed due to over-hydroxylation.
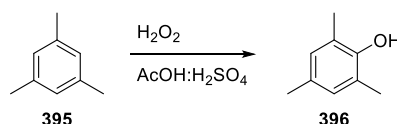
Scheme 126: Oxidation of mesitylene **395** using H_2O_2 under acidic conditions

Other similar transformations have since emerged based upon this process, and major disadvantages such as regioselectivity and over-oxidation of the arene have not yet been overcome using this strategy.[141] An isolated study by Olah in 1991 showed selectivity for the oxidation of naphthalene **397** to 1-naphthol **398** (>98%) over 2-naphthol **399** (Scheme 127).[142] The reaction required a strong acid to activate hydrogen peroxide and low temperatures to provide the phenol shown in moderate yields (26–43%). Selectivity toward 2-naphthol **399** could also be achieved by using a superacidic H_2O_2-HF-BF_3 system at –60 °C.
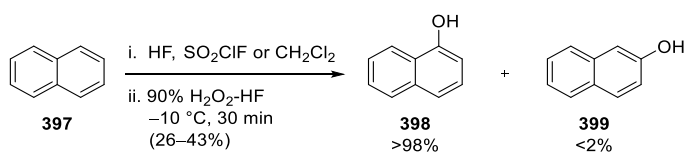
Scheme 127: Regioselective hydroxylation of naphthalene **397**

3.1.1.2 Peroxide Radicals using Copper Chloride or Iodine as Catalysts

Kovacic and coworkers have developed methods for oxidizing arenes in the presence of an organic peroxide and a catalyst, such as copper chloride or iodine.[143] The oxidation of toluene **400** with benzoyl peroxide **167** and catalytic iodine afforded a mixture of aromatic

ester regioisomers **401** in good yield (Scheme 128). The reaction also provided polymerization byproducts and benzoic acid coproducts.
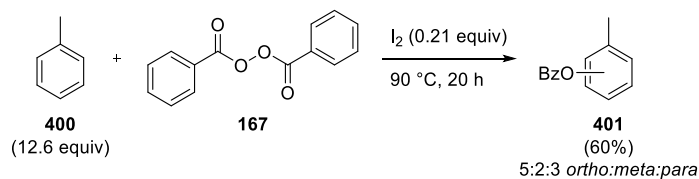
Scheme 128: Iodine catalyzed arene oxygenation using benzoyl peroxide **167**

3.1.1.3 Iron Salts

Some studies have shown that iron salts can also be used to perform arene hydroxylation. Intramolecular processes using molecular oxygen as the oxidant have shown regioselectivity, however, these oxidations occur on the aromatic rings of the ligands attached to iron.[144] A study by Hamilton *et al.* used catalytic iron(III) perchlorate and catechol to oxidize four simple arenes to their corresponding phenols in moderate yields (Scheme 129).[145] In line with other methods, a mixtures of regioisomers was formed under these reaction conditions.
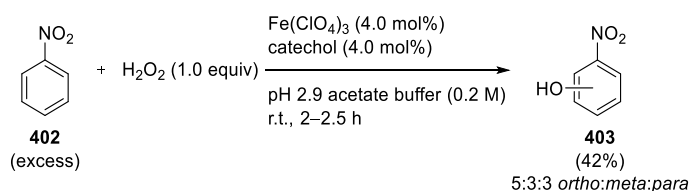
Scheme 129: Iron catalyzed arene oxidation

3.1.1.4 Manganese Complexes

In 2000, Mansuy described a hydroxylation of arenes using hydrogen peroxide and a Mn-porphyrin **405** catalytic system, in conjunction with an ammonium mandelate co-catalyst (Scheme 130).[146] The arenes (*e.g.* anisole **404**) were used in large excess. The method showed *ortho* and *para* selectivity for arenes such as anisole **404**, but the substrate scope reported was limited to only three arenes. Of these, naphthalene **397** was oxidized mainly in the 1-position, whilst ethylbenzene was oxidized at the benzylic carbon.
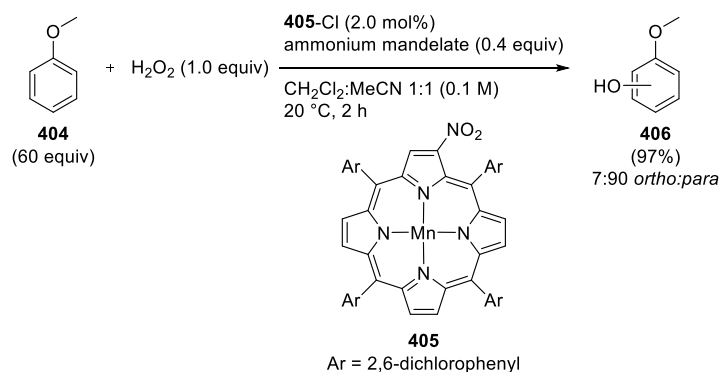
Scheme 130: Mn porphyrin catalyzed hydroxylation of arenes

3.1.1.5   Iridium Derivatives

In 2015, Ritter and coworkers reported a method for selective arene hydroxylation using iridium complexes (Scheme 131).[147] This novel reaction consists of a stepwise process which initially involves the formation of iridium complex **407**. This complex is then treated with excess sodium chlorite in the presence of 2-methyl-2-butene to form intermediate **409**. The crude reaction mixture is then treated with $HBF_4 \cdot OEt_2$ to form the phenol **408** as a single regioisomer. This method was very important as it paved the way to potential regioselective oxidations of electron deficient arenes.
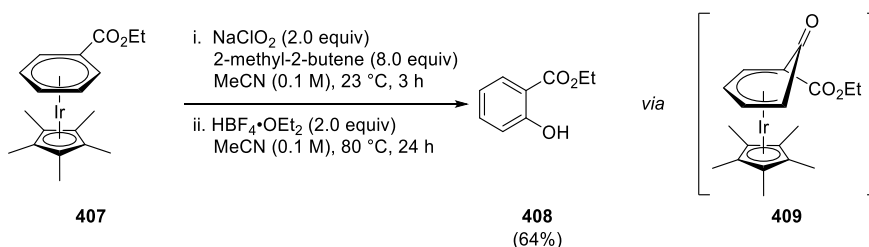
Scheme 131: Iridium mediated arene oxidation

3.1.1.6   Palladium Catalysts

Palladium catalysts for arene oxidations are perhaps the most versatile for the formation of new aromatic C–O bonds.[148] Most of the studies involving Pd-based catalysts were highly regioselective due to the presence of a directing group on the substrate,[149] while reactions without a tethered directing group proceed with lower selectivity.[150] An example by Gevorgyan used a palladium catalyst for a directed synthesis of catechols (Scheme 132).[149c]

Treatment of silanol ethers (e.g. **410**) with PhI(OAc)$_2$ as an oxidant using catalytic Pd(OPiv)$_2$, followed by desilylation with TBAF afforded the catechol products **411**, in excellent yield (88%). The transformation showed very good functional group tolerance and was applicable to a broad range of substrates.
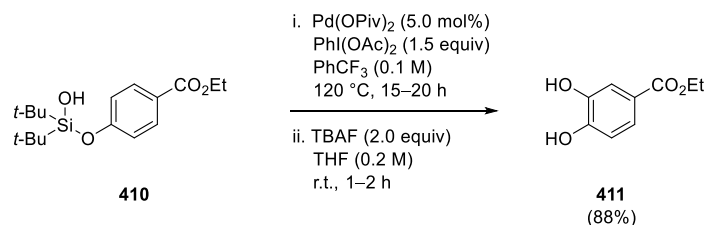
Scheme 132: Pd catalyzed arene oxidation

3.1.1.7 Peracids

In 2005, Bjørsvik developed a method for synthesizing phenols using peracids (Scheme 133).[151] Electron rich aromatic compounds were treated with hydrogen peroxide in acetic acid, with *p*-toluenesulfonic acid as catalyst, to afford a mixture of compounds. An example is shown below where acetophenone derivative **412** was converted to phenol **413**, Baeyer-Villiger/phenol product **414** and Baeyer-Villiger product **415**. It was proposed that the reaction proceeded *via in situ* generated peracetic acid **324**.
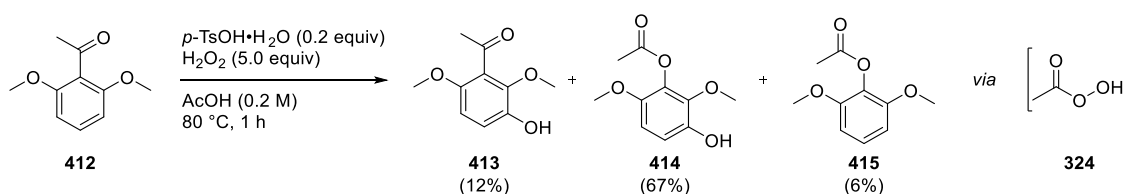
Scheme 133: Peracid mediated arene hydroxylation

3.1.1.8 Phthaloyl Peroxide 106

In 2013, Houk and Siegel published a paper in which >50 aromatic compounds were converted to their corresponding phenols in moderate to excellent yields.[152] The reaction was a phthaloyl peroxide **106** mediated oxidation of arenes that overcame previously described challenges such as over-oxidation,[140,141] selectivity[143,145] and functional group tolerance[151] (Scheme 134). Ester products, such as **416**, were not always isolated, as solvolysis of the crude reaction mixture provided the phenols **396** or **418** in good to excellent overall yields.
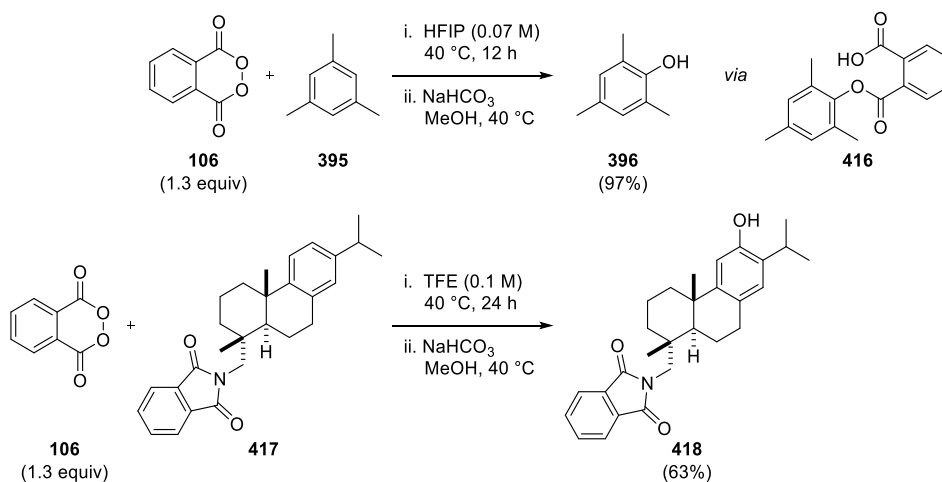
Scheme 134: Phthaloyl peroxide **106** mediated arene oxidation

Despite the significant benefits offered by this novel oxidation process, the use of phthaloyl peroxide **106** is a potential drawback, as this peroxide has been reported to detonate upon heating, shock or ignition.[66,153]

In an attempt to minimize the risk, Siegel and coworkers used a flow reactor to avoid handling phthaloyl peroxide **106** in its pure form (Scheme 135).[154] Nevertheless, after the reaction between the arene and phthaloyl peroxide **106**, the solvent was removed *in vacuo* to afford the crude reaction mixture which was afterward taken through to the hydrolysis step. While this method was safer than using the peroxide directly as a reagent, the *in situ* formed phthaloyl peroxide **106** was used in excess (2.1 equiv), a solvent switch was performed prior to the hydrolysis step, meaning that unreacted peroxide was present in the crude reaction mixtures.
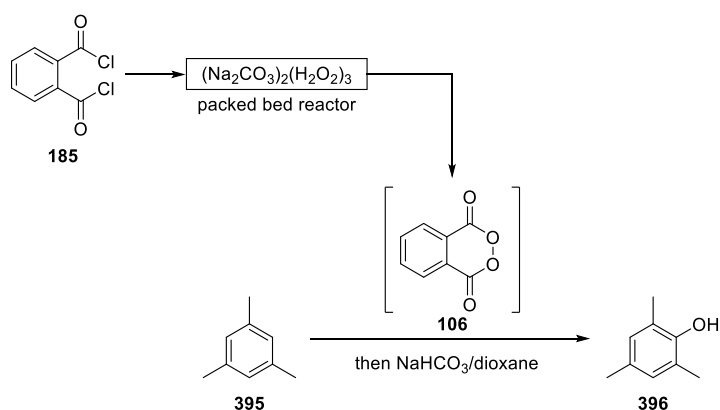
Scheme 135: *In situ* generation of phthaloyl peroxide **106**

3.1.1.9   Conclusions on Arene Oxygenation

Several methods for the formation of new C–O bonds *via* arene oxidation were described in the previous sections. Most of these methods provided mixtures of different regioisomers or had significant byproducts from the reaction (Sections 3.1.1.2, 3.1.1.3 and 3.1.1.7). The selective methods either work for a limited number of substrates (Sections 3.1.1.1, 3.1.1.4 and 3.1.1.5) or required a tethered directing group (Section 3.1.1.6). While many of these transformations could be synthetically useful, the phthaloyl peroxide **106** mediated arene oxidation is a valuable addition because it proceeds for a broad range of substrates (Section 3.1.1.8). A specific disadvantage of using this reagent is that it is highly shock sensitive.

3.1.2   Alternative Peroxide

A safer alternative to phthaloyl peroxide **106** is malonoyl peroxide **90**, which has been shown to be more reactive than phthaloyl peroxide **106** in the dihydroxylation of alkenes.[39,40,41,155] Based on previous knowledge within the group regarding phthaloyl peroxide **106** and its reactivity toward alkenes,[66] we believed that malonoyl peroxide **90** could provide not only a safer, but also a more reactive oxidant for arenes.

90   **106**
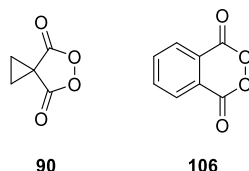
Figure 30: Peroxides used for the dihydroxylation of alkenes

3.1.3   Attribution

This arene oxidation project was carried out with Tomasz Kubczyk, another Ph.D. student in the group. His work focused on reaction optimizations, expanding the substrate scope and radical clocks. Other contributions included pieces of data for the Hammett study, which will be described in Section 3.4.4, and valuable discussions regarding the mechanism of the reaction and EPR analysis. Specific work carried out by Kubczyk reported in this thesis is acknowledged throughout.

3.2   Initial Results and Substrate Scope[131]

A first attempt to oxidize mesitylene **395** with malonoyl peroxide **90** under the conditions reported by Houk and Siegel provided ester **419** in excellent yield upon work-up (94%, Scheme 136). Hydrolysis of **419** was then attempted using the reported conditions (saturated aqueous NaHCO₃ in MeOH).[152] The yields obtained from the ester hydrolysis were unsatisfactory (<60%), however, using MeNH₂ in EtOH to carry out the hydrolysis provided the corresponding phenol **396** in very high yield (92%, Scheme 136). This initial result showed that malonoyl peroxide **90** could perform the oxidation that leads to the formation of a new C–O bond in a similar fashion to phthaloyl peroxide **106**.
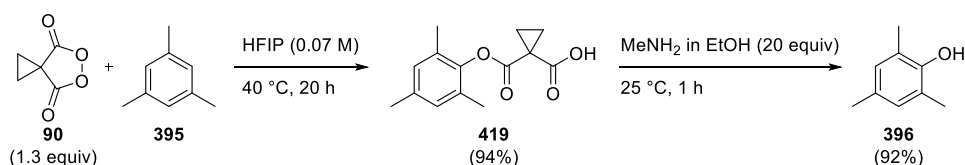
Scheme 136: Malonoyl peroxide **90** mediated oxidation of mesitylene **395** followed by aminolysis of ester **419**

Brief optimizations showed that lowering the reaction temperature to 25 °C, resulted in no compromise in yield (96%), albeit with a longer reaction time (40 h). Increasing the amount of peroxide to two equivalents (25 °C) lowered this reaction time and no byproducts were observed (97%, 20 h). This was very encouraging, as the reaction with phthaloyl peroxide **106** was reported to be sluggish at lower temperatures.[152] Increasing the concentration to 0.5 M significantly decreased reaction time and, once again, no byproducts were observed (98%, 4.5 h, Scheme 137). These reaction conditions were deemed satisfactory and were thus used in exploring the substrate scope.
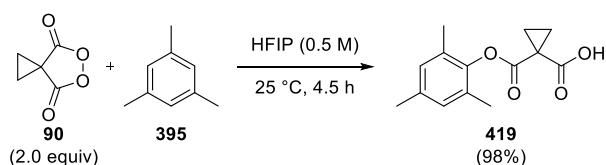
Scheme 137: Optimized reaction conditions for the malonoyl peroxide **90** mediated arene oxidation

Before the reaction could be performed on a range of substrates, it was necessary to confirm the aminolysis method shown in Scheme 136 could be used to liberate the phenol product. The results are summarized in Table 10 below. The ester bond cleavage had already been shown to be effective when using the ester of mesitylene as substrate (Table 10, entry 1),

providing the corresponding phenol **396** in 92% yield for the second step. When using the ester of 1,3,5-triisopropylbenzene as a substrate, phenol **424** was also obtained in very high yield (93%, entry 2). Given these positive results, we deemed this hydrolysis was a robust process.

Table 10: Aminolysis of ester products

Entry	Starting material	Product	Yield Step 1 (%), t (h)[a]	Yield Step 2 (%)[b]
1	**395**	**396**	98 4.5 h	92
2	**423**	**424**	98 2 h	93

[a] Isolated yield and reaction times after Step 1. [b] Isolated yield after Step 2.

In an attempt to compare the reactivity of malonoyl peroxide **90** to phthaloyl peroxide **106** a series of arenes that had been reported by Houk and Siegel were reacted under our optimized reaction conditions (Table 11). Mesitylene **395** and 1,3,5-triisopropylbenzene **423** provided the ester products **419** and **425** in excellent yields of 98% (entries 1 and 2). The reaction times (4.5 h and 2 h) were significantly shorter than those published by Houk and Siegel (12 h at 40 °C for both substrates),[152] which suggested malonoyl peroxide **90** was more reactive than phthaloyl peroxide **106** for these substrates. It was noted that 1,3,5-triisopropylbenzene **423** reacted faster than mesitylene **395**, a trait which was attributed to the fact that the former was more electron rich.

When using a less electron rich arene such as *p*-xylene **426**, the ester product **427** was also isolated in very high yield (97%), but the reaction required heating to 50 °C for 96 h in order to reach completion (entry 3). Having noticed the lower reactivity of *p*-xylene **426**, attempts were made to oxidize benzene **428**, but no products were observed in the ^{1}H NMR of the crude reaction mixture even after a week at reflux (entry 4). These results suggested that electron rich arenes were needed in order to bring about reaction under the conditions examined.

Table 11: Substrate scope for the arene oxidation

Entry	Starting material	Product(s)	Yield (%), t (h)	Comparison[a]
1	395	419	98 / 4.5 h	97% / 12 h
2	423	425	98 / 2 h	95% / 12 h
3	426	427	97[b] / 96 h	86% / 24 h
4	428	–	0[c] / 144 h	N/A
5	400	429 / 429'	63[b] / 1:1[d] / 72 h	46% / 1:1 / 24 h
6	404	430 / 430'	63[c] / 1.6:1[d] / 72 h	45% / 1.4:1 / 14 h
7	431	432	70[e] / 24 h	96% / 8 h
8	433	434	91 / 120 h	63% / 24 h
9	435	436	86[b] / 42 h	N/A
10	437	–	0[b] / 72 h	N/A
11	438	439 / 439'	60 / 3:2[d,f] / 24 h	N/A
12	440	441	40 / 24 h	57% / 24 h

[a] Isolated yield (phenol) as reported by Houk and Siegel.[152] [b] The reaction was performed at 50 °C.
[c] The reaction was performed at 80 °C. [d] Regioisomeric ratio determined by ^{1}H NMR spectroscopy.
[e] 1.1 equiv of malonoyl peroxide 90 used. [f] Isolated yield after two steps.

A decrease in reactivity was also noted when using toluene **400** as the substrate (63% after 72 h), but perhaps the most interesting feature was the regioselectivity of this transformation (entry 5). The new C–O bonds were only formed in the *ortho* and *para* positions on the aromatic ring, while *meta* substituted products were not observed in the ^{1}H NMR spectrum of the crude reaction mixture. The same regioselectivity was observed by Houk and Siegel for the oxidation of toluene **400**.[152] Anisole **404** behaved similarly to toluene **400**, showing *ortho* and *para* regioselectivity and a ratio of 1.6:1 for the two regioisomers which was marginally higher to that reported by Houk and Siegel (1.4:1, entry 6). The *para*-isomer **430** was the major product, presumably due to the steric demands of the –OMe group, The regioselectivity exhibited by these substrates was reflective of electrophilic aromatic substitutions, in which electron donating groups activate the ring and direct the substitution to the *ortho* and *para* positions, stabilizing the generated positive charge in the Wheland intermediate.[156]

Pentamethylbenzene **431** required only 1.1 equivalents of malonoyl peroxide **90**, to give the product **432** in 70% yield, lower than that reported by Houk and Siegel (96%, entry 7).[152] The reaction showed tolerance to halides and aromatic carboxylic acids, providing the esters **434** and **436** in excellent yields of 91% and 86%, respectively (entries 8 and 9). Nitromesitylene **437** was inert to the reaction conditions examined and this was attributed to the highly electron withdrawing nitro group attached to the arene (entry 10), defining a limitation to the process. The reactivity of electron rich arenes was further supported through the reaction of biaryl compound **438** which reacted only on the ring bearing the –OMe group to afford a 3:2 mixture of regioisomers **439** and **439'** (major isomer unknown) in 60% overall yield (entry 11). It could be identified by ^{1}H NMR spectroscopy that no oxidation had occurred on the electron deficient aromatic ring, however, the ester intermediates could not be purified by column chromatography and the crude mixture required treatment with methylamine in order to obtain the phenol products **439** and **439'**. Even though it could not be identified which of the products **439** and **439'** was the major isomer, it was expected that the strongly activating –OMe group would have dominated the regioselectivity induced.[157]

An interesting substrate was aromatic aldehyde **440** which afforded the ester product **441** in 40% yield upon reaction with malonoyl peroxide **90** (entry 9). This was an unexpected reactivity, as **440** has been shown to react in the *para* position to the benzyloxy substituent for brominations or nitrations in electrophilic aromatic substitutions (Scheme 138).[158] The generated HOMO indicated that the phenyl ring of the benzyloxy group was more electron rich than the reactive aromatic ring (Figure 31). The simulated results proved inconclusive for the reactivity of **440** and, in hindsight, it could be possible that the peroxide was directed for nucleophilic attack by the groups adjacent to the reactive carbon.
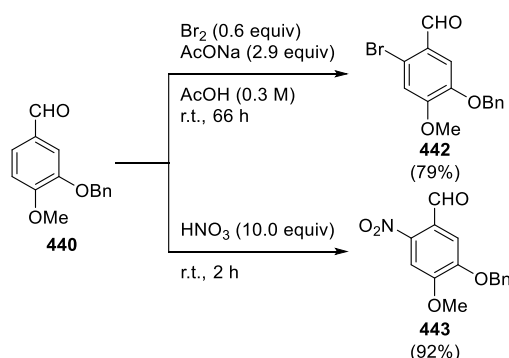
Scheme 138: Bromination and nitration of aldehyde **440**
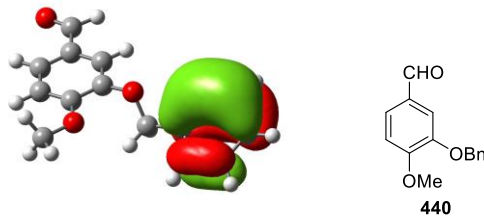
Figure 31: Simulated HOMO of aldehyde **440**

The results shown in Table 11 showed that only electron rich arenes reacted readily, with the more electron deficient substrates requiring 50 °C to react (**400**, **404**, **426** and **435**) and arenes such as **428** and **437** being unreactive. In the >50 examples reported, Houk and Siegel only described arenes with at least one electron donating substituent present on the aromatic ring and no comment was made on electron deficient substrates.[152] After observing the preference toward arenes bearing electron donating groups, it was of interest to discover if malonoyl peroxide **90** could react with a series of electron-deficient arenes **444** (Scheme 139). Acetophenone, methyl benzoate, benzoic acid and benzonitrile proved inert to the reaction conditions examined (2.0 equivalents of malonoyl peroxide **90** in HFIP at 50 °C for 24 h). These results showed a major limitation to the process whereby the reaction only proceeds

with electron rich substates. It should be noted that this limitation could also provide a source of selectivity in substrates containing more than one aromatic ring.
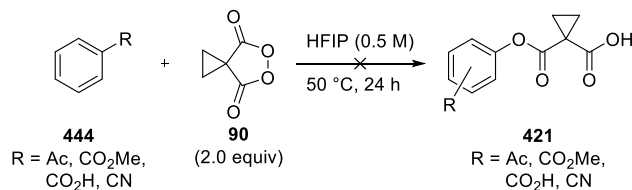
Scheme 139: Unreactive arenes

Overall, malonoyl peroxide **90** reacted in a similar manner to phthaloyl peroxide **106**, which meant it was a useful, safer alternative for the formation of new aromatic C–O bonds. The arene oxidation reaction was effective for electron rich arenes, whereas electron deficient substrates proved unreactive. Moreover, substrates such as toluene **400** and anisole **404** exhibited Friedel-Crafts reactivity patterns, while aldehyde **440** provided a surprising ester product **441**, sparking our interest toward gaining further insight into the transformation.

3.3   Additive Screening

Despite the successful oxidation of arenes, the use of HFIP as solvent represented a potential drawback due to its expense and toxicity. Solvent screening showed that the reaction between 1,3,5-triisopropylbenzene **423** and malonoyl peroxide **90** worked well in halogenated alcohols (Table 12, entries 1–4) and not in standard polar protic (^{i}PrOH, entry 5), nonpolar (CHCl$_3$, entry 6) or polar aprotic solvents (entries 7–11). This was a similar trend to the results reported by Houk and Siegel.[152] Perfluoro *tert*-butanol (PFB, entry 2, >99% after 1 h) performed best, followed by HFIP (entry 1, >99% after 2 h), 2,2,2-trichloroethanol (TCE, entry 3, 96% after 24 h) and 2-chloroethanol (CEO, entry 4, 39% after 24 h). This trend was related to the pK_a values of these solvents: PFB had a pK_a value of 5.4, HFIP 9.3, TCE 12.3, and CEO 14.3. [159,160] This correlation indicated that the lower the pK_a value of the solvent, the faster the reaction.

Table 12: Solvent screening for the arene oxidation

Entry	Solvent	Conversion (%)^a	Time (h)
1	HFIP	>99	2
2	PFB	>99	1
3	TCE	96	24
4	CEO	39	24
5	^{i}PrOH	<5	24
6	CHC$_3$	<5	24
7	EtOAc	<5	24
8	THF	<5	24
9	CH$_2$Cl$_2$	<5	24
10	MeCN	<5	24
11	DME	<5	24

^{a} Conversion determined by ^{1}H NMR spectroscopy of reaction mixture following blow down.

The activity of these halogenated alcohols was even more remarkable, given that the reaction was more than three times slower in AcOH when Houk and Siegel examined it as a potential solvent for the phthaloyl peroxide **106** arene oxidation.[152] The pK_a of AcOH is 4.76,[161] and is significantly lower than that of HFIP (9.3). Based on the previous observation regarding pK_a values, one would expect AcOH to perform in a similar manner to PFB. However, there is a remarkable feature of fluorinated alcohols called the "booster effect", introduced by Berkessel in 2006, which could influence the reaction. Fluorinated alcohols can aggregate to form a hydrogen bond network, increasing the H-bonding capability of these alcohols (Figure 32).[162]
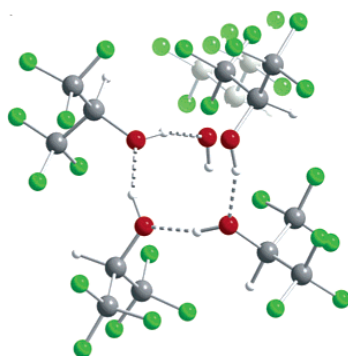
445

Figure 32: Single-crystal X-ray structure of HFIP aggregate **445**[162]

Given that CH$_2$Cl$_2$ had minimal use a solvent for the stoichiometric transformation, with only 3% conversion to ester product **425** and no byproducts after 24 h, together with its low boiling point, it was chosen as solvent for screening potential additives to accelerate the transformation (Figure 33). A series of reactions were carried out using 2.0 equivalents of a fluorinated alcohol with respect to 1,3,5-triisopropylbenzene **423** in the presence of peroxide **90** (2.0 equiv, Figure 33). The reactions proceeded faster with PFB (67% conversion after 24 h) than HFIP (47% after 24 h) or TFE (19% after 24 h). These results followed the previously noted correlation: the lower the pK$_a$ value of the alcohol added, the higher the reaction rate. More importantly, it was shown that fluorinated alcohols can be used as additives, instead of being used as solvents.
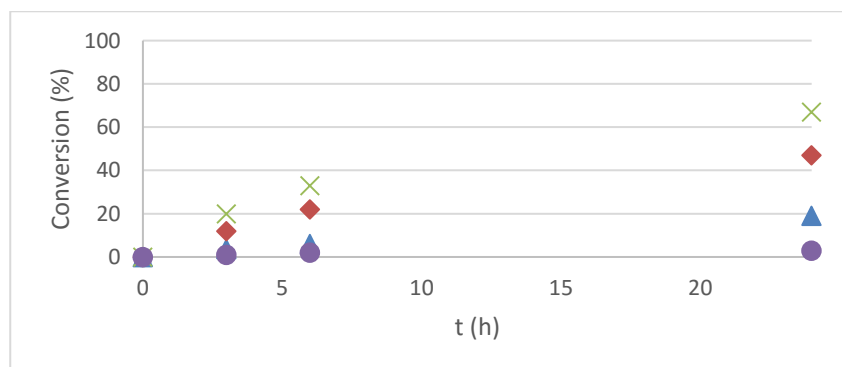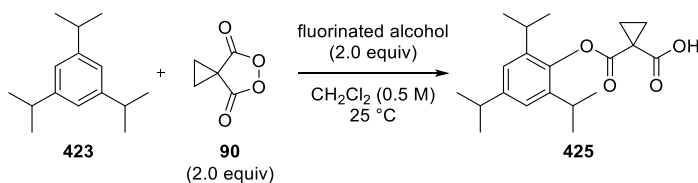
Figure 33: Fluorinated alcohols as additives (✕ PFB, ◆ HFIP, ▲ TFE, ● without additive)

After showing that acidity played an important role, several organic acids were screened as possible additives for the reaction (Figure 34). 1,3,5-Triisopropylbenzene **423** was treated with 2.0 equivalents of malonoyl peroxide **90** in the presence of 2.0 equivalents an acid additive in CH_2Cl_2. It was found that trifluoromethanesulfonic acid (triflic acid or TfOH) was the most efficient additive, the reaction reaching 92% conversion after 3 h, and the only one reaching full conversion under 24 h. This reaction clearly proceeded faster than with any of the fluorinated alcohols examined. This could be reasoned based on the pK_a value of –14 for TfOH, the lowest of all acids examined.[163] Dehydrated *p*-toluenesulfonic acid (pK_a –5.4) was an intriguing additive, reaching 67% conversion after 6 h. After this time, the reaction slowed down to reach 78% conversion after 24 h.[164] Interestingly, when used as its commercially available monohydrate form, *p*-toluenesulfonic acid was less effective (8% conversion after 24 h). This difference suggested that the presence of water significantly slowed down the reaction rate, potentially by interfering with hydrogen bonding. Methanesulfonic acid (pK_a –1.9) displayed a lower conversion of 59% after 24 h, keeping with the observed trend.[164] The pK_a of MsOH is significantly lower than that of PFB (pK_a 5.4) where the reaction reached a conversion of 67% at 24 h. This implied that the rate of the reaction was not solely dependent on acidity, but other factors such as aggregation potentially play a role.[162] A direct correlation between pK_a values and reaction rate was further disproved when TFA (pK_a 0.2) showed a steady increase toward a conversion of 90% over 24 h, higher than the acids examined with lower pK_a values.[165]
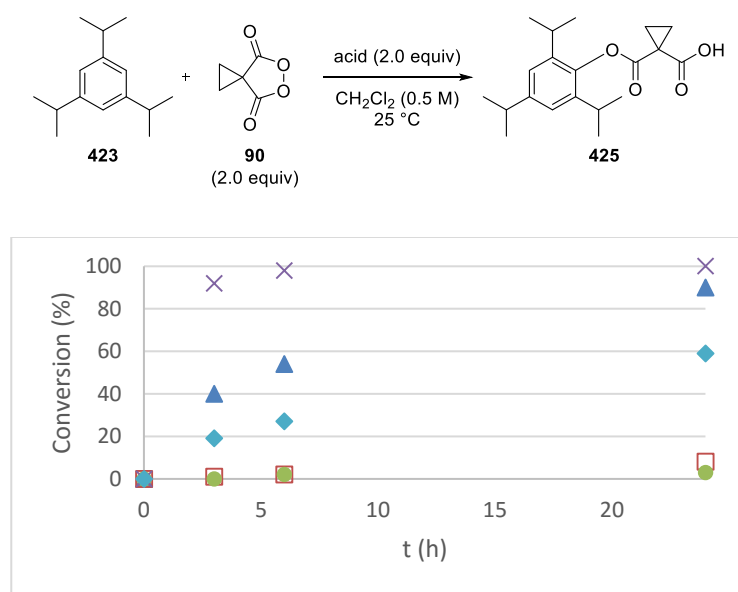
Figure 34: Acids as additives (× TfOH; ▲ TFA; ■ p-TsOH; ◆ MsOH; □ p-TsOH•H_2O; ● without acid additive)

3.3.1   Effect of Water

As seen in Figure 34, using anhydrous *p*-TsOH showed a significantly improved conversion (78% at 24 h) in comparison with *p*-TsOH•H_2O (8% at 24 h). This suggested that water in the reaction mixture may play a detrimental role in the transformation. Thus, 1,3,5-triisopropylbenzene **423** was treated with 2.0 equivalents of malonoyl peroxide **90** in CH_2Cl_2 (0.5 M) in the presence of 2.0 equivalents of TfOH, TFA and MsOH, and 2.0 equivalents of water (Figure 35). Triflic acid on its own showed a >99% conversion after 24 h, but adding 2.0 equivalents of water significantly decreased this conversion to only 46% after 24 h. A similar effect was observed for the other two acids upon addition of 2.0 equivalents of water: 51% conversion at 24 h for TFA and H_2O, and 15% conversion at 24 h for MsOH and H_2O.
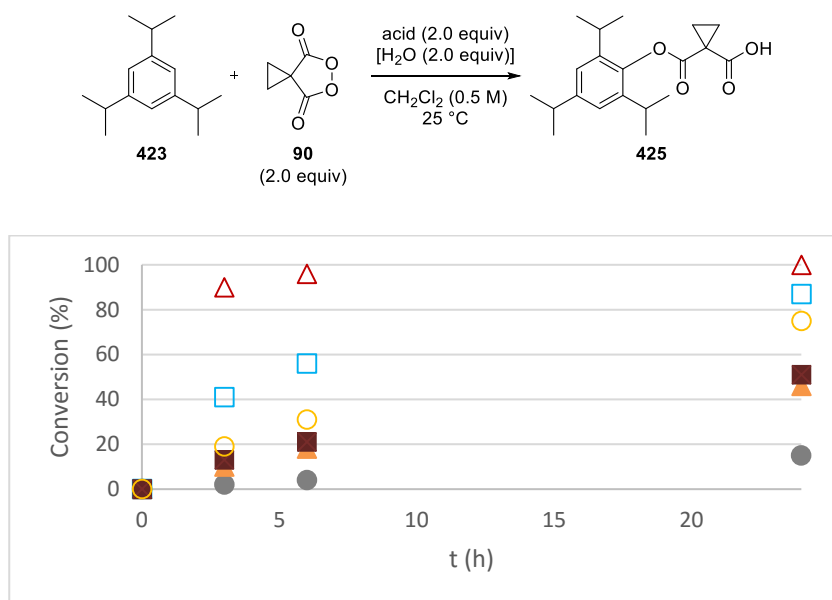
Figure 35: Effect of water on acid for reaction progress (△ TfOH; ☐ TFA; ◯ MsOH; ■ TFA and H_2O; ▲ TfOH and H_2O; ● MsOH and H_2O)

This observed interference in the presence of water could be attributed to a leveling effect of water on pK_a values.[166] Another possibility was that water interfered with acid additives such as **446** in different ways (Scheme 140). For example, malonoyl peroxide **90** could be activated using a generic acid H–X **446** *via* protonation of the carbonyl oxygen to form species **447** and its counterion **448** (Path A). Interference could have occurred *via* hydrogen bonding between malonoyl peroxide **90** and water to form a complex such as **449** (Path B) which would be less susceptible to protonation because of its lower electron density around

the carbonyl oxygen. Another potential disruption of the proposed activation of malonoyl peroxide **90** could be a simple ion pair consisting of hydronium ion **450** and anion **448** (Path C). These pathways would either deactivate the peroxide (Path B) or the additive (Path C), thus slowing down the overall rate of reaction.
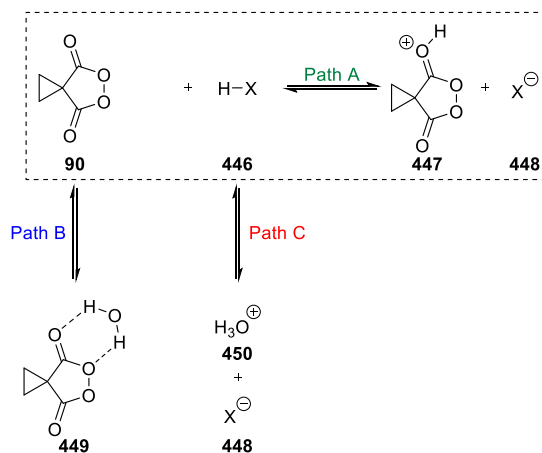
Scheme 140: Proposed pathways for water interference

Based on this observed effect of water on the acid mediated process, Tomasz Kubczyk examined the effect of water in the standard oxidation of mesitylene **395** (2.0 equivalents of malonoyl peroxide **90** in HFIP, Figure 36).[167] The effect of water was shown to be marginal, unless 50.0 equivalents of water were used, in which case the reaction slowed down.
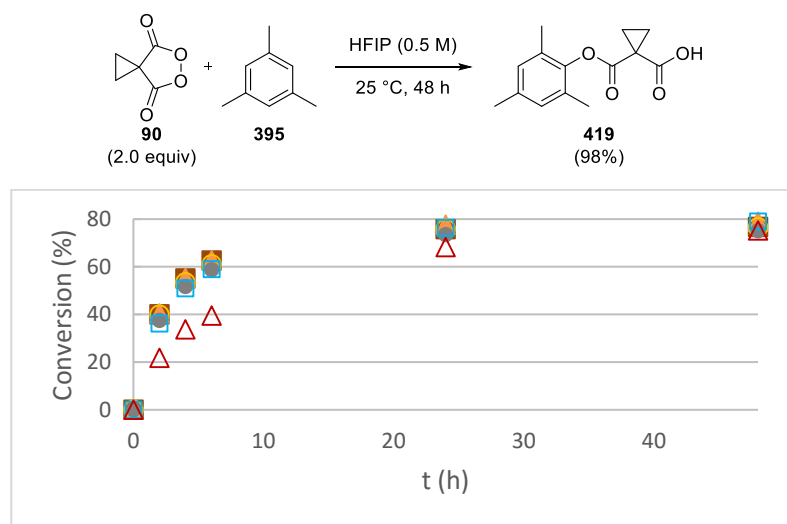
Figure 36: Effect of water equivalents on standard reaction progress
(■ 0.0 equiv; ▲ 1.0 equiv; ○ 2.0 equiv; ● 5.0 equiv; □ 10 equiv; △ 50 equiv)

All of these results suggested that malonoyl peroxide **90** required activation in order to react with the electron-rich arenes to form a new aromatic C–O bond. The successful use of additives has paved the way to a potential acid catalyzed process, meaning that the use of expensive and environmentally harmful solvents such as HFIP could be avoided or minimized in a future study. However, at this stage, it was of interest to obtain a better understanding of the reaction mechanism.

3.4 Mechanistic Investigations

The mechanism proposed by Houk and Siegel for the phthaloyl peroxide arene oxidation was a "reverse rebound" mechanism involving radical intermediates (Scheme 141).[152] The proposed mechanism involved phthaloyl peroxide **106** undergoing homolytic cleavage of the oxygen–oxygen bond to form diradical species **451**, which then reacted with an arene (mesitylene **395**) to form **452**. This intermediate then provided the observed ester **416** *via* hydrogen atom abstraction, which led to the corresponding phenol **396** upon hydrolysis. While this mechanism was proposed when using phthaloyl peroxide **106**, it was of interest if malonoyl peroxide **90** underwent the same or a similar type of mechanism, as shown in Scheme 142.
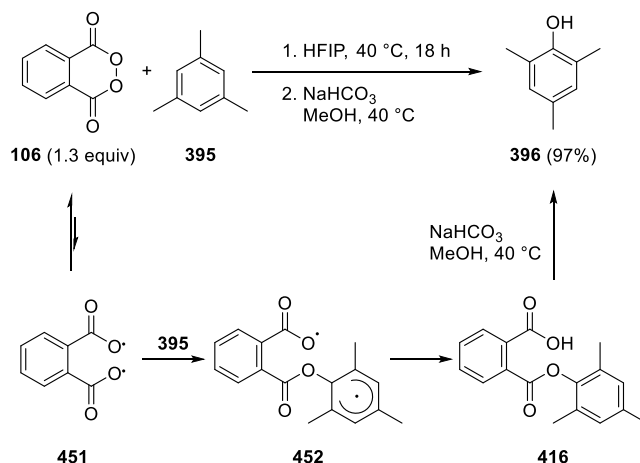
Scheme 141: Reverse rebound mechanism for the phthaloyl peroxide **106** mediated oxidation of arenes
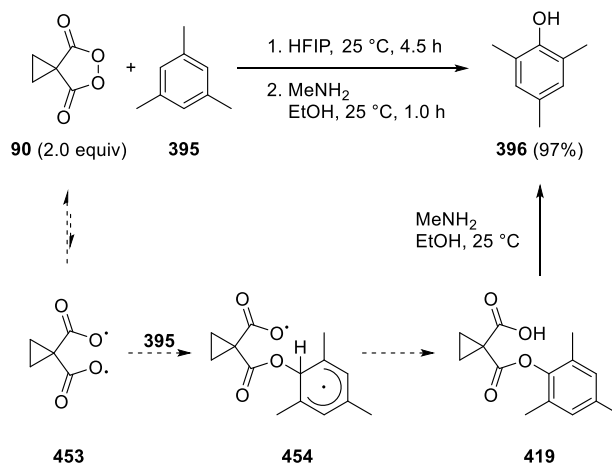
Scheme 142: Reverse rebound mechanism for the malonoyl peroxide **90** mediated oxidation of arenes

When using malonoyl peroxide **90** in the *syn*-dihydroxylation of alkenes, evidence suggested the reaction was an ionic process.[41] It was of interest if the reaction of malonoyl peroxide **90** with arenes occurred through an ionic process or through a "reverse rebound" process, similar to that proposed by Houk and Siegel.

3.4.1   Initial Findings

Initial observations when using malonoyl peroxide **90** for the oxidation of arenes suggested an ionic mechanism, specifically through an electrophilic aromatic substitution, with the rate determining step being the loss of aromaticity upon formation of the new C–O bond, generating Wheland intermediate **455** (Scheme 143). These observations included:

- Friedel-Crafts like reactivity (i.e. toluene **400** and anisole **404** only reacted through *ortho* and *para* positions – Table 11, entries 4 and 9).

- Acids promoted the reaction (Section 3.3), and disruption of H-bonding through the addition of water slowed down the process.

- Only electron-rich arenes reacted with peroxide **90** (Table 11), while electron-deficient substrates such as acetophenone **386** were unreactive under the optimized reaction conditions (Table 12).
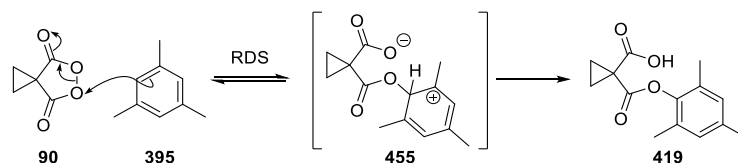
Scheme 143: Possible ionic mechanism for the oxidation of arenes

Preliminary investigations involved a series of parallel reactions using 1,3,5-triisopropylbenzene **423** and malonoyl peroxide **90** in HFIP (Scheme 144): one reaction was exposed to light and air; one exposed to light under an argon atmosphere; one in the dark and exposed to air; and one in the dark under an argon atmosphere. The reactions were monitored by ^{1}H NMR spectroscopy over time. No significant differences were observed, all reactions reaching conversions of 90–92% after 6 h. Performing the same reaction at 4 °C, in the dark and under argon, only decreased the rate (83% conversion after 24 h). All of these investigations combined showed that the reaction proceeds under very mild conditions and does not necessarily require light, oxygen or heat to initiate the process.
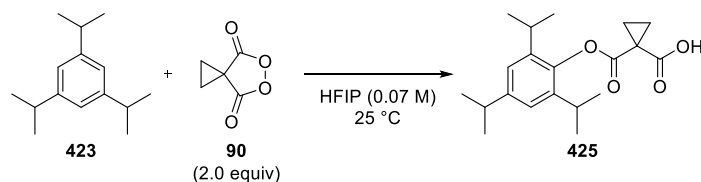
Scheme 144: Standard conditions for reactions in the presence/absence of light/air

3.4.2 DFT Calculations

A set of DFT calculations using Gaussian software on the homolytic bond cleavage of the O–O bond of peroxide **90** was performed using structures previously optimized by Dr. Julian Rowley.[41,69] Inspiration was taken from Houk and Siegel's paper concerning the level of theory used for frequency calculations, *i.e.* the energies of the compounds shown were computed using UB3LYP/6-31+G(d), in a similar manner to the phthaloyl peroxide **106** mediated arene oxidation reported.[152]

Most reactions using malonoyl peroxide **90** were shown to proceed in fluorinated alcohols at 25 °C. 2,2,2-Trifluoroethanol (TFE) was used as solvent in Gaussian, using Houk and Siegel's solvation model, CPCM (conductor polarized continuum model) at 298.15 K (25 °C). Upon simulating the homolytic bond cleavage of malonoyl peroxide **90** to generate diradical species **453** (24.8 kcal mol^{-1}), transition state **TS2** (29.7 kcal mol^{-1}) was found. Based on the high value obtained, it seemed unlikely that such an energy barrier (**TS2**) could be overcome at low temperatures such as 4 °C to form a diradical species **453**, conditions that have been shown to be effective for this transformation.
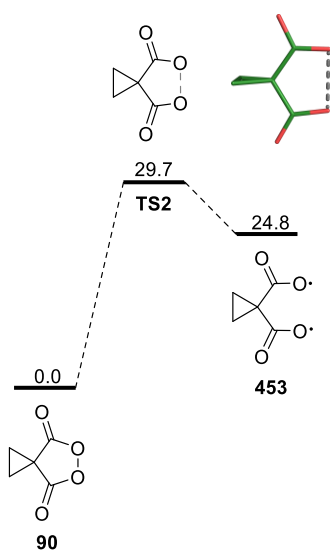
Figure 37: Malonoyl peroxide **90** homolytic cleavage transition state model

3.4.3 Reaction Kinetics

Mechanistic investigations were continued by determining the reaction order. A homogeneous solution of equimolar amounts of mesitylene **395** and malonoyl peroxide **90** in HFIP, using 1,4-dinitrobenzene as an internal standard, was monitored over time by ^{1}H NMR spectroscopy (Figure 38). Both starting materials were consumed at the same rate, giving ester **419** as the only product. No byproducts or coproducts were observed in the ^{1}H NMR spectra.
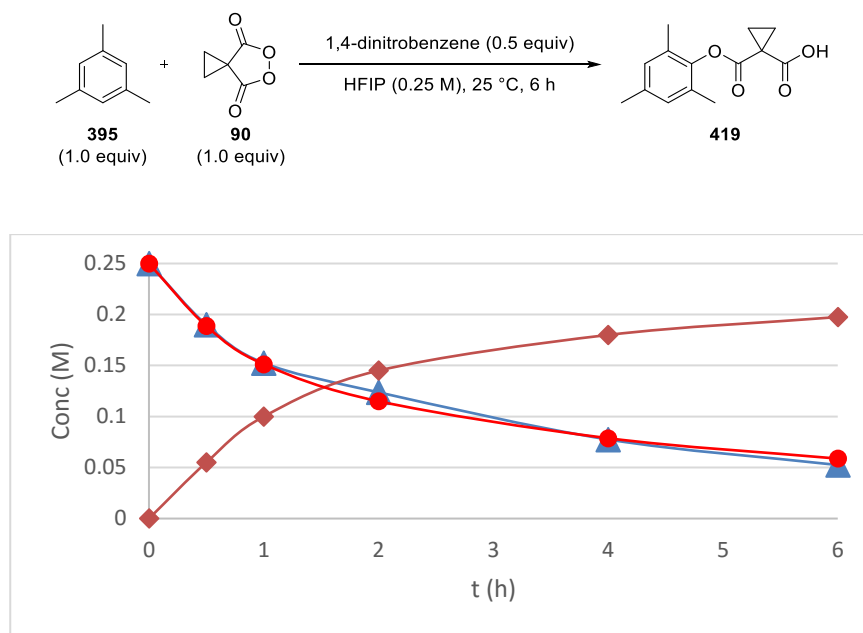
Figure 38: Reaction profile of the malonoyl peroxide **90** (▲, (0.25 M)) mediated oxidation of mesitylene **395** (●, (0.25 M)) leading to single product **419** (◆, (0.25 M))

Following this, the kinetic orders in peroxide **90** and mesitylene **395** were determined. It is generally desirable that a large excess of one of the reagents is used, in order to keep the concentration of one of the reagents constant to minimize error. For this, in a reaction with two components, a 50-fold or 100-fold excess would be ideal. A 10-fold excess is also acceptable, even though the error is larger.[168]

The kinetic order in malonoyl peroxide **90** was determined using a 10-fold excess of mesitylene **395** in HFIP (Figure 39). The reaction was monitored over 3 h measuring the consumption of peroxide **90** (conversion to product) by ^{1}H NMR spectroscopy against an internal standard (1,4-dinitrobenzene). The natural logarithm of the concentration of malonoyl peroxide **90** was plotted over time and a linear graph was obtained. This linear

graph suggested that the kinetic order in malonoyl peroxide **90** was first order, but given the fact that 10% of mesitylene **395** was also consumed the reaction was deemed pseudo first order in malonoyl peroxide **90**.[169]
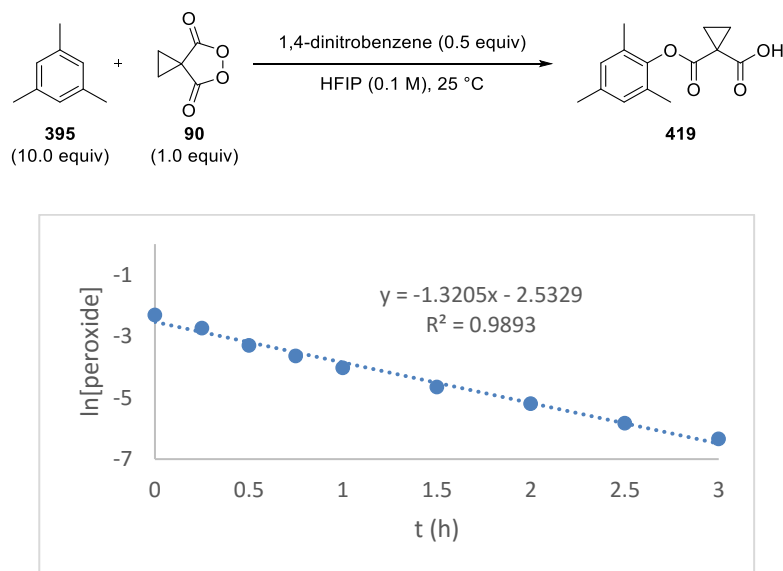
Figure 39: Reaction order in malonoyl peroxide **90**

The same analysis was performed to determine the kinetic order in mesitylene **395** (Figure 40). In this case, a 10-fold excess of malonoyl peroxide **90** was used. Plotting the natural logarithm of the concentration of mesitylene **395** over time generated a linear plot, thus meaning that the kinetic order was also pseudo first order in this reactant.
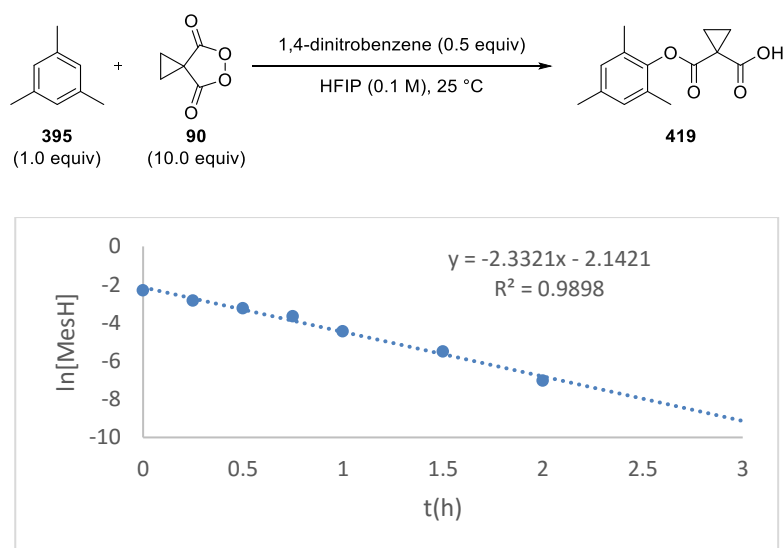
Figure 40: Reaction order in mesitylene **395**

After determining that the reaction was pseudo first order with respect to malonoyl peroxide **90** and mesitylene **395**, along with the equal consumption of both materials over time when used in equimolar amounts, the overall arene oxidation reaction was shown to follow pseudo second order kinetics overall. Thus, the reaction rate equation can be written as such:

$$\text{Rate} = k[\text{arene}][\text{peroxide}] \qquad \text{Equation 1}$$

When using equimolar amounts (*i.e.* [arene] = [peroxide]) such as shown in Figure 38, Equation 1 can be re-written in the following way:

$$\text{Rate} = k[\text{arene}]^2 \qquad \text{Equation 2}$$

Plotting 1/[arene] (*i.e.* 1/[MesH]) over time for the reaction shown in Figure 38 (79% conversion after 6 h) shows a linear relationship with a second order rate constant $k = 2.13 \ \text{M}^{-1}\text{h}^{-1}$ (Figure 41).
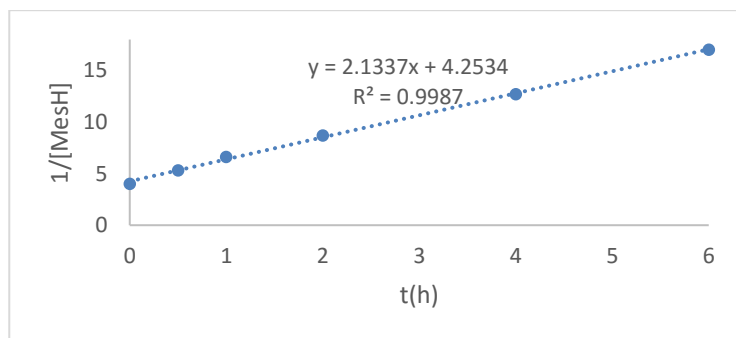
Figure 41: Linear plot of 1/[MesH] over time showing pseudo second order kinetics for the overall reaction

3.4.4   Hammett Analysis

In order to understand more about this transformation, a Hammett analysis was carried out.[170] The purpose of this study was to identify whether the same mechanism was operating for substrates bearing electron donating groups and electron withdrawing groups, as well as to verify if there was development of positive/negative charge in the transition state.

To begin the study, several mesitylene derivatives **456** were examined for their reactivity as substrates under the optimized reaction conditions (Table 13). It was already known that only electron-rich arenes reacted, thus it was no surprise that nitromesitylene **437** (Table 13, entry 7) was unreactive even upon heating (50 °C). Furthermore, 2,4,6-trimethylbenzoic acid **435** (Table 13, entry 6) was unreactive at 25 °C and required a higher temperature (50 °C) to react. These two substrates were excluded from the final Hammett study.

Table 13: Substrate scope for Hammett analysis
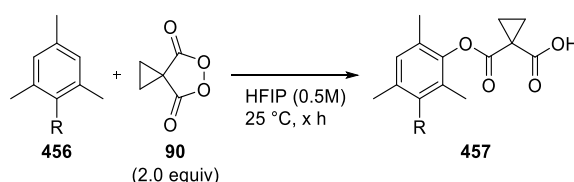
Entry	Compound	R	Yield (%)	t (h)
1	**395**	H	98%	4.5 h
2	**458**	OMe	97%	6 h
3	**433**	Br	91%	120 h
4	**459**	Me	98%	0.5 h
5	**460**	F	96%	8 h
6	**435**	CO$_2$H	86%	42 h[b]
7	**437**	NO$_2$	0%[a]	72 h[b]

[a] No change observed for nitromesitylene **437** under the attempted reaction conditions.
[b] Reaction performed at 50 °C.

The initial rates of the reactions of mesitylene derivatives **395**, **433**, **458–460** were determined in order to generate a Hammett plot. These were determined using the "initial rate method" which consisted of recording conversions over time as long as the plot of the reaction rate was still apparently linear.[171] Mesitylene derivatives **395**, **433**, **458–460** were reacted with one equivalent of malonoyl peroxide **90** using the conditions shown in Figure 42. The rate was determined by monitoring the consumption of the peroxide against an internal standard (1,4-dinitrobenzene) by ^{1}H NMR spectroscopy. The initial rates (slopes of the graphs) were recorded up to 10% conversion and with a minimum of 5 non-zero data points.
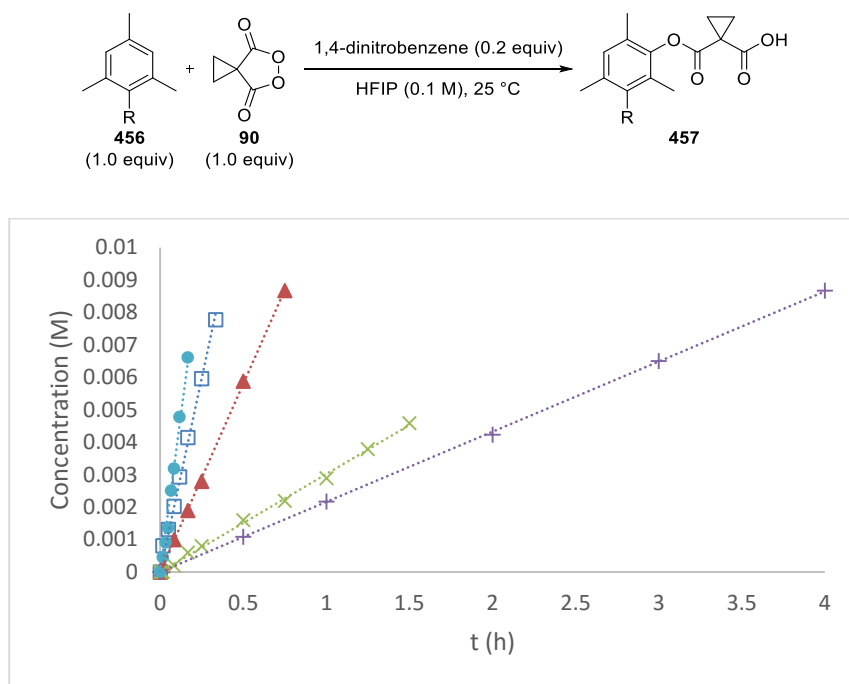
Figure 42: Initial rates of mesitylene derivatives **395, 433, 458–460**
(●, R = Me **459**; □, R = H **395**; ▲, R = OMe **458**; ✕, R = F **460**; +, R = Br **433**)

The initial rates (slopes) were converted to mol dm^{-3} s^{-1} and were reported in Table 14. In order to generate the Hammett plot, the H-substituent was considered the zero point, and the decimal logarithm of the fraction between the rates of all substituents was recorded against it. The σ parameters were chosen according to substrates: the reactive center was in the *meta* position relative to the substituent –R, hence σ_{para} coefficients were not considered; σ_{meta}^{+} and σ_{meta}^{-} parameters were also disregarded since there would be no resonance stabilization from –R substituents on the arene.[170] Thus, literature σ_{meta} values were used, as they only involve the inductive effect.[172]

Table 14: Data used for the Hammett plot

Entry	R	Initial rate (mol dm^{-3} s^{-1}), k	log(k_X/k_H)	σ_{meta}
1	Me	1.08×10^{-5}	0.21	−0.069
2	H	6.64×10^{-6}	0	0
3	OMe	3.22×10^{-6}	−0.31	0.115
4	F	8.33×10^{-7}	−0.90	0.337
5	Br	6.11×10^{-7}	−1.04	0.391

The Hammett plot was generated using the data in Table 14 (Scheme 145). The Hammett plot showed a linear relationship between the σ_{meta} values and the experimental log(k_X/k_H). This implied that the same mechanism was operating when both electron-donating and

electron-withdrawing substituents were attached to the mesitylene derivative.[170] The slope of the line indicated a moderate negative ρ value of –2.7, which is consistent with the build-up of a positive charge during the transition state of the reaction.[41,170] Furthermore, a moderate negative ρ value (i.e. –2.7) is consistent with electrophilic aromatic substitutions, which would support the mechanism proposed in Scheme 143.[173] This value suggests that the mechanism is likely to be ionic, given that free radical pathways tend to show small ρ values.[170,174]
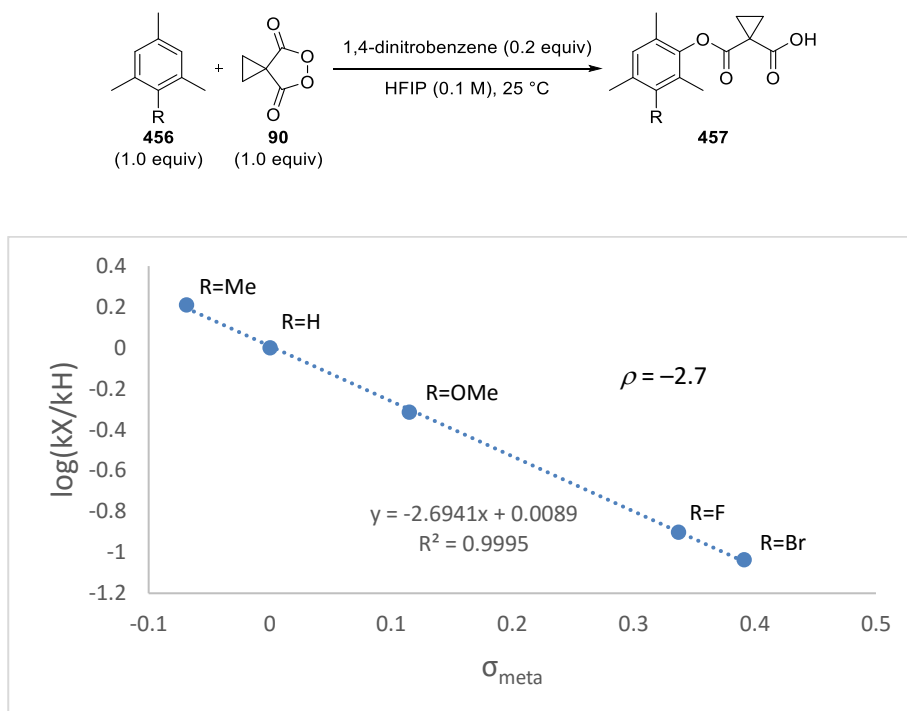
Scheme 145: Hammett plot for the reaction of mesitylene derivatives **395, 435, 458–460**

3.4.5 ^{18}O Labeling Experiments

Further mechanistic investigations were carried out using doubly ^{18}O labeled malonoyl peroxide **462** as a probe.[41,131] This peroxide was prepared from the corresponding dicarboxylic acid **461**. Labeled dicarboxylic acid **461** was synthesized by stirring its non-labeled counterpart **100** in ^{18}O-labeled water under an argon atmosphere at 40 °C for two weeks; the ^{18}OH$_2$ was then removed under reduced pressure and the solid mixture was re-subjected to the same procedure for a further two weeks (Scheme 146). The ^{18}O incorporation was monitored by mass spectrometry (ESI) and after the four weeks, 85% of the dicarboxylic acid had full incorporation of the label (15% bearing three ^{18}O labels). This species was then treated with H$_2$O$_2$•urea and doubly ^{18}O-labeled malonoyl peroxide **462** was

obtained in good yield (77%). It was not possible to unequivocally identify the position of the labels within the molecule, however, subsequent transformations are consistent with structure **462**, shown in Scheme 146.
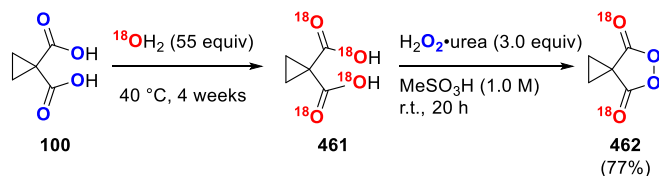
Scheme 146: Synthesis of malonoyl peroxide **462** with two ^{18}O labels incorporated

After preparing the ^{18}O labeled malonoyl peroxide **462**, it was examined in an arene oxidation reaction (Scheme 147). Treatment of mesitylene **395** with 1.35 equivalents of malonoyl peroxide **462** formed ester **463**, with two labels incorporated in its structure, as shown by GC-MS/CI. MS^n analysis using high resolution mass spectrometry suggested that one label (exchangeable) was located within the carboxylic acid terminus of the molecule, and the second was the carbonyl oxygen atom of the ester. Thus, these results suggested exclusive ^{16}O incorporation in the newly formed C–O bond.
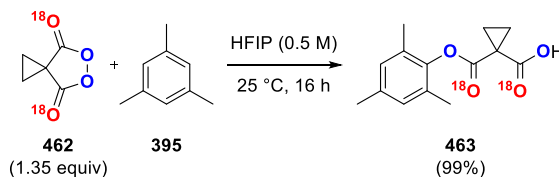
Scheme 147: Synthesis of mesitylene ester **463** having two ^{18}O labels incorporated

To corroborate this finding, a sample of the doubly labeled ester **463** was treated with methylamine and the crude reaction mixture was analyzed by GC-MS/CI (Scheme 148). The observed products were 2,4,6-trimethylphenol **396** with exclusive ^{16}O incorporation in the new C–O bond, amide **464** (bearing two ^{18}O labels), amide **465** (with only one ^{18}O label), and ^{18}O-labeled amide **466**. Amide **465** only showed one label, which was likely because of the carboxylic acid terminus that allowed the ^{18}O label to exchange with ^{16}O from fortuitous moisture, whereas amide **466** originated from decarboxylation of **464** or **465**. The identity of the reaction products in the mixture were confirmed by repeating the same reaction with non-labeled ester **419**. The retention times of the non-labeled products in the mixture corresponded to those in the labeling experiments (Scheme 149). This aminolysis showed that there was exclusive ^{16}O incorporation in the new C–O bond.
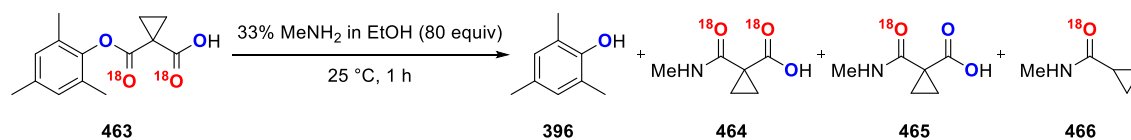
Scheme 148: Aminolysis of doubly ^{18}O-labeled mesitylene ester **463**
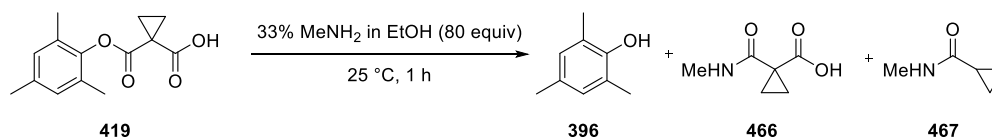
Scheme 149: Aminolysis of mesitylene ester **419**

The results from the labeling experiments were consistent with the ionic process shown in Scheme 143. If the process involved a homolytic bond cleavage of the peroxide O–O bond, as expected in a possible reverse-rebound process (Scheme 142), scrambling of the ^{18}O label across the peroxide would be expected (Scheme 150). This scrambling could have happened *via* rotation around the highlighted C–C bonds in diradical intermediate **469**, and would have been reflected in the products. It is possible that recombination of the diradical **469** to give peroxide **462** was faster than bond rotation, therefore the labels in **469** may not scramble. However, the observed selectivity in C–O bond formation would require addition of **469** to the mesitylene **395** to occur specifically through the unlabeled oxygen atom. This would appear unlikely, therefore we concluded through this labeling study that once again the results were consistent with an ionic mechanism.
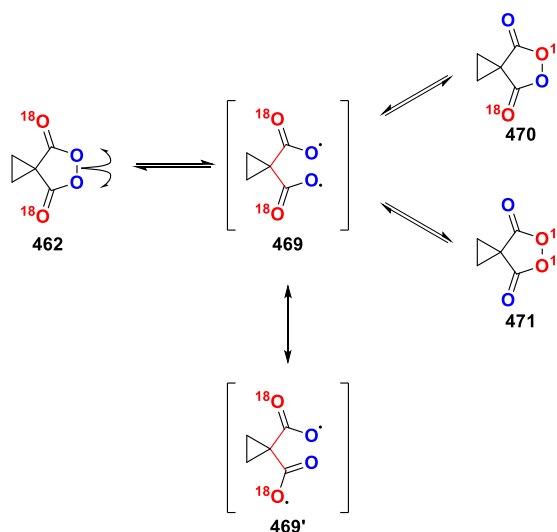
Scheme 150: Malonoyl peroxide **462** potential label scrambling *via* homolytic cleavage of the O–O bond

These findings suggested that malonoyl peroxide **462** did not undergo homolytic bond cleavage of its O–O bond under the reaction conditions examined. The results were particularly interesting since phthaloyl peroxide **106** was known for being able to scramble an [18]O label across the molecule, which was shown experimentally by Fujimori *et al.*[175] The results from the labeling experiments were consistent with the proposed ionic process (Scheme 143), but more mechanistic insights were needed at this stage.

3.4.6   Radical Clocks

Radical clocks are well known and established mechanistic probes for differentiation between ionic and radical transformations.[41,176] Of particular interest was a paper by Murphy and coworkers in which radical clock **472** was used for radical anion identification.[177] Radical clocks have also been isomerized from either their *cis*-**472** or *trans*-**474** isomers *via* a radical cation intermediate **473** (Scheme 151).[178] We believed this reported isomerization was ideal for learning more about the malonoyl peroxide **90** mediated arene oxidation.
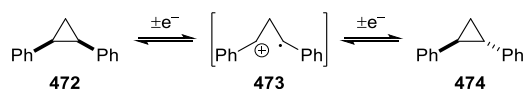
Scheme 151: Radical clock **472** *cis*-to-*trans* isomerization *via* radical cation **473**

Based on the type of radical clock described above and on the known low reactivity of toluene **400** (Section 3.2), Tomasz Kubczyk synthesized and examined a custom *cis*-cyclopropane based mechanistic probe **475** (Scheme 152).[167] This radical clock **475** was reacted with malonoyl peroxide **90** (1.0 equiv) in HFIP for 3 h at 25 °C. No products were purified or isolated at this stage and the crude reaction mixture was treated under aminolysis conditions to afford phenol **476** in very low yield (8%). The relative stereochemistry around the cyclopropane ring could not be determined, therefore the purified sample was methylated in an attempt to determine its structure. Again, the relative stereochemistry of product **477** could not be determined.
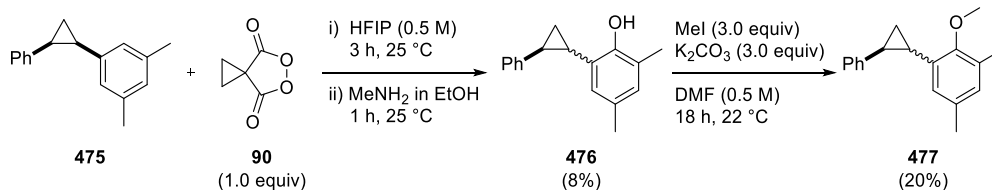
Scheme 152: Reaction of malonoyl peroxide **90** with radical clock **475**

In order to determine the stereochemistry of Tomasz Kubczyk's product **477**, I synthesized authentic samples of both *cis* and *trans* isomers of **477** independently. The first step for both retrosyntheses was the cyclopropanation step (Scheme 153); [177,179] subsequent methylation could lead to **478** and **480**. *trans*-Alkene **478** could be synthesized from the known aldehyde **479** *via* a Wittig or Horner-Wadsworth-Emmons reaction. [180,181] *cis*-Alkene **480** could be synthesized by *syn*-hydrogenation of the alkyne **481**, which could be formed *via* a Sonogashira cross-coupling reaction. [180]
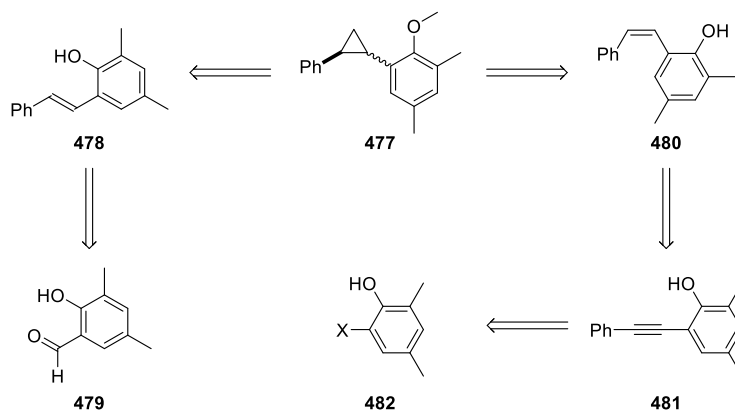
Scheme 153: Retrosyntheses of *cis*- and *trans*-isomers of **477**

The first route examined was the synthesis of the *cis*-alkene **480**, and the corresponding cyclopropanation product ***cis*-477**. First, aryl bromide **484** was synthesized from commercially available 2,4-dimethylphenol **483** in excellent yield (91%, Scheme 154). [182] Next, a Sonogashira coupling using aryl bromide **484** and phenylacetylene **485** was attempted. [167] This method did not provide alkyne **481** and only starting materials were observed. Allowing the reaction to run longer did not influence the transformation. This lack of reactivity was attributed to the presence of the phenolic –OH on aryl bromide **484**, which either hindered the reaction, or was deprotonating under the reaction conditions and interfering with the process.
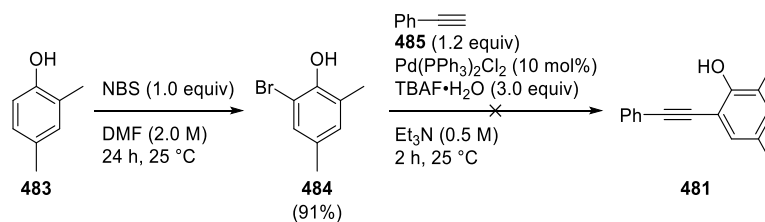
Scheme 154: Attempted synthesis of alkyne **481**

Because the previous attempt to generate alkyne **481** failed, a more reactive aryl halide,[183] aryl iodide **486** was prepared in very high yield (88%, Scheme 155).[184] It has been shown that under Sonogashira reaction conditions, phenolic –OH groups in the *ortho* position relative to the halide can lead to cyclization products such as benzofuran **487**.[185] As a result, in order to avoid this unwanted cyclization, the phenol functionality was methylated to afford anisole derivative **488** in excellent yield (86%).[186] This was reacted under Sonogashira conditions (Scheme 154), but no conversion to **489** was observed. Thus, a modified procedure for bulkier arenes was adopted and provided Sonogashira product **489** in 69% yield (Scheme 155).
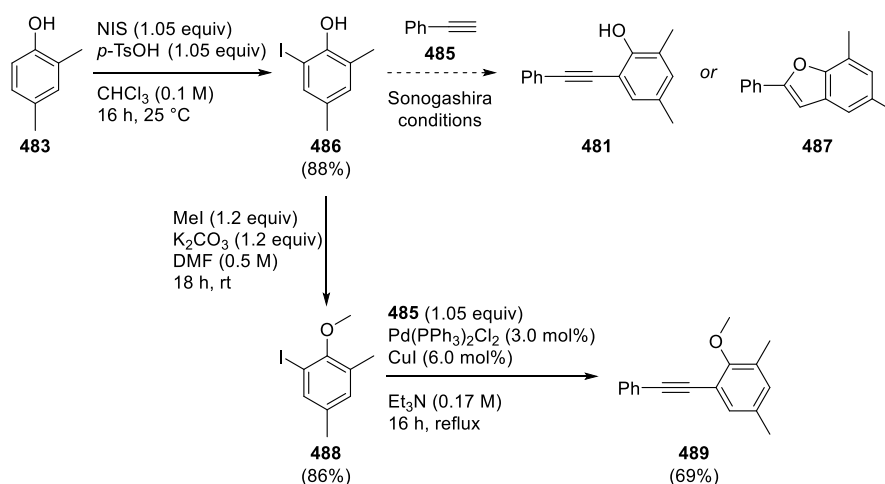
Scheme 155: Synthesis of alkyne **489**

The next step was to generate the *cis*-alkene **490** *via syn*-hydrogenation of alkyne **489**. The first attempt made use of Lindlar catalyst under a hydrogen atmosphere (Scheme 156).[167] However, the reaction resulted in >90% recovery of the starting material. A transfer hydrogenation procedure used for the hydrogenation of encumbered alkynes was applied to **489** and successfully provided *cis*-alkene **490** in 69% yield.[187] Alkene **490** was then reacted under cyclopropanation conditions and target molecule ***cis*-477** was obtained in excellent yield (87%, Scheme 156).[177] Target molecule ***cis*-477** was prepared geometrically pure in five steps from commercially available phenol **483** in 31% overall yield.
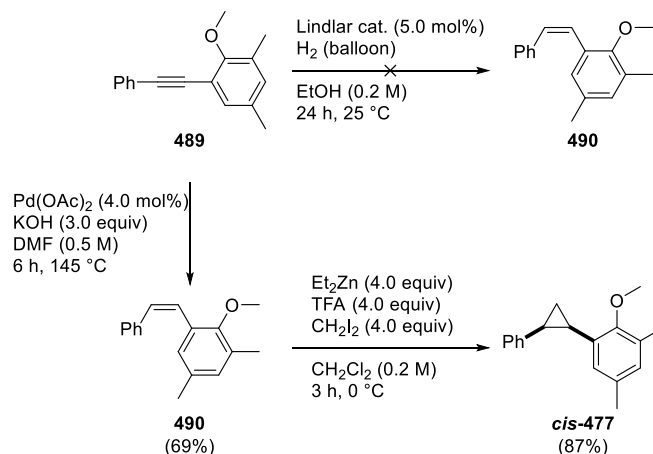
Scheme 156: Synthesis of *cis*-**477**

Comparison of the ^{1}H NMR spectrum of *cis*-**477** with that of **477** (Scheme 152) whose stereochemistry was unknown showed that the two molecules were different. This was not conclusive in unequivocally assigning the relative stereochemistry and the *trans*-alkene *trans*-**477** became the next target compound.

As shown in the rethrosynthesis (Scheme 153), aldehyde **479** was prepared from 2,4-dimethylphenol **483** using a literature preparation.[181] Aldehyde **479** was then reacted under Horner-Wadsworth-Emmons conditions with diethyl benzylphosphonate **491** to obtain *trans*-alkene **478** as a single isomer (Scheme 157).[188] The phenolic –OH of alkene **478** was then methylated under basic conditions to afford alkene **492** in 82% yield.[186] Alkene **492** was then reacted under the cyclopropanation conditions to generate the second target molecule *trans*-**477**.[177] Thus, target molecule *trans*-**477** was prepared geometrically pure in four steps from commercially available phenol **483** in 51% overall yield.
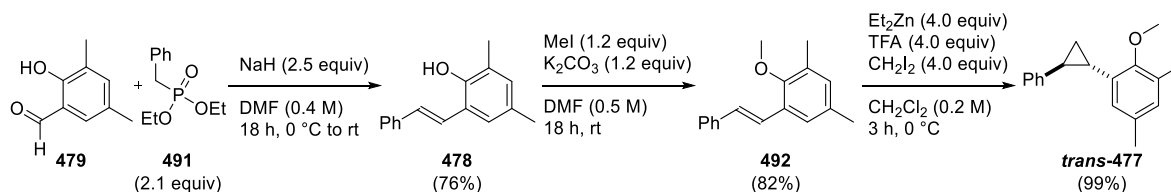
Scheme 157: Synthesis of *trans*-**477**

Comparison of the ^{1}H NMR spectrum of *trans*-**477** with that of compound **477** isolated by Tomasz Kubczyk showed a perfect overlap of the signals. Combining this finding with the

rest of the analytical data confirmed that the cyclopropane ring of radical clock **477** had indeed opened and isomerized under the arene oxidation conditions (Scheme 158).
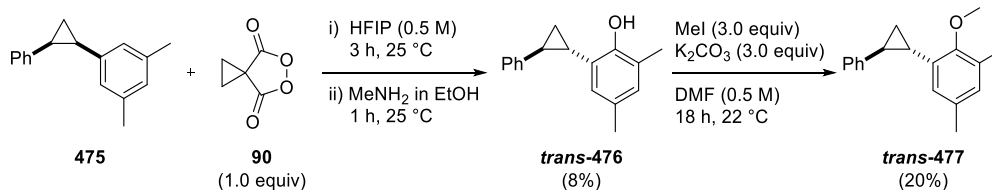
Scheme 158: Reaction of malonoyl peroxide **90** with radical clock **475**

The next step was to find out whether the isomerization occurred without malonoyl peroxide **90**. For that reason, Tomasz Kubczyk stirred the independently synthesized ***cis*-477** and radical clock **475** in HFIP for 24 h at 25 °C (Scheme 159). No change was observed in either case and the starting materials were recovered. This meant that the isomerization had happened during the oxidation reaction and in the presence of malonoyl peroxide **90**.
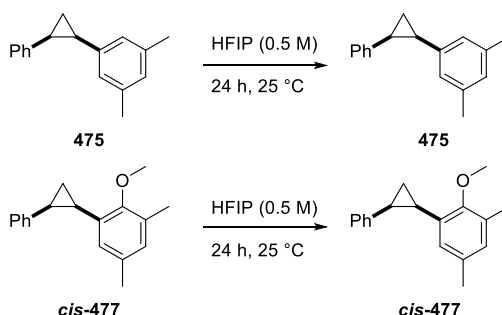
Scheme 159: Testing of isomerization in the absence of malonoyl peroxide **90**

The radical clock used may suggest that a radical mechanism was in operation, but considering the structure and all of the other observations and results so far, there is a possibility that mechanistic probe **477** underwent an ionic ring opening of the cyclopropane ring to form **493** (Scheme 160). With this mechanism, the inversion of stereoconfiguration occurred upon cyclization of proposed intermediate **494**.
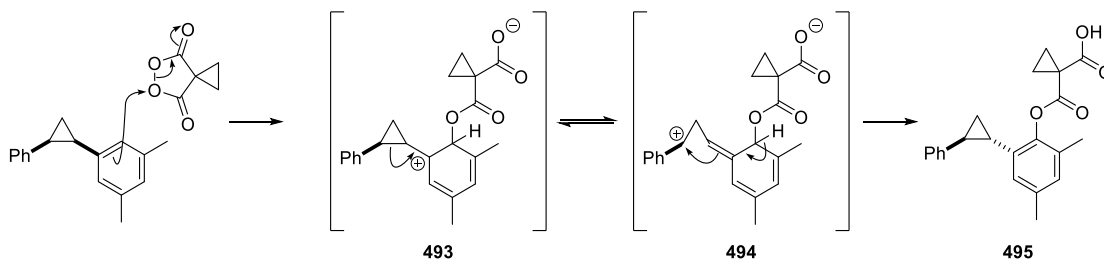
Scheme 160: Possible ionic mechanism for isomerization of radical clock **475**

Radical clock **475** also suggested there was a possibility of a single electron transfer (SET) mechanism to be operating (Scheme 161). This would imply that electron rich arene **475** donated an electron to malonoyl peroxide **90** to form the radical cation **496** and radical anion **497** intermediates which would then combine to form ester product **495**. This sort of mechanism is plausible, but unlikely if considering the ^{18}O labeling experiments (Section 3.4.5), because the oxygen atoms of radical anion **497** would be expected to scramble on formation of the new C–O bond.
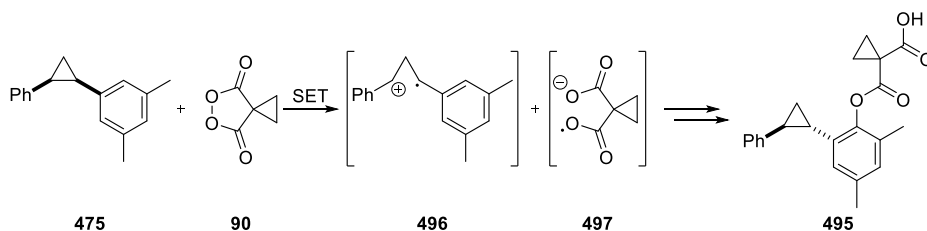
Scheme 161: Possible SET mechanism for isomerization of radical clock **475**

Overall, mechanistic probe **475** was successfully prepared and reacted with malonoyl peroxide **90**. The reaction was investigated and it showed reversal of the stereochemistry of the cyclopropane ring of **475**, but it was inconclusive for the mechanism. Furthermore, reaction of **475** with malonoyl peroxide **90** provided the phenol *trans*-**476** in only 8% yield and other components of the reaction mixture were not identified or isolated.[167] We had no more arene **475** remaining and we decided not to synthesize it again.

3.4.7 EPR Studies

Electron paramagnetic resonance (EPR) spectroscopy experiments were performed in collaboration with Dr. Stephen Sproules from the University of Glasgow who operated the spectrometer and analyzed the generated data. The aim was to find out if there were any noticeable radicals forming during a standard reaction, within the detection limits (ppb) of the spectrometer used, (Bruker ELEXSYS E500 spectrometer operating at 9.5 GHz). All of the experiments in this section were carried out under an inert atmosphere.

EPR spectroscopy is a very sensitive tool for detecting unpaired electrons, which is more sensitive than NMR.[189] The technique is so sensitive that it can detect free radicals at µM concentrations and at ppb levels.[190] Thus, to begin our studies, samples of mesitylene **395** and malonoyl peroxide **90** were scanned in TFE and HFIP to check if any of the two starting

materials displayed any EPR signal; nothing was observed. The components **395** and **90** were also allowed to react in a stoichiometric amount and the reaction was scanned over a period of 18 h. Once again, no radical species were detected by the EPR spectrometer.
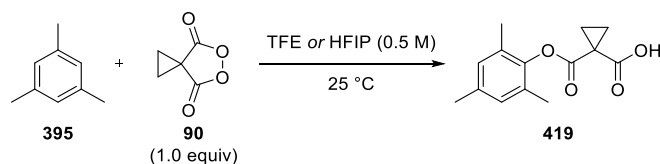
Scheme 162: Standard reaction for EPR studies

After these initial results in which no radicals were detected, Dr. Stephen Sproules suggested to use 5,5-dimethyl-1-pyrroline-*N*-oxide **498** (DMPO) as a spin trap in order to increase our chances of finding a radical species in the reaction mixture. DMPO **498** is a common spin trap used in EPR spectroscopy for the detection of oxygen radical species.[191] It is known to form a longer-lived radical species such as **499** which has a longer half-life on the EPR time scale (Scheme 163).[191,192]
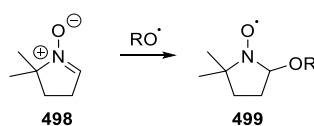
Scheme 163: DMPO **498** as a spin trap for a generic oxygen based radical

The spin trap was then added in an equimolar amount to a standard arene oxidation reaction between mesitylene **395** and malonoyl peroxide **90** which was monitored over 3 h by ¹H NMR against an internal standard and compared to a blank reaction without DMPO **498** (Scheme 164). The conversion after 3 h was 73% with DMPO **498** present in the mixture and 68% in the absence of the spin trap. This error was considered acceptable, but more importantly, there were no byproducts/coproducts observed in the ¹H NMR spectra recorded. Thus, DMPO **498** was considered ideal as a spin trap for EPR studies.
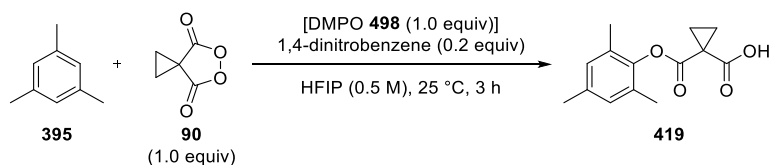
Scheme 164: Testing of DMPO **498** in a standard oxidation of mesitylene **395**

Initially, 0.5 M solutions of DMPO **498** in TFE and HFIP were examined by EPR to determine if there were any traces of radical species. No radicals were observed and these standard solutions could be used for further studies. A 0.5 M solution of malonoyl peroxide **90** (in TFE or HFIP) was mixed with two equivalents of DMPO **498** (0.5 M solution in TFE or HFIP) and no radical species were detected over 24 h (Scheme 165). Mesitylene **395** (1.0 equiv) was added to the two solutions of malonoyl peroxide **90** in TFE and HFIP, after which 0.5 M solutions of DMPO **498** in TFE or HFIP (2.0 equiv) were added. Once again, no radical species were observed over a period of 24 h.
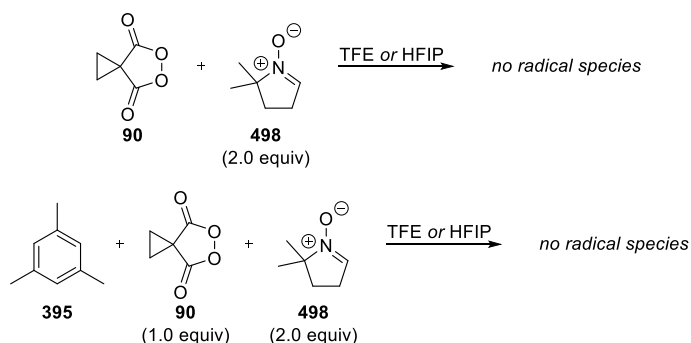
Scheme 165: Mixtures with DMPO **498** for EPR spectroscopy

Radical species were not detected by EPR spectroscopy, with or without a spin trap (DMPO **498**). EPR spectroscopy is known to be highly sensitive and to be able to detect radicals present in parts per billion. As none were observed in the experiments carried out, these results provided further evidence that radical species were not involved in this arene oxidation process.

3.5   Conclusions

Malonoyl peroxide **90** has been shown to be an effective reagent for the direct formation of aromatic C–O bonds. The advantages of using malonoyl peroxide **90** over phthaloyl peroxide **106** are its thermal and shock stability, bench stability for >3 months and its higher reactivity. The C–H functionalizations using **90** were performed under mild conditions (generally 25 °C), in the presence of moisture and air and without the need for specialized protocols (e.g. degassing solvents, inert atmosphere). A general reaction scheme is shown below for the oxidation of mesitylene **395** in HFIP at 25 °C, with the newly formed C–O bond highlighted in red (Scheme 166).
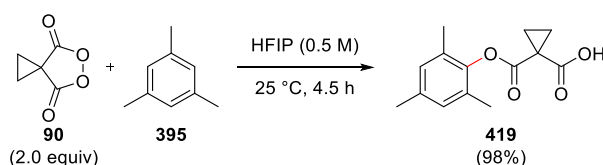
Scheme 166: Oxidation of mesitylene **395** using malonoyl peroxide **90**

The reaction profile indicated traits typical to an ionic process:

- Friedel-Crafts reactivity patterns were exhibited.
- Only electron rich arenes reacted.
- Hydrogen bond donors accelerated the reactions
- Reactions were the same in the presence or absence of light and/or air.

Extensive mechanistic studies were performed, including Hammett analysis, isotopic labeling and EPR studies, which were all consistent with an ionic mechanism. As a result, it was proposed that the reaction was an electrophilic aromatic substitution (Scheme 167), with mesitylene **395** attacking an oxygen of the weak peroxide O–O bond to form an intermediate such as **500**, which, upon protonation and rearomatization, led to ester product **463**.
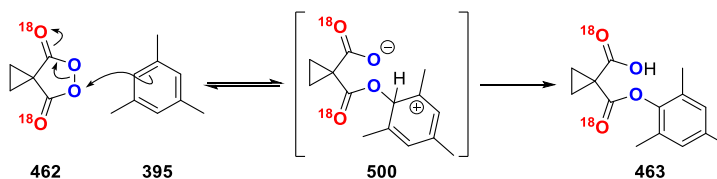
Scheme 167: Proposed mechanism for the oxidation of arenes

It was also shown that acids can act as additives to accelerate the reaction (Section 3.3), triflic acid being the most efficient (Scheme 168). Two equivalents of this strong acid converted 93% of 1,3,5-triisopropylbenzene **423** in the presence of peroxide **90** to the corresponding ester **425** in 3 h, without any observed byproducts/coproducts. This remarkable result paves the way for a potential acid-catalyzed arene oxidation. Furthermore, if this mode of activation significantly improves the reactivity of malonoyl peroxide **90**, it may also be extended to the oxidation of electron deficient arenes.
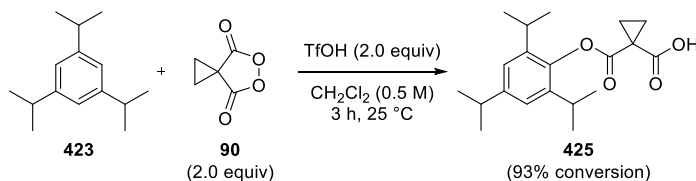
Scheme 168: Triflic acid-mediated oxidation of 1,3,5-triisopropylbenzene **423**

Chapter 4: Experimental

4.1   General Experimental Details

Commercially available solvents and reagents were used without further purification or drying and all reactions performed under an air atmosphere unless otherwise stated. Dry solvents were used directly from a PureSolv MD 5 Solvent Purification System by Innovative Technology Inc., and handled under inert atmosphere without further purification. Flash chromatography was carried out using Merck Kieselgel 60 H silica. Analytical thin layer chromatography was carried out using aluminum-backed plates coated with Merck Kieselgel 60 GF254 that were visualized under UV light (at 254 nm) or stained using $KMnO_4$. Nuclear magnetic resonance (NMR) spectra were recorded on a Bruker Avance III or a Bruker Avance spectrometer, operating at 400 MHz (^{1}H) and 101 MHz (^{13}C), respectively, or Bruker Avance DRX spectrometer, operating at 500 MHz (^{1}H) and 125 MHz (^{13}C), or Bruker Avance II spectrometer, operating at 600 MHz (^{1}H). Chemical shifts were reported in parts per million (ppm) in the scale relative to $CHCl_3$, 7.26 ppm for ^{1}H NMR and 77.16 for ^{13}C NMR; DMSO-d_6, 2.50 ppm for ^{1}H NMR and 39.52 for ^{13}C NMR; acetone-d_6, 2.05 for ^{1}H NMR and 206.26 for ^{13}C NMR. Multiplicities are abbreviated as: s, singlet; d, doublet; appd, apparent doublet; t, triplet; appt, apparent triplet; q, quartet; dd, doublet of doublets; appdd, apparent doublet of doublets; apptd, apparent triplet of doublets; appdq, apparent doublet of quartets; ddd, doublet of doublets of doublets; dtd, doublet of triplets of doublets; t appd, triplet of apparent doublets; appp, apparent pentet; hept, heptet; dhept, doublet of heptets; m, multiplet; br, broad. Coupling constants are measured in Hertz (Hz). Low-resolution mass spectra (LRMS) were recorded on an Agilent 6130 single quadrupole with APCI/ESI dual source, on a ThermoQuest Finnigan LCQ DUO electrospray, or on an Agilent 7890A GC system, equipped with a 30 m DB5MS column connected to a 5975C inert XL CI MSD with Triple-Axis Detector. High-resolution mass spectra (HRMS) were obtained courtesy of the EPSRC National Mass Spectrometry Facility at Swansea University, UK. Infrared spectra were recorded on a Shimadzu IRAffinity-1 equipped with ATR (Attenuated Total Reflectance) or on an Agilent 5500a FTIR equipped with ATR and were reported in cm^{-1}. Melting points were obtained on a Stuart SMP11 device. *In vacuo* refers to evaporation under reduced pressure using a rotary evaporator connected to a diaphragm pump, followed by the removal of trace volatiles using a high vacuum (oil) pump.

4.2   Syntheses of Malonoyl Hydroxylamines 115–117 and Related Compounds

Malonic acid 100[44]

100
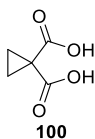
To 500 mL 50% aq. NaOH, benzyltriethylammonium chloride (56.5 g, 248 mmol, 1.0 equiv) was added. The resulting suspension was vigorously stirred using a mechanical stirrer and a mixture of diethyl malonate **108** (37.5 mL, 248 mmol, 1.0 equiv) and 1,2-dibromoethane (31.9 mL, 334 mmol, 1.35 equiv) was added. The reaction mixture was stirred for 2 h at room temperature and then the contents of the flask were transferred to a 2 L Erlenmeyer flask with water (3 × 50 mL). The resulting mixture was cooled down to 15 °C in an ice bath after which it was acidified with 500 mL HCl (37%, 12 M) over 1.5 h, keeping the temperature below 25 °C. The aqueous layer was extracted with Et$_2$O (3 × 300 mL). All ether layers were combined and washed with 500 mL brine, and then dried (MgSO$_4$). The solvent was removed under vacuum and the resulting white-yellow solids were triturated with petroleum ether to afford the title compound **21** as white solids (24.5 g, 192 mmol, 78%).

m.p. 132–133 °C (lit. 132–133 °C);[193] ^{1}H NMR (400 MHz, DMSO-*d$_6$*) δ 1.31 (s, 4H); ^{13}C NMR (101 MHz, DMSO-*d$_6$*) δ 171.8, 27.3, 16.2; LRMS (APCI/ESI) *m/z* 129.1 [M–H]⁻; IR (ATR)/cm⁻¹ 2988, 2820, 1705.

Malonic acid chloride 107[194]

107
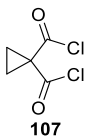
Dicarboxylic acid **100** (7.0 g, 54 mmol) was weighed into a pre-dried round bottom flask, and then SOCl$_2$ (54 mL, 0.65 mmol) was added to it. The flask was equipped with a condenser and a drying tube (CaCl$_2$) and the mixture was gently refluxed (76 °C) for 2 h. SOCl$_2$ was removed by rotary evaporation followed by 30 min under high vacuum to afford acyl chloride **107** as a brown liquid (7.0 g, 42 mmol, 78%).

^{1}H NMR (400 MHz, CDCl$_3$) δ 2.01 (s, 4H); ^{13}C NMR (101 MHz, CDCl$_3$) δ 168.5, 45.9, 21.5; IR (ATR)/cm^{-1} 3115, 1763, 1271.

N-Boc-Malonoyl hydroxylamine 115

115
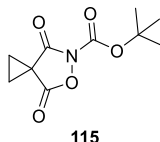
N-Boc-Hydroxylamine **109** (3.2 g, 24.0 mmol) was weighed into a pre-dried round bottom flask and dry dioxane (48 mL) was added. The mixture was cooled down to 0 °C and Et$_3$N (6.7 mL, 48.0 mmol) was added, followed by dropwise addition of acyl chloride **107** (4 g, 24.0 mmol). The reaction mixture was allowed to warm up to room temperature over 1.5 h and was stirred for 3 additional hours at 20 °C. The mixture was then diluted with water (30 mL) and was extracted with EtOAc (3 × 50 mL). The organic extracts were combined and washed with 0.2 M HCl (30 mL), brine (50 mL) and dried (MgSO$_4$). The solution was concentrated and remaining volatiles were removed under high vacuum to provide a yellow oil which was triturated with Et$_2$O. The resulting solids were filtered and washed with cold Et$_2$O (3 × 10 mL) to afford the title compound as a white powder (2.4 g, 17.6 mmol, 73%).

m.p. 91–92 °C dec; ^{1}H NMR (400 MHz, CDCl$_3$) δ 2.03–1.95 (m, 4H), 1.60 (s, 9H); ^{13}C NMR (101 MHz, CDCl$_3$) δ 168.7, 165.8, 144.5, 87.1, 28.1, 24.5, 23.3; HRMS (FTMS-NSI): calculated for C$_{11}$H$_{18}$NO$_6$ 260.1129 [M+MeOH+H]$^+$, found 260.1129; IR (ATR)/cm^{-1} 2964, 1820, 1782, 1705.

N-Cbz-Malonoyl hydroxylamine 116

116
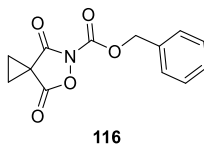
N-Cbz-Hydroxylamine **110** (2.0 g, 12.0 mmol) was weighed into a pre-dried round bottom flask and dry dioxane (24 mL) was added. The mixture was cooled down to 0 °C and Et$_3$N (3.4 mL, 24.0 mmol) was added, followed by dropwise addition of acyl chloride **107** (2.0 g,

12.0 mmol). The reaction mixture was allowed to warm up to room temperature over 1.5 h and was stirred for 1.5 additional h at 20 °C. The mixture was then diluted with water (15 mL) and was extracted with EtOAc (3 × 30 mL). The organic extracts were combined and washed with 0.2 M HCl (15 mL), brine (30 mL) and dried (MgSO$_4$). The solution was concentrated and the crude was chromatographed on silica gel (EtOAc:petroleum ether, 1:1, R_f = 0.6) to afford the title compound as a white solid (770 mg, 2.95 mmol, 25%).

m.p. 108–109 °C; ^{1}H NMR (400 MHz, CDCl$_3$) δ 7.47–7.43 (m, 2H), 7.42–7.36 (m, 3H), 5.40 (s, 2H), 2.06–1.99 (m, 4H); ^{13}C NMR (101 MHz, CDCl$_3$) δ 168.3, 165.5, 146.0, 134.1, 129.2, 128.9, 128.8, 70.0, 24.3, 23.6; HRMS (FTMS-NSI): calculated for C$_{14}$H$_{19}$N$_2$O$_6$ 311.1238 [M+MeOH+NH$_4$]$^+$, found 311.1242; IR (ATR)/cm^{-1} 3098, 2924, 1815, 1763, 1747.

N-Tosylhydroxylamine 114[195]

114
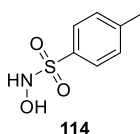
Hydroxylamine hydrochloride **111** (600 mg, 8.6 mmol) was dissolved in MeOH/H$_2$O (3:2, 5 mL) and was then treated with MgO (350 mg, 8.6 mmol), after which a solution of TsCl (820 mg, 4.3 mmol) in THF (30 mL) and MgO (170 mg, 4.3 mmol) were subsequently added. The reaction mixture was vigorously stirred at 20 °C, and was filtered through a pad of celite and a short plug of silica gel, using EtOAc as eluent. The resulting organic solution was dried (MgSO$_4$) and the solvent was evaporated to provide the title compound (670 mg, 3.6 mmol, 83%).

m.p. 127–128 °C, (lit. 129 °C);[196] ^{1}H NMR (400 MHz, CDCl$_3$) δ 7.87–7.82 (m, 2H), 7.40–7.35 (m, 2H), 2.46 (s, 3H); ^{13}C NMR (101 MHz, CDCl$_3$) δ 130.0, 129.7, 129.5, 128.9, 21.9; LRMS (EI) *m/z* 186.1 [M–H]$^-$; IR (ATR)/cm^{-1} 3377, 3254, 1595, 1159.

Diethyl cyclopropane-1,1-dicarboxylate 120[197]

120
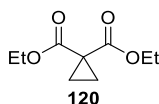
K_2CO_3 (64 g, 464 mmol) and tetrabutylammonium hydrogensulfate (1.0 g, 2.9 mmol) were dissolved in DMSO (50 mL) and then a mixture of diethylmalonate **108** (9.5 mL, 63 mmol) and 1,2-dibromoethane (10 mL, 116 mmol) was added. The reaction mixture was stirred for 24 h at 20 °C after which it was poured into 300 mL water. This was followed by extraction with Et_2O (5 × 100 mL) and the combined organic extracts were washed with brine (100 mL) and dried ($MgSO_4$). The solvent was removed and the resulting oil was distilled under vacuum (100 °C, 20 mbar) to afford the title compound **120** as a colorless oil (8.3 g, 44.6 mmol, 71%).

^{1}H NMR (400 MHz, $CDCl_3$) δ 4.20 (q, *J* = 7.1 Hz, 4H), 1.43 (s, 4H), 1.28 (t, *J* = 7.1 Hz, 6H); ^{13}C NMR (101 MHz, $CDCl_3$) δ 170.0, 61.5, 28.4, 16.5, 14.2; LRMS (APCI/ESI) *m/z* 187.1 [M+H]$^+$; IR (ATR)/cm^{-1} 2982, 1720.5, 1173, 1130.

Malonoyl hydroxylamine 117

117
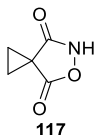
Procedure 1

To a pre-dried round bottom flask, *N*-Boc malonoyl hydroxylamine **115** (227 mg, 1.0 mmol) was weighed. Dry CH_2Cl_2 (5 mL) was added and the solution was cooled down to 0 °C. Trifluoroacetic acid (TFA, 1.53 mL, 20.0 mmol) was added dropwise, keeping the temperature of the mixture at 0 °C. After addition of TFA, the solution was allowed to warm up to 20 °C over 1.5 h. The solvent was removed *in vacuo* and the crude reaction mixture was triturated with petroleum ether to afford the title compound as a white powder (123 mg, 0.97 mmol, 97%).

Procedure 2

To a solution of hydroxylamine (3.3 mL, 53.2 mmol) and EtONa (3.36 g, 53.2 mmol) in EtOH (10 mL) at 0 °C, diester **120** (4.0 mL, 21.3 mmol) in EtOH (5 mL) was added. The reaction was stirred at 0 °C for 1.5 h, then at 25 °C for 16 h. Afterward, the solvent was removed *in vacuo* and the remaining solids were dissolved carefully in a minimum amount of 3.0 M HCl. The resulting aqueous solution was extracted with CH_2Cl_2 (5 × 15 mL) and the combined organic extracts were dried ($MgSO_4$) and concentrated. The resulting pale yellow solids were crystallized ($CHCl_3$/petroleum ether) to afford the title compound as a white powder (790 mg, 6.2 mmol, 29%).

m.p. 100–101 °C, (lit. 103–105 °C);[45] ^{1}H NMR (400 MHz, $CDCl_3$) δ 7.80 (br, 1H), 1.97–1.92 (m, 4H); ^{13}C NMR (101 MHz, $CDCl_3$) δ 174.8, 172.2, 23.4, 22.1; LRMS (APCI/ESI) *m/z* 128.1 [M + H]$^+$; HRMS (APCI) calculated for $C_5H_6O_3N_1$ [M+H]$^+$ 128.0342, found 128.0339; IR (ATR)/cm^{-1} 3024, 1703, 1659.

4.3 Reactions of Malonoyl Hydroxylamines with Morpholine 133

N-Boc-Morpholine 134[198]

134
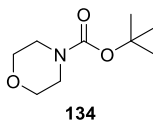
N-Boc-Malonoyl hydroxylamine **115** (102 mg, 0.45 mmol) was dissolved in a vial containing $CHCl_3$ (0.9 mL) and then morpholine **133** (33 μL, 0.375 mmol) was added. The mixture was stirred for 4 h at 40 °C and then the solvent was vacuumed down. The resulting mixture was chromatographed on silica gel (EtOAc:petroleum ether, 1:1) to afford the title compound as a white solid (43 mg, 0.23 mmol, 61%).

m.p. 57–58 °C, (lit. 57–60 °C);[198] ^{1}H NMR (400 MHz, $CDCl_3$) δ 3.66–3.60 (m, 4H), 3.43–3.38 (m, 4H), 1.46 (s, 9H); ^{13}C NMR (101 MHz, $CDCl_3$) δ 154.8, 80.0, 66.8, 44.2, 28.5; IR (ATR)/cm^{-1} 2978, 2966, 1690.

***N*-Cbz-Morpholine 135[199]**

135
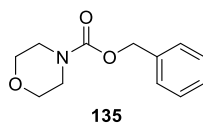
N-Cbz-Malonoyl hydroxylamine **116** (118 mg, 0.45 mmol) was dissolved in a vial containing CHCl₃ (0.9 mL) and then morpholine **133** (33 µL, 0.375 mmol) was added. The mixture was stirred for 16 h at 40 °C and then the solvent was vacuumed down. The resulting mixture was chromatographed using silica gel (EtOAc:petroleum ether, 1:1) to afford the title compound as a white-yellow solid (61 mg, 0.27 mmol, 72%).

m.p. 46–47 °C, lit. 47–50 °C;[199] ^{1}H NMR (500 MHz, CDCl₃) δ 7.40–7.30 (m, 5H), 5.15 (s, 2H), 3.65 (s, 4H), 3.50 (dd, *J* = 6.1, 3.7 Hz, 4H); ^{13}C NMR (125 MHz, CDCl₃) δ 155.4, 136.7, 128.7, 128.3, 128.1, 67.4, 66.7, 44.3; LRMS (EI) *m/z* 222.1 [M+H]⁺; IR (ATR)/cm⁻¹ 2962, 2857, 1697.

4.4   Nitriles Generated in the Attempted Synthesis of Imidoperoxide 140

Malononitrile 142[200]

142

Malononitrile **143** (5.0 g, 75.7 mmol) was dissolved in THF (100 mL). Then, 1,2-dibromoethane (13 mL, 151.4 mmol) was added, followed by K₂CO₃ (31.0 g, 224 mmol). The reaction mixture was refluxed for 2 h and then it was cooled down to room temperature. The solvent was removed and water (200 mL) was added to dissolve excess K₂CO₃. The aqueous layer was extracted with Et₂O (3 × 150 mL), and the resulting organic phase was washed with brine (100 mL), dried (MgSO₄) and concentrated. The resulting brown oil was distilled using a Kugelrohr apparatus (130 °C, 15 mbar) to afford dinitrile **142** as a colorless oil (1.8 g, 19.5 mmol, 26%).

^{1}H NMR (400 MHz, CDCl₃) δ 1.83 (s, 4H); ^{13}C NMR (100 MHz, CDCl₃) δ 115.3, 18.7, −1.2; IR (ATR)/cm⁻¹ 3117, 3032, 2253, 1429.

1-Cyanocyclopropane-1-carboxamide 145[201]

145
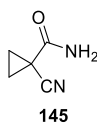
Cyclopropyl malononitrile **142** (92 mg, 1.0 mmol) was dissolved in $MeSO_3H$ (1 mL) and then H_2O_2•urea (282 mg, 3.0 mmol) was added to the solution. The resulting mixture was stirred for 48 h at 20 °C and then it was diluted with EtOAc (10 mL) and cold water (5 mL). The layers were separated and the aqueous layer was extracted again with EtOAc (3×10 mL). The combined organics were washed with sat. $NaHCO_3$ (10 mL), brine (10 mL), dried ($MgSO_4$) and concentrated. The crude mixture was chromatographed on silica gel (EtOAc:petroleum ether, 1:1) to obtain the title compound **145** as a white solid (37 mg, 0.34 mmol, 34%).

m.p. 157–158 °C, lit. 158–160;[201] ^{1}H NMR (400 MHz, $CDCl_3$) δ 6.37 (br, 1H), 5.67 (br, 1H), 1.71 (dd, J = 8.2, 4.4 Hz, 2H), 1.54 (dd, J = 8.2, 4.4 Hz, 2H); ^{13}C NMR (101 MHz, DMSO-*d6*) δ 167.1, 120.2, 16.5, 13.4; IR (ATR)/cm^{-1} 3390, 3180, 2929, 2249.

4.5   Payne Epoxidation Reactions

General procedure for the Payne epoxidations (General Procedure 1)

To a pre-dried flask, $KHCO_3$ (20.2 mg, 0.2 mmol), *E*- or *Z*-stilbene (180.3 mg, 1.0 mmol), H_2O_2•urea (564 mg, 6.0 mmol) were weighed. Then, dry MeOH (2 mL) and benzonitrile **147** (0.62 mL, 6.0 mmol) were added. The reaction was monitored against an internal standard, 1,4-dinitrobenzene (16.8 mg, 0.1 mmol) over 24 h at 50 °C. Mini work-ups were performed using water and CH_2Cl_2 and the reactions were examined by ^{1}H NMR.

Reactions using the nitriles shown in Table 2 were followed this procedure.

E-Stilbene oxide 139[202]

139
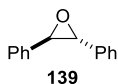
Procedure 1

The reaction was set up according to General Procedure 1 and was quenched with water (10 mL) after 24 h, followed by extraction of the aqueous mixture with CH_2Cl_2 (3 × 10 mL). The combined organic layers were then dried ($MgSO_4$) and concentrated. The crude reaction mixture was then chromatographed on silica gel (EtOAc:petroleum ether, 1:9) to afford the title compound as a white solid (79 mg, 0.44 mmol, 44%).

Procedure 2

E-stilbene **68** (180.3 mg, 1.0 mmol) and $NaHCO_3$ (100.8 mg, 1.2 mmol) were stirred in CH_2Cl_2 (4 mL) and *m*-CPBA (269 mg, 1.2 mmol) was then added. The reaction mixture was stirred at 20 °C for 16 h and the solvent was removed *in vacuo*. The crude mixture was chromatographed on silica gel (EtOAc:petroleum ether, 1:9) to afford the title compound as a white solid (178 mg, 0.91 mmol, 91%).

m.p. 68–68 °C (lit. 68–69 °C);[202] ^{1}H NMR (400 MHz, $CDCl_3$) δ 7.43–7.32 (m, 10H), 3.88 (s, 2H); ^{13}C NMR (101 MHz, DMSO) δ 137.3, 128.7, 128.5, 125.7, 63.0; LRMS (CI) *m/z* 197.1 [M+H]$^+$; IR (ATR)/cm^{-1} 3061, 2988, 2924, 1452.

Z-Stilbene oxide 25[202]

25
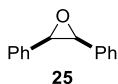
Z-Stilbene **162** (180.3 mg, 173 µL, 1.0 mmol) and $NaHCO_3$ (100.8 mg, 1.2 mmol) were stirred in CH_2Cl_2 (4 mL) and *m*-CPBA (269 mg, 1.2 mmol) was then added. The reaction mixture was stirred at 20 °C for 16 h and the solvent was removed *in vacuo*. The crude mixture was chromatographed on silica gel (EtOAc:petroleum ether, 1:9) to afford **25** as a white solid (160 mg, 0.81 mmol, 81%).

m.p. 35–36 °C, (lit. 35–37 °C);[202] ^{1}H NMR (400 MHz, CDCl$_3$) δ 7.20–7.12 (m, 10H), 4.36 (s, 2H); ^{13}C NMR (101 MHz, CDCl$_3$) δ 134.5, 127.9, 127.7, 127.0, 59.9; LRMS (CI) *m/z* 197.1 [M + H]$^+$; IR (ATR)/cm^{-1} 3061, 3030, 2976, 1497.

4.6   Syntheses of Phthaloyl Hydroxylamines 183 and 184

N-Boc phthaloyl hydroxylamine 183[203]

183
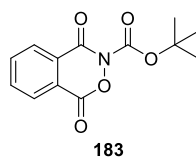
A pre-dried three-neck round bottom flask placed under an argon atmosphere at 0 °C was charged with dry CH$_2$Cl$_2$ (300 mL) and then phthaloyl chloride **185** (10.0 mL, 1.0 equiv, 68 mmol) was added *via* syringe. A solution of Et$_3$N (23.6 mL, 2.5 equiv, 170 mmol) and *N*-Boc-hydroxylamine **109** (13.6 g, 1.5 equiv, 102 mmol) in dry CH$_2$Cl$_2$ (50 mL) was added dropwise to the mixture at 0 °C. The reaction mixture was allowed to warm up to room temperature over 6 h, after which it was quenched using HCl (2.0 M, 100 mL) and allowed to stir for a further 20 min. The CH$_2$Cl$_2$ layer was collected and the resulting aqueous layer was extracted with EtOAc (2 × 100 mL). The organic solutions were combined, dried (MgSO$_4$) and concentrated. The sticky off-white crude solids was triturated with Et$_2$O (100 mL), the resulting solids were dissolved in THF (125 mL) and the filtrate was concentrated *in vacuo* to afford the title compound as a white solid (5.7–10.1 g, 22–38 mmol, 32–56%).

m.p. 154–155 °C (dec, gas evolution at 132–133 °C); ^{1}H NMR (400 MHz, CDCl$_3$) δ 8.40–8.33 (m, 1H), 8.27–8.24 (m, 1H), 7.98–7.86 (m, 2H), 1.64 (s, 9H); ^{13}C NMR (101 MHz, CDCl$_3$) δ 158.8, 156.4, 146.3, 136.1, 135.1, 130.0, 129.8, 128.9, 124.0, 86.9, 28.1; HRMS (FTMS-NSI): calculated for C$_{14}$H$_{21}$N$_2$O$_6$ 313.1394 [M+MeOH+NH$_4$]$^+$, found 313.1397; IR (ATR)/cm^{-1} 2982, 1781, 1760, 1712.

Phthaloyl hydroxylamine 184[203,204]

184
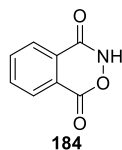
A 50 mL round bottom flask equipped with a stir bar was charged with phthaloyl hydroxylamine **183** (2.1 g, 1.0 equiv, 8.0 mmol) followed by the addition of CH_2Cl_2 (8 mL). The mixture was stirred at room temperature until **183** was dissolved and then TFA (6.2 mL, 10.0 equiv, 80 mmol) was added in one portion. The resulting mixture was stirred for 1 h after which the solvent was removed *in vacuo* and the resulting crude was triturated with Et_2O to afford the title compound as a white powder (1.05 g, 6.4 mmol, 80%).

m.p. 220–221 °C (dec, lit. 222–224 °C);[204] ^1H NMR (400 MHz, DMSO-d_6) δ 12.83 (s, br, 1H), 8.18 (d, J = 7.7 Hz, 1H), 8.09–7.93 (m, 3H); ^{13}C NMR (101 MHz, CDCl$_3$) δ 158.6, 135.9, 134.2, 128.6, 125.5, 123.3 (2 carbons not observed); LRMS (APCI) *m/z* 162.0 [M–H]⁻; HRMS (FTMS-NSI): calculated for $C_8H_6NO_3$ 164.0342 [M+H]⁺, found 164.0340; IR (ATR)/cm⁻¹ 3026, 2837, 1760, 1729.

4.7 Syntheses of Alkylidene Phthalides (Substrate Scope)

4.7.1 General Procedure for Alkylidene Phthalide Formation (General Procedure 2)

A pre-dried Schlenk flask placed under an argon atmosphere at –78 °C was charged with a solution of LiHMDS in THF (1.0 M, 2.0 equiv, 1.0 mmol). A solution of the ketone in THF (0.7 M, 1.0 equiv, 0.5 mmol) was added dropwise to the LiHMDS solution at –78 °C. The resulting mixture was allowed to stir at the same temperature for 30 min after which a solution of **183** in THF (0.25 M, 2.0 equiv, 1.0 mmol) was added dropwise at –78 °C and the mixture was stirred for an additional hour. The mixture was then quenched with a saturated solution of (NH$_4$)$_2$SO$_4$ (4.0 mL, aq.) and was extracted with EtOAc (3 × 15 mL). The combined organic layers were dried (MgSO$_4$) and the resulting solution was concentrated and subjected to column chromatography on silica gel (1:9 EtOAc:petroleum ether) to afford the pure product(s).

(*E*)-3-(1-Oxo-1-(*p*-tolyl)propan-2-ylidene)isobenzofuran-1(3H)-one 241[67]

241
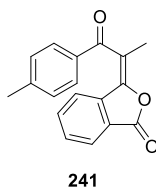
Alkylidene phthalide **241** was prepared as a 5.5:1 *E*/*Z* mixture of diastereomers according to General Procedure 2 using 4'-methylpropiophenone **240** (80 µL, 1.0 equiv, 0.5 mmol). The title compound was isolated as a white solid (115 mg, 0.42 mmol, 83%). The *Z*-isomer was not isolated.

m.p. 114–115 °C (lit. 119–120 °C);[67] ^{1}H NMR (400 MHz, CDCl$_3$) δ 7.94–7.87 (m, 3H), 7.50–7.44 (m, 2H), 7.34–7.28 (m, 2H), 7.28–7.23 (m, 1H), 2.44 (s, 3H), 2.31 (s, 3H); ^{13}C NMR (101 MHz, CDCl$_3$) δ 196.3, 166.5, 145.8, 145.0, 137.3, 134.7, 133.1, 130.2, 130.0, 129.9, 125.6, 125.5, 123.3, 119.6, 22.0, 16.4; LRMS (CI) *m/z* 278.9 [M+H]$^+$; HRMS (FTMS-NSI) calculated for C$_{18}$H$_{15}$O$_3$ [M+H]$^+$ 279.1016, found 279.1017; IR (ATR)/cm^{-1} 2978, 2919, 1768, 1658.

(*E*)-3-(1-Oxo-1-(*m*-tolyl)propan-2-ylidene)isobenzofuran-1(3H)-one 258

258
major

501
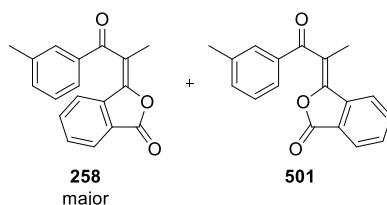
Alkylidene phthalides **258** and **501** were prepared as a 4:1 *E*/*Z* mixture of diastereomers according to General Procedure 2 using 3'-methylpropiophenone (77 µL, 1.0 equiv, 0.5 mmol). The major isomer was isolated as a white solid (65 mg, 0.23 mmol, 47%). The *Z*-isomer **498** was not isolated.

E-isomer **258**

m.p. 91–92 °C; ^{1}H NMR (400 MHz, CDCl$_3$) δ 7.92–7.87 (m, 1H), 7.83–7.79 (m, 1H), 7.79–7.75 (m, 1H), 7.49–7.41 (m, 3H), 7.38 (appt, *J* = 7.6 Hz, 1H), 7.30–7.24 (m, 1H), 2.41 (s, 3H), 2.30 (s, 3H); ^{13}C NMR (101 MHz, CDCl$_3$) δ 196.8, 166.3, 145.2, 139.2, 137.3, 135.6,

135.3, 134.6, 130.2, 130.0, 129.1, 127.1, 125.6, 125.5, 123.3, 119.4, 21.4, 16.4; LRMS (CI) *m/z* 279.0 [M+H]$^+$; HRMS (FTMS-NSI) calculated for C$_{18}$H$_{15}$O$_3$ [M+H]$^+$ 279.1016, found 279.1019; IR (ATR)/cm^{-1} 2919, 1790, 1660.

Z-isomer **501**

relevant ^{1}H NMR shifts (400 MHz, CDCl$_3$) δ 8.01–7.95 (m, 2H), 7.71–7.61 (m, 2H), 7.43–7.38 (m, 1H), 7.37–7.31 (m, 1H), 2.45 (s, 3H), 2.40 (s, 3H); LRMS (CI) *m/z* 279.0 [M+H]$^+$; IR (ATR)/cm^{-1} 3058, 1773, 1732.

(*E*)-3-(1-Oxo-1-(o-tolyl)propan-2-ylidene)isobenzofuran-1(3H)-one 259 and (*Z*)-3-(1-oxo-1-(*o*-tolyl)propan-2-ylidene)isobenzofuran-1(3H)-one 502

259
major

502
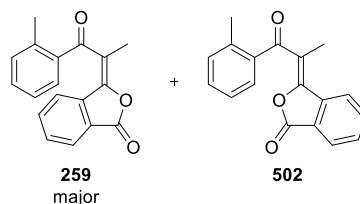
Alkylidene phthalides **259** and **502** were prepared in a 3.5:1 *E/Z* mixture of diastereomers according to General Procedure 2 using 2'-methylpropiophenone (77 µL, 1.0 equiv, 0.5 mmol). The title compounds were isolated as white solids (*E*-isomer: 45 mg, 0.16 mmol, 32%; *Z*-isomer: 36 mg, 0.13 mmol, 26%).

E-isomer **259**

m.p. 137–138 °C; ^{1}H NMR (400 MHz, CDCl$_3$) δ 7.95–7.90 (m, 1H), 7.63 (dd, *J* = 7.7, 1.2 Hz, 1H), 7.57–7.49 (m, 3H), 7.45 (apptd, *J* = 7.5, 1.3 Hz, 1H), 7.35 (d, *J* = 7.7 Hz, 1H), 7.28–7.22 (m, 1H), 2.63 (s, 3H), 2.22 (s, 3H); ^{13}C NMR (101 MHz, CDCl$_3$) δ 198.7, 166.3, 147.0, 139.9, 137.3, 135.8, 134.8, 132.7, 132.5, 130.9, 130.6, 126.3, 125.8, 125.6, 123.8, 120.9, 21.3, 16.3; LRMS (CI) *m/z* 279.0 [M+H]$^+$; HRMS (FTMS-NSI) calculated for C$_{18}$H$_{15}$O$_3$ [M+H]$^+$ 279.1016, found 279.1018; IR (ATR)/cm^{-1} 2922, 1773, 1651.

Z-isomer **502**

m.p. 113–114 °C; ^{1}H NMR (400 MHz, CDCl$_3$) δ 8.01–7.96 (m, 2H), 7.83 (td, *J* = 7.7, 1.1 Hz, 1H), 7.69–7.64 (m, 1H), 7.54 (dd, *J* = 7.7, 1.2 Hz, 1H), 7.42 (apptd, *J* = 7.5, 1.4 Hz, 1H), 7.31 (d, *J* = 7.6 Hz, 1H), 7.24 (t, *J* = 7.5 Hz, 1H), 2.59 (s, 3H), 2.49 (s, 3H); ^{13}C NMR (101 MHz, CDCl$_3$) δ 198.0, 165.5, 145.8, 138.8, 138.4, 137.8, 134.8, 132.0, 131.9, 130.9, 130.2, 126.2, 126.0, 125.7, 124.4, 119.1, 21.2, 14.6; LRMS (CI) *m/z* 279.0 [M+H]$^+$; HRMS (FTMS-NSI) calculated for C$_{18}$H$_{15}$O$_3$ [M+H]$^+$ 279.1016, found 279.1019; IR (ATR)/cm^{-1} 2926, 1777, 1640.

(*E*)-3-(1-Oxo-1-phenylpropan-2-ylidene)isobenzofuran-1(3H)-one 187[67]

187
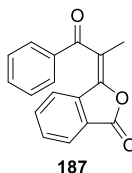
Alkylidene phthalide **187** was prepared as a 4.5:1 *E*/*Z* mixture of diastereomers according to General Procedure 2 using propiophenone **186** (65 µL, 1.0 equiv, 0.5 mmol). The title compound (*E*-isomer) was isolated as a white solid (101 mg, 0.38 mmol, 76%). The *Z*-isomer was not isolated.

m.p. 107–108 °C (lit. 78–79 °C);[67] ^{1}H NMR (400 MHz, CDCl$_3$) δ 8.03–7.96 (m, 2H), 7.93–7.84 (m, 1H), 7.67–7.58 (m, 1H), 7.54–7.40 (m, 4H), 7.29–7.22 (m, 1H), 2.29 (s, 3H); ^{13}C NMR (101 MHz, CDCl$_3$) δ 196.6, 166.2, 145.3, 137.1, 135.6, 134.6, 134.4, 130.2, 129.7, 129.2, 125.5, 125.4, 123.2, 119.2, 16.3; LRMS (CI) *m/z* 265.0 [M+H]$^+$; HRMS (FTMS-NSI) calculated for C$_{17}$H$_{13}$O$_3$ [M+H]$^+$ 265.0859, found 265.0862; IR (ATR)/cm^{-1} 3060, 2919, 1779, 1653.

(*E*)-3-(1-(4-Methoxyphenyl)-1-oxopropan-2-ylidene)isobenzofuran-1(3H)-one 260[67]

260
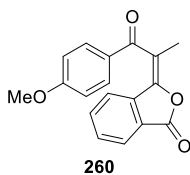
Alkylidene phthalide **260** was prepared as a 6:1 *E/Z* mixture of diastereomers according to General Procedure 2 using 4'-methoxypropiophenone (82 mg, 1.0 equiv, 0.5 mmol). The title compound was isolated as a white solid (82 mg, 0.28 mmol, 56%). The *Z*-isomer was not isolated.

m.p. 128–129 °C (lit. 119–120 °C);[67] ^{1}H NMR (600 MHz, CDCl$_3$) δ 8.00–7.96 (m, 2H), 7.92–7.87 (m, 1H), 7.49–7.43 (m, 2H), 7.25–7.21 (m, 1H), 6.99–6.94 (m, 2H), 3.88 (s, 3H), 2.31 (s, 3H); ^{13}C NMR (101 MHz, CDCl$_3$) δ 195.1, 166.4, 164.8, 144.6, 137.3, 134.6, 132.2, 130.1, 128.5, 125.6, 125.5, 123.2, 119.6, 114.6, 55.7, 16.5; LRMS (CI) *m/z* 295.1 [M+H]$^+$; HRMS (FTMS-NSI) calculated for C$_{18}$H$_{15}$O$_4$ [M+H]$^+$ 295.0965, found 295.0964; IR (ATR)/cm^{-1} 3183, 2842, 1773, 1653.

(*E*)-3-(1-(4-Bromophenyl)-1-oxopropan-2-ylidene)isobenzofuran-1(3H)-one 261

261
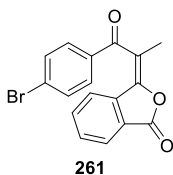
Alkylidene phthalide **261** was prepared as a 3:1 *E/Z* mixture of diastereomers according to General Procedure 2 using 4'-bromopropiophenone (107 mg, 1.0 equiv, 0.5 mmol). The title compound was isolated as a white solid (70 mg, 0.20 mmol, 41%). The *Z*-isomer **298** was isolated after isomerization of the pure *E*-isomer **261** (Refer to page 159 for procedure and data)

m.p. 117–118 °C (dec); ^{1}H NMR (400 MHz, CDCl$_3$) δ 7.93–7.89 (m, 1H), 7.88–7.83 (m, 2H), 7.68–7.63 (m, 2H), 7.52–7.46 (m, 2H), 7.28–7.22 (m, 1H), 2.29 (s, 3H); ^{13}C NMR (101 MHz, CDCl$_3$) δ 195.6, 166.1, 145.7, 137.0, 134.7, 134.4, 132.7, 131.1, 130.5, 129.9, 125.7, 125.6, 123.2, 118.5, 16.3; LRMS (CI) *m/z* 343.0 [M(^{79}Br)+H]$^+$, 345.0 [M(^{81}Br)+H]$^+$; HRMS (FTMS-NSI): calculated for C$_{17}$H$_{12}$^{79}BrO$_3$ 342.9964 [M+H]$^+$, and for C$_{17}$H$_{12}$^{81}BrO$_3$

344.9944 [M+H]$^+$, found 342.9969 [M(^{79}Br)+H]$^+$, 344.9947 [M(^{81}Br)+H]$^+$; IR (ATR)/cm^{-1} 2982, 1781, 1653.

(*E*)-3-(2-Oxo-1,2-diphenylethylidene)isobenzofuran-1(3H)-one 231[84]

231
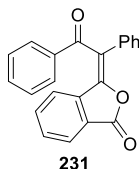
Alkylidene phthalide **231** was prepared as a 3:1 *E/Z* mixture of diastereomers according to General Procedure 2 using 2-phenylacetophenone **170** (98 mg, 1.0 equiv, 0.5 mmol). The title compound was isolated as a white solid (96 mg, 0.19 mmol, 39%). The *Z*-isomer was not isolated.

m.p. 132–133 °C (lit. 160–161 °C);[84] ^{1}H NMR (400 MHz, CDCl$_3$) δ 8.12–8.06 (m, 2H), 7.98–7.93 (m, 1H), 7.72–7.65 (m, 2H), 7.62–7.55 (m, 1H), 7.55–7.49 (m, 2H), 7.49–7.42 (m, 2H), 7.42–7.36 (m, 3H), 7.35–7.29 (m, 1H); ^{13}C NMR (101 MHz, CDCl$_3$) δ 195.0, 166.5, 143.8, 137.9, 136.3, 134.8, 134.6, 132.8, 130.6, 130.3, 129.5, 129.3, 129.0, 125.8, 124.9, 123.6, 122.3 (1 carbon missing); LRMS (CI) *m/z* 327.0 [M+H]$^+$; HRMS (FTMS-NSI) calculated for C$_{22}$H$_{15}$O$_3$ [M+H]$^+$ 327.1016, found 327.1017; IR (ATR)/cm^{-1} 3060, 1773, 1651.

(*E*)-3-(1-Oxo-1-phenylbutan-2-ylidene)isobenzofuran-1(3H)-one 262 and (*Z*)-3-(1-oxo-1-phenylbutan-2-ylidene)isobenzofuran-1(3H)-one 503

262   **503**
major
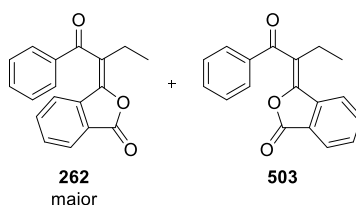
Alkylidene phthalides **262** and **503** were prepared as a 5:1 *E/Z* mixture of diastereomers according to General Procedure 2 using butyrophenone (73 µL, 1.0 equiv, 0.5 mmol). The title compounds were isolated as white solids (*E*-isomer: 56 mg, 0.20 mmol, 40%; *Z*-isomer: 10 mg, 0.04 mmol, 7%).

E-isomer **262**

m.p. 101–102 °C; ^{1}H NMR (400 MHz, CDCl$_3$) 8.05–7.97 (m, 2H), 7.90–7.85 (m, 1H), 7.65–7.59 (m, 1H), 7.52–7.46 (m, 2H), 7.45–7.39 (m, 2H), 7.20–7.14 (m, 1H), 2.79 (q, *J* = 7.6 Hz, 2H), 1.13 (t, *J* = 7.6 Hz, 3H); ^{13}C NMR (101 MHz, CDCl$_3$) δ 196.5, 166.3, 144.3, 137.3, 136.1, 134.5, 134.4, 130.2, 129.7, 129.2, 125.5, 125.4, 125.0, 123.1, 23.8, 12.7; LRMS (CI) *m/z* 279.0 [M+H]$^+$; HRMS (FTMS-NSI) calculated for C$_{18}$H$_{15}$O$_3$ [M+H]$^+$ 279.1016, found 279.1020; IR (ATR)/cm^{-1} 2969, 1779, 1653.

Z-isomer **503**

m.p. 77–78 °C (dec); ^{1}H NMR (400 MHz, CDCl$_3$) δ 7.99–7.89 (m, 4H), 7.81 (td, *J* = 7.8, 1.1 Hz, 1H), 7.63 (td, *J* = 7.7, 0.7 Hz, 1H), 7.61–7.56 (m, 1H), 7.49–7.43 (m, 2H), 2.92 (q, *J* = 7.6 Hz, 2H), 1.30 (t, *J* = 7.6 Hz, 3H); ^{13}C NMR (101 MHz, CDCl$_3$) δ 195.9, 165.6, 143.7, 137.8, 137.0, 135.0, 133.8, 130.7, 129.7, 128.8, 126.2, 126.1, 124.4, 123.8, 22.5, 13.0; LRMS (CI) *m/z* 279.0 [M+H]$^+$; HRMS (FTMS-NSI) calculated for C$_{18}$H$_{15}$O$_3$ [M+H]$^+$ 279.1016, found 279.1019; IR (ATR)/cm^{-1} 2973, 1777, 1658.

(*E*)-3-(3-Methyl-1-oxo-1-phenylbutan-2-ylidene)isobenzofuran-1(3H)-one 263 and 3-methyl-1-oxo-1-phenylbutan-2-yl 2-((tert-butoxycarbonyl)carbamoyl)benzoate 267
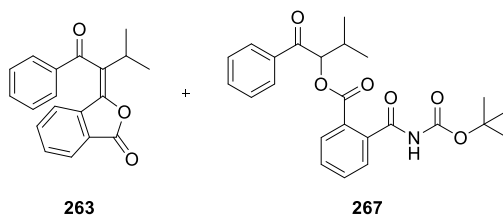
Alkylidene phthalide **263** and *α*-oxygenation product **267** were prepared according to General Procedure 2 using isovalerophenone **266** (84 µL, 1.0 equiv, 0.5 mmol). The alkylidene phthalide **263** was isolated as a white solid (28 mg, 0.10 mmol, 19%) and the *α*-oxygenation product **267** was isolated as a colorless oil (25 mg, 0.06 mmol, 12%).

Alkylidene phthalide **263**: m.p. 101–102 °C; ^{1}H NMR (400 MHz, CDCl$_3$) δ 8.08–8.02 (m, 2H), 7.92–7.86 (m, 1H), 7.66–7.60 (m, 1H), 7.53–7.46 (m, 2H), 7.46–7.35 (m, 2H), 7.04–6.99 (m, 1H), 3.45 (hept, *J* = 7.0 Hz, 1H), 1.22 (d, *J* = 7.0 Hz, 6H); ^{13}C NMR (101 MHz, CDCl$_3$) δ 196.3, 166.4, 142.7, 137.5, 137.0, 134.6, 134.5, 130.0, 129.8, 129.3, 128.4, 125.6,

125.4, 123.0, 29.9, 21.4; LRMS (CI) *m/z* 293.1 [M+H]$^+$; HRMS (FTMS-NSI) calculated for C$_{19}$H$_{17}$O$_3$ [M+H]$^+$ 293.1172, found 293.1175; IR (ATR)/cm^{-1} 2973, 1777, 1658.

α-Oxygenation product **267**: ^{1}H NMR (400 MHz, CDCl$_3$) δ 8.21–8.14 (m, 1H), 7.92 (s, br, 1H), 7.83–7.76 (m, 1H), 7.73–7.64 (m, 2H), 7.50–7.43 (m, 2H), 7.36–7.23 (m, 3H), 5.76 (d, *J* = 9.7 Hz, 1H), 2.71 (dhept, *J* = 9.7, 6.7 Hz, 1H), 1.51 (s, 9H), 1.09 (d, *J* = 6.7 Hz, 6H); ^{13}C NMR (101 MHz, CDCl$_3$) δ 167.8, 163.8, 155.6, 144.5, 134.7, 132.8, 131.6, 131.5, 130.3, 129.4, 129.3, 128.7, 128.3, 125.9, 124.7, 83.4, 28.2, 26.4, 22.7; HRMS (FTMS-NSI) calculated for C$_{24}$H$_{31}$O$_6$N$_2$ [M+NH$_4$]$^+$ 443.2177, found 443.2171; IR (ATR)/cm^{-1} 3292, 2960, 1777, 1738, 1667.

(*Z*)-3-(3-Oxopentan-2-ylidene)isobenzofuran-1(3H)-one 264[83]

230   **264**
major
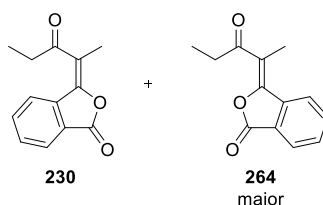
Alkylidene phthalides **230** and **264** were prepared as a 1:6 *E*/*Z* mixture of diastereomers according to General Procedure 2 using 3-pentanone (53 µL, 1.0 equiv, 0.5 mmol). The major isomer **264** (*Z*) was isolated as a white solid (48 mg, 0.22 mmol, 44%). The *E*-isomer was not isolated.

Z-isomer **264**

m.p. 130–131 °C (lit. 135–136 °C);[83] ^{1}H NMR (400 MHz, CDCl$_3$) δ 8.04–7.98 (m, 1H), 7.95 (d, *J* = 8.0 Hz, 1H), 7.80 (td, *J* = 7.6, 1.1 Hz, 1H), 7.66 (td, *J* = 7.6, 0.8 Hz, 1H), 3.08 (q, *J* = 7.2 Hz, 2H), 2.30 (s, 3H), 1.16 (t, *J* = 7.2 Hz, 3H); ^{13}C NMR (101 MHz, CDCl$_3$) δ 202.4, 165.6, 148.7, 139.1, 135.1, 131.2, 126.3, 125.7, 125.3, 118.2, 37.7, 13.2, 8.6; LRMS (CI) *m/z* 217.1 [M+H]$^+$; HRMS (FTMS-NSI) calculated for C$_{13}$H$_{13}$O$_3$ [M+H]$^+$ 217.0859, found 217.0859; IR (ATR)/cm^{-1} 2980, 2922, 1792, 1660.

E-isomer **230** relevant ^{1}H NMR shifts (400 MHz, CDCl$_3$) δ 8.10 (d, *J* = 8.0 Hz, 1H), 7.92 (d, *J* = 7.6 Hz, 1H), 7.72–7.65 (m, 1H), 7.61–7.55 (m, 1H), 2.77 (q, *J* = 7.2 Hz, 2H), 2.30 (s, 3H), 1.21 (t, *J* = 7.2 Hz, 3H).

(*E*)-3-(2-Oxocyclohexylidene)isobenzofuran-1(3H)-one 239

239
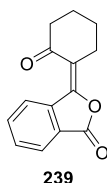
Alkylidene phthalide **239** was prepared according to General Procedure 2 using cyclohexanone **160** (52 µL, 1.0 equiv, 0.5 mmol). The title compound was isolated as a yellow solid (72 mg, 0.32 mmol, 63%). The structure was identified by analogy to alkylidene phthalide **265**. No NOESY signals were observed for this molecule, further supporting the *E*-isomer was formed as major; *E/Z* ratio n.d. due to unavailable data of the minor isomer.

m.p. 92–93 °C (dec); ^{1}H NMR (400 MHz, CDCl$_3$) δ 8.40 (d, *J* = 8.1 Hz, 1H), 7.95–7.90 (m, 1H), 7.73–7.66 (m, 1H), 7.59 (td, *J* = 7.5, 0.8 Hz, 1H), 3.01–2.94 (m, 2H), 2.66–2.58 (m, 2H), 2.03–1.94 (m, 2H), 1.92–1.83 (m, 2H); ^{13}C NMR (101 MHz, CDCl$_3$) δ 202.2, 166.2, 148.9, 137.2, 135.2, 131.4, 126.3, 126.0, 125.4, 122.0, 42.9, 29.0, 24.5, 23.9; LRMS (CI) *m/z* 229.1 [M+H]$^+$; HRMS (FTMS-NSI) calculated for C$_{14}$H$_{13}$O$_3$ [M+H]$^+$ 229.0859, found 229.0860; IR (ATR)/cm^{-1} 2947, 2870, 1779, 1673.

(*E*)-3-(2-Oxocyclopentylidene)isobenzofuran-1(3H)-one 265

265
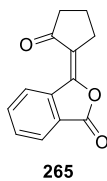
Alkylidene phthalide **265** was prepared according to General Procedure 2 using cyclopentanone **373** (44 µL, 1.0 equiv, 0.5 mmol). The title compound was isolated as a yellow solid (86 mg, 0.40 mmol, 80%). The structure was identified by X-Ray crystallography; *E/Z* ratio n.d. due to unavailable data of the minor isomer.

m.p. 139–140 °C; ^{1}H NMR (400 MHz, CDCl$_3$) δ 9.14 (d, *J* = 8.0 Hz, 1H), 7.99–7.89 (m, 1H), 7.85–7.73 (m, 1H), 7.65 (td, *J* = 7.5, 0.7 Hz, 1H), 3.13–3.05 (m, 2H), 2.54 (appt, *J* = 7.8 Hz, 2H), 2.10 (appp, *J* = 7.5 Hz, 2H); ^{13}C NMR (101 MHz, CDCl$_3$) δ 207.1, 166.7, 150.3, 136.8, 135.6, 132.1, 127.0, 125.8, 125.5, 120.9, 41.0, 29.3, 20.3; LRMS (CI) *m/z* 215.1 [M+H]$^+$; HRMS (FTMS-NSI) calculated for C$_{13}$H$_{11}$O$_3$ [M+H]$^+$ 215.0703, found 215.0704; IR (ATR)/cm^{-1} 2947, 2870, 1779, 1673.

Ethyl (*E*)-2-(3-oxoisobenzofuran-1(3H)-ylidene)propanoate 222[80,82]

222
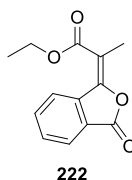
Alkylidene phthalide **222** was prepared as a 6.5:1 *E/Z* mixture of diastereomers according to General Procedure 1 using ethyl propionate (58 µL, 1.0 equiv, 0.5 mmol). The title compound was isolated as a yellow solid (90 mg, 0.39 mmol, 77%).

m.p. 72–73 °C (lit. 71–73 °C);[80] ^{1}H NMR (400 MHz, CDCl$_3$) δ 8.56 (d, *J* = 8.1 Hz, 1H), 7.98–7.91 (m, 1H), 7.73 (apptd, *J* = 7.6, 1.2 Hz, 1H), 7.60 (apptd, *J* = 7.6, 0.8 Hz, 1H), 4.36 (q, *J* = 7.1 Hz, 2H), 2.27 (s, 3H), 1.39 (t, *J* = 7.1 Hz, 3H); ^{13}C NMR (101 MHz, CDCl$_3$) δ 167.4, 166.0, 151.8, 137.0, 135.0, 131.1, 126.6, 126.4, 125.5, 113.2, 61.5, 15.0, 14.4; LRMS (CI) *m/z* 233.1 [M+H]$^+$; HRMS (FTMS-NSI) calculated for C$_{13}$H$_{13}$O$_4$ [M+H]$^+$ 233.0808, found 233.0809; IR (ATR)/cm^{-1} 2917, 2850, 1783, 1708.

4.7.2 Reaction with *N*-Methoxyphthalimide 243

Synthesis of *N*-methoxyphthalimide 243[205]

243
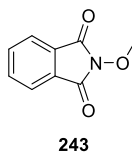
N-Hydroxyphthalimide (3.26 g, 1.0 equiv, 20.0 mmol) was weighed into a round bottom flask, after which DMF (50 mL) was added and was followed by the addition of iodomethane (1.37 mL, 1.1 equiv, 22 mmol) and slow addition of DBU (3.00 mL, 1.0 equiv, 20.0 mmol) over 5 min. The reaction mixture was stirred for 1 h, after which it was poured into ice cold HCl (1.0 M, 500 mL). The resulting solids were filtered and washed with water (200 mL) and left to air dry overnight to afford the title compound as white solids (2.2 g, 12.4 mmol, 62%).

m.p. 132–133 °C (lit. 134–135 °C);[205] ^{1}H NMR (400 MHz, CDCl$_3$) δ 7.92–7.82 (m, 2H), 7.80–7.71 (m, 2H), 4.07 (s, 3H); ^{13}C NMR (101 MHz, CDCl$_3$) δ 163.4, 134.7, 129.0, 123.7, 66.0; LRMS (CI) *m/z* 177.9 [M+H]$^+$; HRMS (FTMS-NSI) calculated for C$_9$H$_8$O$_3$N [M+H]$^+$ 178.0499, found 178.0497; IR (ATR)/cm^{-1} 3002, 2947, 1731.

N-Methoxy-2-(2-methyl-3-oxo-3-(*p*-tolyl)propanoyl)benzamide 244

244
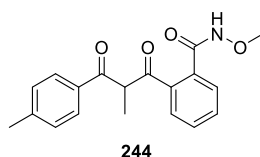
Compound **244** was prepared according to General Procedure 2 using 4'-methylpropiophenone **240** (80 µL, 1.0 equiv, 0.5 mmol) and *N*-methoxyphthalimide **243** (177 mg, 2.0 equiv, 1.0 mmol). The title compound was isolated after flash chromatography on silica gel (1:1, EtOAc:petroleum ether) as white solids (80 mg, 0.25 mmol, 49%).

m.p. 133–134 °C (dec); ^{1}H NMR (400 MHz, CDCl$_3$) δ 7.86–7.80 (m, 3H), 7.70–7.63 (m, 2H), 7.55 (ddd, *J* = 7.5, 6.8, 1.8 Hz, 1H), 7.30–7.25 (m, 2H), 7.03 (s, br, 1H), 3.85 (s, 3H), 3.61 (q, *J* = 7.2 Hz, 1H), 2.42 (s, 3H), 1.38 (d, *J* = 7.2 Hz, 3H); ^{13}C NMR (101 MHz, CDCl$_3$) δ 205.8, 165.5, 145.1, 142.4, 133.4, 133.1, 130.3, 129.7, 129.0, 128.7, 124.9, 124.0, 94.8,

65.3, 44.2, 21.8, 15.2; LRMS (MALDI) *m/z* 324.08 [M–H]⁻; HRMS (FTMS-NSI) calculated for $C_{19}H_{20}O_4N$ [M+H]⁺ 326.1387, found 326.1390; IR (ATR)/cm⁻¹ 3339, 2943, 1718, 1647, 1604.

4.8 Reactions of Alkylidene Phthalides

4.8.1 *E to Z Isomerization*[96]

(Z)-3-(1-(4-Bromophenyl)-1-oxopropan-2-ylidene)isobenzofuran-1(3H)-one 298

298
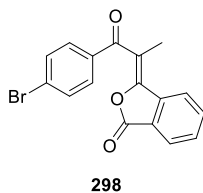
Alkylidene phthalide **261** (103 mg, 1.0 equiv, 0.3 mmol) was weighed into a 7 mL vial equipped with a stir bar, after which H_2SO_4 conc. (1.5 mL) was added and the mixture became yellow. After 2.5 h, ice was carefully added to the mixture until it remained cold. Then, the mixture was dissolved in EtOAc (60 mL) and the resulting organic solution was washed with water (3 × 30 mL), a saturated solution of $NaHCO_3$ (2 × 40 mL), brine (40 mL), dried ($MgSO_4$) and concentrated. *Note:* The reaction reaches an equilibrium between the two isomers (3:1 *Z/E*) at 2.5 h and allowing it to run longer can lead to byproducts. The crude reaction mixture was then subjected to column chromatography on silica gel (5:1 to 1:1, EtOAc:petroleum ether) to afford *Z*-alkylidene phthalide **298** as white solids (67 mg, 0.20 mmol, 65%) and recover *E*-alkylidene phthalide **261** (29 mg, 0.06 mmol, 18%).

m.p. 161–162 °C; ¹H NMR (400 MHz, CDCl₃) δ 7.99–7.94 (m, 2H), 7.86–7.79 (m, 1H), 7.79–7.74 (m, 2H), 7.69–7.63 (m, 1H), 7.62–7.57 (m, 2H), 2.44 (s, 3H); ¹³C NMR (101 MHz, CDCl₃) δ 195.0, 165.4, 144.7, 138.0, 135.4, 135.0, 132.1, 131.1, 131.0, 129.1, 126.3, 125.9, 124.2, 117.0, 14.9; LRMS (CI) *m/z* 343.0 [M(⁷⁹Br) + H]⁺, 345.0 [M(⁸¹Br) + H]⁺; HRMS (FTMS-NSI): calculated for $C_{17}H_{12}$⁷⁹BrO_3 342.9964 [M + H]⁺, and for $C_{17}H_{12}$⁸¹BrO_3 344.9944 [M + H]⁺, found 342.9969 [M(⁷⁹Br) + H]⁺, 344.9946 [M(⁸¹Br) + H]⁺; IR (ATR)/cm⁻¹ 2922, 1768, 1657.

4.8.2   Reaction with Methylamine

N^1,N^2-Dimethylphthalamide 26

291
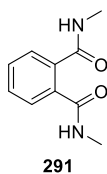
Alkylidene phthalide **241** (56 mg, 1.0 equiv, 0.2 mmol) was weighed into a 7 mL vial equipped with a stir bar, after which $MeNH_2$ in EtOH (33% w/v, 2.0 mL, 80 equiv, 16 mmol) was added at 25 °C and the mixture turned orange. The reaction mixture was allowed to stir at 25 °C for 2 h, followed by removal of the solvent and 4'-methylpropiophenone **240** in a blowdown apparatus at 40 °C for 18 h, to afford the title compound as a white solid (36 mg, 0.19 mmol, 95%)

m.p. 180–181 °C (boiled, lit. 185 °C);[206] ^{1}H NMR (400 MHz, CDCl$_3$) δ 7.59–7.52 (m, 2H), 7.47–7.40 (m, 2H), 6.85 (s, br, 2H), 2.95 (s, 3H), 2.94 (s, 3H); ^{13}C NMR (101 MHz, CDCl$_3$) δ 170.1, 134.7, 130.3, 128.6, 27.0; LRMS (CI) *m/z* 162.0 [M–MeNH]˙; HRMS (FTMS-NSI) calculated for $C_{10}H_{13}O_2N_2$ [M+H]$^+$ 193.0972, found 193.0969; IR (ATR)/cm^{-1} 3231, 3071, 1625.

4.8.3   Epoxidation Reactions

(*E*)-3-(1-Hydroxy-1-(*p*-tolyl)propan-2-ylidene)isobenzofuran-1(3H)-one   293   (Luche reduction of alkylidene phthalide 241)[94]

293
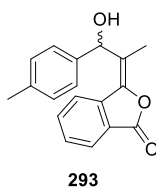
A Schlenk flask under an argon atmosphere was charged with alkylidene phthalide **241** (283 mg, 1.0 equiv, 1.0 mmol) and CeCl$_3$•7H$_2$O (760 mg, 2.0 equiv, 2.0 mmol). MeOH (10 mL) and the minimum amount of EtOAc required to solubilize alkylidene phthalide **241** were then added, and the reaction mixture was cooled down to 0 °C, after which NaBH$_4$ (154 mg, 4.0 equiv, 4.1 mmol) was added portion-wise over 1 min. After 15 min, the reaction was quenched with a saturated solution of NH$_4$Cl (10 mL, aq.) and was extracted with CH$_2$Cl$_2$

(3 × 25 mL). The combined organic solutions were dried (MgSO₄), concentrated, and the crude reaction mixture was subjected to column chromatography on silica gel (1:5, EtOAc:petroleum ether) to isolate the title compound as a white solid (188 mg, 0.67 mmol, 66%).

m.p. 167–168 °C; ¹H NMR (400 MHz, CDCl₃) δ 8.00–7.95 (m, 1H), 7.91 (d, *J* = 8.1 Hz, 1H), 7.70 (apptd, *J* = 7.8, 1.1 Hz, 1H), 7.58–7.52 (m, 1H), 7.32 (d, *J* = 8.0 Hz, 2H), 7.18 (d, *J* = 8.0 Hz, 2H), 6.36 (d, *J* = 4.2 Hz, 1H), 2.35 (s, 3H), 2.13 (d, *J* = 4.2 Hz, 1H), 1.98 (s, 3H); ¹³C NMR (101 MHz, CDCl₃) δ 166.9, 143.4, 138.0, 137.8, 137.6, 134.7, 129.5, 126.2, 126.0, 125.7, 124.8, 123.3, 70.4, 21.2, 12.4; LRMS (CI) *m/z* 263.1 [M–OH]⁺; HRMS (FTMS-NSI) calculated for $C_{18}H_{17}O_3$ [M+H]⁺ 281.1172, found 281.1175; IR (ATR)/cm⁻¹ 3462, 2921, 1744.

rel-(1R,3'R)-3'-((S)-hydroxy(p-tolyl)methyl)-3'-methyl-3H-spiro[isobenzofuran-1,2'-oxiran]-3-one 294[91]
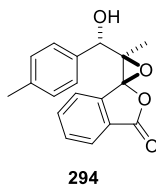
294

Alkylidene phthalide **293** (42 mg, 1.0 equiv, 0.15 mmol) was weighed into a 7 mL vial equipped with a stir bar, followed by the addition of CH₂Cl₂ (0.5 mL). The mixture was cooled down to 0 °C and then *m*-CPBA (61 mg, 1.8 equiv, 0.27 mmol) was added over 1 min. The reaction mixture was allowed to warm up to room temperature and was stirred for 18 h, after which it was diluted with CH₂Cl₂ (10 mL) and the resulting organic solution was washed with a solution of Na₂S₂O₃ (10 %, 2 × 10 mL, aq.), a saturated solution of NaHCO₃ (2 × 10 mL, aq.). The combined aqueous layers were extracted with CH₂Cl₂ (2 × 15 mL) and the combined organic solutions were dried (MgSO₄), concentrated *in vacuo*, and the crude reaction mixture was subjected to column chromatography on silica gel (1:5, EtOAc:petroleum ether) to isolate the title compound as a white solid (36–41 mg, 0.12–0.14 mmol, 81–92%, 95% pure, 20:1 *d.r.**).

m.p. 120–121 °C (dec); ¹H NMR, major (400 MHz, CD₃CN) δ 8.01–7.97 (m, 1H), 7.86–7.74 (m, 3H), 7.05–7.01 (m, 2H), 7.01–6.95 (m, 2H), 5.19 (d, *J* = 4.6 Hz, 1H), 4.08 (d, *J* =

4.6 Hz, 1H), 2.23 (s, 3H), 1.46 (s, 3H); ^{13}C NMR, major (101 MHz, CD$_3$CN) δ 167.4, 142.8, 138.3, 137.6, 136.1, 132.7, 129.9, 129.5, 126.7, 126.4, 125.3, 94.0, 73.1, 72.6, 21.0, 13.4; LRMS (CI) *m/z* 278.9 [M–OH]$^{•}$; HRMS (FTMS-NSI) calculated for C$_{18}$H$_{16}$O$_4$Na [M+Na]$^+$ 319.0941, found 319.0936; IR (ATR)/cm^{-1} 3523, 2930, 1768.

*ature: What appears to be the minor diastereomer could be observed after purification but was not separated from the major. ^{1}H NMR, minor, identified signals (400 MHz, CD$_3$CN) δ 7.44–7.38 (m, 2H), 7.26–7.22 (m, 2H), 5.12 (d, 3.6 Hz, 1H), 3.76 (d, 3.6 Hz, 1H), 2.36 (s, 3H), 1.41 (s, 3H).

rel-(*S*)-((1*S*,3'*R*)-3'-Methyl-3-oxo-2,3-dihydrospiro[indene-1,2'-oxiran]-3'-yl)(p-tolyl)methyl acetate 31^{95}

295
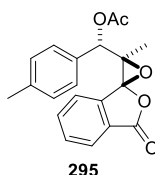
Epoxide **294** (41 mg, 1.0 equiv, 0.14 mmol) was weighed into a 7 mL vial equipped with a stir bar, after which dry CH$_2$Cl$_2$ (0.6 mL), a crystal of DMAP (0.4 mg, 0.02 equiv, 3.0 µmol), Et$_3$N (25 µL, 1.3 equiv, 0.18 mmol) and Ac$_2$O (17 µL, 1.3 equiv, 0.18 mmol) were subsequently added. The mixture was allowed to stir at room temperature for 0.5 h after which water (15 mL) was added and the resulting mixture was extracted with CH$_2$Cl$_2$ (3 × 15 mL). The combined organic solution was dried (MgSO$_4$) and concentrated to provide the title compound as a white solid (46 mg, 0.14 mmol, 91%, 95% pure, 20:1 *d.r.**).

m.p. 93–94 °C (dec); ^{1}H NMR (400 MHz, CD$_3$CN) δ 8.03–7.98 (m, 1H), 7.94–7.87 (m, 2H), 7.84–7.75 (m, 1H), 7.11–7.04 (m, 2H), 6.98–6.90 (m, 2H), 6.37 (s, 1H), 2.25 (s, 3H), 2.24 (s, 3H), 1.56 (s, 3H); ^{13}C NMR (101 MHz, CD$_3$CN) δ 171.0, 167.2, 142.2, 139.3, 136.4, 133.8, 132.9, 130.3, 129.6, 126.9, 126.5, 125.1, 93.6 74.7, 70.1, 21.1, 21.0, 14.4; HRMS (FTMS-NSI) calculated for C$_{20}$H$_{18}$O$_5$Na [M+Na]$^+$ 361.1046, found 361.1045; IR (ATR)/cm^{-1} 2919, 2850, 1783, 1738.

*ature: What appears to be the minor diastereomer could be observed after work-up but was not separated from the major. ^{1}H NMR, minor, identified signals (400 MHz, CD$_3$CN) δ 7.41–7.36 (m, 2H), 7.30–7.24 (m, 2H), 6.08 (s, 1H), 1.56 (s, 3H).

**(*E*)-2-(3-Oxoisobenzofuran-1(3H)-ylidene)-1-(*p*-tolyl)propyl acetate 28[95]**
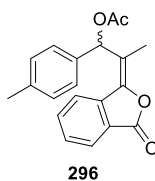
296

Alkylidene phthalide **293** (42 mg, 1.0 equiv, 0.15 mmol) was weighed into a 7 mL vial equipped with a stir bar, after which dry CH_2Cl_2 (0.6 mL), a crystal of DMAP (0.4 mg, 0.02 equiv, 3.0 µmol), Et_3N (25 µL, 1.2 equiv, 0.18 mmol) and Ac_2O (17 µL, 1.2 equiv, 0.18 mmol) were subsequently added. The mixture was allowed to stir at room temperature for 0.5 h after which water (15 mL) was added and the resulting mixture was extracted with CH_2Cl_2 (3 × 15 mL). The combined organic solution was dried ($MgSO_4$) and concentrated to provide the title compound as a white solid (37 mg, 0.11 mmol, 77%).

m.p. 119–120 °C; ^1H NMR (400 MHz, $CDCl_3$) δ 8.14 (d, *J* = 8.1 Hz, 1H), 8.01–7.93 (m, 1H), 7.80–7.70 (m, 1H), 7.60–7.51 (m, 1H), 7.41 (s, 1H), 7.25–7.20 (m, 2H), 7.20–7.13 (m, 2H), 2.34 (s, 3H), 2.21 (s, 3H), 1.98 (s, 3H); ^{13}C NMR (101 MHz, $CDCl_3$) δ 170.3, 166.7, 144.3, 138.1, 137.7, 134.9, 134.4, 129.7, 129.5, 126.2, 125.9, 125.7, 123.7, 120.4, 71.7, 21.2, 21.1, 12.8; LRMS (CI) *m/z* 263.1 [M–OAc]$^{•}$; HRMS (FTMS-NSI) calculated for $C_{20}H_{18}O_4Na$ [M+Na]$^+$ 345.1097, found 345.1097; IR (ATR)/cm^{-1} 3021, 2855, 1770, 1738.

Chapter 4: Experimental

4.9 Baeyer-Villiger Reactions

4.9.1 General BV Procedure – Small Scale (General Procedure 3)

To a flame dried crimp top vial under argon, 1,4-dinitrobenzene (17 mg, 0.1 mmol, 0.1 equiv), KHCO$_3$ (20 mg, 0.2 mmol, 0.2 equiv) was weighed, followed by urea hydrogen peroxide (564 mg, 6.0 mmol, 6.0 equiv). The ketone (1.0 mmol, 1.0 equiv) was added at this stage if it was a solid. The vial was then sealed and evacuated, followed by backfilling with argon (repeated three times). Afterward, the solvent (2.0 mL), benzonitrile **147** (0.62 mL, 6.0 mmol, 6.0 equiv) and, if it was a liquid, the ketone (1.0 mmol, 1.0 equiv), were added via syringe. The reaction was allowed to run for the specified time and temperature. Aliquots (0.2 mL) were removed at different times and were then diluted in 0.5 mL CDCl$_3$ to record conversion. Optimizations shown in Table 7 followed this procedure, as well as monitoring reactions shown in Table 8 and Table 9.

4.9.2 General BV Procedure – Large Scale (General Procedure 4)
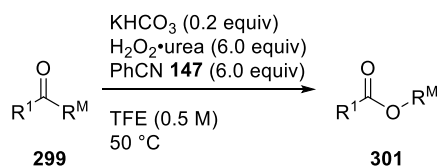
To a flame dried crimp top vial under argon, KHCO$_3$ (80 mg, 0.8 mmol, 0.2 equiv) was weighed, followed by urea hydrogen peroxide (2.26 g, 24 mmol, 6.0 equiv). The ketone (4.0 mmol, 1.0 equiv) was added at this stage if it was a solid. The vial was then sealed and evacuated, followed by backfilling with argon (repeated three times). Afterward, the solvent (8.0 mL), benzonitrile (2.48 mL, 24 mmol, 6.0 equiv) and, if it was a liquid, the ketone (4.0 mmol, 1.0 equiv), were added via syringe. The reaction was allowed to run for the specified time at 50 °C, after which it was cooled down to room temperature. The pressure was released with a needle, then the vial was opened. The mixture was diluted with CH$_2$Cl$_2$ (40 mL) and water (20 mL). The layers were separated and the resulting aqueous solution was extracted with CH$_2$Cl$_2$ (2 × 40 mL). The combined organic layers were dried (MgSO$_4$), concentrated in vacuo, and the crude product was subjected to flash chromatography on silica gel (5:1 petroleum ether:EtOAc) to afford the corresponding product(s).

ε-Caprolactone 161[207]
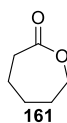
Lactone **161** was prepared according to General Procedure 4 using cyclohexanone **160** (0.44 mL, 4.0 mmol). The title compound was isolated as a colorless oil (321 mg, 2.8 mmol, 70%).

^{1}H NMR (400 MHz, CDCl$_3$) δ 4.28–4.17 (m, 2H), 2.71–2.57 (m, 2H), 1.90–1.80 (m, 2H), 1.81–1.69 (m, 4H); ^{13}C NMR (101 MHz, CDCl$_3$) δ 176.3, 69.4, 34.7, 29.4, 29.1, 23.1; LRMS (CI) *m/z* 115.0 [M+H]$^+$; IR (ATR)/cm^{-1} 2988, 2901, 1726.

5-Methyloxepan-2-one 366[208]
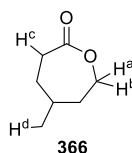
Lactone **366** was prepared according to General Procedure 4 using 4-methylcyclohexanone **365** (0.49 mL, 4.0 mmol). The title compound was isolated as a colorless oil (421 mg, 3.3 mmol, 82%).

^{1}H NMR (400 MHz, CDCl$_3$) δ 4.28 (ddd, *J* = 12.9, 5.7, 1.9 Hz, 1H, H^a), 4.17 (appdd, *J* = 12.7, 10.4 Hz, 1H, H^b), 2.71–2.56 (m, 2H, H^c), 1.98–1.83 (m, 2H), 1.82–1.71 (m, 1H), 1.50 (appdtd, *J* = 15.2, 10.8, 1.8 Hz, 1H), 1.33 (appdtd, *J* = 13.9, 11.5, 2.4 Hz, 1H), 0.99 (d, *J* = 6.6 Hz, 3H, H^d); ^{13}C NMR (101 MHz, CDCl$_3$) δ 176.3, 68.3, 37.4, 35.4, 33.4, 30.9, 22.3; LRMS (CI) *m/z* 129.0 [M+H]$^+$; HRMS (SIR-CI) calculated for C$_7$H$_{13}$O$_2$ [M+H]$^+$ 129.0910, found 129.0910; IR (ATR)/cm^{-1} 2988, 2901, 1717.

5-(*tert*-Butyl)oxepan-2-one 315[209]

315

Lactone **315** was prepared according to General Procedure 4 using 4-*tert*-butylcyclohexanone **314** (617 mg, 4.0 mmol). The title compound was isolated as a white solid (554 mg, 3.3 mmol, 81%).

m.p. 49–50 °C (lit. 49 °C);[209] ^{1}H NMR (400 MHz, CDCl$_3$) δ 4.32 (ddd, J = 12.9, 5.9, 1.8 Hz, 1H, H^a), 4.14 (appdd, J = 12.9, 10.4 Hz, 1H, H^b), 2.69 (ddd, J = 14.3, 7.5, 1.4 Hz, 1H, H^c), 2.61–2.51 (m, 1H, H^d), 2.13–1.95 (m, 2H), 1.58–1.44 (m, 1H), 1.38–1.28 (m, 2H), 0.88 (s, 9H); ^{13}C NMR (101 MHz, CDCl$_3$) δ 176.5, 68.8, 50.9, 33.6, 30.5, 27.6, 23.9; LRMS (CI) *m/z* 171.1 [M+H]$^+$; HRMS (FTMS-NSI) calculated for C$_{10}$H$_{19}$O$_2$ [M+H]$^+$ 171.1380, found 171.1377; IR (ATR)/cm^{-1} 2987, 2961, 1717.

5-Phenyloxepan-2-one 330[210]

330
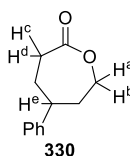
Lactone **330** was prepared according to General Procedure 4 using 4-phenylcyclohexanone **329** (697 mg, 4.0 mmol). The title compound was isolated as a white solid (629 mg, 3.3 mmol, 83%).

m.p. 95–96 °C (lit. 100–101 °C);[210] ^{1}H NMR (400 MHz, CDCl$_3$) δ 7.36–7.29 (m, 2H), 7.26–7.21 (m, 1H), 7.21–7.16 (m, 2H), 4.40 (ddd, J = 13.0, 5.3, 2.3 Hz, 1H, H^a), 4.32 (ddd, J = 13.0, 10.0, 1.0 Hz, 1H, H^b), 2.90–2.71 (m, 3H, H^{c-e}), 2.20–1.98 (m, 3H), 1.91–1.80 (m, 1H); ^{13}C NMR (101 MHz, CDCl$_3$) δ 176.0, 145.1, 128.9, 127.0, 126.7, 68.4, 47.4, 36.9, 33.8, 30.5; LRMS (CI) *m/z* 191.1 [M+H]$^+$; HRMS (FTMS-NSI) calculated for C$_{12}$H$_{15}$O$_2$ [M+H]$^+$ 191.1067, found 191.1064; IR (ATR)/cm^{-1} 2960, 2943, 1740.

7-Methyloxepan-2-one 312[207]
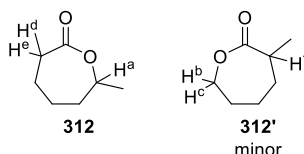
Lactone **312** was prepared according to General Procedure 4 using 2-methylcyclohexanone **311** (0.49 mL, 4.0 mmol). The title compound was isolated as a colorless oil (468 mg, 3.7 mmol, 91%, 15:1 mixture of regioisomers).

^{1}H NMR (400 MHz, CDCl$_3$) δ 4.43 (appdq, J = 8.3, 6.4 Hz, 1H, major, H^a), 4.31–4.15 (m, 2H, minor, H^b, H^c), 2.72–2.52 (m, 2H, major, H^d, H^e, 1H, minor, H^f), 1.99–1.83 (m, 3H, major, 2H, minor), 1.72–1.51 (m, 3H, major, 4H, minor), 1.34 (d, J = 6.4 Hz, 3H, major, 2H, minor), 1.18 (d, J = 6.7 Hz, 3H, minor); ^{13}C NMR (101 MHz, CDCl$_3$, major isomer) δ 175.7, 76.9, 36.4, 35.1, 28.4, 23.0, 22.7; LRMS (CI) m/z 129.0 [M+H]$^+$; IR (ATR)/cm^{-1} 2987, 2901, 1716.

7-Ethyloxepan-2-one 368[211]
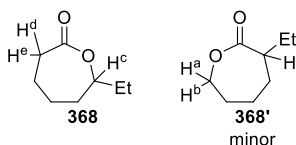
Lactone **368** was prepared according to General Procedure 4 using 2-ethylcyclohexanone **367** (0.56 mL, 4.0 mmol). The title compound was isolated as a colorless oil (410 mg, 2.9 mmol, 72%, 12:1 mixture of regioisomers).

^{1}H NMR (400 MHz, CDCl$_3$) δ 4.26–4.24 (m, 2H, minor, H^a, H^b), 4.16 (t appd, J = 7.8, 5.3 Hz, 1H, major, H^c), 2.71–2.54 (m, 2H, major, H^d, H^e), 2.49–2.39 (m, 1H, minor, H^f), 2.03–1.84 (m, 3H, major, 2H, minor), 1.80–1.67 (m, 1H, major, 2H, minor), 1.66–1.51 (m, 4H, major, 2H, minor), 1.47–1.37 (m, 2H, minor), 0.98 (t, J = 7.4 Hz, 3H, major), 0.95 (t, J = 7.6 Hz, 3H, minor); ^{13}C NMR (101 MHz, CDCl$_3$, major isomer) δ 175.9, 81.9, 35.1, 29.5, 28.5, 23.2, 10.0; LRMS (CI) m/z 143.1 [M+H]$^+$; HRMS (TOF-EI) calculated for C$_8$H$_{14}$O$_2$ [M+•] 142.0994, found 142.0997; IR (ATR)/cm^{-1} 2970, 2931, 1721.

7-Phenyloxepan-2-one 370[212]

370 **370'** minor
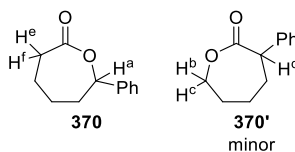
Lactone **370** was prepared according to General Procedure 4 using 2-phenylcyclohexanone **369** (697 mg, 4.0 mmol). The title compound was isolated as a white solid (683 mg, 3.6 mmol, 90%, 20:1 mixture of regioisomers).

m.p. 68–69 °C (lit. 67–68 °C);[212] ^{1}H NMR (400 MHz, CDCl$_3$) δ 7.42–7.27 (m, 5H, each isomer), 5.29 (appd, J = 9.4 Hz, 1H, major, H^a), 4.40–4.35 (m, 2H, minor, H^b, H^c), 3.91–3.86 (m, 1H, minor, H^d), 2.77 (appdd, J = 7.7, 3.7 Hz, 2H, major, H^e, H^f), 2.18–1.97 (m, 4H, each isomer), 1.84–1.64 (m, 2H, each isomer); ^{13}C NMR (101 MHz, CDCl$_3$, major isomer) δ 175.0, 140.9, 128.7, 128.3, 126.0, 82.3, 37.6, 35.1, 28.8, 23.0; LRMS (CI) *m/z* 191.1 [M+H]$^+$; HRMS (FTMS-NSI) calculated for C$_{12}$H$_{15}$O$_2$ [M+H]$^+$ 191.1067, found 191.1063; IR (ATR)/cm^{-1} 2928, 2868, 1717.

1,4,8-Trioxaspiro[4.6]undecan-9-one 372

372
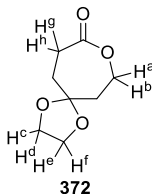
Lactone **372** was prepared according to General Procedure 4 using 1,4-dioxaspiro[4.5]decan-8-one **371** (625 mg, 4.0 mmol). The title compound was isolated as a colorless oil (244 mg, 1.4 mmol, 36%).

^{1}H NMR (400 MHz, CDCl$_3$) δ 4.28–4.19 (m, 2H, H^a, H^b), 3.96–3.91 (m, 4H, H^{c-f}), 2.70–2.60 (m, 2H, H^g, H^h), 2.00–1.92 (m, 2H), 1.91–1.81 (m, 2H); ^{13}C NMR (101 MHz, CDCl$_3$) δ 175.5, 107.8, 64.8, 64.3, 39.0, 32.7, 28.8; LRMS (CI) *m/z* 173.1 [M+H]$^+$; HRMS (FTMS-NSI) calculated for C$_8$H$_{13}$O$_4$ [M+H]$^+$ 173.0808, found 173.0804; IR (ATR)/cm^{-1} 2970, 2889, 1729.

(4*R*,7*S*)-7-Isopropyl-4-methyloxepan-2-one 327[134]
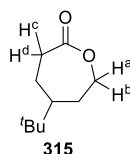

327
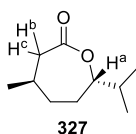
Lactone **327** was prepared according to General Procedure 4 using (–)-menthone **325** (0.69 mL, 4.0 mmol). The title compound was isolated as a colorless oil (344 mg, 2.0 mmol, 51%).

$[\alpha]_D^{20}$ –20.56° (c 0.72, CHCl$_3$), lit. –19.7°;[134] ^{1}H NMR (400 MHz, CDCl$_3$) δ 4.03 (appdd, J = 9.2, 4.5 Hz, 1H, H^a), 2.65–2.39 (m, 2H, H^b, H^c), 2.03–1.77 (m, 4H), 1.66–1.52 (m, 1H), 1.35–1.21 (m, 1H), 1.03 (d, J = 6.7 Hz, 3H), 0.97 (d, J = 6.8 Hz, 3H), 0.96 (d, J = 6.8 Hz, 3H); ^{13}C NMR (101 MHz, CDCl$_3$) δ 175.1, 84.9, 42.7, 37.6, 33.5, 31.1, 30.5, 24.1, 18.5, 17.3; LRMS (CI) *m/z* 171.1 [M+H]$^+$; HRMS (FTMS-NSI) calculated for C$_{10}$H$_{19}$O$_2$ [M+H]$^+$ 171.1380, found 171.1376; IR (ATR)/cm^{-1} 2970, 2928, 1722.

Tetrahydro-2H-pyran-2-one 374[213]

374
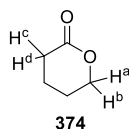
Lactone **374** was prepared according to General Procedure 4 using cyclopentanone **373** (0.36 mL, 4.0 mmol). The title compound was isolated as a colorless oil (118 mg, 1.1 mmol, 30%).

^{1}H NMR (400 MHz, CDCl$_3$) δ 4.38–4.29 (m, 2H, H^a, H^b), 2.54 (appt, J = 7.1 Hz, 2H, H^c, H^d), 1.97–1.78 (m, 4H); ^{13}C NMR (101 MHz, CDCl$_3$) δ 171.5, 69.5, 29.9, 22.4, 19.2; LRMS (CI) *m/z* 104.0 [M+H]$^+$; IR (ATR)/cm^{-1} 2970, 2934, 1724.

Dihydrofuran-2(3H)-one 376[213]

376
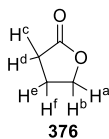
Lactone **376** was prepared according to General Procedure 4 using cyclobutanone **375** (0.30 mL, 4.0 mmol). The title compound was isolated as a colorless oil (292 mg, 3.4 mmol, 85%).

^{1}H NMR (400 MHz, CDCl$_3$) δ 4.33 (appt, J = 7.0 Hz, 2H, H^a, H^b), 2.57–2.44 (m, 2H, H^c, H^d), 2.35–2.18 (m, 2H, H^e, H^f); ^{13}C NMR (101 MHz, CDCl$_3$) δ 177.8, 68.6, 27.9, 22.3; LRMS (CI) *m/z* 87.0 [M+H]$^+$; IR (ATR)/cm^{-1} 2988, 2901, 1763.

rel-(1R,3R,6S,8S)-4-Oxatricyclo[4.3.1.1³,⁸]undecan-5-one 378[214]

378
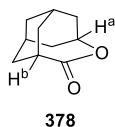
Lactone **378** was prepared according to General Procedure 4 using 2-adamantanone **377** (600 mg, 4.0 mmol). The title compound was isolated as a white solid (545 mg, 3.3 mmol, 82%).

m.p. >250 °C (lit. 288–290 °C);[214] ^{1}H NMR (400 MHz, CDCl$_3$) δ 4.51–4.43 (m, 1H, H^a), 3.06 (appt, J = 5.8 Hz, 1H, H^b), 2.14–1.88 (m, 8H), 1.86–1.78 (m, 2H), 1.77–1.70 (m, 2H); ^{13}C NMR (101 MHz, CDCl$_3$) δ 179.1, 73.3, 41.4, 35.9, 33.9, 31.1, 26.0; LRMS (CI) *m/z* 167.0 [M+H]$^+$; HRMS (FTMS-NSI) calculated for C$_{10}$H$_{15}$O$_2$ [M+H]$^+$ 167.1067, found 167.1063; IR (ATR)/cm^{-1} 2988, 2911, 1717.

4.10 Safety Warning!

Peroxides are particularly dangerous. These procedures should be carried out by knowledgeable laboratory workers. DSC data for malonoyl peroxide **90** is given in Tomkinson et al., *J. Am. Chem. Soc.* **2010**, *132*, 14409 (page S89, Supporting Information) and shows an onset temperature of 114.5 °C.

4.11 Synthesis of Malonoyl Peroxide 90

90
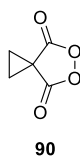
Dicarboxylic acid **100** (4.0 g, 30.7 mmol, 1.0 equiv) was weighed into a 100 mL round bottom flask equipped with a stir bar and wrapped in parafilm. The flask was immersed into a water bath and methanesulfonic acid (31.0 mL, 1.0 M) was added. Urea hydrogen peroxide (8.7 g, 93 mmol, 3.0 equiv) was added in three portions over one minute and the flask was loosely capped and allowed to stir over 18–20 h behind a blast shield. Afterward, the reaction was diluted with EtOAc (40 mL) and ice (40 mL) and stirred for 10 min. The layers were separated and the aqueous layer was extracted again with EtOAc (2 × 40 mL). The organic layers were combined and washed with a saturated solution of $NaHCO_3$ (3 × 40 mL), brine (40 mL) and dried ($MgSO_4$). The solvent was then removed to afford malonoyl peroxide **90** as a white solid (3.0-3.2 g, 23-25 mmol, 76-81%).

m.p. 77–78 °C; ^1H NMR (400 MHz, $CDCl_3$) δ 2.10 (s, 4H); ^{13}C NMR (101 MHz, $CDCl_3$) δ 172.3, 23.8, 19.9; IR (ATR)/cm^{-1}: 3121, 1829, 1788.

4.12 Arene Oxidation – Substrates

4.12.1 General Procedure for the Oxidation of Arenes (General Procedure 5)

Malonoyl peroxide **4** (77 mg, 0.60 mmol) was weighed directly into the reaction vial. Then, 1,1,1,3,3,3-hexafluoroisopropanol (0.6 mL) was added, followed by the addition of the arene (0.30 mmol). The vial was sealed with a screw cap and placed in a heating block set to 25 °C unless noted otherwise and the reaction was allowed to stir for the specified time. Upon completion, the mixture was diluted with EtOAc (20 mL) and stirred with a saturated solution of $Na_2S_2O_5$ in water (20 mL) for 2 h. The layers were then separated and the aqueous solution was extracted again with EtOAc (2 × 20 mL). The organic extracts were combined and washed with brine (20 mL) and dried ($MgSO_4$). The solution was concentrated and, if needed, the crude was chromatographed on silica gel (EtOAc) to afford the target compound.

4.12.2 Aromatic Esters shown in Table 11

Mesitylene ester 419

419
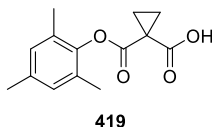
Ester **419** was prepared according to General Procedure 5 using mesitylene **395** (42 μL, 0.30 mmol). The title compound was isolated after work-up as a white solid (74 mg, 0.30 mmol, 99%).

Reaction time: 4.5 h.

m.p. 74–75 °C; ^{1}H NMR (400 MHz, CDCl$_3$) δ 12.35 (s, br, 1H), 6.89 (s, 2H), 2.28 (s, 3H), 2.11–2.04 (m, 10H); ^{13}C NMR (101 MHz, CDCl$_3$) δ 174.4, 170.5, 144.8, 136.5, 129.7, 129.3, 25.4, 22.5, 20.8, 16.2; LRMS (ESI) *m/z* 249.1 [M+H]$^+$; HRMS (FTMS-NSI) calculated for C$_{14}$H$_{17}$O$_4$ [M+H]$^+$ 249.1121, found 249.1124; IR (ATR)/cm^{-1} 2917, 1753, 1682.

1,3,5-Triisopropylbenzene ester 425

425
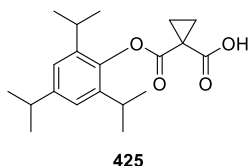
Ester **425** was prepared according to General Procedure 5 using 1,3,5-triisopropylbenzene **423** (73 μL, 0.3 mmol). The title compound was isolated after work-up as a yellow solid (99 mg, 0.3 mmol, 99%).

Reaction time: 2 h.

m.p. 121–122 °C; ^{1}H NMR (400 MHz, CDCl$_3$) δ 12.34 (s, br, 1H) 7.01 (s, 2H), 2.90 (hept, *J* = 6.8 Hz, 1H), 2.69 (hept, *J* = 6.8 Hz, 2H), 2.07 (s, 4H), 1.25 (d, *J* = 6.9 Hz, 6H), 1.22 (d, *J* = 6.8 Hz, 6H), 1.18 (d, *J* = 6.8 Hz, 6H); ^{13}C NMR (101 MHz, CDCl$_3$) δ 175.5, 170.5, 148.0, 142.4, 139.5, 122.3, 34.3, 27.9, 25.3, 24.2, 24.1, 22.9, 22.6; LRMS (ESI) *m/z* 333.2 [M+H]$^+$; HRMS (FTMS-NSI) calculated for C$_{20}$H$_{29}$O$_4$ [M+H]$^+$ 333.2060, found 333.2063; IR (ATR)/cm^{-1} 2961, 1746, 1688.

p-Xylene ester 427

427
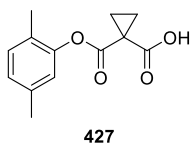
Ester **427** was prepared according to General Procedure 5 using *p*-xylene **426** (37 μL, 0.30 mmol). The title compound was isolated after work-up as a colorless oil (68 mg, 0.29 mmol, 97%).

Reaction time: 96 h.

^{1}H NMR (400 MHz, CDCl$_3$) δ 11.19 (s, br, 1H), 7.13 (d, J = 7.7 Hz, 1H), 7.01 (d, J = 7.8 Hz, 1H), 6.80 (s, 1H), 2.33 (s, 3H), 2.11 (s, 3H), 2.05–2.00 (m, 4H); ^{13}C NMR (101 MHz, CDCl$_3$) δ 174.4, 170.6, 148.0, 137.5, 131.3, 127.9, 126.4, 121.8, 25.6, 22.5, 20.9, 15.7; LRMS (ESI) *m/z* 233.1 [M–H]$^-$; HRMS (FTMS-CI) calculated for C$_{13}$H$_{13}$O$_4$ [M–H]$^-$ 233.0819, found 233.0821; IR (ATR)/cm^{-1} 2955, 2924, 1749, 1694.

Toluene esters 429 and 429'

429   **429'**
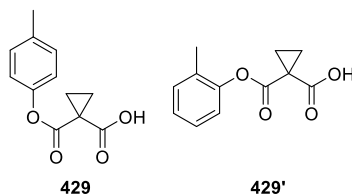
Esters **429** and **429'** were prepared according to General Procedure 5 using toluene **400** (107 μL, 1.0 mmol), malonoyl peroxide **90** (256 mg, 2.0 mmol) in HFIP (2.0 mL). A 1:1 mixture of the title compounds was obtained after work-up as a colorless oil (138 mg, 0.63 mmol, 63%).

Reaction time: 72 h.

Temperature: 50 °C.

^{1}H NMR (400 MHz, CDCl$_3$) δ 11.67 (s, br, 2H), 7.29–7.18 (m, 5H), 7.01–6.97 (m, 1H), 6.94 (d, J = 8.5 Hz, 2H), 2.36 (s, 3H), 2.17 (s, 3H), 2.07–1.98 (m, 8H); ^{13}C NMR (101 MHz, CDCl$_3$) δ 174.9, 174.3, 170.7, 170.6, 148.2, 147.3, 136.8, 131.6, 130.3, 129.7, 127.4, 127.1, 121.4, 120.8, 25.6, 22.7, 22.6, 21.0, 16.2; LRMS (ESI) *m/z* 219.1 [M–H]$^-$; IR (ATR)/cm^{-1} 3030, 2096, 1748, 1694.

Anisole esters 430 and 430'

430   **430'**
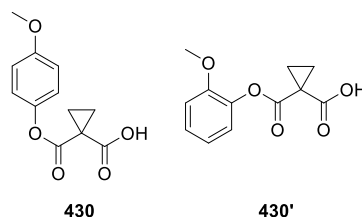
Esters **430** (major) and **430'** were prepared according to General Procedure 5 using anisole **404** (107 μL, 1.0 mmol). A 1:1.6 mixture of the title compounds was obtained after work-up as a yellow oil (138 mg, 0.60 mmol, 63%).

Reaction time: 72 h.

Temperature: 50 °C.

^{1}H NMR (400 MHz, CDCl$_3$) δ 11.67 (br, s, 2H), 7.28–7.22 (m, 1H), 7.05–6.88 (m, 7H), 3.83 (s, 3H), 3.80 (s, 3H), 2.14–2.07 (m, 2H), 2.04–1.97 (m, 6H); ^{13}C NMR (101 MHz, CDCl$_3$) δ 174.9, 174.3, 170.7, 170.6, 148.2, 147.3, 136.8, 131.6, 130.3, 129.7, 127.4, 127.1, 121.4, 120.8, 25.6, 22.7, 22.6, 21.0, 16.2; LRMS (ESI) *m/z* 219.1 [M–H]$^-$; IR (neat)/cm^{-1}: 3119, 2839, 1757, 1694.

Pentamethylbenzene ester 432

432
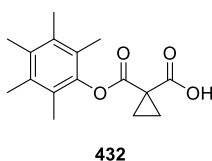
Ester **432** was prepared according to General Procedure 5 using pentamethylbenzene **431** (100 mg, 0.67 mmol) and malonoyl peroxide **90** (95 mg, 0.74 mmol) in HFIP (1.34 mL). The title compound was isolated as a dark yellow solid (128 mg, 0.46 mmol, 70%) after work-up.

Reaction time: 24 h.

m.p. 144–147 °C; ^{1}H NMR (400 MHz, CDCl$_3$) δ 11.95 (s, br, 1H), 2.22 (s, 9H), 2.14–2.10 (m, 2H), 2.09–2.02 (m, 8H); ^{13}C NMR (101 MHz, CDCl$_3$) δ 174.5, 170.6, 144.8, 134.0, 133.8, 124.8, 25.4, 22.4, 16.7, 16.5, 13.4; HRMS (FTMS-NSI) calculated for C$_{16}$H$_{21}$O$_4$ [M+H]$^+$ 277.1434, found 277.1433; IR (ATR)/cm^{-1}: 3022, 2930, 1732, 1705, 1144.

Bromomesitylene ester 434

434
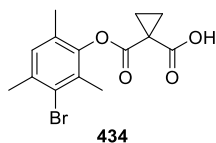
Ester **434** was prepared according to General Procedure 5 using 2-bromomesitylene **433** (55 µL, 0.36 mmol). After work-up, the title compound was isolated as a white solid (107 mg, 0.33 mmol, 91%).

Reaction time: 120 h.

m.p. 157–160 °C; ^{1}H NMR (400 MHz, CDCl$_3$) δ 11.78 (s, br, 1H), 7.01 (s, 1H), 2.38 (s, 3H), 2.20 (s, 3H), 2.09–2.03 (m, 7H); ^{13}C NMR (101 MHz, CDCl$_3$) δ 173.8, 170.3, 144.9, 137.1, 130.3, 129.7, 128.4, 125.4, 25.5, 23.7, 22.5, 17.3, 16.2; LRMS (ESI) *m/z* 326.9 [M(^{79}Br)+H]$^+$, 329.0 [M(^{81}Br)+H]$^+$; HRMS (FTMS-NSI): calculated for C$_{14}$H$_{16}$^{79}BrO$_4$ 327.0226 [M+H]$^+$, and for C$_{14}$H$_{16}$^{81}BrO$_4$ 329.0206 [M+H]$^+$, found 327.0225 [M(^{79}Br)+H]$^+$, 329.0203 [M(^{81}Br)+H]$^+$; IR (ATR)/cm^{-1} 2900, 1743, 1684, 1130.

2,4,6-Trimethyl benzoic acid ester 436

436
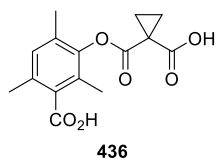
Ester **436** was prepared according to General Procedure 5 using 2,4,6-trimethylbenzoic acid **435** (49 mg, 0.30 mmol). After the standard work-up procedure, the crude was re-dissolved in EtOAc (20 mL), and extracted with a saturated solution of NaHCO$_3$ (aq., 3×20 mL). The resulting aqueous solution was slowly acidified with HCl (1.0 M) until cloudy (pH 1), extracted with EtOAc (3×20 mL), and dried (MgSO$_4$). The solvent was removed under reduced pressure to afford a white oily solid which was triturated with petroleum ether to afford the title compound as a white solid (75 mg, 0.26 mmol, 86%).

Reaction time: 42 h.

Temperature: 50 °C.

m.p. 179–180 °C (dec); ^{1}H NMR (400 MHz, acetone-d_6) δ 9.63 (s, br, 2H), 7.01 (s, 1H), 2.30 (s, 3H), 2.17 (s, 3H), 2.15 (s, 3H), 1.72–1.61 (m, 4H); ^{13}C NMR (101 MHz, acetone-d_6) δ 170.4, 170.0, 169.4, 146.6, 134.8, 132.8, 132.0, 130.8, 127.7, 28.0, 19.3, 17.6, 16.2, 13.6; LRMS (ESI) *m/z* 290.9 [M–H]$^{-}$; HRMS (FTMS-NSI) calculated for $C_{15}H_{15}O_6$ [M–H]$^{-}$ 291.0874, found 291.0872; IR (ATR)/cm^{-1} 2967, 1765, 1730, 1684.

3-Benzyloxy-4-methoxybenzaldehyde ester 441

441

Ester **441** was prepared according to General Procedure 5 using 3-benzyloxy-4-methoxybenzaldehyde **440** (73 mg, 0.30 mmol). After work-up, the crude reaction mixture was passed through a plug of silica gel using EtOAc as eluent. Evaporation of the solvent provided ester **441** as a colorless oil (43 mg, 0.12 mmol, 40%).

Reaction time: 24 h.

^{1}H NMR (400 MHz, CDCl$_3$) δ 11.83 (s, br, 1H), 9.80 (s, 1H), 7.58 (d, *J* = 8.7 Hz, 1H), 7.41–7.31 (m, 5H), 7.02 (d, *J* = 8.7 Hz, 1H), 5.04 (s, 2H), 4.02 (s, 3H), 2.02–1.77 (m, 4H); ^{13}C NMR (101 MHz, CDCl$_3$) δ 188.1, 174.0, 170.1, 158.8, 142.8, 140.6, 136.7, 129.7, 128.8, 128.7, 128.4, 122.3, 110.1, 75.8, 56.6, 25.8, 23.0; LRMS (ESI) *m/z* 393.1 [M+Na]$^{+}$; HRMS (FTMS-NSI) calculated for $C_{20}H_{17}O_7$ [M–H]$^{-}$ 369.0980, found 369.0976; IR (ATR)/cm^{-1} 2925, 1759, 1690, 1597.

4.12.3 Aromatic Esters used in the Hammett Analysis (Table 13)

2,4,6-Trimethylanisole ester 504

504
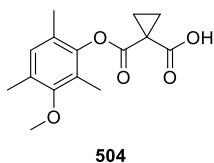
Ester **504** was prepared according to General Procedure 5 using 2,4,6-trimethylanisole **458** (47 µL, 0.30 mmol). The crude product obtained after work-up was passed through an –NH$_2$ cartridge using CH$_2$Cl$_2$ (20 mL) to remove all impurities. Afterwards, the cartridge was flushed with a saturated solution of HCl in Et$_2$O (20 mL); the resulting ether solution was removed *in vacuo* to afford the title compound as a colorless oil (81 mg, 0.29 mmol, 98%).

Reaction time: 6 h.

^{1}H NMR (400 MHz, CDCl$_3$) δ 10.19 (s, br, 1H), 6.89 (s, 1H), 3.69 (s, 3H), 2.24 (s, 3H), 2.07–1.99 (m, 10H); ^{13}C NMR (101 MHz, CDCl$_3$) δ 173.5, 170.9, 155.6, 145.4, 130.2, 129.5, 124.9, 123.2, 60.2, 25.6, 22.2, 15.9, 15.8, 9.9; LRMS (ESI) *m/z* 279.1 [M+H]$^+$; HRMS (FTMS-APCI) calculated for C$_{14}$H$_{17}$O$_4$ [M+H]$^+$ 279.1227, found 279.1225; IR (ATR)/cm^{-1} 3015, 2932, 1747, 1697.

Isodurene 459

459
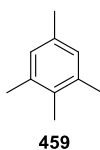
To a pre-dried Schlenk flask equipped with a stirrer, under an argon atmosphere at –78 °C, 2.4 mL dry Et$_2$O were added *via* syringe. Then 2-bromomesitylene **433** (1.22 mL, 8.0 mmol, 1.0 equiv) was added. A [1.52 M] solution of *t*-butyllityhium in pentane (10.5 mL, 16.0 mmol, 2.0 equiv) was slowly added to the flask over a period of 10–15 min at –78 °C. The mixture was allowed to warm up to room temperature over 1.5 h and was checked by ^{1}H NMR for consumption of 2-bromomesitylene **433**. The white mixture was cooled down to -78 °C again and iodomethane (1.49 mL, 24.0 mmol, 3.0 equiv) was added to it dropwise over 20 min. The mixture was then stirred overnight, allowing it to warm up to room

temperature. Then CH_2Cl_2 (20 mL) and water (10 mL) were added to the mixture and the biphasic solution was stirred for 30 min at room temperature. The layers were separated and the aqueous was further extracted with CH_2Cl_2 (2 × 20 mL), after which the organic layers were combined, washed with brine (20 mL), dried ($MgSO_4$) and the solvent was removed *in vacuo*. The resulting crude was distilled under reduced pressure (72 °C, 12 mbar) using a Vigreux column to afford the title compound as a colorless oil (541 mg, 4.0 mmol, 50%).

^{1}H NMR (400 MHz, $CDCl_3$) δ 6.85 (s, 2H), 2.29–2.24 (m, 9H), 2.15 (s, 3H); ^{13}C NMR (101 MHz, $CDCl_3$) δ 136.4, 134.7, 132.0, 128.5, 20.9, 20.6, 15.1; LRMS (CI) *m/z* 135.1 [M+H]$^+$ HRMS (FTMS-APCI) calculated for $C_{10}H_{15}$ [M+H]$^+$ 135.1168, found 135.1168; IR (ATR)/cm^{-1} 2999, 2916, 1485.

Isodurene ester 505

505
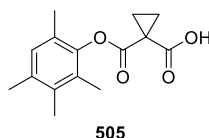
Ester **505** was prepared according to General Procedure 5 using isodurene **459** (15 µL, 0.10 mmol). The title compound was pure after work-up as a colorless oil (26 mg, 0.10 mmol, 99%).

Reaction time: 30 min.

^{1}H NMR (400 MHz, $CDCl_3$) δ 6.90 (s, 1H), 2.24 (s, 3H), 2.16 (s, 3H), 2.11–2.04 (m, 7H), 2.02 (s, 3H); ^{13}C NMR (101 MHz, $CDCl_3$) δ 174.6, 170.5, 145.0, 135.2, 134.6, 129.9, 127.8, 126.0, 25.3, 22.8, 20.5, 16.1, 15.8, 13.2; LRMS (ESI) *m/z* 261 [M–H]$^-$; HRMS (FTMS-NSI) calculated for $C_{15}H_{19}O_4$ [M+H]$^+$ 263.1278, found 263.1278; IR (ATR)/cm^{-1} 2924, 2868, 1748, 1694.

2-Fluoromesitylene ester 506

506
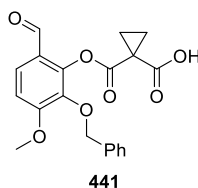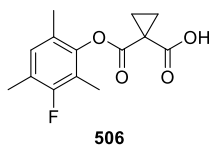
Ester **506** was prepared according to General Procedure 5 using 2-fluoromesitylene **460** (43 µL, 0.30 mmol). After the standard work-up procedure, the crude was triturated with petroleum ether to afford the title compound as a white solid (77 mg, 0.29 mmol, 96%).

Reaction time: 8 h.

m.p. 105–180 °C; ^{1}H NMR (400 MHz, CDCl$_3$) δ 10.70 (s, 1H), 6.89 (d, $^4J_{HF}$ = 8.2 Hz, 1H), 2.22 (s, 3H), 2.09-2.00 (m, 10H); ^{13}C NMR (101 MHz, CDCl$_3$) δ, 173.8, 170.4, 158.0 (d, $^1J_{CF}$ = 243.4 Hz), 145.0 (d, $^3J_{CF}$ = 6.7 Hz), 130.0 (d, $^3J_{CF}$ = 6.0 Hz), 124.5 (d, $^4J_{CF}$ = 4.0 Hz), 123.2 (d, $^2J_{CF}$ = 18.3 Hz), 117.4 (d, $^2J_{CF}$ = 20.6 Hz), 25.5, 22.6, 15.85, 14.5 (d, $^3J_{CF}$ = 3.1 Hz), 8.9 (d, $^3J_{CF}$ = 4.5 Hz); ^{19}F NMR (376 MHz, CDCl$_3$) δ 120.90 (s, 1F); LRMS (ESI) *m/z* 264.9 [M–H]$^-$; HRMS (FTMS-NSI) calculated for C$_{14}$H$_{14}$O$_4$F$_1$ [M–H]$^-$ 265.0882, found 265.0877; IR (ATR)/cm^{-1} 2988, 2887, 1753, 1694.

4.12.4 Aminolysis of Ester Intermediates (General Procedure 6)

The crude product of the arene oxidation (1.0 equiv) was dissolved in the minimum amount of EtOH. To this solution, MeNH$_2$ in EtOH (33% MeNH$_2$ w/v, 20 equiv MeNH$_2$) was added and the mixture was stirred for 1 h at 25 °C. The solvent was then removed *in vacuo* and the resulting crude was chromatographed on silica gel using the specified solvent system for each substrate.

2,4,6-Trimethylphenol 396

396
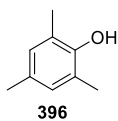
2,4,6-trimethylphenol **396** was prepared according to General Procedure 6 using ester **419** (50 mg, 0.20 mmol). The crude was chromatographed on silica gel (EtOAc:petroleum ether, 1:1) to afford 2,4,6-trimethylphenol **396** as a beige solid (25 mg, 0.18 mmol, 92%).

^{1}H NMR (400 MHz, CDCl$_3$) δ 6.79 (s, 2H), 2.24–2.21 (m, 9H); ^{13}C NMR (101 MHz, CDCl$_3$) δ 150.0, 129.4, 129.3, 122.9, 20.5, 15.9; LRMS (EI) *m/z* 136.08 [M•]; IR (ATR)/cm^{-1} 3389, 2972, 2914.

2,4,6-Triisopropylphenol 424

424
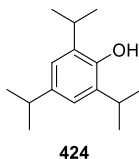
2,4,6-triisopropylphenol **424** was prepared according to General Procedure 6 using ester **425** (67 mg, 0.20 mmol). The crude was chromatographed on silica gel (EtOAc:petroleum ether, 1:1) to afford 2,4,6-triisopropylphenol **424** as a brown oil (41 mg, 0.19 mmol, 93%).

^{1}H NMR (400 MHz, CDCl$_3$) δ 6.93 (s, 2H), 4.63 (s, 1H), 3.16 (hept, *J* = 6.7 Hz, 2H), 2.86 (hept, *J* = 6.9 Hz, 1H), 1.29 (d, *J* = 6.9 Hz, 12H), 1.25 (d, *J* = 6.9 Hz, 6H); ^{13}C NMR (101 MHz, CDCl$_3$) δ 148.1, 140.9, 133.5, 121.5, 34.0, 27.5, 24.5, 22.9; LRMS (EI) *m/z* 220.11 [M•]; HRMS (FTMS-APCI) calculated for C$_{15}$H$_{25}$O$_1$ [M+H]$^+$ 221.1900, found 221.1898; IR (ATR)/cm^{-1} 2959, 2928, 2868.

Biaryl phenols 439 and 439'
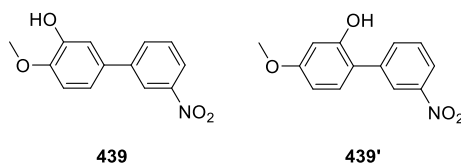
The crude reaction mixture after reacting biaryl compound **438** (69 mg, 0.30 mmol) with malonoyl peroxide **90** (0.60 mmol) according to General Procedure 5, was subjected to aminolysis using General Procedure 6. The crude of the aminolysis reaction mixture was chromatographed on silica gel (EtOAc:petroleum ether, 4:1) to afford a 3:2 mixture of the two isomers **439** and **439'** as a yellow oil (44 mg, 0.18 mmol, 60%).

^{1}H NMR (400 MHz, CDCl$_3$) δ 8.45–8.35 (m, 2H), 8.22–8.11 (m, 2H), 7.91–7.80 (m, 2H), 7.65–7.53 (m, 2H), 7.28–7.19 (m, 3H), 7.14 (dd, *J* = 8.3, 2.1 Hz, 1H), 6.96 (d, *J* = 8.3 Hz, 1H), 6.62 (d, *J* = 8.4 Hz, 1H), 6.52 (s, 1H), 5.71 (s, 1H), 5.11 (s, 1H), 3.95 (s, 3H), 3.84 (s, 3H); ^{13}C NMR (101 MHz, CDCl$_3$) δ 161.3, 153.6, 147.2, 146.3, 142.6, 139.5, 135.3, 132.7, 132.2, 124.2, 121.9, 121.7, 119.1, 113.5, 111.2, 107.4, 102.4, 56.2, 55.6; LRMS (EI) *m/z* 245.08 [M•]; IR (ATR)/cm^{-1} 3468, 2928, 1616, 1514.

4.13 Procedures used for Additive Screening

4.13.1 General Procedure for Additive Screening (General Procedure 7)
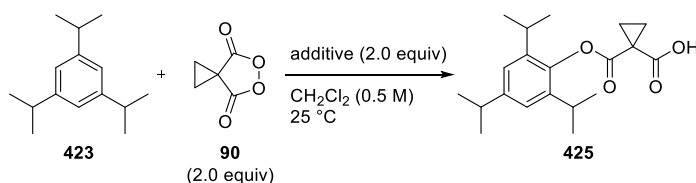
Malonoyl peroxide **90** (51 mg, 0.40 mmol, 2.0 equiv) was weighed into a 1.5 mL vial and CH$_2$Cl$_2$ (0.4 mL) was added. Afterward, 1,3,5-triisopropylbenzene **423** (48 µL, 0.20 mmol, 1.0 equiv) and the additive (0.40 mmol, 2.0 equiv) were added. 20 µL aliquots were taken at the specified times and the solvent was evaporated carefully under compressed air. The aliquots were diluted in 0.6 mL CDCl$_3$ and the conversion of the 1,3,5-triisopropylbenzene **423** to its corresponding ester **425** was monitored by ^{1}H NMR spectroscopy.

4.13.2 General procedure for the Effect of Water on the Acid Mediated Oxidation (General Procedure 7)
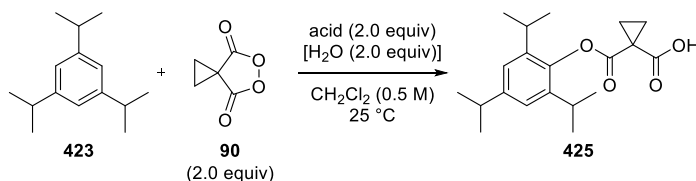
Malonoyl peroxide **90** (25 mg, 0.20 mmol, 2.0 equiv) was weighed into a 1.5 mL vial. CH_2Cl_2 (0.2 mL) was added, followed by the acid (0.20 mmol, 2.0 equiv), 1,3,5-triisopropylbenzene **425** (24 µL, 0.10 mmol, 1.0 equiv) and water (3.5 µL, 0.20 mmol, 2.0 equiv) when required. 20 µL aliquots were taken at the specified times and evaporated carefully under compressed air. The aliquots were diluted in 0.6 mL $CDCl_3$ and the conversion of the 1,3,5-triisopropylbenzene **423** to its corresponding ester **425** was monitored by ^1H NMR spectroscopy.

4.14 Reaction Kinetics

4.14.1 Overall Reaction
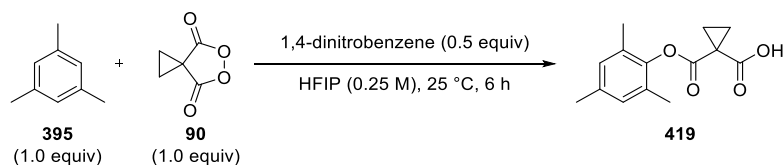
Malonoyl peroxide **90** (32 mg, 0.25 mmol, 1.0 equiv) was weighed into a 7 mL vial. Then, a 0.125 M standard solution of 1,4-dinitrobenzene in HFIP (1.0 mL, 0.5 equiv 1,4-dinitrobenzene) was added and a 40 µL aliquot was diluted in 0.5 mL $CDCl_3$ to record the initial ratio (internal standard *vs* peroxide). Mesitylene **395** (35 µL, 0.25 mmol, 1.0 equiv) was added and the reaction was stirred at 25 °C. 40 µL aliquots were sampled at different times and were immediately diluted in $CDCl_3$ (0.5 mL); this stopped the reaction, providing identical ^1H NMR spectra after 3 h of standing. The results are an average of two runs (Figure 43).
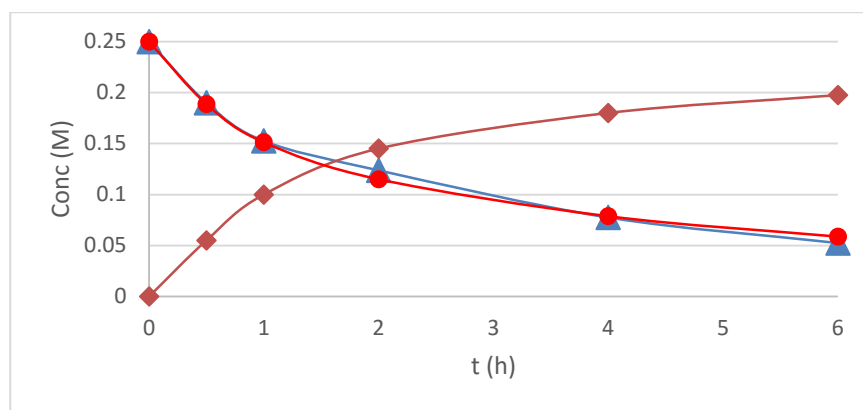
Figure 43: Reaction profile of the malonoyl peroxide **90** (▲, (0.25 M)) mediated oxidation of mesitylene **395** (●, (0.25 M)) leading to single product **419** (◆, (0.25 M))
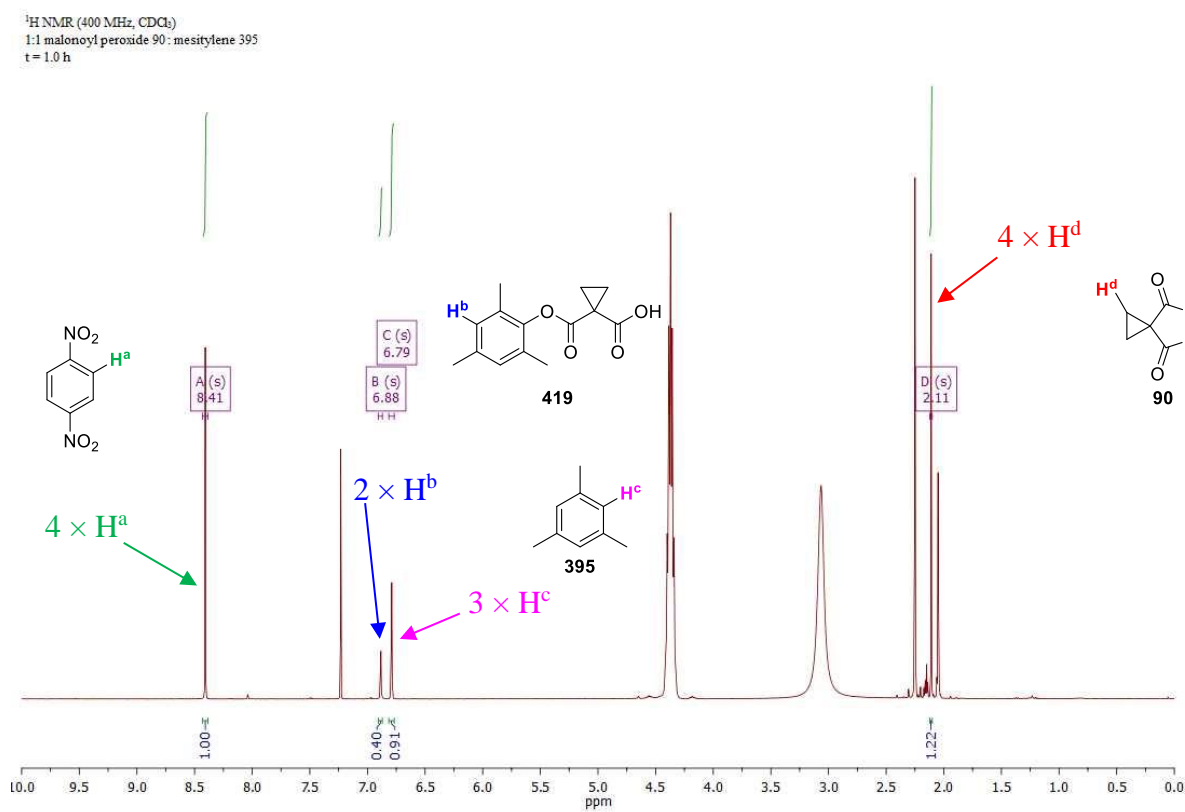
Figure 44: Sample ^{1}H NMR spectrum of the arene oxidation reaction at t = 1.0 h showing the signals used to determine conversion

4.14.2 Reaction Order in Malonoyl Peroxide 90
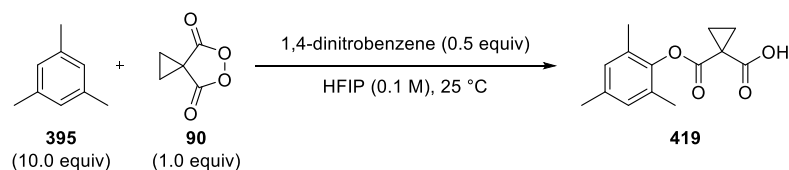
Malonoyl peroxide **90** (32 mg, 0.25 mmol, 1.0 equiv) was weighed into a 7 mL vial. Then, a 0.02 M standard solution of 1,4-dinitrobenzene in HFIP (2.5 mL, 0.2 equiv 1,4-dinitrobenzene) was added and a 40 µL aliquot was diluted in 0.5 mL CDCl₃ to record the initial ratio (internal standard *vs* peroxide). Mesitylene **395** (348 µL, 2.5 mmol, 10.0 equiv) was added and the reaction was stirred at 25 °C. 40 µL aliquots were sampled at different times and were immediately diluted in CDCl₃ (0.5 mL); this stopped the reaction, providing identical ¹H NMR spectra after 3 h of standing. The results shown are an average of two runs.

Table 15: Raw data used for determining the reaction order in malonoyl peroxide **90**

t(h)	[peroxide]	[prod]	[MesH]	perox corr	perox inte	prod integ	MesH int	ln[perox]	ln[perox/p]	1/[perox]
0	0.1	0	1	5.1	5.1	0	50	-2.30259	0	10
0.25	0.065106	0.042745	0.9576	3.43	3.43	2.18	47.88	-2.73175	-0.42916	15.35967
0.5	0.03714	0.06549	0.934667	2.02	2.02	3.34	46.73333	-3.29307	-0.99048	26.92537
0.75	0.026364	0.076863	0.927467	1.47	1.47	3.92	46.37333	-3.63574	-1.33316	37.93005
1	0.017847	0.085882	0.924533	1.02	1.02	4.38	46.22667	-4.02594	-1.72335	56.03272
1.5	0.009603	0.088627	0.906133	0.57	0.57	4.52	45.30667	-4.6457	-2.34311	104.1359
2	0.005594	0.095294	0.904533	0.31	0.31	4.86	45.22667	-5.18607	-2.88348	178.7642
2.5	0.002964	0	0	0.2	0.2			-5.82107	-3.51848	337.3325
3	0.001765	0	0	0.09	0.09			-6.33977	-4.03719	566.6667

4.14.3 Reaction Order in Mesitylene 395
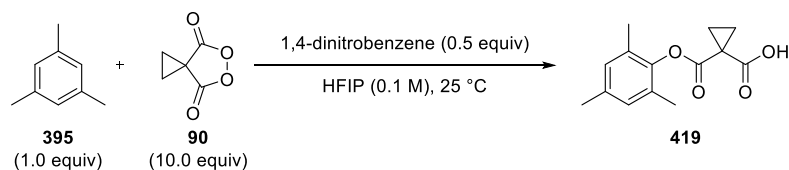
Malonoyl peroxide **90** (320 mg, 2.5 mmol, 10.0 equiv) was weighed into a 7 mL vial. Then, a 0.02 M standard solution of 1,4-dinitrobenzene in HFIP (2.5 mL, 0.2 equiv 1,4-dinitrobenzene) was added. Mesitylene **395** (35 µL, 0.25 mmol, 1.0 equiv) was added and the reaction was stirred at 25 °C. 40 µL aliquots were sampled at different times and were immediately diluted in CDCl₃ (0.5 mL); this stopped the reaction, providing identical ¹H NMR spectra after 3 h of standing. The results shown are an average of two runs.

Table 16: Raw data used for determining the reaction order in mesitylene **395**

t(h)	[peroxide	[prod]	[MesH]	perox integration	prod integration x 2	MesH int x 4/3	ln[MesH]	1/[MesH]	ln([MesH]/[MesH0]
0	1	0	0.1	45.36	0	5.2	-2.30259	10	0
0.25	1.01433	0.01778	0.05871	46.01	2	2.973	-2.8352	17.0338	-0.53261
0.5	0	0.04793	0.03935	0	3.08	2	-3.23523	25.4122	-0.93265
0.75	0	0.06536	0.02602	0	3.7	1.307	-3.64885	38.4305	-1.34627
1	0	0.08206	0.01179	0	4.42	0.88	-4.44009	84.7826	-2.13751
1.5	0	0.09065	0.00406	0	4.72	0.333	-5.50583	246.121	-3.20324
2	0	0.09538	0.00089		4.88	0.093	-7.01955	1118.28	-4.71696
2.5	0	0.09692	0		5.2	0			
3	0	0.1	0		5.2				

4.15 Procedures for Hammett Analysis

4.15.1 General Procedure 8

To a 7 mL vial, malonoyl peroxide **90** (38 mg, 0.30 mmol, 1.0 equiv) was weighed. A standard solution of 1,4-dinitrobenzene in HFIP ((0.01 M), 3.0 mL, 0.20 equiv 1,4-dinitrobenzene) was then added. A 100 µL aliquot was taken and diluted in CDCl$_3$ (0.5 mL) to record the initial ratio (internal standard *vs* peroxide). Afterward, the arene (0.30 mmol, 1.0 equiv) was added and the reaction was stirred at 25 °C. 100 µL aliquots were taken at the specified times and were immediately diluted in CDCl$_3$ (0.5 mL); this slowed down the reaction, providing identical ^{1}H NMR spectra after 3 h of standing. All reactions were performed in duplicate.

Mesitylene 395

395
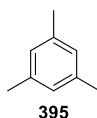
General Procedure 8 was applied to mesitylene **395** (42 µL, 0.30 mmol, 1.0 equiv). The consumption of peroxide was monitored against the internal standard at the following time intervals (min): 1, 3, 5, 7, 10, 15, 20, 25, 30.

2,4,6-Trimethylanisole 458

458
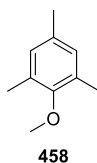
General Procedure 8 was applied to 2,4,6-trimethylanisole **458** (47 µL, 0.30 mmol, 1.0 equiv). The consumption of peroxide was monitored against the internal standard at the following time intervals (min): 1, 5, 10, 15, 30, 45, 60, 75, 90.

2-Fluoromesitylene 460

460
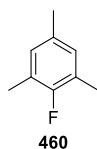
General Procedure 8 was applied to 2-fluoromesitylene **460** (43 µL, 0.30 mmol, 1.0 equiv). The consumption of peroxide was monitored against the internal standard at the following time intervals (min): 1, 5, 10, 15, 30, 45, 60, 75, 90.

2-Bromomesitylene 433

433
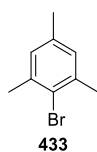
General Procedure 8 was applied to 2-bromomesitylene **433** (45 µL, 0.30 mmol, 1.0 equiv). The consumption of peroxide was monitored against the internal standard at the following time intervals (h): 0.5, 1, 2, 3, 4.

Isodurene 459

459
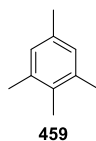
To a 7 mL vial, a standard solution of 1,4-dinitrobenzene in HFIP ((0.01 M), 2.0 mL, 0.20 equiv 1,4-dinitrobenzene) was added. Isodurene **459** (30 µL, 0.20 mmol, 1.0 equiv) was then added. A 100 µL aliquot was taken and diluted in CDCl$_3$ (0.5 mL) to record the initial ratio (internal standard *vs* isodurene). Malonoyl peroxide **90** (26 mg, 0.20 mmol, 1.0 equiv) was then added. 100 µL aliquots were retrieved at the specified time intervals and quenched in vials containing CDCl$_3$ (0.6 mL) and a saturated solution of Na$_2$S$_2$O$_5$ in water (0.8 mL). The organic layers were pipetted out and filtered through a short plug of MgSO$_4$ directly into the NMR tube. The data was recorded at the following time intervals (min): 1, 2, 3, 4, 5, 7, 10.

Raw Data

[prod] vs time

t(h)	R=H	R=Br	R=Me	R=OMe	R=F
0	0	0	0	0	0
0.016667	0.000808		0.000456	0.0002	0
0.033333			0.000911		
0.05	0.001313		0.001367		
0.066667			0.002503		
0.083333	0.00202		0.003184	0.000999	0.0002
0.116667	0.002929		0.004782		
0.166667	0.004141		0.006609	0.001897	0.000599
0.25	0.00596		0	0.002795	0.000798
0.333333	0.007778		0		
0.416667	0.010404		0		
0.5	0.011717	0.001083	0	0.005884	0.001599
0.75	0		0	0.008678	0.002196
1	0	0.00217	0	0.010076	0.002892
1.25	0		0	0.011972	0.003789
1.5	0		0	0.014071	0.004591
1.75	0		0	0	0
2	0	0.004232	0	0	0
3	0	0.006508	0	0	0
4	0	0.008678	0	0	0

Figure 45: Data used for determination of initial rates used in the Hammett analysis
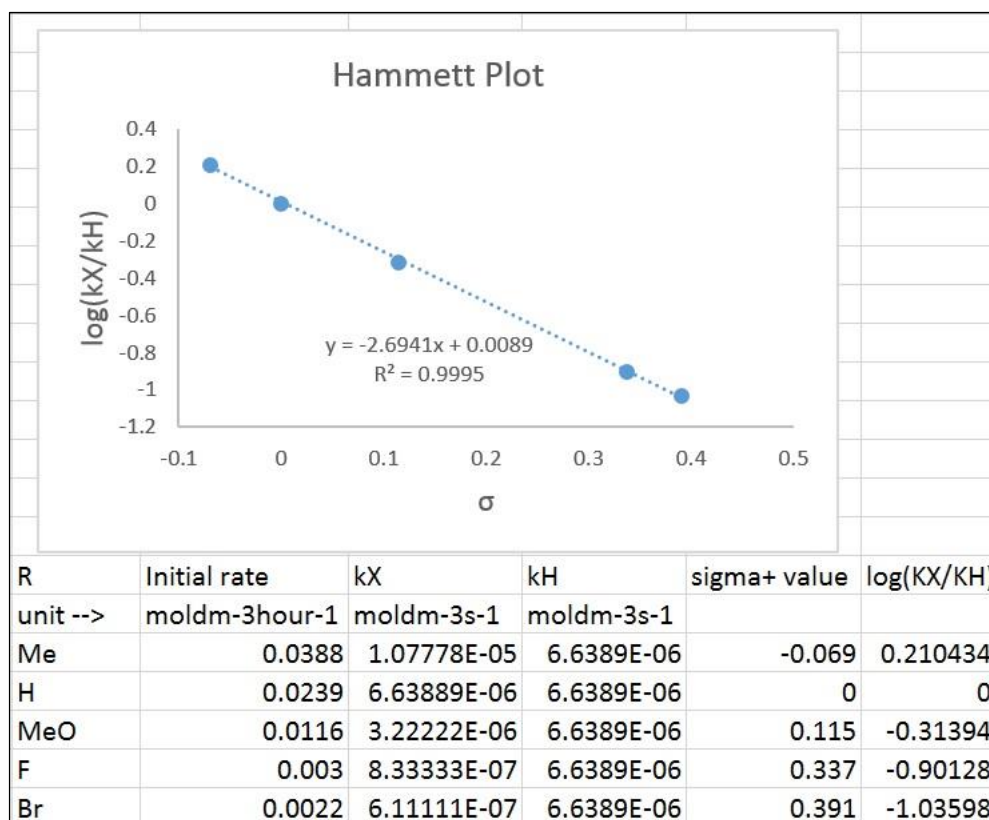
Figure 46: Data used for the generation of the Hammett plot

R	Initial rate	kX	kH	sigma+ value	log(KX/KH)
unit -->	moldm-3hour-1	moldm-3s-1	moldm-3s-1		
Me	0.0388	1.07778E-05	6.6389E-06	-0.069	0.210434
H	0.0239	6.63889E-06	6.6389E-06	0	0
MeO	0.0116	3.22222E-06	6.6389E-06	0.115	-0.31394
F	0.003	8.33333E-07	6.6389E-06	0.337	-0.90128
Br	0.0022	6.11111E-07	6.6389E-06	0.391	-1.03598

4.16 ^{18}O Labeling Experiments

Malonic acid 461
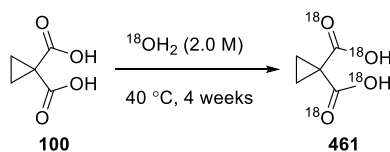
Malonic acid **100** (260 mg, 2.0 mmol, 1.0 equiv) was weighed in a 5 mL round bottom flask; the flask was sealed under argon and ^{18}OH$_2$ (97% ^{18}O incorporation, 1.0 mL, 55 mmol, 26.5 equiv) was added. The mixture was stirred for 14 days at 40 °C and then the ^{18}OH$_2$ was carefully removed under reduced pressure, ensuring that no air or moisture from the atmosphere contaminated the sample. The resulting solid compound was re-dissolved in ^{18}OH$_2$ (97% ^{18}O incorporation, 1.0 mL, 55 mmol, 26.5 equiv) and stirred for another 14 days at 40 °C. Afterward, the ^{18}OH$_2$ was removed under reduced pressure to afford the ^{18}O

enriched malonic acid **461** in quantitative yield (white solid). The title compound was stored under Ar at –18 °C.

The spectral data matched that of cyclopropyl malonic acid **21**. LRMS (ESI) *m/z* 137.1 [M–H]⁻, (85% abundance) and 134.9 [M–H]⁻, (15% abundance).

¹⁸O labeled malonoyl peroxide 462
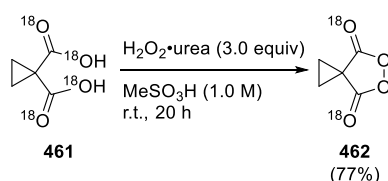
¹⁸O enriched cyclopropyl malonic acid **461** (62 mg, 0.45 mmol, 1.0 equiv) was weighed in a 7 mL vial, then MeSO₃H (0.45 mL, 1.0 M) was added. H₂O₂•urea (127 mg, 1.4 mmol, 3.0 equiv) was then carefully added and the mixture was allowed to react for 20 h at room temperature. The mixture was then diluted in EtOAc (10 mL) and stirred with ice (10 mL) for 15 min until the ice melted. The layers were separated and the aqueous layer was further extracted with EtOAc (2 × 10 mL). The organic extracts were combined and washed with saturated NaHCO₃ (aq., 3 × 10 mL), brine (10 mL), and dried (MgSO₄). The solvent was removed under reduced pressure to afford malonoyl peroxide **462** as a white solid (46 mg, 0.35 mmol, 77%).

The spectral data matches that of malonoyl peroxide **90**.

¹⁸O labeled mesitylene ester 463
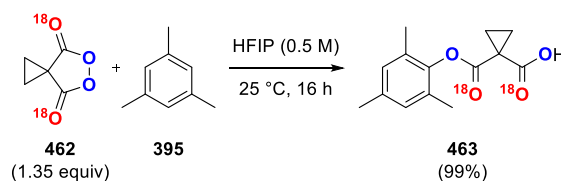
The ¹⁸O labeled peroxide **462** (30 mg, 0.23 mmol, 1.35 equiv) was weighed into a 1.5 mL vial and then HFIP (0.23 mL, 0.5 M) was added. Mesitylene **395** (23 µL, 0.17 mmol, 1.0 equiv) was added *via* syringe to the mixture. The reaction was stirred for 6 h and the mixture was diluted in EtOAc (10 mL) and stirred with saturated Na₂S₂O₅ (aq., 10 mL) for

2 h at room temperature. The layers were separated and the aqueous phase was further extracted with EtOAc (2 × 10 mL). The organic extracts were combined and dried (MgSO$_4$). Removal of the solvent *in vacuo* afforded doubly labelled ester **463** (45 mg, 0.17 mmol, 99%).

The ^{1}H and ^{13}C NMR spectra matched that of non-labeled ester **419**; LRMS (ESI) *m/z* 252.9, 250.9 [M+H]$^+$, with fragmentation of these ions using LRMS and HRMS showing no ^{18}O attached to the aromatic ring; IR (ATR)/cm^{-1} 2919, 1721, 1673.

Aminolysis of mesitylene esters 463 and 419

The ester bond was cleaved using MeNH$_2$ and the crude reaction mixture was analyzed using a GC Agilent 7890A GC system, equipped with a 30 m ×250 µm × 0.25 µm DB5MS column connected to a 5975C inert XL CI MSD with Triple-Axis Detector. GC program: 40 °C (4 min), then 20 °C/min to 320 °C (hold 10 min).
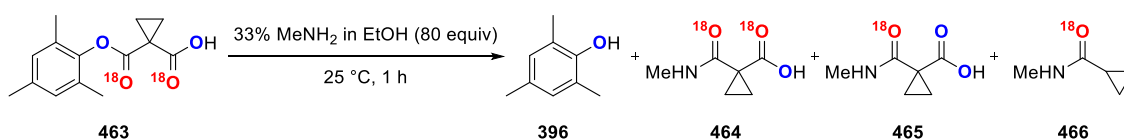
^{18}O labeled ester **463** (10 mg, 0.040 mmol, 1.0 equiv) was weighed into a 1.5 mL vial and MeNH$_2$ in EtOH (33 wt%, 0.4 mL, 80.0 equiv) was added. The reaction was stirred for 1 h at 25 °C and then the solvent was removed under reduced pressure. The resulting crude mixture (10 mg) was analyzed by GCMS/CI, providing three signals:

1. Retention time (min): 7.918; *m/z* 102.0 [M+H]$^+$; decarboxylated amide **466** with one ^{18}O label.
2. Retention time (min): 9.348; *m/z* 137.1 [M+H]$^+$; 2,4,6-trimethylphenol **396**, no ^{18}O label.
3. Retention time (min): 10.671; *m/z* 147.9 [M+H]$^+$; amide **464** with two ^{18}O labels and amide **465** with one ^{18}O label.
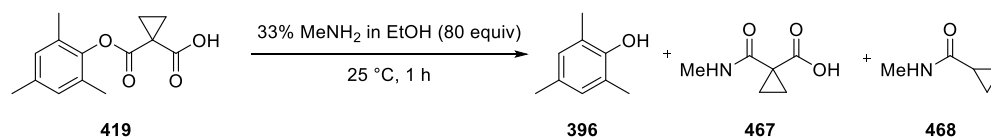
Ester **419** (50 mg, 0.20 mmol, 1.0 equiv) was weighed into a 7 mL vial and MeNH$_2$ in EtOH (33 wt%, 2.0 mL, 80.0 equiv) was added. The reaction was stirred for 1 h at 25 °C and then the solvent was removed under reduced pressure. The resulting crude mixture (64 mg) was analyzed by GCMS/CI, providing three signals:

1. Retention time (min): 8.111; *m/z* 100.0 [M+H]$^+$; decarboxylated amide **468**.
2. Retention time (min): 9.398; *m/z* 137.1 [M+H]$^+$; 2,4,6-trimethylphenol **396**.
3. Retention time (min): 10.834; *m/z* 143.9 [M+H]$^+$; amide **467**.

The crude for this reaction was chromatographed on silica gel (EtOAc:petroleum ether, 1:1) to afford 2,4,6-trimethylphenol **396** as a beige solid (15 mg, 0.11 mmol, 56%). *Note*: 2,4,6-trimethylphenol **396** is volatile (220 °C (lit.)[215]).

4.17 Synthesis of Authentic Samples of Radical Clock Potential Products

2-Bromo-3,5-dimethylphenol 484[182]
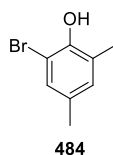
To a solution of 2,4-dimethylphenol **482** (6.04 mL, 50 mmol) in DMF (25 mL), a solution of *N*-bromosuccinimide (8.9 g, 50 mmol) in DMF was added dropwise at 25 °C. The reaction was allowed to stir for 24 h at 25 °C and was then quenched with water (250 mL). The aqueous solution was extracted with a mixture of toluene and hexane (1:19, 3 × 100 mL) and the combined organic extracts were washed with water (2 × 100 mL), brine (100 mL) and dried (MgSO4). The solution was filtered and concentrated to afford the title compound as a green liquid (9.1 g, 45.3 mmol, 91%).

^{1}H NMR (400 MHz, CDCl$_3$) δ 7.13–7.09 (m, 1H), 6.90–6.85 (m, 1H), 5.37 (s, 1H), 2.26 (s, 3H), 2.23 (s, 3H); ^{13}C NMR (101 MHz, CDCl$_3$) δ 148.3, 131.3, 130.8, 129.5, 125.5, 109.9, 20.3, 16.7; LRMS (CI) *m/z* 200.0 [M (^{79}Br) +H]$^+$ 202.0 [M (^{81}Br) +H]$^+$; HRMS

(FTMS-APCI) calculated for $C_8H_9O_1{}^{79}Br$ [M+H]$^+$ 199.9831, $C_8H_9O_1{}^{79}Br$ [M+H]$^+$ 201.9811, found 199.9831 and 201.9809; IR (ATR)/cm^{-1} 3514, 2972, 2920, 1481.

2-iodo-3,5-dimethylphenol 486

486
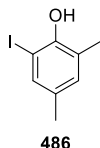
p-Toluenesulfonic acid monohydrate (8.00 g, 42 mmol) and *N*-iodosuccinimide (9.44 g, 42 mmol) were charged to a round bottom flask and then CHCl$_3$ (400 mL) was added, followed by the 2,4-dimethylphenol **482** (4.84 mL, 40 mmol) and the mixture was stirred for 16 h at 25 °C. The reaction was then quenched with a saturated solution of NaHCO$_3$ (100 mL). The layers were separated and the organic phase was washed with water (150 mL), brine (150 mL), dried (MgSO$_4$) and concentrated to afford the title compound as a brown liquid (8.8 g, 35.2 mmol, 88%).

^{1}H NMR (400 MHz, CDCl$_3$) δ 7.33–7.28 (m, 1H), 6.92–6.87 (m, 1H), 5.10 (s, 1H), 2.26 (s, 3H), 2.21 (s, 3H); ^{13}C NMR (101 MHz, CDCl$_3$) δ 150.8, 135.8, 135.78, 135.7, 132.5, 132.4, 131.7, 124.6, 85.8, 20.0, 17.2; LRMS (CI) *m/z* 248.0 [M]$^+$; HRMS (FTMS-APCI) calculated for C_8H_9O [M]$^+$ 247.9693, found 247.9691; IR (ATR)/cm^{-1} 3477, 3350, 2920.

1-iodo-2-methoxy-3,5-dimethylbenzene 488[186]

488
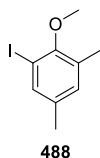
2-Iodo-3,5-dimethylphenol **488** (4.96 g, 20 mmol) was weighed into a round bottom flask, DMF (40 mL) was added, then K$_2$CO$_3$ (3.32 g, 24 mmol) followed by iodomethane (1.5 mL, 24 mmol). The reaction was stirred at 22 °C for 18 h and was then quenched with 10% NH$_4$OH (100 mL), extracted with Et$_2$O (2 × 50 mL); the ether extracts were combined, washed with water (3 × 100 mL), dried (MgSO$_4$) and the solvent was evaporated to afford the title compound as a brown liquid (4.52 g, 17.2 mmol, 86%).

^{1}H NMR (400 MHz, CDCl$_3$) δ 7.46–7.41 (m, 1H), 6.97–6.92 (m, 1H), 3.75 (s, 3H), 2.30 (s, 3H), 2.23 (s, 3H); ^{13}C NMR (101 MHz, CDCl$_3$) δ 156.0, 137.4, 135.7, 132.4, 131.8, 91.8, 60.4, 20.3, 17.1; LRMS (CI) *m/z* 263.0 [M+H]$^+$; HRMS (FTMS-APCI) calculated for C$_9$H$_{12}$OI [M+H]$^+$ 262.9927, found 262.9926; IR (ATR)/cm^{-1} 2980, 2970, 1472.

2-methoxy-1,5-dimethyl-3-(phenylethynyl)benzene 489[216]

489
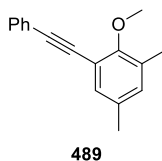
A flask was loaded with dichlorobis(triphenylphosphine)palladium(II) (316 mg, 3 mol%, 0.45 mmol), CuI (171 mg, 6 mol%, 0.90 mmol), and triphenylphosphine (236 mg, 6 mol%, 0.90 mmol). A degassed mixture of triethylamine (90 mL) and 1-iodo-2-methoxy-3,5-dimethylbenzene **488** (3.93 g, 15 mmol) was transferred *via* cannula into the flask containing the solids. Phenylacetylene **485** (1.73 mL, 15.75 mmol) was added and the reaction was stirred under reflux conditions for 16 h. The resulting suspension was diluted with Et$_2$O (100 mL) and was washed successively with a saturated, aqueous solution of NH$_4$Cl (2 × 100 mL), water (100 mL), and brine (100 mL). The organic layer was collected, dried (MgSO4), filtered, and concentrated. The crude was then chromatographed on silica gel using a gradient from petroleum ether (to remove the Glaser coupling product) to petroleum ether:EtOAc (9:1) to afford alkyne **489** as a light brown oil (2.7 g, 69% yield).

^{1}H NMR (400 MHz, CDCl$_3$) δ 7.57–7.52 (m, 2H), 7.38–7.32 (m, 3H), 7.16 (dd, *J* = 1.6, 0.6 Hz, 1H), 6.97 (dd, *J* = 1.5, 0.7 Hz, 1H), 3.95 (s, 3H), 2.27 (d, *J* = 3.7 Hz, 6H); ^{13}C NMR (101 MHz, CDCl$_3$) δ 157.5, 134.0, 133.8, 133.0, 132.4, 131.6, 131.5, 131.0, 128.4, 123.8, 116.4, 93.1, 86.4, 60.7, 20.6, 16.1; LRMS (CI) *m/z* 237.1 [M+H]$^+$; HRMS (FTMS-APCI) calculated for C$_{17}$H$_{17}$O [M+H]$^+$ 237.1274, found 237.1273; IR (ATR)/cm^{-1} 2980, 2956, 1597.

(*Z*)-2-methoxy-1,5-dimethyl-3-styrylbenzene 490[187]

490
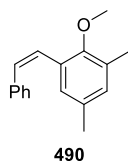
To a pre-dried pressure resistant vial under N$_2$, Pd(OAc)$_2$ (18 mg, 4 mol%, 0.08 mmol) KOH (337 mg, 6.0 mmol) and alkyne **489** (473 mg, 2.0 mmol) were weighed and the vial was sealed with a crimp cap, re-evacuated and filled with N$_2$. Dry DMF (4 mL) was then added and the reaction was stirred at 145 °C for 6 h. The mixture was allowed to cool down to room temperature and was filtered through Celite, washed with CH$_2$Cl$_2$ and concentrated. The crude was chromatographed on silica gel using petroleum ether:Et$_2$O (19:1) to afford the *cis*-alkene **490** as white needles (330 mg, 1.38 mmol, 69%).

m.p. 35–36 °C; ^{1}H NMR (400 MHz, CDCl$_3$) δ 7.30–7.25 (m, 2H), 7.24–7.14 (m, 3H), 6.90–6.87 (s, 1H), 6.85–6.81 (m, 1H), 6.70 (d, *J* = 12.3 Hz, 1H), 6.61 (d, *J* = 12.3 Hz, 1H), 3.76 (s, 3H), 2.27 (s, 3H), 2.09 (s, 3H); ^{13}C NMR (101 MHz, CDCl$_3$) δ 154.8, 137.3, 132.9, 131.2, 130.9, 130.5, 129.0, 128.5, 128.2, 127.2, 126.5, 60.8, 20.7, 16.1; LRMS (CI) *m/z* 239.1 [M+H]$^+$; HRMS (FTMS-APCI) calculated for C$_{17}$H$_{19}$O [M+H]$^+$ 239.1430, found 239.1431; IR (ATR)/cm^{-1} 3497, 2945, 2924.

2-hydroxy-3,5-dimethylbenzaldehyde 479[181]

479
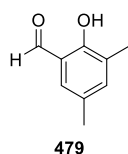
To a 3-neck round bottom flask under Ar equipped with a condenser, 2,4-dimethylphenol **483** (3.6 mL, 30 mmol) was charged and then dry MeCN (150 mL, dried over 4Å molecular sieves) was added. This was followed up by Et$_3$N (15.6 mL, 113 mmol, stored over KOH) and MgCl$_2$ (4.29 g, 45 mmol, dried under reduced pressure at 120 °C). The suspension turned pink and was stirred for 20 min at 25 °C. Dry paraformaldehyde (6.1 g, 203 mmol, dried over P$_2$O$_5$ in a desiccator) was then added and the mixture was heated under reflux conditions for 3 h. During this time, it became yellow. The reaction was quenched with 5% HCl (250 mL), followed by stirring for 30 min. The resulting mixture

was extracted with Et_2O (5 × 100 mL), the organics were combined and washed with brine (200 mL), dried ($MgSO_4$), concentrated and the resulting crude was cromatographed on silica gel using petroleum ether:Et_2O (19:1) to afford the title compound as yellow needles (3.69 g, 24.6 mmol, 82%).

m.p. 23–24 °C; ^{1}H NMR (400 MHz, CDCl$_3$) δ 11.07 (s, 1H), 9.83 (s, 1H), 7.24–7.19 (m, 1H), 7.19–7.15 (m, 1H), 2.30 (s, 3H), 2.24 (s, 3H); ^{13}C NMR (101 MHz, CDCl$_3$) δ 196.8, 158.1, 139.2, 131.1, 128.7, 126.7, 119.9, 20.4, 15.1; LRMS (CI) *m/z* 151.1 [M+H]$^+$; HRMS (FTMS-APCI) calculated for $C_9H_{11}O_2$ [M+H]$^+$ 151.0754, found 151.0751; IR (ATR)/cm^{-1} 2949, 2841, 1645.

(*E*)-2,4-dimethyl-6-styrylphenol 478
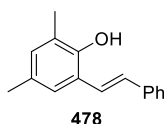
To a pre-dried flask under Ar, NaH (400 mg, 10 mmol, 60% suspension) was charged. Then, dry DMF (10 mL) was added, followed by dropwise addition of diethyl benzylphosphonate **491** (1.5 mL, 8.4 mmol) at 0 °C. The mixture was then stirred for 30 min at 0 °C after which the aldehyde **479** (600 mg, 4.0 mmol) was added dropwise at 0 °C and the mixture was allowed to warm up to room temperature overnight. The mixture was diluted with EtOAc (100 mL), washed with water (2 × 50 mL), brine (50 mL), dried ($MgSO_4$) and concentrated. The crude was chromatographed on silica gel using petroleum ether:EtOAc (9:1) to obtain *trans*-alkene **478** as white solids (670 mg, mmol, 76%).

m.p. 97–98 °C; ^{1}H NMR (400 MHz, CDCl$_3$) δ 7.55–7.50 (m, 2H), 7.39–7.31 (m, 3H), 7.20–7.16 (m, 1H), 7.08 (d, *J* = 16.4 Hz, 1H), 6.89–6.86 (m, 1H), 4.75 (s, 1H), 2.28 (s, 3H), 2.25 (s, 3H); ^{13}C NMR (101 MHz, CDCl$_3$) δ 149.4, 137.8, 131.0, 130.3, 129.8, 128.9, 128.8, 128.8, 128.7, 127.7, 126.6, 125.4, 124.2, 123.6, 123.6, 20.7, 16.0; LRMS (CI) *m/z* 223.1 [M+H]$^+$; HRMS (FTMS-APCI) calculated for $C_{16}H_{17}O$ [M+H]$^+$ 225.1274, found 225.1272, calculated for $C_{16}H_{15}O$ [M-H]$^-$ 223.1117, found 223.1118; IR (ATR)/cm^{-1} 3400, 2980, 2918, 1475.

(*E*)-2-methoxy-1,5-dimethyl-3-styrylbenzene 492[186]

492
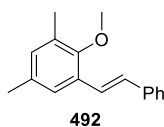
Alkene **478** (449 mg, 2 mmol) was weighed into a round bottom flask, followed by addition of DMF (4 mL), K_2CO_3 (332 mg, 2.4 mmol) and iodomethane (0.15 mL, 2.4 mmol). The reaction was allowed to run at 25 °C for 18 h and was quenched with 10% NH_4OH (aq., 10 mL), extracted with Et_2O (2 × 10 mL), washed with water (3 × 20 mL), dried ($MgSO_4$), and concentrated under reduced pressure to afford the title compound **492** as a colorless oil (392 mg, 1.64 mmol, 82%).

^{1}H NMR (400 MHz, CDCl$_3$) δ 7.57–7.52 (m, 2H), 7.43–7.34 (m, 3H), 7.30–7.27 (m, 1H), 7.11 (d, *J* = 16.5 Hz, 1H), 6.95–6.90 (m, 1H), 3.74 (s, 3H), 2.32 (s, 3H), 2.28 (s, 3H); ^{13}C NMR (101 MHz, CDCl$_3$) δ 154.5, 138.0, 133.5, 131.5, 131.2, 130.3, 129.5, 128.8, 127.6, 126.7, 124.6, 123.7, 61.1, 21.0, 16.0; LRMS (CI) *m/z* 239.1 [M+H]$^+$; HRMS (FTMS-APCI) calculated for $C_{17}H_{19}O$ [M+H]$^+$ 239.1430, found 239.1430; IR (ATR)/cm^{-1} 2987, 2922, 2920, 1474.

4.17.1 General Procedure for Cyclopropanation (General Procedure 9)[177]

WARNING: Neat diethylzinc is extremely flammable and must be handled carefully with all safety precautions present (including a water-free fire extinguisher).

A solution of Et_2Zn (0.51 mL, 5.0 mmol) in dry CH_2Cl_2 (2.5 mL) under Ar was prepared and was cooled down to 0 °C. To the Et_2Zn solution, TFA (0.37 mL, 5 mmol) in dry CH_2Cl_2 (1.25 mL) was slowly added using a syringe pump over 1 h and the mixture was stirred at 0 °C for another 30 min. Diiodomethane (0.40 mL, 5.0 mmol) in dry CH_2Cl_2 (1.25 mL) was then added at 0 °C and the mixture was stirred for 40 min at 0 °C. The alkene (297 mg, 1.25 mmol) in dry CH_2Cl_2 (1.25 mL) was added at 0 °C (turned yellow) and the reaction was allowed to warm up to room temperature overnight (turned red). The reaction was quenched with a saturated solution of NH_4Cl (aq., 10 mL) *via* syringe pump over 1 h at 0 °C, extracted with CH_2Cl_2 (3 × 15 mL), and the combined organic extracts were washed with a saturated solution of $NaHCO_3$ (aq., 2 × 25 mL), distilled water (30 mL), brine (30 mL), dried ($MgSO_4$), and concentrated to afford the cyclopropanation product.

Cis-2-methoxy-1,5-dimethyl-3-(2-phenylcyclopropyl)benzene *cis*-477
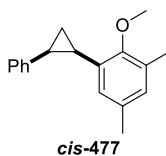
cis-477

Cyclopropanation product ***cis*-477** was obtained from alkene **490** according to General Procedure 9 as a sticky yellow solid (276 mg, 1.09 mmol, 87%, >90% pure) after work-up. A small sample (30 mg) was subjected to preparative TLC using petroleum ether:Et_2O (19:1) for full characterization.

m.p. 91–92 °C; ^{1}H NMR (400 MHz, $CDCl_3$) δ 7.17–6.93 (m, 5H), 6.73–6.67 (m, 1H), 6.44–6.33 (m, 1H), 3.66 (s, 3H), 2.69–2.60 (m, 1H), 2.58–2.47 (m, 1H), 2.17 (s, 3H), 2.07 (s, 3H), 1.52–1.35 (m, 2H); ^{13}C NMR (101 MHz, $CDCl_3$) δ 156.4, 138.9, 132.1, 130.4, 130.0, 129.5, 128.7, 127.8, 127.2, 125.7, 60.2, 25.0, 20.9, 20.0, 16.2, 11.4; LRMS (CI) *m/z* 253.2 [M+H]$^{+}$; HRMS (FTMS-APCI) calculated for $C_{18}H_{21}O$ [M+H]$^{+}$ 253.1587, found 253.1586; IR (ATR)/cm^{-1} 2961, 2920, 1260.

Trans-2-methoxy-1,5-dimethyl-3-(2-phenylcyclopropyl)benzene *trans*-477
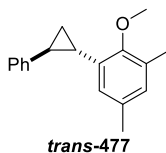
trans-477

Cyclopropanation product ***trans*-477** was obtained from alkene **492** according to General Procedure 9 as a yellow oil after work-up (315 mg, 99%, >95% pure).

^{1}H NMR (400 MHz, $CDCl_3$) δ 7.35–7.28 (m, 2H), 7.23–7.17 (m, 3H), 6.88–6.85 (m, 1H), 6.64–6.60 (m, 1H), 3.67 (s, 3H), 2.52–2.45 (m, 1H), 2.31–2.30 (m, 1H), 2.30, (s, 3H), 2.29 (s, 3H), 2.16–2.09 (m, 1H), 1.52–1.40 (m, 2H); ^{13}C NMR (101 MHz, $CDCl_3$) δ 155.4, 142.8, 134.8, 133.4, 130.7, 129.3, 128.5, 126.0, 125.8, 122.9, 60.6, 27.7, 22.0, 21.1, 17.5, 16.1; LRMS (CI) *m/z* 253.2 [M+H]$^{+}$; HRMS (FTMS-APCI) calculated for $C_{18}H_{21}O$ [M+H]$^{+}$ 253.1587, found 253.1588; IR (ATR)/cm^{-1} 3024, 2988, 2924, 2866.

4.18 EPR Experiments

Blank testing
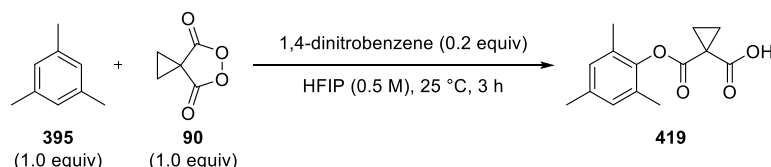
Malonoyl peroxide **90** (26 mg, 0.20 mmol, 1.0 equiv) was weighed into a 1.5 mL vial equipped with a stir bar. A standard solution of 1,4-dinitrobenzene in HFIP ((0.04 M), 0.4 mL, 0.20 equiv 1,4-dinitrobenzene) was then added and a 20 µL aliquot was diluted in CDCl$_3$ to record the initial ratio (^{1}H NMR) between the internal standard and malonoyl peroxide **90**. Mesitylene **395** (28 µL, 0.20 mmol, 1.0 equiv) was then added and the reaction was monitored by ^{1}H NMR over 3 h. The reaction showed 52% conversion after 1 h and 73% after 3 h with no byproducts/coproducts.
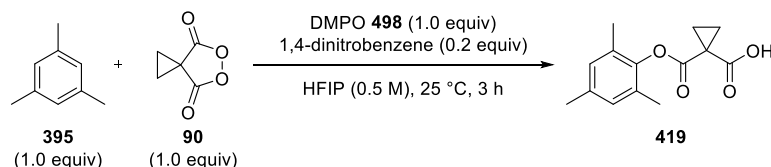
Malonoyl peroxide **90** (26 mg, 0.20 mmol, 1.0 equiv) was weighed into a 1.5 mL vial equipped with a stir bar. A standard solution of 1,4-dinitrobenzene in HFIP [0.04 M] (0.4 mL, 0.20 equiv 1,4-dinitrobenzene) was then added and a 20 µL aliquot was diluted in CDCl$_3$ to record the initial ratio (^{1}H NMR) between the internal standard and malonoyl peroxide **90**. DMPO **498** (23 mg, 0.20 mmol) and mesitylene **395** (28 µL, 0.20 mmol, 1.0 equiv) were then added and the reaction was monitored by ^{1}H NMR over 3 h. The reaction showed 48% conversion after 1 h and 68% after 3 h with no byproducts/coproducts.

Purification of DMPO[217]

Commercially available (Fluorochem, 5 g, brown solid with a low melting point) 5,5-dimethyl-1-pyrroline-*N*-oxide **498** (DMPO, 1.6 g) was weighed directly into a 10 mL round bottom flask which was equipped with a Vigreux column and a short-path condenser with three 10 mL round bottom flasks as fractions. The system was placed under vacuum

(4.1 mbar) and the Vigreux column and the upper part of the short-path condenser were covered in glass wool and aluminum foil. The oil bath was heated to 140 °C and the vapor temperature of DMPO was 88 °C at 4.1 mbar. A heat gun must be used occasionally to warm up the upper part of the condenser (otherwise DMPO will condense as a colorless oil at the top of the condenser). 1.2 g of DMPO (colorless oil) were distilled in a 10 mL round bottom flask and stored under argon. The collected DMPO became a crystalline white solid after storing it at –24 °C.

Sample preparation for EPR studies

(0.5 M) Solutions of DMPO **498**, malonoyl peroxide **90** and mesitylene **395** in 2,2,2-trifluoroethanol (TFE) were prepared under nitrogen. The EPR spectrometer was calibrated using a (0.05 M) solution of TEMPO in TFE.

Blank samples of the (0.5 M) solutions of DMPO **498** and malonoyl peroxide **90** in TFE were first subjected to EPR spectroscopy (0.2 mL of each).

0.1 mL of the (0.5 M) solution of malonoyl peroxide **90** in TFE was mixed with 0.2 mL of the (0.5 M) solution of DMPO **498** in TFE and the resulting sample was monitored by EPR spectroscopy.

To 0.1 mL of the (0.5 M) solution of malonoyl peroxide **90** in TFE, mesitylene **395** (5.6 μL, 0.04 mmol) was added and the resulting mixture was analyzed by EPR spectroscopy. This mixture was then combined with 0.2 mL of the (0.5 M) solution of DMPO **498** in TFE and the resulting mixture was analyzed by EPR spectroscopy.

The experiments were repeated using HFIP as a solvent and all of the experiments were performed in duplicate.

No radicals were observed by EPR spectroscopy in any of the experiments performed.

4.19 DFT Calculations

DFT calculations were performed using the Gaussian09 pack of programs.[69] Optimizations of ground states and transition states were performed at the (U)B3LYP/6-31G level of theory.[218] These optimized structures were then characterized using frequency calculations at the UB3LYP/6-31+G(d) level of theory and evaluated by a SCRF (self-consistent reaction field) with 2,2,2-trifluoroethanol CPCM (conductor polarized continuum model) solvation.[219] Frequency data was analyzed *via* a classical approach where fully converged local minima (peroxide **90** and diradical species **453**) contain no imaginary frequencies and transition states (**TS2**) have one imaginary frequency.

Chapter 5: Appendix

Chapter 5: Appendix

5.1   X-Ray Crystallographic Data

X-Ray Data for Phthaloyl Hydroxylamine 184

Table 1. Crystal data and structure refinement for 2015ncs0253.

Identification code	shelx
Empirical formula	C8 H5 N O3
Formula weight	163.13
Temperature	100(2) K
Wavelength	0.71073 Å
Crystal system	Monoclinic
Space group	P 2_1
Unit cell dimensions	a = 3.6735(2) Å α= 90°.
	b = 7.3529(3) Å β= 94.078(5)°.
	c = 12.6780(8) Å γ = 90°.
Volume	341.58(3) Å^3
Z	2
Density (calculated)	1.586 Mg/m^3
Absorption coefficient	0.124 mm^{-1}
F(000)	168
Crystal size	0.056 x 0.054 x 0.010 mm^3
Theta range for data collection	3.205 to 27.470°.
Index ranges	-4<=h<=4, -9<=k<=9, -14<=l<=16
Reflections collected	5642
Independent reflections	1553 [R(int) = 0.0369]
Completeness to theta = 27.000°	99.9 %
Absorption correction	Semi-empirical from equivalents
Max. and min. transmission	1.00000 and 0.67857
Refinement method	Full-matrix least-squares on F^2
Data / restraints / parameters	1553 / 1 / 114
Goodness-of-fit on F^2	1.127
Final R indices [I>2sigma(I)]	R1 = 0.0377, wR2 = 0.1008
R indices (all data)	R1 = 0.0381, wR2 = 0.1013
Absolute structure parameter	0.3(14)
Extinction coefficient	n/a
Largest diff. peak and hole	0.384 and -0.190 e.Å^{-3}

Chapter 5: Appendix
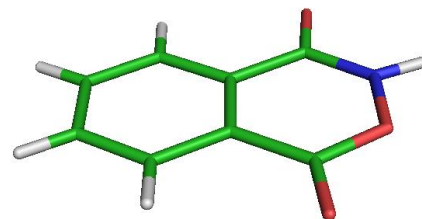
X-Ray Data for (*E*)-3-(1-Oxo-1-(*p*-tolyl)propan-2-ylidene)isobenzofuran-1(3H)-one 241
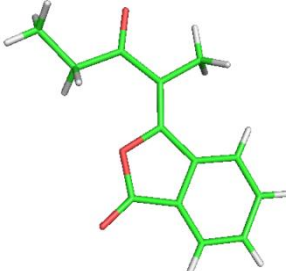
Table 1. Crystal data and structure refinement for tom_dragan.

Identification code	tom_dragan
Empirical formula	C18 H14 O3
Formula weight	278.29
Temperature	123(2) K
Wavelength	0.71073 Å
Crystal system	Monoclinic
Space group	P21/c
Unit cell dimensions	a = 8.3556(7) Å α= 90°.
	b = 23.574(2) Å β= 101.850(8)°.
	c = 7.2667(7) Å γ = 90°.
Volume	1400.9(2) Å^3
Z	4
Density (calculated)	1.320 Mg/m^3
Absorption coefficient	0.089 mm^{-1}
F(000)	584
Crystal size	0.33 x 0.12 x 0.06 mm^3
Theta range for data collection	2.99 to 26.99°.
Index ranges	-10<=h<=10, -27<=k<=30, -9<=l<=9
Reflections collected	9509
Independent reflections	3064 [R(int) = 0.0415]
Completeness to theta = 26.99°	99.9 %
Absorption correction	Semi-empirical from equivalents
Max. and min. transmission	1.00000 and 0.86508
Refinement method	Full-matrix least-squares on F^2
Data / restraints / parameters	3064 / 0 / 192
Goodness-of-fit on F^2	1.057
Final R indices [I>2sigma(I)]	R1 = 0.0474, wR2 = 0.0975
R indices (all data)	R1 = 0.0739, wR2 = 0.1101
Largest diff. peak and hole	0.207 and -0.207 e.Å^{-3}

Chapter 5: Appendix

X-Ray Data for (Z)-3-(3-Oxopentan-2-ylidene)isobenzofuran-1(3H)-one 264

Table 2. Crystal data and structure refinement for tom_draganad724.

Identification code	tom_draganad724
Empirical formula	C13 H12 O3
Formula weight	216.23
Temperature	123(2) K
Wavelength	0.71073 Å
Crystal system	Monoclinic
Space group	$P2_1/c$
Unit cell dimensions	a = 7.5288(10) Å α= 90°.
	b = 12.3360(17) Å β= 98.416(12)°.
	c = 11.5691(17) Å γ = 90°.
Volume	1062.9(3) Å^3
Z	4
Density (calculated)	1.351 Mg/m^3
Absorption coefficient	0.096 mm^{-1}
F(000)	456
Crystal size	0.35 x 0.24 x 0.10 mm^3
Theta range for data collection	3.30 to 26.00°.
Index ranges	-9<=h<=7, -11<=k<=15, -7<=l<=14
Reflections collected	4431
Independent reflections	2086 [R(int) = 0.0509]
Completeness to theta = 26.00°	99.8 %
Absorption correction	Semi-empirical from equivalents
Max. and min. transmission	1.00000 and 0.80501
Refinement method	Full-matrix least-squares on F^2
Data / restraints / parameters	2086 / 0 / 148
Goodness-of-fit on F^2	1.051
Final R indices [I>2sigma(I)]	R1 = 0.0528, wR2 = 0.1268
R indices (all data)	R1 = 0.0862, wR2 = 0.1523
Extinction coefficient	0.0045(14)
Largest diff. peak and hole	0.203 and -0.242 e.Å^{-3}
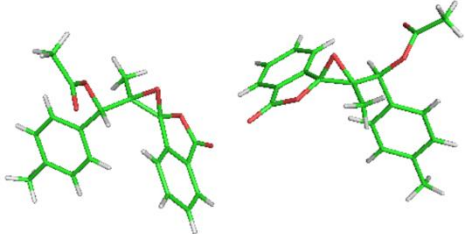
X-Ray Data for (*E*)-3-(2-Oxocyclopentylidene)isobenzofuran-1(3H)-one 265

Table 3. Crystal data and structure refinement for tom_ad792.

Identification code	shelx
Empirical formula	$C_{13} H_{10} O_3$
Formula weight	214.21
Temperature	123(2) K
Wavelength	1.5418 Å
Crystal system	Monoclinic
Space group	$P\,2_1/c$
Unit cell dimensions	a = 7.9297(3) Å α= 90°.
	b = 18.8834(9) Å β= 99.417(4)°.
	c = 13.5491(8) Å γ = 90°.
Volume	2001.50(17) $Å^3$
Z	8
Density (calculated)	1.422 Mg/m^3
Absorption coefficient	0.834 mm^{-1}
F(000)	896
Crystal size	0.3 x 0.25 x 0.08 mm^3
Theta range for data collection	4.052 to 73.057°.
Index ranges	-8<=h<=9, -23<=k<=17, -12<=l<=16
Reflections collected	7712
Independent reflections	3928 [R(int) = 0.0369]
Completeness to theta = 70.000°	99.7 %
Absorption correction	Semi-empirical from equivalents
Max. and min. transmission	1.00000 and 0.78295
Refinement method	Full-matrix least-squares on F^2
Data / restraints / parameters	3928 / 0 / 289
Goodness-of-fit on F^2	1.012
Final R indices [I>2sigma(I)]	R1 = 0.0551, wR2 = 0.1355
R indices (all data)	R1 = 0.0883, wR2 = 0.1622
Extinction coefficient	n/a
Largest diff. peak and hole	0.480 and -0.197 e.Å^{-3}

X-Ray Data for rel-(*S*)-((1*S*,3'*R*)-3'-Methyl-3-oxo-2,3-dihydrospiro[indene-1,2'-oxiran]-3'-yl)(p-tolyl)methyl acetate 295

Table 4. Crystal data and structure refinement for tom_dragan_ad816.

Identification code	tom_dragan_ad816
Empirical formula	C20 H18 O5
Formula weight	338.34
Temperature	123(2) K
Wavelength	1.54180 Å
Crystal system	Monoclinic
Space group	$P2_1/n$
Unit cell dimensions	a = 19.1520(5) Å α= 90°.
	b = 7.9401(2) Å β= 100.480(2)°.
	c = 23.1026(5) Å γ = 90°.
Volume	3454.58(15) Å^3
Z	8
Density (calculated)	1.301 Mg/m^3
Absorption coefficient	0.771 mm^{-1}
F(000)	1424
Crystal size	0.4 x 0.3 x 0.08 mm^3
Theta range for data collection	3.31 to 73.11°.
Index ranges	-23<=h<=23, -9<=k<=8, -25<=l<=28
Reflections collected	32509
Independent reflections	6868 [R(int) = 0.0387]
Completeness to theta = 70.00°	100.0 %
Absorption correction	Semi-empirical from equivalents
Max. and min. transmission	1.00000 and 0.78528
Refinement method	Full-matrix least-squares on F^2
Data / restraints / parameters	6868 / 0 / 457
Goodness-of-fit on F^2	1.039
Final R indices [I>2sigma(I)]	R1 = 0.0452, wR2 = 0.1212
R indices (all data)	R1 = 0.0540, wR2 = 0.1296
Largest diff. peak and hole	0.262 and -0.218 e.Å^{-3}

Chapter 5: Appendix

X-Ray Data for (*E*)-3-(1-(4-Bromophenyl)-1-oxopropan-2-ylidene)isobenzofuran-1(3H)-one 261

Table 1. Crystal data and structure refinement for tom_ad838.

Identification code	tom_ad838
Empirical formula	C17 H11 Br O3
Formula weight	343.17
Temperature	123(2) K
Wavelength	0.71073 Å
Crystal system	Triclinic
Space group	P-1
Unit cell dimensions	a = 6.7129(6) Å α= 105.975(7)°.
	b = 7.9713(7) Å β= 90.902(7)°.
	c = 13.4227(11) Å γ = 93.030(7)°.
Volume	689.21(10) Å^3
Z	2
Density (calculated)	1.654 Mg/m^3
Absorption coefficient	2.989 mm^{-1}
F(000)	344
Crystal size	0.35 x 0.15 x 0.05 mm^3
Theta range for data collection	3.16 to 28.98°.
Index ranges	-8<=h<=8, -10<=k<=10, -16<=l<=17
Reflections collected	6652
Independent reflections	3354 [R(int) = 0.0420]
Completeness to theta = 27.00°	99.8 %
Absorption correction	Semi-empirical from equivalents
Max. and min. transmission	1.00000 and 0.52974
Refinement method	Full-matrix least-squares on F^2
Data / restraints / parameters	3354 / 0 / 190
Goodness-of-fit on F^2	1.019
Final R indices [I>2sigma(I)]	R1 = 0.0394, wR2 = 0.0751
R indices (all data)	R1 = 0.0595, wR2 = 0.0833
Largest diff. peak and hole	0.472 and -0.530 e.Å^{-3}

Chapter 5: Appendix
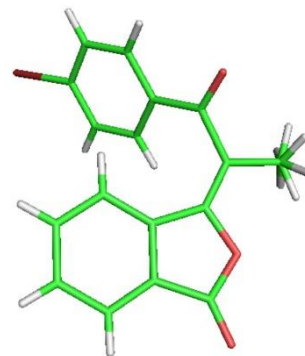
X-Ray Data for (*Z*)-3-(1-(4-Bromophenyl)-1-oxopropan-2-ylidene)isobenzofuran-1(3H)-one 298

Table 1. Crystal data and structure refinement for ad_recoll.

|		
Identification code	ad_recoll	
Empirical formula	$C_{17} H_{11} Br O_3$	
Formula weight	343.17	
Temperature	123(2) K	
Wavelength	1.54180 Å	
Crystal system	MONOCLINIC	
Space group	$P2_1/c$	
Unit cell dimensions	a = 4.0933(3) Å	α= 90°.
	b = 13.4305(7) Å	β= 91.787(5)°.
	c = 25.2057(17) Å	γ = 90°.
Volume	1385.01(16) $Å^3$	
Z	4	
Density (calculated)	1.646 Mg/m^3	
Absorption coefficient	4.115 mm^{-1}	
F(000)	688	
Crystal size	0.4 x 0.02 x 0.01 mm^3	
Theta range for data collection	3.51 to 70.29°.	
Index ranges	-4<=h<=4, -16<=k<=16, -30<=l<=30	
Reflections collected	6765	
Independent reflections	2518 [R(int) = 0.0827]	
Completeness to theta = 70.00°	96.6 %	
Absorption correction	Semi-empirical from equivalents	
Max. and min. transmission	1.00000 and 0.58675	
Refinement method	Full-matrix least-squares on F^2	
Data / restraints / parameters	2518 / 0 / 190	
Goodness-of-fit on F^2	1.011	
Final R indices [I>2sigma(I)]	R1 = 0.0598, wR2 = 0.1472	
R indices (all data)	R1 = 0.0703, wR2 = 0.1586	
Largest diff. peak and hole	1.311 and -0.682 e.$Å^{-3}$	
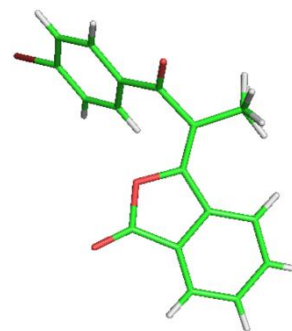
5.2   Selected ¹H NMR Data

¹H NMR of the crude reaction mixture from the formation of alkylidene phthalide 261

¹H NMR (400 MHz, CDCl₃), crude
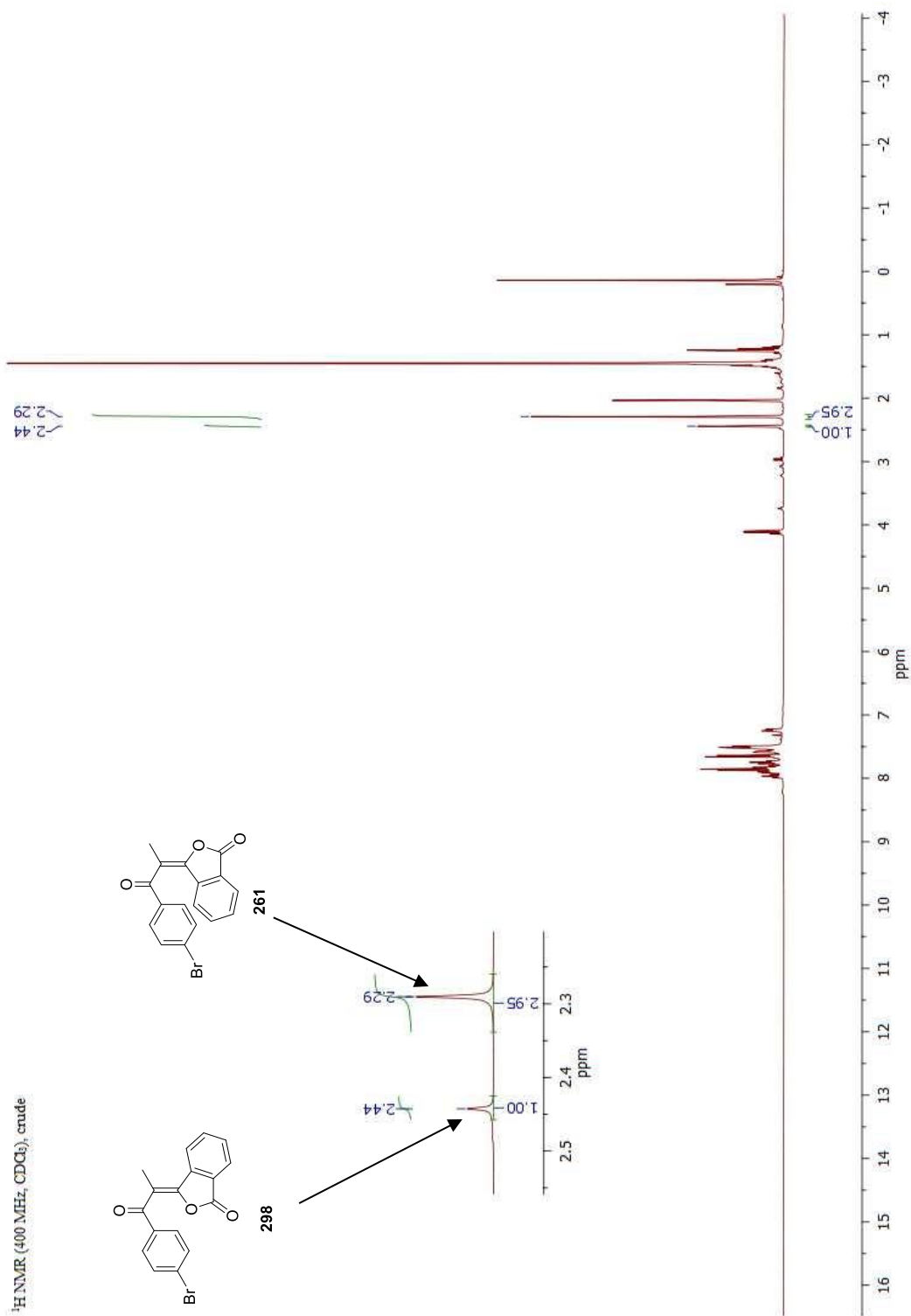
¹H NMR of alkylidene phthalide 261
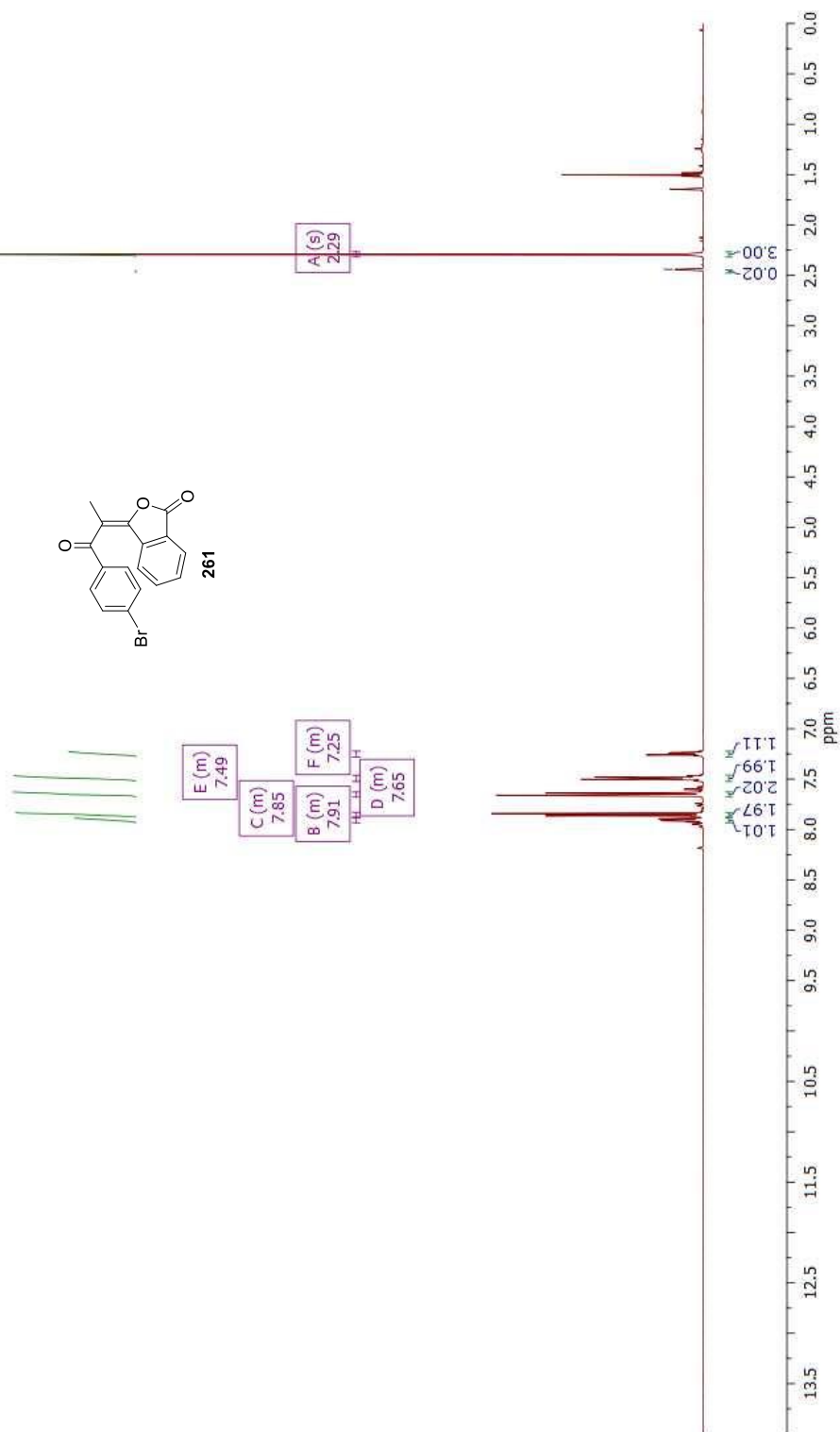
¹H NMR (400 MHz, CDCl₃)

¹H NMR of alkylidene phthalide 298

¹H NMR (400 MHz, CDCl₃)
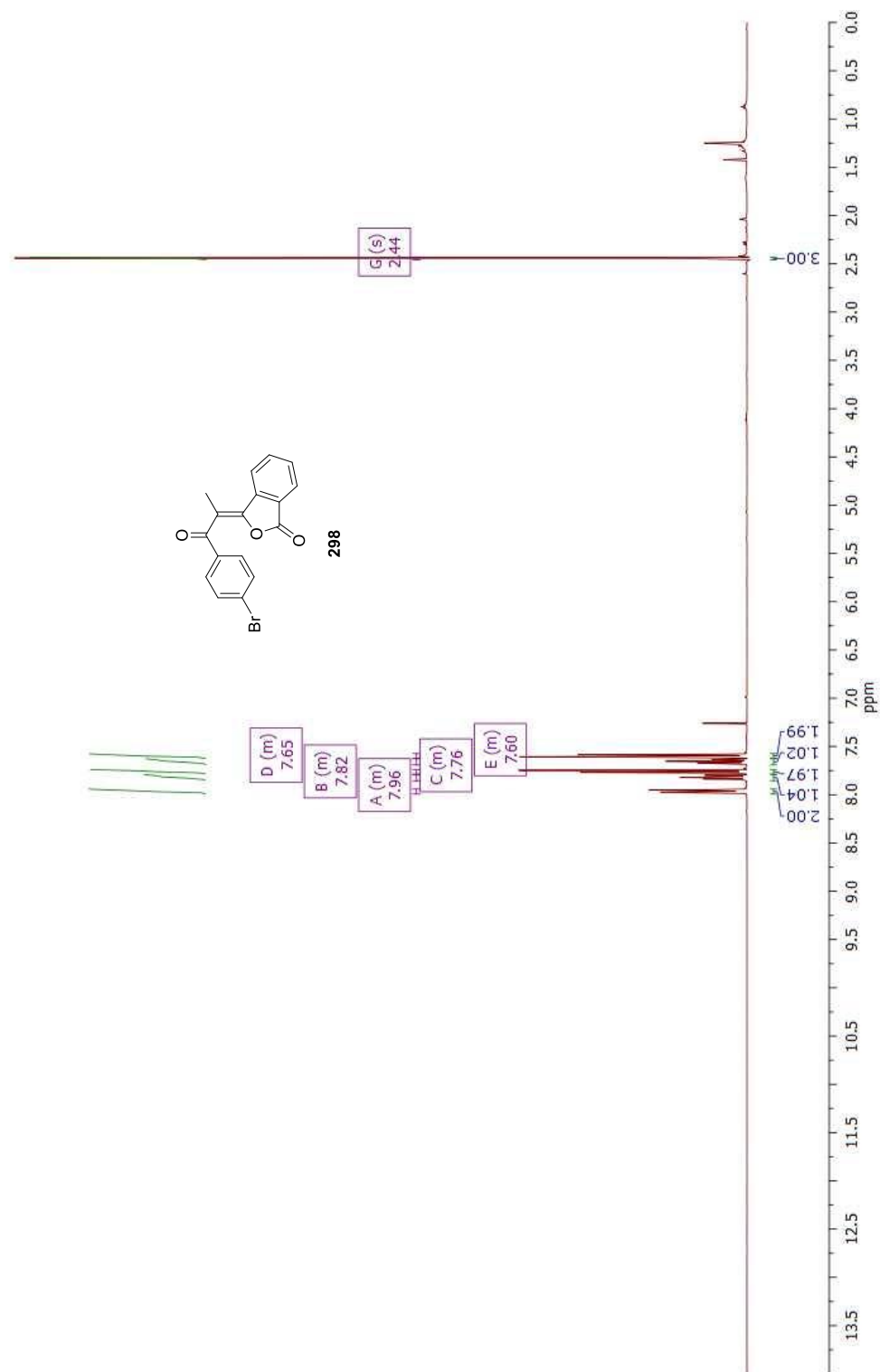
¹H NMR of the crude reaction mixture from the BV oxidation of 2-methylhexanone 311

¹H NMR (400 MHz, CDCl₃), crude
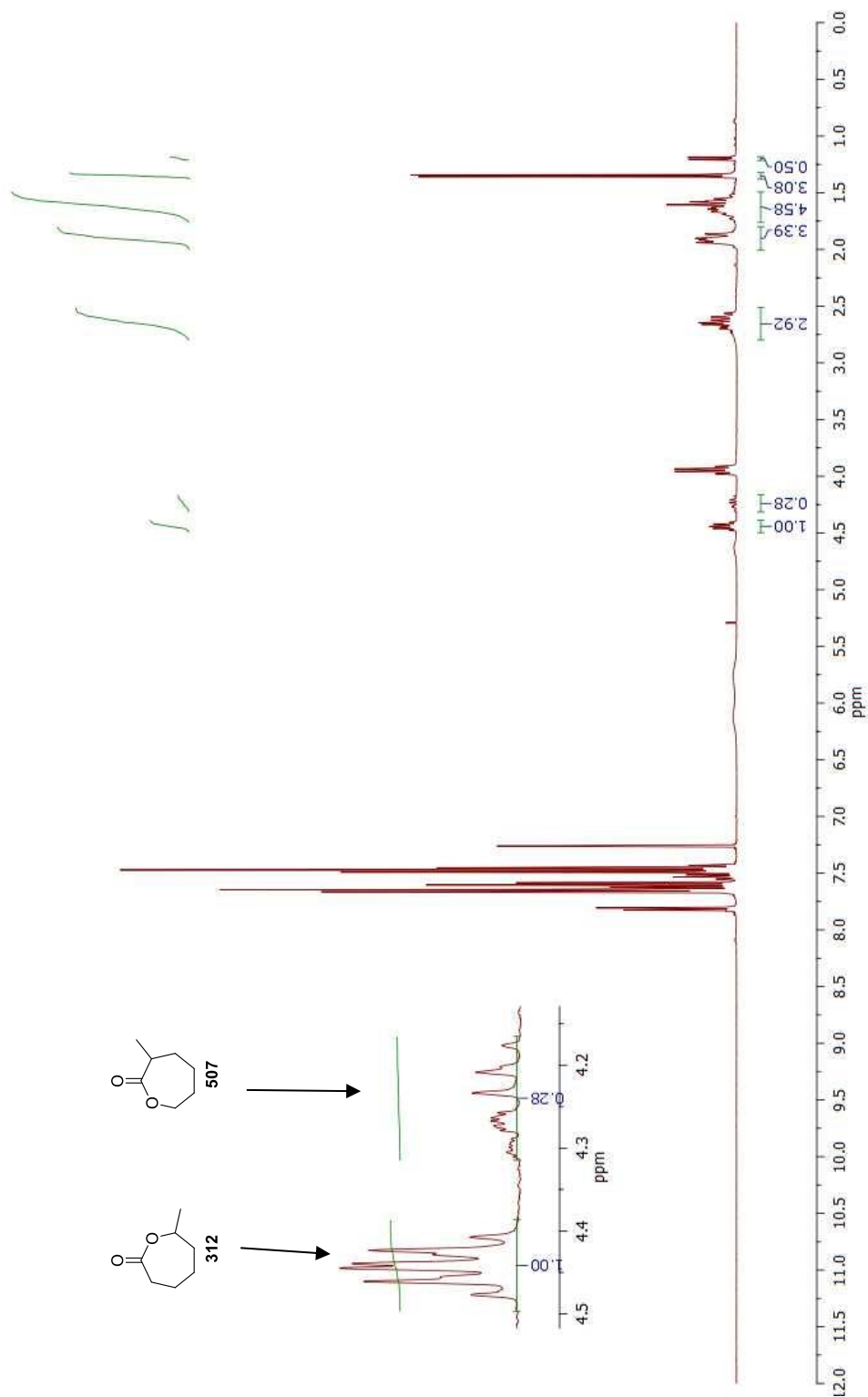
Hammett analysis: ^{1}H NMR of the reaction between 2-fluoromesitylene 458 and peroxide 90 at t=0 min
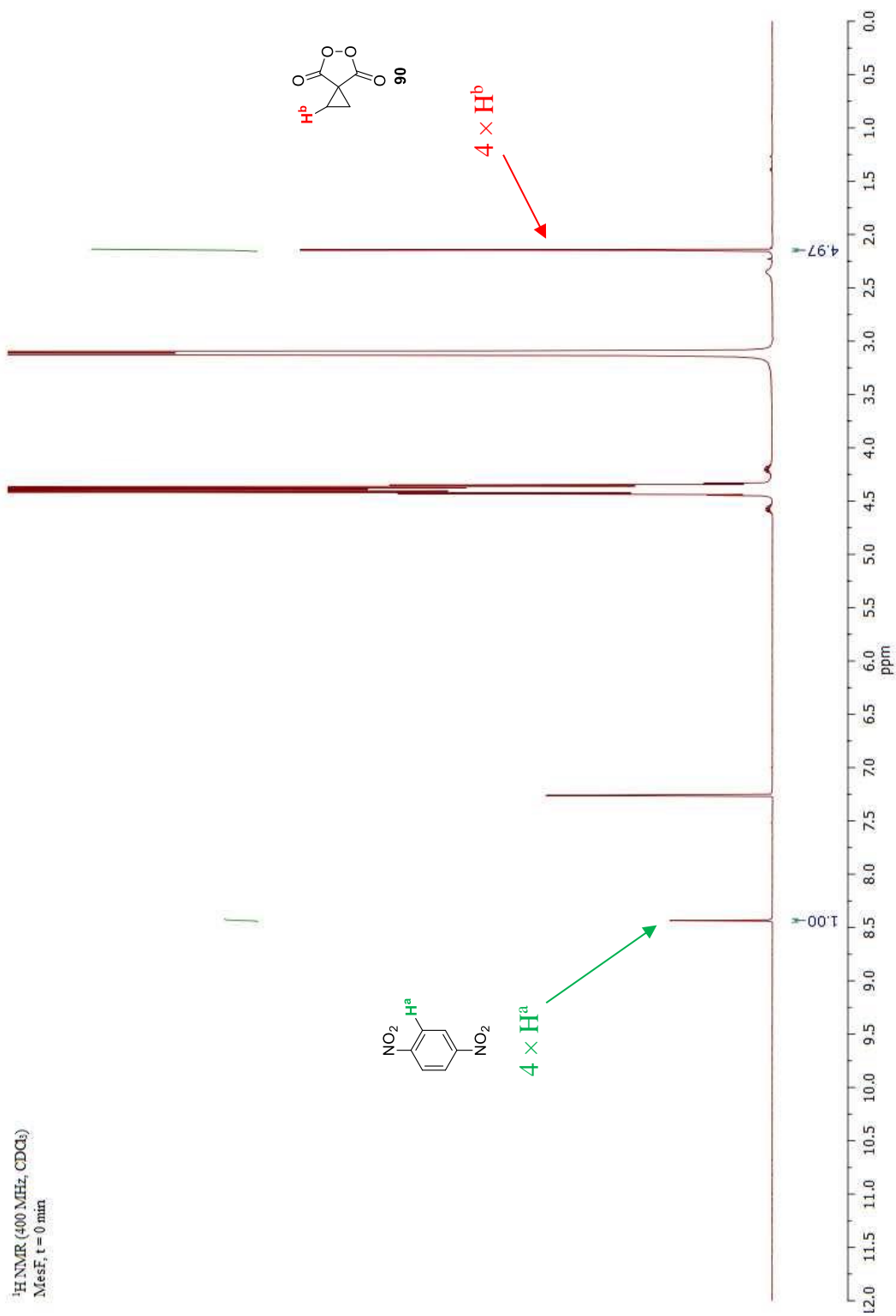
^{1}H NMR (400 MHz, CDCl$_3$)
MesF, t = 0 min

Hammett analysis: ^{1}H NMR of the reaction between 2-fluoromesitylene 458 and peroxide 90 at t=10 min
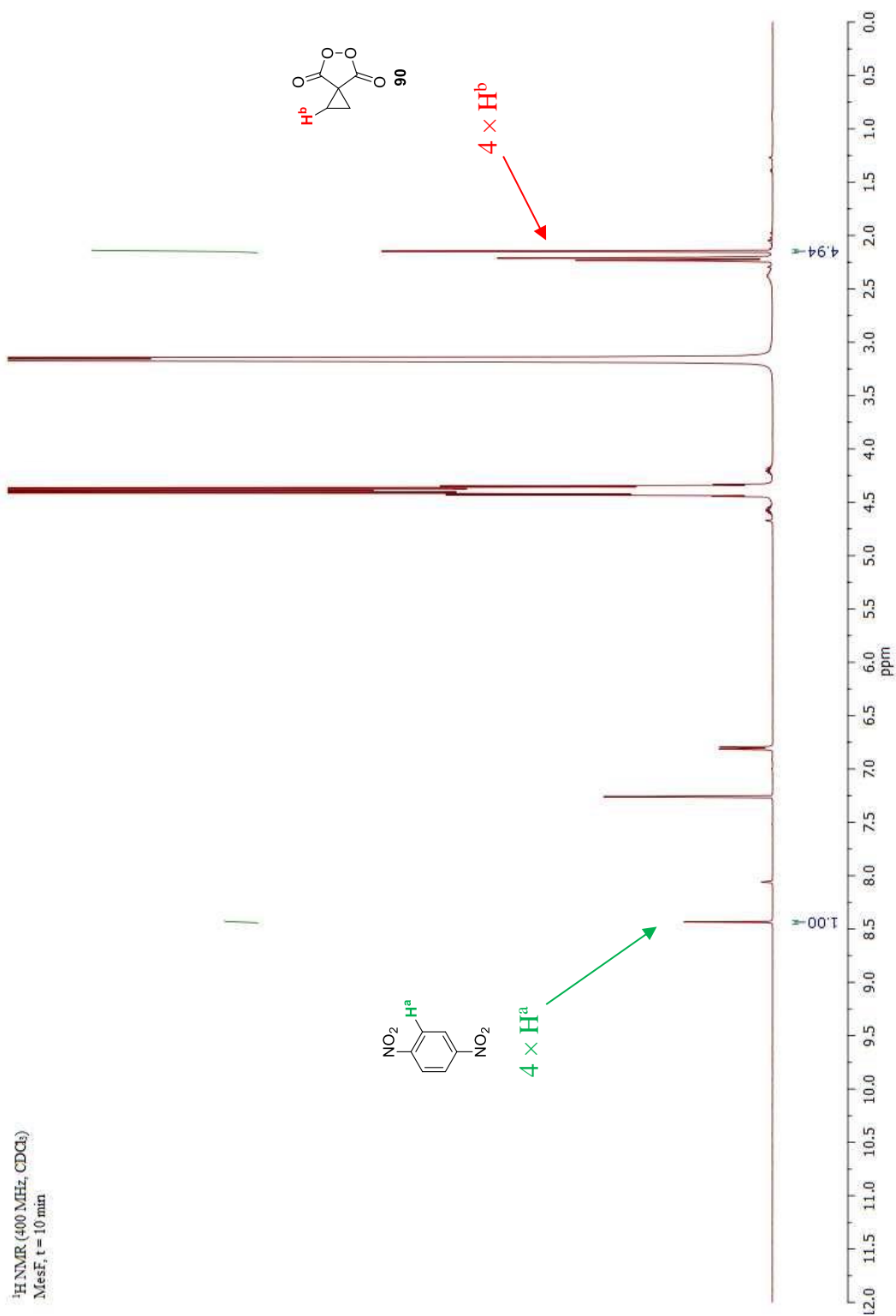
^{1}H NMR (400 MHz, CDCl$_3$)
MesF, t = 10 min

Hammett analysis: ^{1}H NMR of the reaction between 2-fluoromesitylene 458 and peroxide 90 at t=30 min

^{1}H NMR (400 MHz, CDCl$_3$)
MesF, t = 30 min
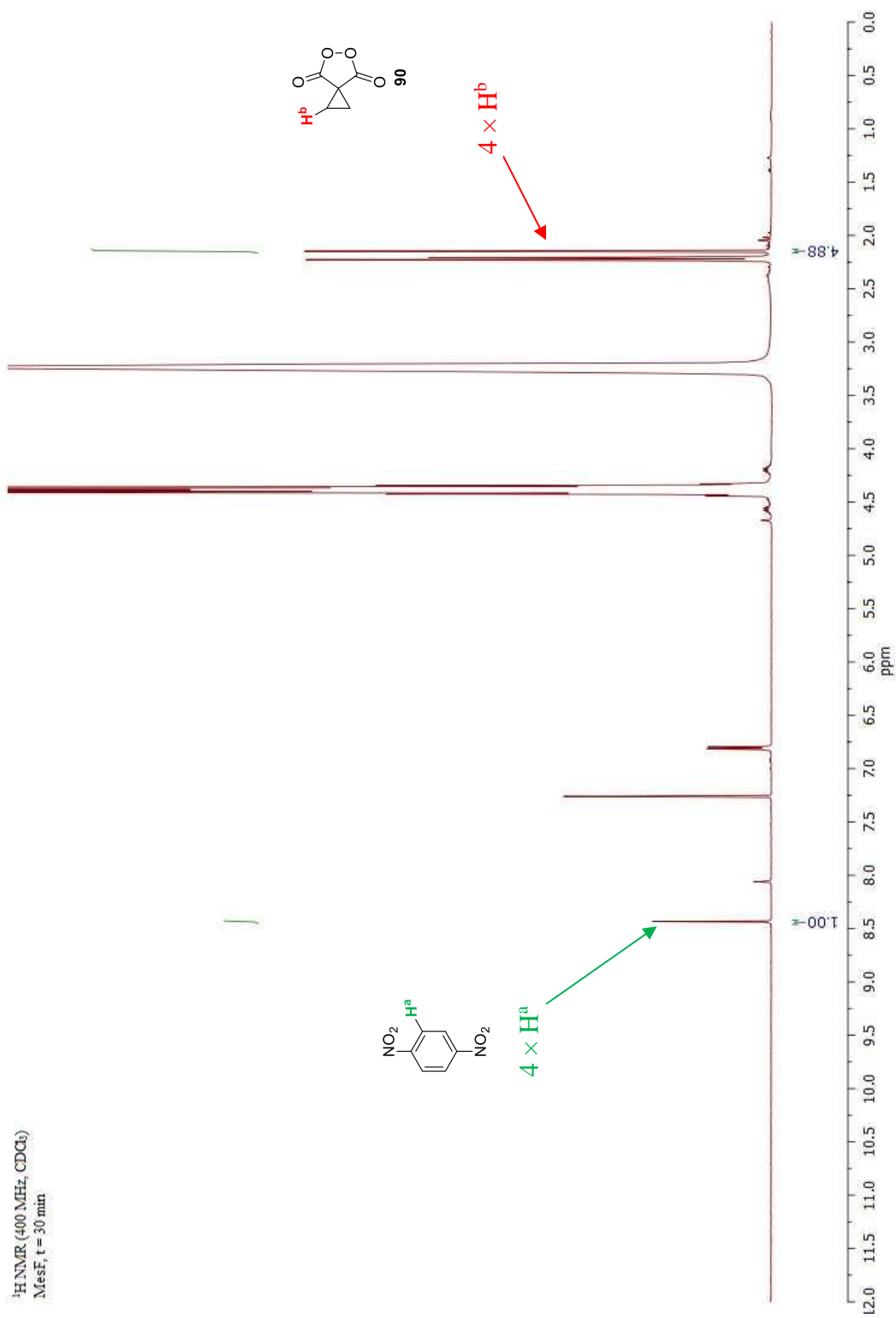
5.3 Selected Mass Spectrometry Data

Reaction of mesitylene 395 with ^{18}O labeled peroxide 462

462
(1.35 equiv)

395

463
(99%)
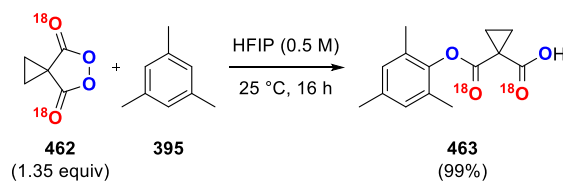
HRMS Analysis of 463 showing [M+H]$^+$ ion at 253.1208, showing incorporation of two ^{18}O labels

HRMS MS^2 analysis of [M+H]$^+$ ion at 253.1208, showing loss of H$_2$O and H$_2$^{18}O
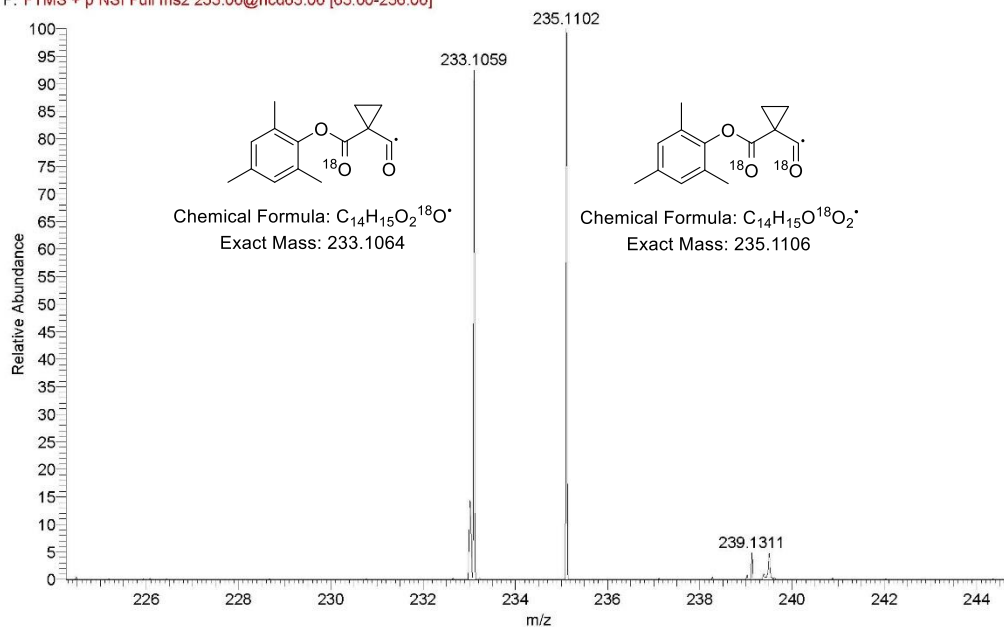
HRMS MS^2 analysis of [M+H]$^+$ ion at 253.1208, showing loss of H$_2$O and H$_2$^{18}O
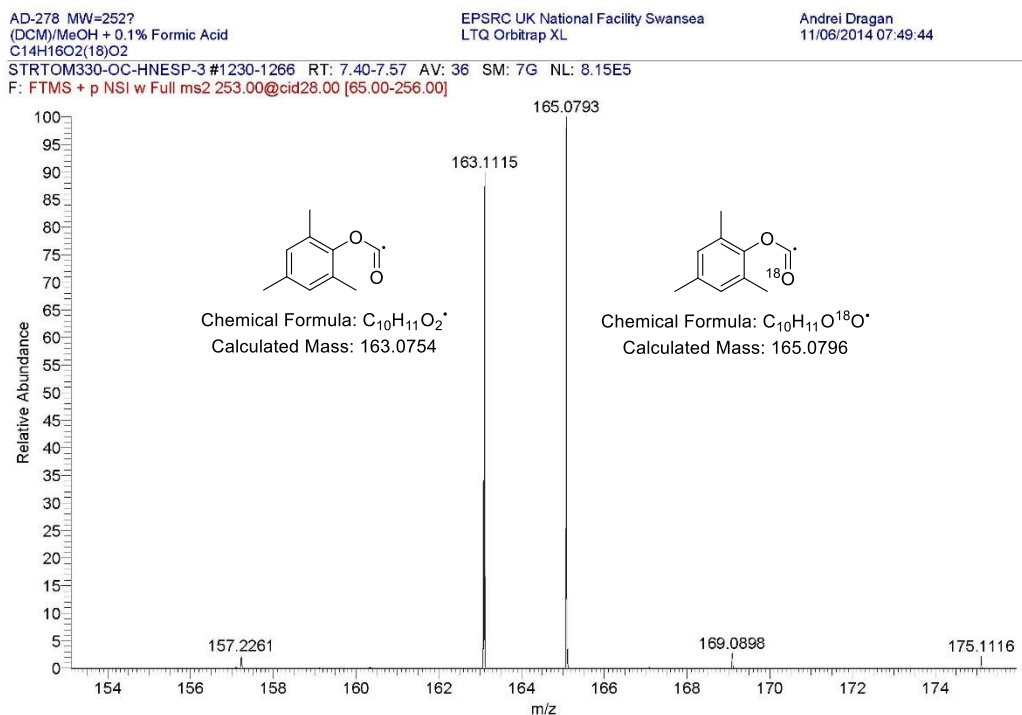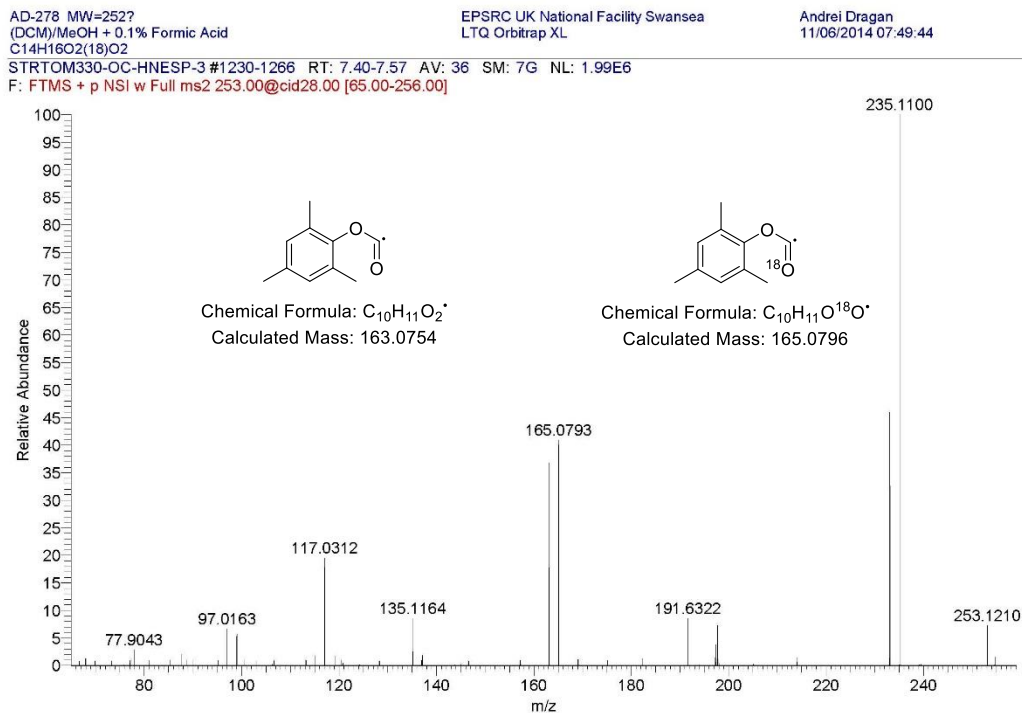
HRMS MS^2 analysis of [M+H]$^+$ ion at 253.1208, showing ^{16}O label attached to arene
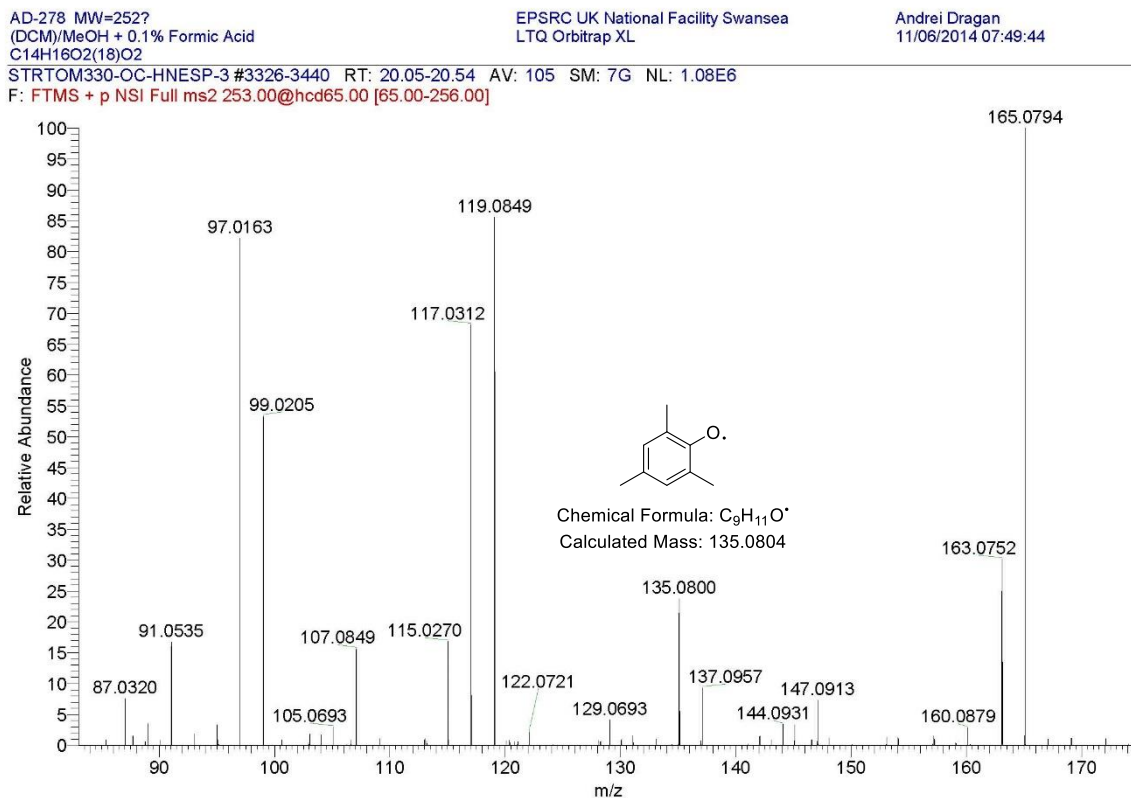
Note: The obtained value at 137.0957 did not fit the acceptable tolerance window for HRMS of ± 10.00 ppm. A theoretical isotope for the labeled species is shown below.

Chemical Formula: $C_9H_{11}{}^{18}O\bullet$
Calculated Mass: 137.0852
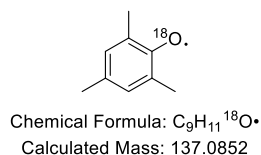
HRMS MS^3 analysis of [M+H]$^+$ ion at 253.1208 and ion at 235.17, showing ^{16}O label attached to arene
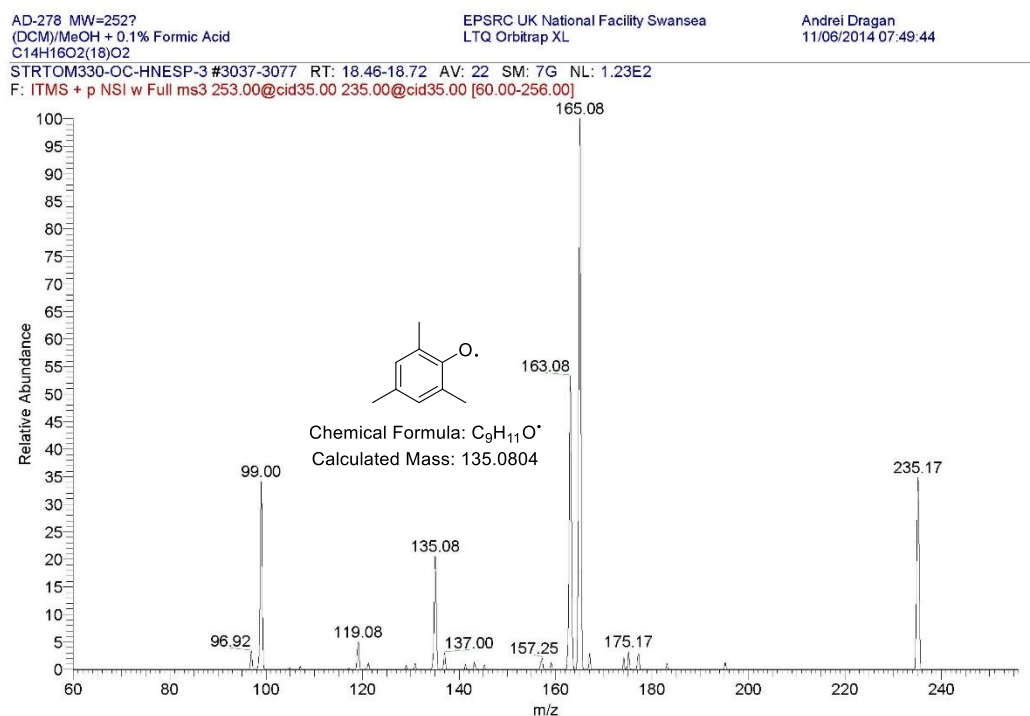
Note: Sensitivity was poor when using FTMS and a different method (ITMS) was used for MS^3 analysis, hence the accuracy of this method is based on only two decimal places.

Cleavage of ester C—O bond using MeNH₂ followed by GC/LRMS (CI) analysis of crude reaction mixture

GC spectrum of crude reaction mixture after aminolysis of ^{18}O labeled ester **463**
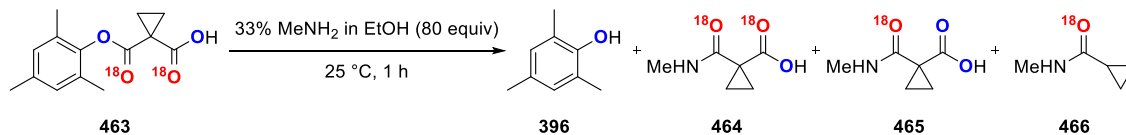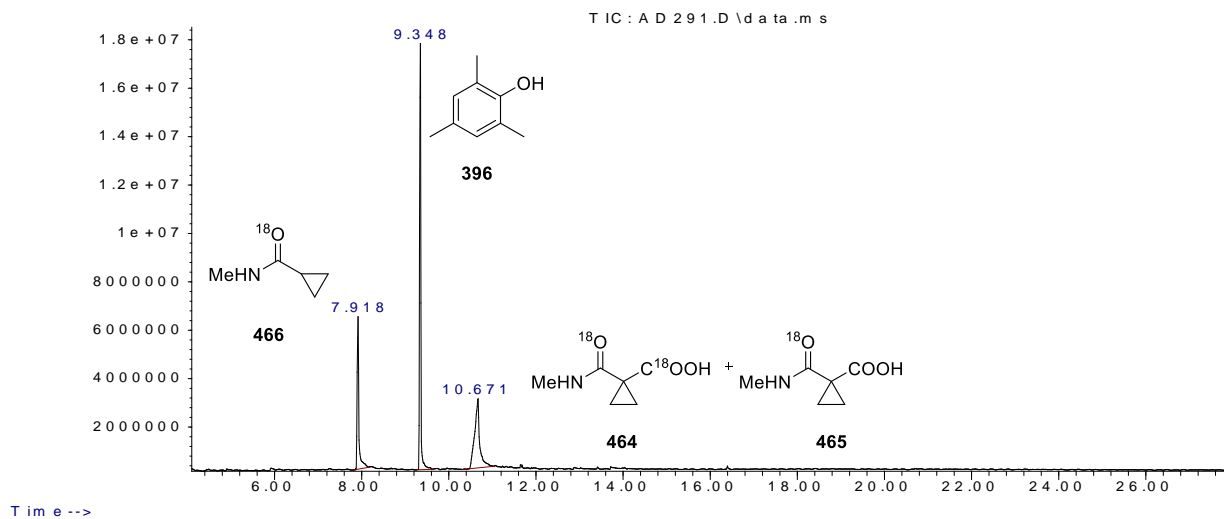
GC spectrum of crude reaction mixture after aminolysis of non-labeled ester **419**
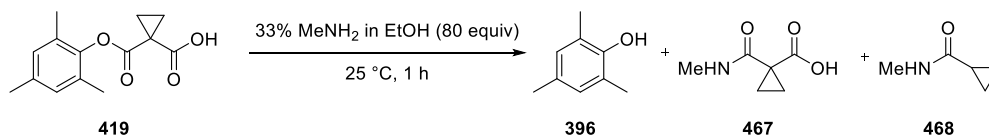
MS (CI) of GC peak at 7.918 min showing [M+H]⁺ of ¹⁸O labeled decarboxylated amide **466** upon cleavage of doubly ¹⁸O labeled ester **463**
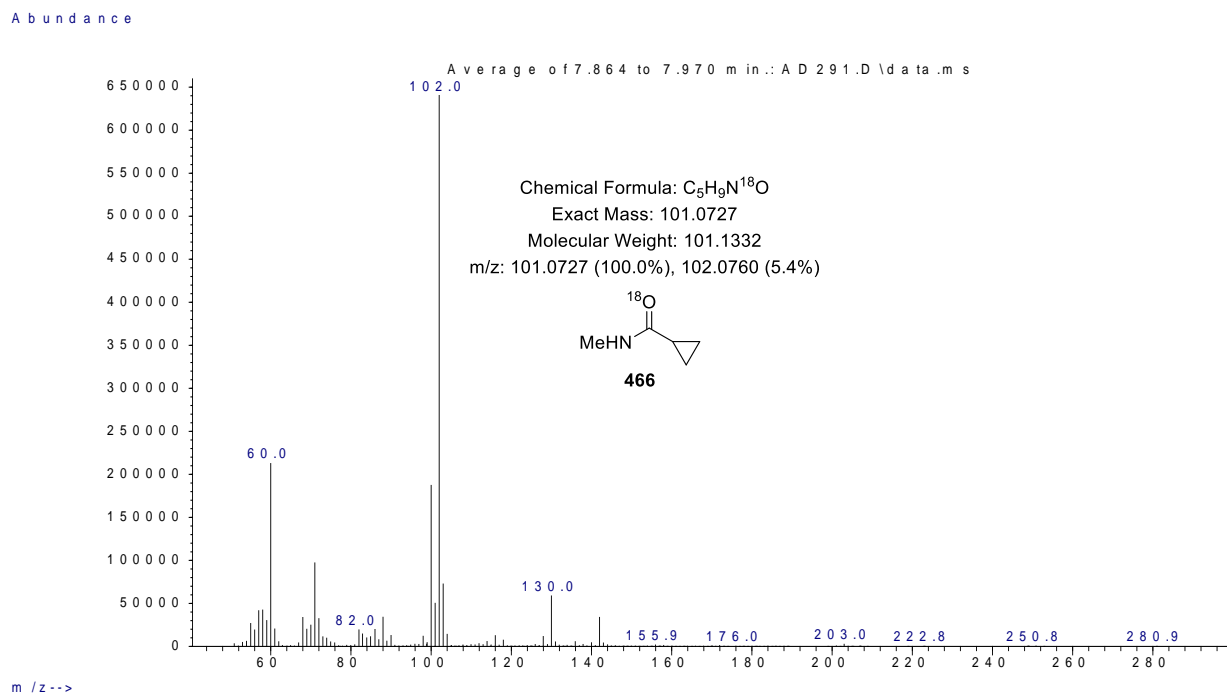
MS (CI) of GC peak at 8.111 min showing [M+H]⁺ of decarboxylated amide **468** upon cleavage of non-labeled ester **419**
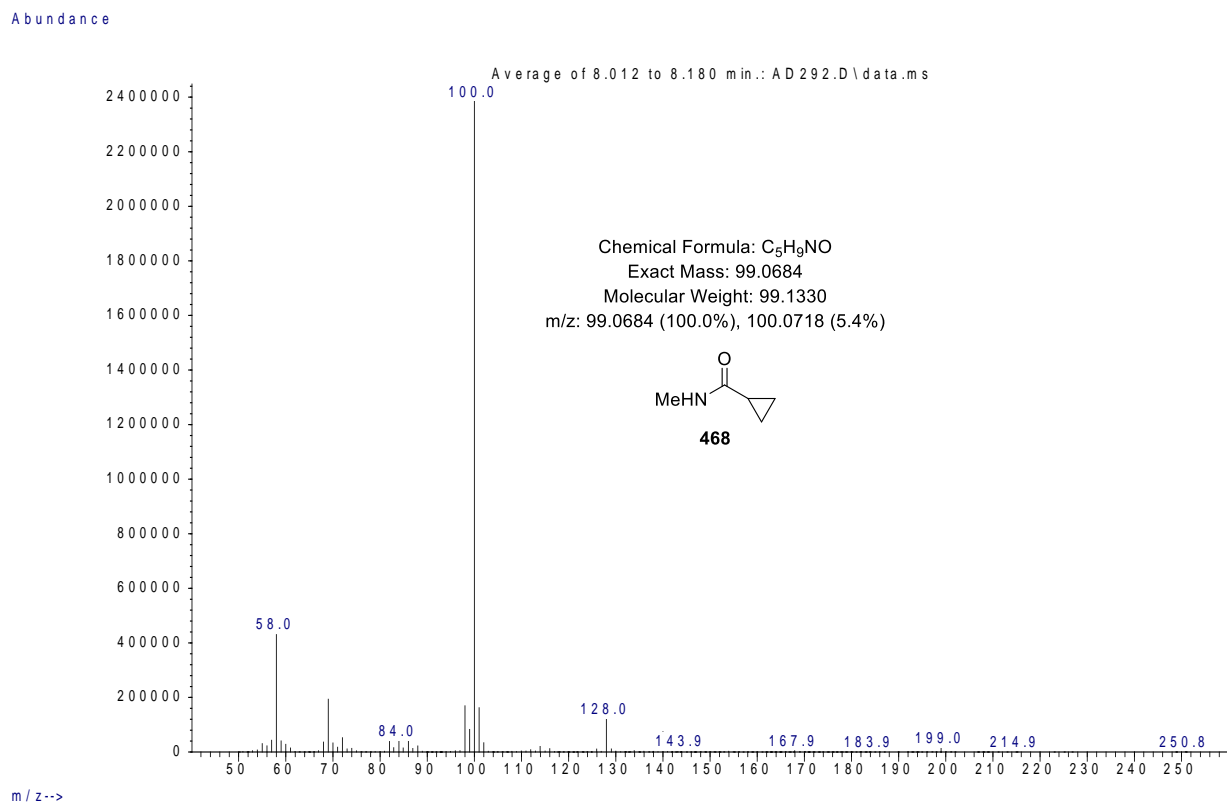
MS (CI) of GC peak at 9.348 min showing [M+H]$^+$ of phenol **396** upon cleavage of doubly ^{18}O labeled ester **463**
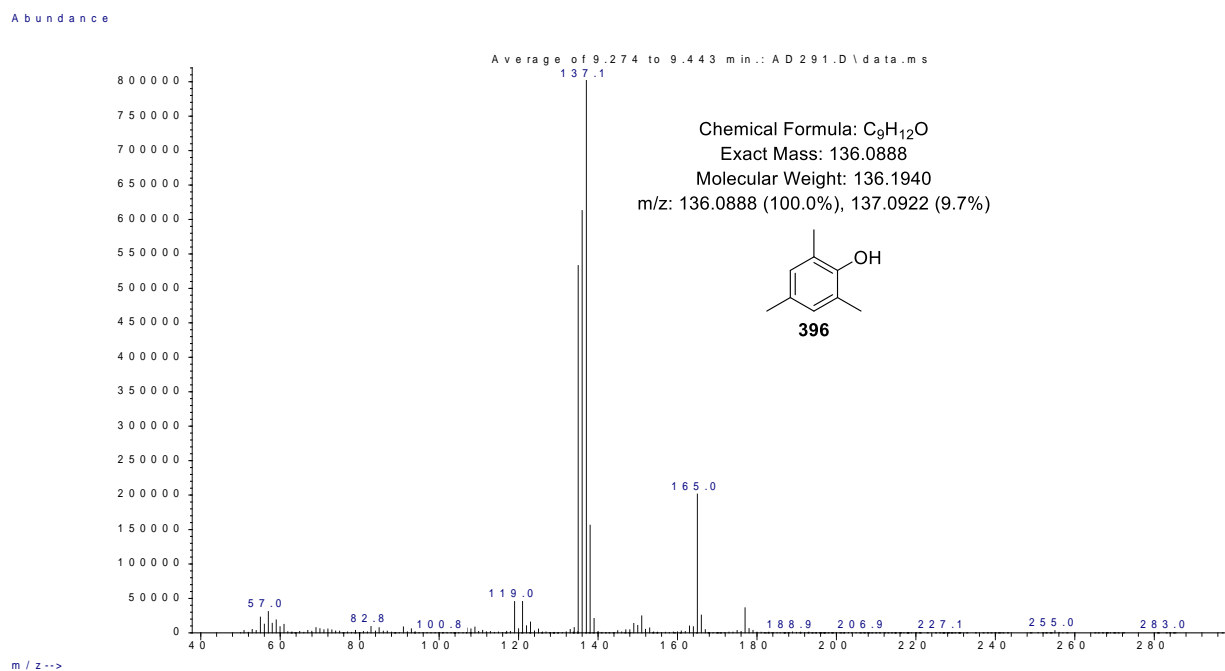
MS (CI) of GC peak at 9.398 min showing [M+H]$^+$ of phenol **396** upon cleavage of non-labeled ester **419**
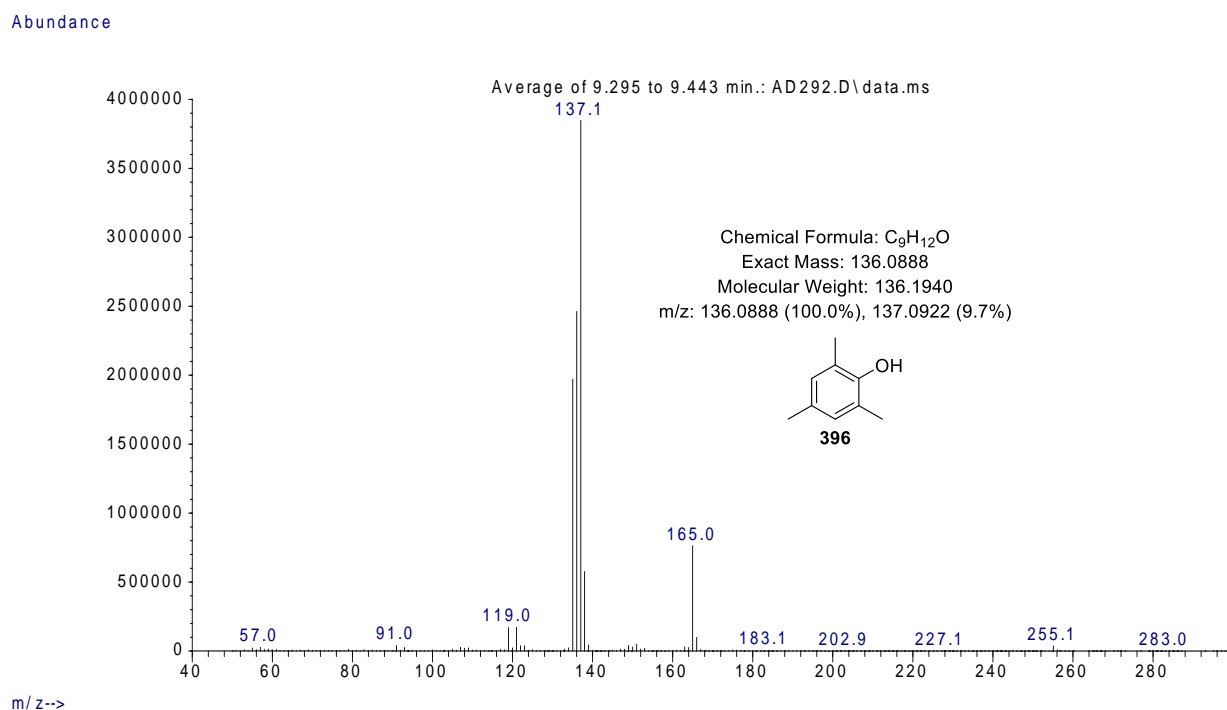
MS (CI) of GC peak at 10.671 min showing [M+H]$^+$ of ^{18}O labeled amides **464** and **465** upon cleavage of doubly ^{18}O labeled ester **463**
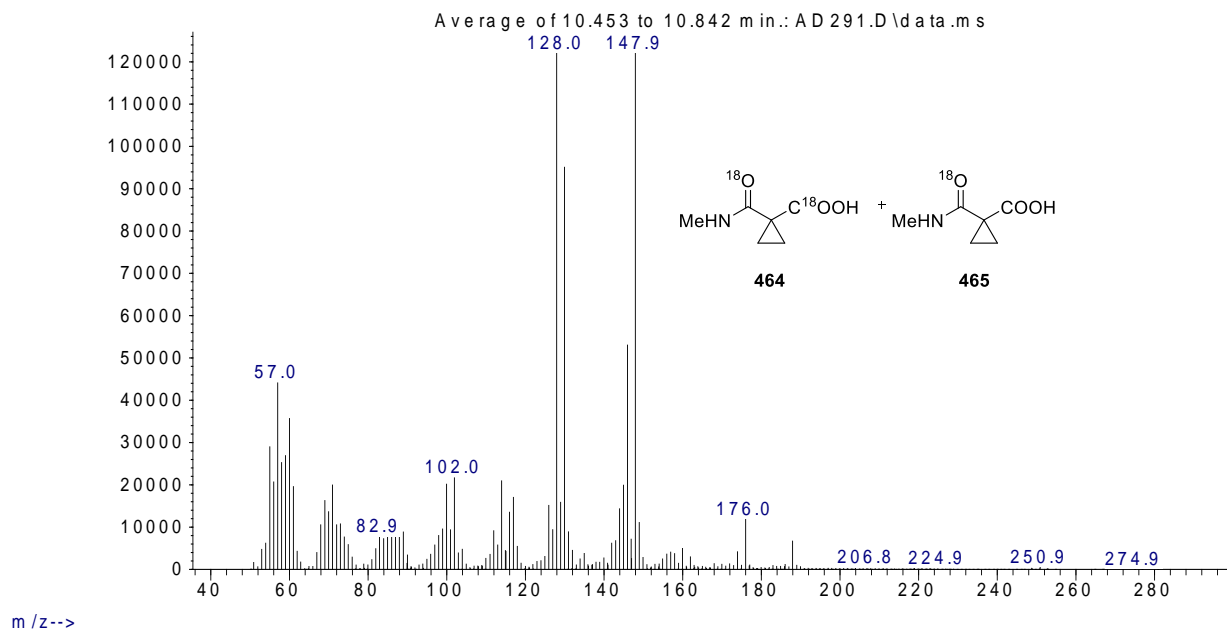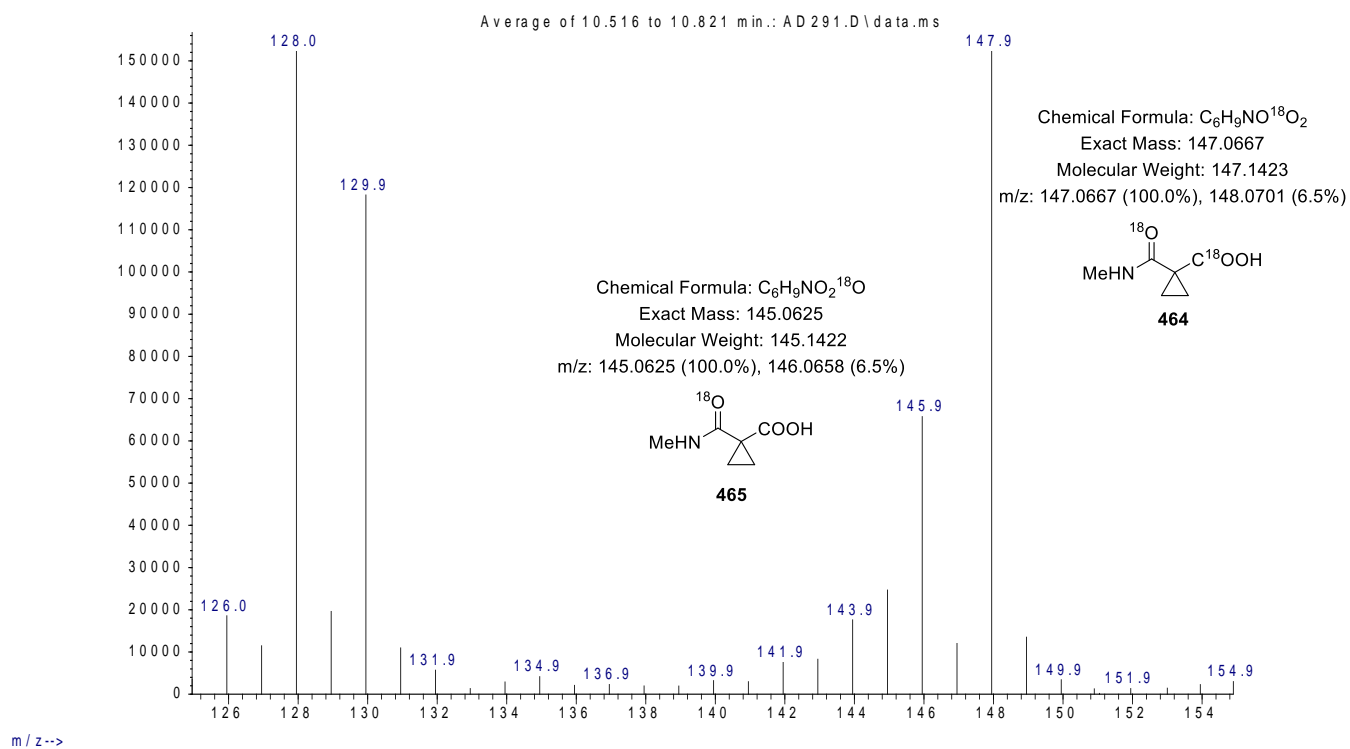
MS (CI) of GC peak at 10.834 min showing $[M+H]^+$ of amide **467** upon cleavage of non-labeled ester **419**

Abundance

Average of 10.516 to 10.947 min.: AD 292.D \data.ms

Chemical Formula: C$_6$H$_9$NO$_3$
Exact Mass: 143.0582
Molecular Weight: 143.1420
m/z: 143.0582 (100.0%), 144.0616 (6.5%)

m / z -->
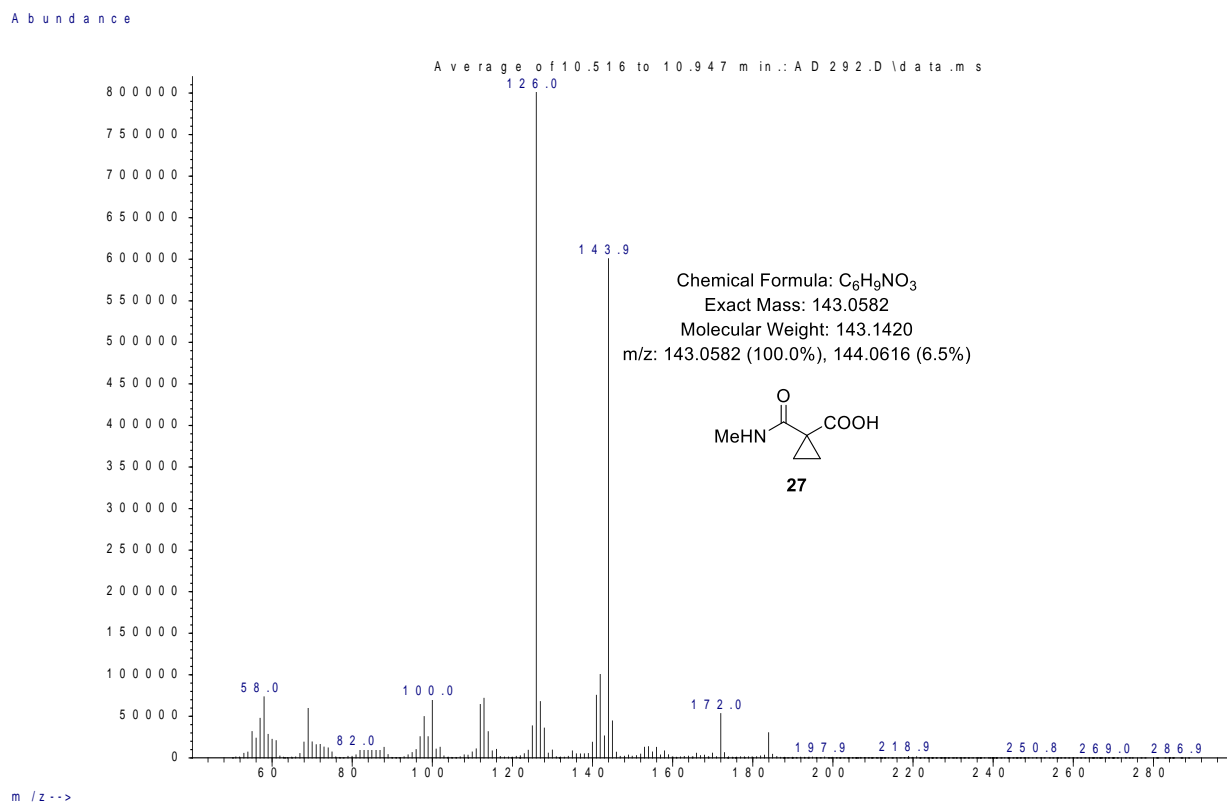
5.4   Cartesian Coordinates

The number of imaginary frequencies relate to structures optimized at the (U)B3LYP/6-31+G(d) level of theory, using 2,2,2-trifluoroethanol (TFE) CPCM model.

All Gibbs Free Energies were calculated at 298.15 K.

Peroxide 90

Gibbs Free Energy (in Hartrees), B3LYP/6-31+G(d) in TFE: –493.676511

Number of imaginary frequencies: 0

O	4.32923300	-1.05445300	0.93896000
C	3.35719900	-1.37479800	0.30400400
O	3.45848100	-1.51658800	-1.07120700
C	1.97127900	-1.67441000	0.69314600
C	1.25266500	-2.00472900	-0.54639600
O	2.14715000	-1.90930700	-1.60109500
C	1.28187900	-0.94046000	1.85535700
C	1.63731100	-2.36080300	2.02802000
O	0.11049500	-2.31772700	-0.76574700
H	1.89307000	-0.18403000	2.33666700
H	0.85407500	-3.10924200	1.96653400
H	2.50162600	-2.61600200	2.63236800
H	0.24549900	-0.67725800	1.67085100
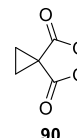
Peroxide homolytic cleavage transition state (TS2)

Gibbs Free Energy (in Hartrees), UB3LYP/6-31+G(d) in TFE: –493.629200

Number of imaginary frequencies: 1 (–228.63 cm^{-1})

TS2

C	-0.00201000	1.58114600	-0.74888200
C	0.00306800	1.58712400	0.73992400
H	-0.91029200	1.84513800	-1.27897600
H	0.92783100	1.79462000	-1.26346300
H	-0.90145400	1.85558800	1.27418400
H	0.93654100	1.80486900	1.24608800
C	-0.02134600	0.22753600	0.00109600
O	-1.18607200	-1.88430000	0.01210900
O	1.11709700	-1.87858500	0.00140300
C	-1.22517200	-0.61069400	0.00846500
C	1.28777700	-0.56408900	0.00004100
O	-2.39939000	-0.03033600	0.01090100
O	2.37347100	0.04569000	-0.00236200
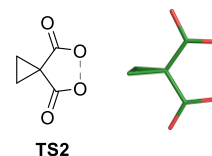
Diradical species 469

Gibbs Free Energy (in Hartrees), UB3LYP/6-31+G(d) in TFE: –493.637030

Number of imaginary frequencies: 0

C	-4.13972000	0.11480700	1.05920300
C	-2.69503200	-0.09702000	0.87732900
H	-4.79591500	0.02556400	0.19981700
H	-4.58542600	-0.10199200	2.02421600
H	-2.31947800	-0.33856900	-0.11136500
H	-2.10877300	-0.46419600	1.71314700
C	-3.21099700	1.35656400	1.03796800
O	-3.02774600	3.43715400	-0.22507300
O	-2.78378900	3.25854900	2.50683200
C	-3.24154300	2.18866500	-0.18188500
C	-2.95229400	2.01418900	2.33488400
O	-3.48470000	1.73404800	-1.33742500
O	-2.87427400	1.39379900	3.43487500
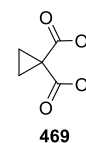
Chapter 6: References

1. (a) Whang, Z.; Cui, Y.-T.; Xu, Z.-B.; Qu, J. *J. Org. Chem.* **2008**, *73*, 2270–2274. (b) Liu, Y.-K.; Li, R.; Yue, L.; Li, B.-J.; Chen, Y.-C.; Wu, Y.; Ding, L.-S. *Org. Lett.* **2006**, *8*, 1521-1524. (c) Morán-Ramallal, R.; Liz, R.; Gotor, V. *J. Org. Chem.* **2010**, *75*, 6614-6624.

2. (a) Shivani; Pujala, B.; Chakraborti, A. K. *J. Org. Chem.* **2007**, *72*, 3713–3722. (b) Azizi, N.; Saidi, M. R. *Org. Lett.* **2005**, *7*, 3649–3651.

3. Li, G.; Chang, H.-T.; Sharpless, K. B. *Angew. Chem. Int. Ed.* **1996**, *35*, 451–454.

4. Morán-Ramallal, R.; Liz, R.; Gotor, V. *J. Org. Chem.* **2010**, *75*, 6614–6624.

5. Degennaro, L.; Trinchera, P.; Luisi, R. *Chem. Rev.* **2014**, *114*, 7881–7929.

6. Vesely, J.; Ibrahem, I.; Zhao, G.-L.; Rios, R.; Córdova, A. *Angew. Chem. Int. Ed.* **2007**, *46*, 778–781.

7. Hashimoto, T.; Osuna Gálvez, A.; Maruoka, K. *J. Am. Chem. Soc.* **2013**, *135*, 17667–17670.

8. Arai, K.; Lucarini, S.; Salter, M. M.; Ohta, K.; Yamashita, Y.; Kobayashi, S. *J. Am. Chem. Soc.* **2007**, *129*, 8103–8111.

9. Kumar, M.; Kureshi, R. I.; Saravanan, S.; Verma, S.; Jakhar, A.; Khan, N. H.; Abdi, S. H. R.; Bajaj, H. C. *Org. Lett.* **2014**, *16*, 2798–2801.

10. Gao, Bo; Wen, Y.; Yang, Z.; Huang, X.; Liu, X.; Feng, X. *Adv. Synth. Catal.* **2008**, *350*, 385–390.

11. Sharpless, K. B.; Patrick, D. W.; Truesdale, L. K.; Biller, S. A. *J. Am. Chem. Soc.* **1975**, *97*, 2305–2307.

12. Luttrell, W. E; Giles, C. B.; *J. Chem. Health Saf.* **2007**, *14*, 40–41.

13. Sharpless, K. B.; Chong, A. O.; Oshima, K. *J. Org. Chem.* **1976**, *41,* 177–179.

14. Li, G.; Chang, H.-T.; Sharpless, K. B. *Angew. Chem. Int. Ed.* **1996**, *35*, 451–454.

15. Jacobsen, E. N.; Markó, I.; Mungall, W. S.; Schröder, G.; Sharpless, K. B.; *J. Am. Chem. Soc.* **1988**, *110*, 1968–1970.

16. Rudolph, J.; Sennhenn, P. C.; Vlaar, C. P.; Sharpless, K. B. *Angew. Chem. Int. Ed.* **1996**, *35*, 2810–2813.

17. Donohoe, T. J.; Callens, C. K. A.; Flores, A.; Lacy, A. R.; Rathi, A. H. *Chem. Eur. J.* **2011**, *17*, 58–76.

18. Munz, D.; Strassner, T. *J. Org. Chem.* **2010**, *75*, 1491–1497.

19. Muñiz, K. *Chem. Soc. Rev.* **2004**, *33*, 166–174.

20. Donohoe, T. J.; Churchill, G. H.; Wheelhouse, K. M. P.; Glossop, P. A. *Angew. Chem. Int. Ed.* **2006**, *45*, 8025–8028.

21. Beaumont, S.; Pons, V.; Retailleau, P.; Dodd, R. H.; Dauban, P. *Angew. Chem. Int. Ed.* **2010**, *49*, 1634–1637.

22. Dequirez, G.; Ciesielski, J.; Retailleau, P.; Dauban, P. *Chem. Eur. J.* **2014**, *20*, 8929–8933.

23. Bäckvall, J.-E. *Tetrahedron Lett.* **1975**, *16*, 2225–2228.

24. Liu, G.; Stahl, S. *J. Am. Chem. Soc.* **2006**, *128*, 7179–7181.

25. Muñiz, K.; Iglesias, A.; Fang, Y. *Chem. Commun.* **2009**, *2009*, 5591–5593.

26. Khusnutdinova, J. R.; Maiorana, A. S.; Zavalij, P. Y.; Vedernikov, A. N. *Inorg. Chim. Acta* **2011**, *369*, 274–283.

27. (a) Michaelis, D. J.; Shaffer, C. J.; Yoon, T. P. *J. Am. Chem. Soc.* **2007**, *129*, 1866–1867. (b) Michaelis, D. J.; Ischay, M. A.; Yoon, T. P. *J. Am. Chem. Soc.* **2008**, *130*, 6610–6615. (c) Michaelis, D. J.; Williamson, K. S.; Yoon, T. P. *Tetrahedron* **2009**, *65*, 5118–5124. (d) DePorter, S. M.; Jacobsen, A. C.; Partridge, K. M.; Williamson, K. S.; Yoon, T. P. *Tetrahedron Lett.* **2010**, *51*, 5223–5225.

28. Williamson, K. S.; Yoon, T. P. *J. Am. Chem. Soc.* **2010**, *132*, 4570–4571.

29. Williamson, K. S.; Yoon, T. P. *J. Am. Chem. Soc.* **2012**, *134*, 12370–12373.

30. Liu, G.-S.; Zhang, Y.-Q.; Yuan, Y.-A.; Xu, H. *J. Am. Chem. Soc.* **2013**, *135*, 3343–3346.

31. Miyazawa, K.; Koike, T.; Akita, M. *Chem. Eur. J.* **2015**, *21*, 11677–11680.

32. Dangerfield, E. M.; Timmer, M. S. M.; Stocker, B. L. *Org. Lett.* **2009**, *11*, 535–538.

33. Mahoney, J. M.; Smith, C. R.; Johnston, J. N. *J. Am. Chem. Soc.* **2005**, *127*, 1354–1355.

34. Garigipati, R. S.; Freyer, A. J.; Whittle, R. R.; Weinreb, S. M. *J. Am. Chem. Soc.* **1984**, *106*, 7861–7867.

35. Moriyama, K.; Izumisawa, Y.; Togo, H. *J. Org. Chem.* **2012**, *77*, 9846–9851.

36. Schmidt, V. A.; Alexanian, E. J. *J. Am. Chem. Soc.* **2011**, *133*, 11402–11405.

37. Han, B.; Yang, X.-L.; Fang, R.; Yu, W.; Wang, C.; Duan, X.-Y.; Liu, S. *Angew. Chem. Int. Ed.* **2012**, *124*, 8946–8950.

38. Li, Y.; Hartmann, M.; Daniliuc, C. G.; Studer, A. *Chem. Commun.* **2015**, *51*, 5706–5709.

39. Griffith, J. C.; Jones, K. M.; Picon, S.; Rawling, M. J.; Kariuki, B. M.; Campbell, M.; Tomkinson, N. C. O. *J. Am. Chem. Soc.* **2010**, *132*, 14409–14411.

40. Picon, S.; Rawling, M. J.; Campbell, M.; Tomkinson, N. C. O. *Org. Lett.* **2012**, *14*, 6250–6253.

41. Rawling, M. J.; Rowley, J. H.; Campbell, M.; Kennedy, A. R.; Parkinson, J. A.; Tomkinson, N. C. O. *Chem. Sci.* **2014**, *5*, 1777–1785

42. (a) Patnaik, P. *A Comprehensive Guide to the Hazardous Properties of Chemical Substances*, 3rd ed.; Wiley, **2007**; pp. 259–266. (b) Pohanish, R. P.; Greene, S. A. *Wiley Guide to Chemical Incompatibilities*, 3rd ed.; Wiley, **2009**. (c) AkzoNobel website, "*Safety of organic peroxides*" (PDF). Retrieved on April 18, 2016.

43. Sharba, A. H. K.; Al-Bayati, R. H.; Rezki, N.; Aouad, M. R. *Molecules* **2005**, *10*, 1153–1160.

44. Singh, R. K.; Danishefsky, S. *Org. Synth.* **1990**, *Coll. Vol. 7*, 411.

45. Zinner, G.; Ruthe, H.; Böse, D. *Pharmazie* **1974**, *29*, 16–20.

46. Richon, A. B.; Maragoudakis, M. E.; Wasvary, J. S. *J. Med. Chem.* **1982**, *25*, 745–747.

47. Dmowski, W.; Wolniewicz, A. *J. Fluorine Chem.* **2000**, *102*, 141–146.

48. For details, please refer to Kevin Jones' Ph.D. Thesis, Cardiff University, **2010**.

49. Kerr, J. A. *Strengths of Chemical Bonds* (pp. 9-52–9-75) in *CRC Handbook of Chemistry and Physics, Internet Version 2005,* David R. Lide, ed., <http://www.hbcpnetbase.com>, CRC Press, Boca Raton, FL, **2005**.

50. (a) Payne, G. B.; Williams, P. H. *J. Org. Chem.* **1961**, *26*, 651–659. (b) Payne, G. B.; Deming, P. H.; Williams, P. H. *J. Org. Chem.* **1961**, *26*, 659–663.

51. Ji, L.; Wang, Y.-N.; Qian, C.; Chen, X.-Z. *Synth. Commun.* **2013**, *43*, 2256–2264.

52. Lavoisier, T.; Rodriguez, J. *Synth. Commun.* **1996**, *26*, 525–530.

53. Please refer to COSHH forms regarding peroxide handling.

54. Radziszewski, B. *Ber. Dtsch. Chem. Ges.* **1885**, *18*, 355–356.

55. Nielsen, D. U.; Taaning, R. H.; Lindardt, A. T.; Gøgsig, T. M.; Skrydstrup, T. *Org. Lett.* **2011**, *13*, 4454–4457.

56. von Holleben, M. L. A.; Livotto, P. R.; Schuch, C. M. *J. Braz. Chem. Soc.* **2001**, *12*, 42–46.

57. Vacque, V.; Dupuy, N.; Sombret, B.; Huvenne, J. P.; Legrand, P. *J. Mol. Struct.* **1996**, *384*, 165–174.

58. von Baeyer, A.; Villiger, V. *Ber. Dtsch. Chem. Ges.* **1899**, *32*, 3625–3633.

59. ten Brink, G.-J.; Arends, I. W. C. E.; Sheldon, R. A. *Chem. Rev.* **2004**, *104*, 4105–4123.

60. (a) Jadhav, M. S.; Righi, P.; Marcantoni, E.; Bencivenni, G. *J. Org. Chem.* **2012**, *77*, 2667–2674. (b) Demoulin, N.; Lifchits, O.; List, B. *Tetrahedron* **2012**, *68*, 7568–7574. (c) Lifchits, O.; Demoulin, N.; List, B. *Angew. Chem. Int. Ed.* **2011**, *50*, 9680–9683. (d) Kano, T.; Mii, H.; Maruoka, K. *J. Am. Chem. Soc.* **2009**, *131*, 3450–3451. (e) Vaismaa, M. J. P.; Yau, S. C.; Tomkinson, N. C. O. *Tetrahedron Lett.* **2009**, *50*, 3625–3627.

61. Davis, F. A.; Sheppard, A. C.; Chen, B.-C.; Haque, M. S. *J. Am. Chem. Soc.* **1990**, *112*, 6679–6690.

62. Cecere, G.; König, C. M.; Alleva, J. L.; MacMillan, D. W. C. *J. Am. Chem. Soc.* **2013**, *135*, 11521–11524.

63. (a) Vidal, J.; Guy, L.; Stérin, S.; Collet, A. *J. Org. Chem.* **1993**, *58*, 4791–4793. (b) Vidal, J.; Damestoy, S.; Guy, L.; Hannachi, J.-C.; Aubry, A.; Collet, A. *Chem. Eur. J.* **1997**, *3*, 1691–1709.

64. Enders, D.; Poiesz, C.; Joseph, R. *Tetrahedron: Asymmetry* **1998**, *9*, 3709–3716.

65. Armstrong, A.; Edmonds, I. D.; Swarbrick, M. E.; Treweeke, N. R. *Tetrahedron* **2005**, *61*, 8423–8442.

66. (a) Greene, F. D. *J. Am. Chem. Soc.* **1956**, *78*, 2246–2250. (b) Greene, F. D. *J. Am. Chem. Soc.* **1956**, *78*, 2250–2254. (c) Greene, F. D.; Rees, W. W. *J. Am. Chem. Soc.* **1958**, *80*, 3432–3437. (d) Greene, F. D. *J. Am. Chem. Soc.* **1959**, *81*, 1503–1506. (e) Greene, F. D.; Rees, W. W. *J. Am. Chem. Soc.* **1960**, *82*, 890–893. (f) Greene, F. D.; Rees, W. W. *J. Am. Chem. Soc.* **1960**, *82*, 893–896. (g) Yuan, C.; Axelrod, A.; Varela, M.; Danysh, L.; Siegel, D. *Tetrahedron Lett.* **2011**, *52*, 2540–2542.

67. Mor, S.; Dhawan, S. N.; Kapoor, M.; Kumar, D. *Tetrahedron* **2007**, *63*, 594–597.

68. Godenschwager, P. F.; Collum, D. B. *J. Am. Chem. Soc.* **2008**, *130*, 8726–8732.

69. Gaussian 09, Revision A.02, Frisch, M. J.; Trucks, G. W.; Schlegel, H. B.; Scuseria, G. E.; Robb, M. A.; Cheeseman, J. R.; Scalmani, G.; Barone, V.; Mennucci, B.; Petersson, G. A.; Nakatsuji, H.; Caricato, M.; Li, X.; Hratchian, H. P.; Izmaylov, A. F.; Bloino, J.; Zheng, G.; Sonnenberg, J. L.; Hada, M.; Ehara, M.; Toyota, K.; Fukuda, R.; Hasegawa, J.; Ishida, M.; Nakajima, T.; Honda, Y.; Kitao, O.; Nakai, H.; Vreven, T.; Montgomery, J. A.; Peralta, J. E.; Ogliaro, F.; Bearpark, M.; Heyd, J. J.; Brothers, E.; Kudin, K. N.; Staroverov, V. N.; Kobayashi, R.; Normand, J.; Raghavachari, K.; Rendell, A.; Burant, J. C.; Iyengar, S. S.; Tomasi, J.; Cossi, M.; Rega, N.; Millam, J. M.; Klene, M.; Knox, J. E.; Cross, J. B.; Bakken, V.; Adamo, C.; Jaramillo, J.; Gomperts, R.; Stratmann, R. E.; Yazyev, O.; Austin, A. J.; Cammi,

R.; Pomelli, C.; Ochterski, J. W.; Martin, R. L.; Morokuma, K.; Zakrzewski, V. G.; Voth, G. A.; Salvador, P.; Dannenberg, J. J.; Dapprich, S.; Daniels, A. D.; Farkas, Ö.; Foresman, J. B.; Ortiz, J. V.; Cioslowski J.; Fox, D. J. **2009**.

70. Karmakar, R.; Pahari, P.; Mal. D. *Chem. Rev.* **2014**, *114*, 6213–6284.

71. Kundu, N. G.; Pal, M. *J. Chem. Soc., Chem. Commun.* **1993**, 86–88.

72. (a) Uchiyama, M.; Ozawa, H.; Takuma, K.; Matsumoto, Y.; Yonehara, M.; Hiroya, K.; Sakamoto, T. *Org. Lett.* **2006**, *8*, 5517–5520. (b) Terada, M.; Kanazawa, C. *Tetrahedron Lett.* **2007**, *48*, 933–935.

73. Duchêne, A.; Thibonnet, J.; Parrain, J.-L.; Anselmi, E.; Abarbri, M. *Synthesis* **2007**, 597–607.

74. Jithunsa, M.; Ueda, M.; Miyata, O. *Org. Lett.* **2011**, *13*, 518–521.

75. Park, J. H.; Bhilare, S. V.; Youn, S. W. *Org. Lett.* **2011**, *13*, 2228–2231.

76. Yang, H.; Hu, G.-Y.; Chen, J.; Wang, Y.; Wang, Z.-H. *Bioorg. Med. Chem. Lett.* **2007**, *17*, 5210–5213.

77. Bedoya, L. M.; del Olmo, E.; Sancho, R.; Barboza, B.; Beltrán, M.; García-Cadenas, A. E.; Sánchez-Palomino, S.; López-Pérez, J. L.; Muñoz, E.; San Feliciano, A.; Alcamí, J. *Bioorg. Med. Chem. Lett.* **2006**, *16*, 4075–4079.

78. Zimmer, H.; Barry, R. D. *J. Org. Chem.* **1962**, *27*, 1602–1604.

79. Safari, J.; Naeimi, H.; Khakpour, A. A.; Jondani, R. S.; Khalili, S. D. *J. Mol. Catal. A: Chem.* **2007**, *270*, 236–240.

80. Abell, A. D.; Clark, B. M.; Robinson, W. T. *Aust. J. Chem.* **1988**, *41*, 1243–1249.

81. Dallavalle, S.; Nannei, R.; Merlini, L.; Bava, A.; Nasini, G. *Synlett.* **2005**, 2676–2678.

82. Coelho, F.; Veronese, D.; Pavam, C. H.; de Paula, V. I.; Buffon, R. *Tetrahedron* **2006**, *62*, 4563.

83. Lee, K. Y.; Kim, J. M.; Kim, J. N. *Synlett.* **2003**, 357–360.

84. Kato, H.; Tezuka, H.; Yamaguchi, K.; Nowada, K.; Nakamura, Y. *J. Chem. Soc., Perkin Trans. 1* **1978**, 1029–1036.

85. Helmers, R. *Acta Chem. Scand.* **1965**, *19*, 2139–2150.

86. (a) Hunter, C. A.; Sanders, J. K. M. *J. Am. Chem. Soc.* **1990**, *112*, 5525–5534. (b) Cockroft, S. L.; Hunter, C. A.; Lawson, K. R.; Perkins, J.; Urch, C. J. *J. Am. Chem. Soc.* **2005**, *127*, 8594–8595. (c) Sinnokrot, M. O.; Sherrill, C. D. *J. Phys. Chem. A* **2006**, *110*, 10656–10668.

87.   Sinnokrot, M. O.; Valeev, E. F.; Sherrill, C. D. *J. Am. Chem. Soc.* **2002**, *124*, 10887–10893.

88.   (a) Braun, M. *Fundamentals and Transition-state Models. Aldol Additions of Group 1 and 2 Enolates*. In *Modern Aldol Reactions*; Mahrwald, R., Ed.; Wiley-VCH: Weinheim, **2004**; Part 1, pp. 1–61. (b) Carey, F. A.; Sundberg, R. J. *Addition, Condensation and Substitution Reactions of Carbonyl Compounds*. In *Advanced Organic Chemistry*; Carey, F. A. and Sundberg, R. J., Ed.; Springer: New York, **2007**; Part A: Structure and Mechanisms, pp. 682–697. (c) Carey, F. A.; Sundberg, R. J. *Reactions of Carbon Nucleophiles with Carbonyl Compounds*. In *Advanced Organic Chemistry*; Carey, F. A. and Sundberg, R. J., Ed.; Springer: New York, **2007**; Part B: Reactions and Synthesis, pp. 63–200.

89.   (a) Ireland, R. E.; Mueller, R. H.; Willard, A. K. *J. Am. Chem. Soc.* **1976**, *98*, 2868–2877. (b) Godenschwager, P. F.; Collum, D. B. *J. Am. Chem. Soc.* **2008**, *130*, 8726–8732.

90.   Crimmins, M. T.; King, B. W.; Tabet, E. A.; Chaudary, K. *J. Org. Chem.* **2001**, *66*, 894–902.

91.   Ngo, K.-S.; Cheung, K.-K.; Brown, G. D. *J. Chem. Res. (S)* **1998**, 80–81.

92.   (a) Davies, S. G.; Fletcher, A. M.; Thomson, J. E. *Org. Biomol. Chem.* **2014**, *12*, 4544–4549. (b) Henbest, H. B.; Wilson, R. A. L. *J. Chem. Soc.* **1957**, 1958–1965.

93.   Luche, J. L. *J. Am. Chem. Soc.* **1978**, *100*, 2226–2227.

94.   Manna, M. S.; Mukherjee, S. *J. Am. Chem. Soc.* **2015**, *137*, 130–133.

95.   Dittmer, D. C.; Zhang, Y.; Discordia, R. P. *J. Org. Chem.* **1994**, *59*, 1004–1010.

96.   Mukhopadhyay, R.; Kundu, N. G. *Tetrahedron* **2001**, *57*, 9475–9480.

97.   (a) Mislow, K.; Brenner, J. *J. Am. Chem. Soc.* **1953**, *75*, 2318–2322. (b) Hawthorne, M. F.; Emmons, W. D.; McCallum, K. S. *J. Am. Chem. Soc.* **1958**, *80*, 6393–6398.

98.   Li, J. *Name Reactions*; Springer: Berlin, Heidelberg, 2009, pp. 10–12.

99.   Renz, M.; Meunier, B. *Eur. J. Org. Chem.* **1999**, *1999*, 737–739.

100.   (a) Heaney, H. *Aldrichimica Acta* **1993**, *26*, 35–45. (b) Cooper, M. S.; Heaney, H.; Newbold, A. J.; Sanderson, W. R. *Synlett* **1990**, 533–535.

101.   (a) McKillop, A.; Sanderson, W. R. *Tetrahedron* **1995**, *51*, 6145–6166. (b) Muzart, J. *Synthesis* **1995**, *47*, 1325–1347. (c) McKillop, A.; Sanderson, W. R. *J. Chem. Soc. Perkin Trans. 1* **2000**, 471–476.

102.   Corma, A.; Nemeth, L. T.; Renz, M.; Valencia, S. *Nature* **2001**, *412*, 423–425.

103. Renz, M.; Blasco, T.; Corma, A.; Fornés, V.; Jensen, R.; Nemeth, L. *Chem. Eur. J.* **2002**, *8*, 4708–4717.

104. (a) Hao, X.; Yamazaki, O.; Yoshida, A.; Nishikido, J. *Green Chem.* **2003**, *5*, 524–528. (b) Lei, Z.; Zhang, Q.; Wang, R.; Ma, G.; Jia, C. *J. Organomet. Chem.* **2006**, *691*, 5767–5773. (c) Kirumakki, S.; Samarajeewa, S.; Harwell, R.; Mukherjee, A.; Herber, R. H.; Clearfield, A. *Chem. Commun.* **2008**, 5556–5558. (d) Luo, H. Y.; Bui, L.; Gunther, W. R.; Min, E.; Román-Leshov, Y. *ACS Catal.* **2012**, *2*, 2695–2699. (e) Hara, T.; Hatakeyama, M.; Kim, A.; Ichikuni, N.; Shimazu, S. *Green Chem.* **2012**, *14*, 771–777.

105. Zhang, X.; Ye, J.; Yu, L.; Shi, X.; Zhang, M.; Xu, Q.; Lautens, M. *Adv. Synth. Catal.* **2015**, *357*, 955–960.

106. Martins, L. M. D. R. S.; Alegria, E. C. B. A.; Smoleński, P.; Kuznetsov, M. L.; Pombeiro, A. J. L. *Inorg. Chem.* **2013**, *52*, 4534–4546.

107. Uyanik, M.; Nakashima, D.; Ishihara, K. *Angew. Chem. Int. Ed.* **2012**, *51*, 9093–9096.

108. (a) Conte, V.; Floris, B.; Galloni, P.; Mirruzzo, V.; Scarso, A.; Sordi, D.; Strukul, G *Green Chem.* **2005**, *7*, 262–266. (b) Michelin, R. A.; Pizzo, E.; Scarso, A.; Sgarbossa, P.; Strukul, G.; Tassan, A. *Organometallics* **2005**, *24*, 1012–1017. (c) Del Todesco Frisone, M.; Pinna, F; Strukul, G. *Organometallics* **1993**, *12*, 148–156.

109. Gusso, A.; Baccin, C.; Pinna, F.; Strukul, G. *Organometallics* **1994**, *13*, 3442–3451.

110. Cavarzan, A.; Bianchini, G.; Sgarbossa, P.; Lefort, L.; Gladiali, S.; Scarso, A.; Strukul, G. *Chem. Eur. J.* **2009**, *15*, 7930–7939.

111. Malkov, A. V.; Friscourt, F.; Bell, M.; Swarbrick, M. E.; Kočovský, P. *J. Org. Chem.* **2008**, *73*, 3996–4003.

112. Watanabe, A.; Uchida, T.; Ito, K.; Katsuki, T. *Tetrahedron* **2002**, *43*, 4481–4485.

113. Watanabe, A.; Uchida, T.; Irie, R.; Katsuki, T. *Proc. Natl. Acad. Sci. USA* **2004**, *101*, 5737–5742.

114. Ríos, M. Y.; Salazar, E.; Olivo, H. F. *Green Chem.* **2007**, *9*, 459–462.

115. Kotlewska, A. J.; van Rantwijk, F.; Sheldon, R. A.; Arends, I. W. C. E. *Green Chem.* **2011**, *13*, 2154–2160.

116. Peris, G.; Miller, S. J. *Org. Lett.* **2008**, *10*, 3049–3052.

117. Romney, D. K.; Colvin, S. M.; Miller, S. J. *J. Am. Chem. Soc.* **2014**, *136*, 14019–14022.

118. Xu, S.; Wang, Z.; Zhang, X.; Zhang, X.; Ding, K. *Angew. Chem. Int. Ed.* **2008**, *47*, 2840–2843.

119. Mazzini, C.; Lebreton, J.; Furstoss, R. *J. Org. Chem.* **1996**, *61*, 8–9.

120. Murahashi, S.-I.; Ono, S.; Imada, Y. *Angew. Chem. Int. Ed.* **2002**, *41*, 2366–2368.

121. Okazaki, H.; Hanaya, K.; Shoji, M.; Hada, N.; Sugai, T. *Tetrahedron* **2013**, *69*, 7931–7935.

122. Frank, W. C. *Tetrahedron: Asymmetry* **1998**, *9*, 3745–3749.

123. (a) Wong, O. A.; Shi, Y. *Chem. Rev.* **2008**, *108*, 3958–3987. (b) Burke, C. P.; Shu, L.; Shi, Y. *J. Org. Chem.* **2007**, *72*, 6320–6323.

124. Wang, Z.-H.; Tu, Y.; Frohn, M.; Zhang, J.-R.; Shi Y. *J. Am. Chem. Soc.* **1997**, *119*, 11224–11235.

125. Uraguchi, D.; Tsutsumi, R.; Ooi, T. *J. Am. Chem. Soc.* **2013**, *135*, 8161–8164.

126. Jiménez-Sanchidrián, C.; Hidalgo, J. M.; Llamas, R.; Ruiz, J. R. *Appl. Catal., A: Gen.* **2006**, *312*, 86–94.

127. Ruiz, J. R.; Jiménez-Sanchidrián, C.; Llamas, R. *Tetrahedron* **2006**, *62*, 11697–11703.

128. Llamas, R.; Jiménez-Sanchidrián, C.; Ruiz, J. R. *Appl. Catal., B* **2007**, *72*, 18–25.

129. (a) Llamas, R.; Jiménez-Sanchidrián, C.; Ruiz, J. R. *Tetrahedron* **2007**, *63*, 1435–1439. (b) For a review on surface-based catalysts used in the Baeyer-Villiger reaction, please refer to Jiménez-Sanchidrián, C.; Ruiz, J. R. *Tetrahedron* **2008**, *64*, 2011–2026.

130. For details, please refer to Tyne Bradley's Masters' thesis, University of Strathclyde, **2014**.

131. Dragan, A.; Kubczyk, T. M.; Rowley, J. H.; Sproules, S.; Tomkinson. N. C. O. *Org. Lett.* **2015**, *17*, 2618–2621.

132. Picon, S.; Rawling, M.; Campbell, M.; Tomkinson, N. C. O. *Org. Lett.* **2012**, *14*, 6250–6253.

133. Neimann, K.; Neumann, R. *Org. Lett.* **2000**, *2*, 2861–2863.

134. Fink, M. J.; Fischer, T. C.; Rudroff, F.; Dudek, H.; Fraaije, M. W.; Mihovilovic, M. D. *J. Mol. Catal. B: Enzym.* **2011**, *73*, 9–16.

135. Friess, S. L.; Frankenburg, P. E. *J. Am. Chem. Soc.* **1952**, *74*, 2679–2680.

136. Crudden, C. M.; Chen, A. C.; Calhoun, L. A. *Angew. Chem. Int. Ed.* **2000**, *39*, 2852–2855.

137. (a) Noyori, R.; Kobayashi, H.; Sato, T. *Tetrahedron Lett.* **1980**, *21*, 2573. (b) Noyori, R.; Sato, T.; Kobayashi, H. *Tetrahedron Lett.* **1980**, *21*, 2569.

138. (a) Quideau, S.; Deffieux, D.; Douat-Casassus, C.; Pouysegu, L. *Angew. Chem. Int. Ed.* **2011**, *50*, 586–621. (b) Rappoport, Z. *The Chemistry of Phenols*; Wiley-VCH: Weinheim, **2003**. (c) George, T.; Mabon, R.; Sweeney, G.; Sweeney, J. B.; Tavassoli, A. *J. Chem. Soc., Perkin Trans. 1* **2000**, 2529–2574. (d) Tyman, J. H. P. *Synthetic and Natural Phenols*; Elsevier: New York, **1996**.

139. González, C.; Castedo, L. Synthesis of phenols. In *The Chemistry of Phenols*; Rappoport, Z., Ed.; John Wiley & Sons: Chichester, **2003**; Part 1, pp. 395–490.

140. Derbyshire, D. H.; Waters, W. A. *Nature* **1950**, *165*, 401–401.

141. (a) Hart, H.; Buehler, C. A. *J. Org. Chem.* **1964**, *29*, 2397–2400. (b) Olah, G. A.; Ohnishi, R. *J. Org. Chem.* **1978**, *43*, 865–867. (c) Olah, G. A.; Fung, A. P.; Keumi, T. *J. Org. Chem.* **1981**, *46*, 4305–4306.

142. Olah, G. A.; Keumi, T.; Lecoq, J. C.; Fung, A. P.; Olah, J. A. *J. Org. Chem.* **1991**, *56*, 6148–6151.

143. (a) Kovacic, P.; Kurz, M. E. *J. Am. Chem. Soc.* **1966**, *88*, 2068–2069. (b) Kovacic, P.; Kurz, M. E. *Tetrahedron Lett.* **1966**, *7*, 2689–2692. (c) Kovacic, P.; Reid, C. G.; Brittain, M. J. *J. Org. Chem.* **1970**, *35*, 2152–2156.

144. (a) Hegg, E. L.; Ho, R. Y. N.; Que, L., Jr. *J. Am. Chem. Soc.* **1999**, *121*, 1972–1973. (b) Yamashita, M.; Furutachi, H.; Tosha, T.; Fujinami, S.; Wataru, S.; Maeda, Y.; Takahashi, K.; Tanaka, K.; Kitagawa, T.; Suzuki, M. *J. Am. Chem. Soc.* **2007**, *129*, 2–3.

145. Hamilton, G. A.; Hanifin, J. W.; Friedman, J. P. *J. Am. Chem. Soc.* **1966**, *88*, 5269–5272.

146. Bartoli, J.-F.; Mouries-Mansuy, V.; Le Barch-Ozette, K.; Palacio, M.; Battioni, P.; Mansuy, D. *Chem. Commun.* **2000**, 827–828.

147. D'Amato, E. M.; Neumann, C. N.; Ritter, T. *Organometallics* **2015**, *34*, 4626–4631.

148. For a mini-review on Pd catalyzed arene oxygenations, please refer to Neufeldt S. N.; Sanford, M. S. *Acc. Chem. Res.* **2012**, *45*, 936–946.

149. (a) Zhang, Y.-H.; Yu, J.-Q. *J. Am. Chem. Soc.* **2009**, *131*, 14654–14655. (b) Powers, D. C.; Xiao, D. Y.; Geibel, M. A. L.; Ritter, T. *J. Am. Chem. Soc.* **2010**, *132*, 14530–14536. (c) Huang, C.; Ghavtadze, N.; Chattopadhyay, B.; Gevorgyan, V. *J. Am. Chem. Soc.* **2011**, *133*, 17630–17633. (d) Gulevich, A. V.; Melkonyan, F. S.; Sarkar, D.; Gevorgyan, V. *J. Am. Chem. Soc.* **2012**, *134*, 5528–5531. (e) Rao, Y. *Synlett.*

2013, *24*, 2472–2476. (f) Liang, Y.-F.; Wang, X.; Yuan, Y.; Liang, Y.; Li, X.; Jiao, N. *ACS Catal.* **2015**, *5*, 6148–6152.

150. Emmert, M. H.; Cook, A. K.; Xie, Y. J.; Sanford, M. J. *Angew. Chem. Int. Ed.* **2011**, *50*, 9409–9412.

151. Bjørsvik, H.-R.; Occhipinti, G.; Gambarotti, C.; Cerasino, L.; Jensen, V. R. *J. Org. Chem.* **2005**, *70*, 7290–7296.

152. Yuan, C.; Liang, Y.; Hernandez, T.; Berriochoa, A.; Houk, K. N.; Siegel, D. *Nature* **2013**, *499*, 192–196.

153. Jones, M., Jr.; DeCamp, M. R. *J. Org. Chem.* **1971**, *36*, 1536–1539.

154. Eliasen, A. M.; Thedford, R. P.; Claussen, K. R.; Yuan, C.; Siegel, D. *Org. Lett.* **2014**, *16*, 3628–3631.

155. Rawling, M. J.; Tomkinson, N. C. O. *Org. Biomol. Chem.* **2013**, *11*, 1434–1440.

156. Clayden, J.; Greeves, N.; Warren, S.; Wothers, P. *Organic Chemistry*, 1st ed.; Oxford University Press, **2001**; pp. 547–579.

157. Carey, F. A. *Reactions of Arenes: Electrophilic Aromatic Substitution*. In *Organic Chemistry*, 4th ed.; McGraw-Hill, **2000**; pp. 443–486.

158. (a) Bolton, R. E.; Moody, C. J.; Rees, C. W.; Tojo, G. *J. Chem. Soc., Perkin Trans. 1* **1987**, 931–935. (b) Jin, J.-W.; Zhang, L.; Meng, G.-R.; Zhu, J.-H.; Zhang, Q. *Synth. Commun.* **2014**, *44*, 346–351.

159. Murto, J. *Acta. Chem. Scand.* **1964**, *18*, 1043–1053.

160. Dyatkin, B. L.; Mochalina, E. P.; Knunyants, I. L. *Tetrahedron* **1965**, *21*, 2991–2995.

161. Ripin, D. H.; Evans, D. A. (November 4, 2005). "*pKa Table*" (PDF). Retrieved January 27, 2016.

162. Berkessel, A.; Adrio, J. A.; Hüttenhain, D.; Neudörfl, J. M. *J. Am. Chem. Soc.* **2006**, *128*, 8421–8426.

163. Bordwell, F. G. *Acc. Chem. Res.* **1988**, *21*, 456–463.

164. Guthrie, J. P. *Can. J. Chem.* **1978**, *56*, 2342–2354.

165. Eidman, K. F.; Nichols, P. J. *e-EROS Encyclopedia of Reagents for Organic Synthesis* **2006**, Trifluoroacetic acid.

166. Clayden, J.; Greeves, N.; Warren, S.; Wothers, P. *Organic Chemistry*, 1st ed.; Oxford University Press, **2001**; pp. 181–197.

167. For details, please refer to Tomasz Kubczyk's Ph.D. Thesis, University of Strathclyde, **2015**.

168. (a) Scott, R. A.; Lukehart, C. M. *Applications of Physical Methods to Inorganic and Bioinorganic Chemistry*, 1st ed.; John Wiley & Sons, **2007**; pp. 469–486. (b) Hawley, D. K.; McClure, W. R. *Proc. Natl. Acad. Sci. USA*, **1980**, *77*, 6381–6385. (c) Fedor, M. J. *Determination of Kinetic Parameters for Hammerhead and Hairpin Ribozymes* in *Methods in Molecular Biology, vol. 252: Ribozymes and siRNA Protocols*, 2nd ed.; Humana Press Inc., Totowa, New Jersey, **2004**; pp. 19–32. (d) Pape, T.; Wintermeyer, W.; Rodnina, M. V. *Nature Struct. Biol.* **2000**, *7*, 104–107. (e) Gavutis, M.; Jaks, E.; Lamken, P.; Piehler, J. *Biophys. J.* **2006**, *90*, 3345–3355.

169. (a) Capellos, C.; Bielski, B. H. J. *Kinetic Systems: Mathematical Description of Chemical Kinetics in Solution*, 1st ed.; John Wiley & Sons Inc., New York, **1972**. (b) Corbett, J. F. *J. Chem. Educ.* **1972**, *49*, 663–663.

170. Clayden, J.; Greeves, N.; Warren, S.; Wothers, P. *Organic Chemistry*, 1st ed.; Oxford University Press, **2001**; pp. 1090–1100.

171. Casado, J.; López-Quintela, M. A.; Lorenzo-Barral, F. M. *J. Chem. Educ.* **1986**, *63*, 450–452.

172. (a) Brown, H. C.; Okamoto, Y. *J. Am. Chem. Soc.* **1958**, *80*, 4979–4987. (b) Hansch, C.; Leo, A.; Taft, R. W. *Chem. Rev.* **1991**, *91*, 165–195.

173. (a) Matsumoto, T.; Furutachi, H.; Nagatomo, S.; Tosha, T.; Fujinami, S.; Kitagawa, T.; Suzuki, M. *J. Organomet. Chem.* **2007**, *692*, 111–121. (b) Matsumoto, T.; Furutachi, H.; Kobino, M.; Tomii, M.; Nagatomo, S.; Tosha, T.; Osako, T.; Fujinami, S.; Itoh, S.; Kitagawa, T.; Suzuki, M. *J. Am. Chem. Soc.* **2006**, *128*, 3874–3875. (c) Dabbagh, H. A.; Ghaelee, S. *J. Org. Chem.* **1996**, *61*, 3439–3445.

174. Smith, M. B.; March, J. *March's Advanced Organic Chemistry: Reactions, Mechanisms, and Structure*, 6th ed.; John Wiley & Sons, **2007**; pp. 412.

175. Fujimori, K.; Oshibe, Y.; Hirose, Y.; Oae, S. *J. Chem. Soc., Perkin Trans. 2* **1996**, 413–417.

176. (a) Newcomb, M. *Tetrahedron* **1993**, *49*, 1151–1176. (b) Huang, H.; Chang, W.-C.; Lin, G.-M.; Romo, A.; Pai, P.-J.; Russell, W. K.; Russell, D. H.; Liu, H.-W. *J. Am. Chem. Soc.* **2014**, *136*, 2944–2947. (c) Roschek, B., Jr.; Tallman, K. A.; Rector, C. L.; Gillmore, J. G.; Pratt, D. A.; Punta, C.; Porter, N. A. *J. Org. Chem.* **2006**, *71*, 3527–3532. (d) Newcomb, M.; Choi, S.-Y.; Horner, J. H. *J. Org. Chem.* **1999**, *64*, 1225–1231. (e) Choi, S.-Y.; Toy, P. H.; Newcomb, M. *J. Org. Chem.* **1998**, *63*, 8609–8613. (f) Liu, K. E.; Johnson, C. C.; Newcomb, M.; Lippard, S. J. *J. Am. Chem. Soc.*

1993, *115*, 939–947. (g) Hollis, R.; Hughes, L.; Bowry, V. W.; Ingold, K. U. *J. Org. Chem.* **1992**, *57*, 4284–4287.

177. Cahard, E.; Schoenebeck, F.; Garnier, J.; Cutulic, S. P. Y.; Zhou, S.; Murphy, J. A. *Angew. Chem. Int. Ed.* **2012**, *51*, 3673–3676.

178. (a) Inoue, Y.; Shimoyama, H.; Yamasaki, N.; Tai, A. *Chem. Lett.* **1991**, 593–596. (b) Valyocsik, E. W.; Sigal, P. *J. Org. Chem.* **1971**, *36*, 66–72.

179. Simmons, H. E.; Smith, R. D. *J. Am. Chem. Soc.* **1958**, *80*, 5323–5324.

180. Li, J. J. *Name Reactions. A Collection of Detailed Reaction Mechanisms*, 4th ed.; Springer, Berlin, **2009**.

181. Knight, P. D.; O'Shaughnessy, P. N.; Munslow, I. J.; Kimberley, B. S.; Scott, P. *J. Organomet. Chem.* **2003**, *683*, 103–113.

182. Weller, D. D.; Stirchak, E. P. *J. Org. Chem.* **1983**, *48*, 4873–4879.

183. (a) Patrick, G. L. *Case Study 2. Palladium-catalysed reactions in drug synthesis*. In Patrick, G. L., *An Introduction to Drug Synthesis*, 1st ed.; Oxford University Press, United Kingdom, **2015**; pp. 211–220. (b) Sheppard, T. D. *Org. Biomol. Chem.* **2009**, *7*, 1043–1052.

184. Unpublished conditions developed within the Burley group at the University of Strathclyde were used.

185. (a) Gruijters, B. W. T.; Broeren, M. A. C.; van Delft, F. L.; Sijbesma, R. P.; Hermkens, P. H. H.; Rutjes, F. P. J. T. *Org. Lett.* **2006**, *8*, 3163–3166. (b) Wang, R.; Mo, S.; Lu, Y.; Shen, Z. *Adv. Synth. Catal.* **2011**, *353*, 713–718. (c) Jiang, Y.; Gao, B.; Huang, W.; Liang, Y.; Huang, G.; Ma, Y. *Synth. Commun.* **2009**, *39*, 197–204.

186. Francke, R.; Schnakenburg, G.; Waldvogel, S. R. *Eur. J. Org. Chem.* **2010**, *2010*, 2357–2362.

187. Li, J.; Hua, R.; Liu, T. *J. Org. Chem.* **2010**, *75*, 2966–2970.

188. Johnson, S. M.; Connelly, S.; Wilson, I. A.; Kelly, J. W. *J. Med. Chem.* **2008**, *51*, 6348–6358.

189. Junk, M. J. N. *Electron Paramagnetic Resonance Theory*. In Junk, M. J. N. ed., *Assessing the Functional Structure of Molecular Transporters by EPR Spectroscopy*, Springer-Verlag Berlin Heidelberg, **2012**, Chapter 2, pp. 7–52.

190. (a) Wertz, J. E.; Bolton, J. R. *Electron Spin Resonance Elementary Theory and Practical Applications*, Springer Netherlands, **1986**. (b) Church, D. F. *Anal. Chem.* **1994**, *66*, 419A–427A. (c) Chalfont, G. R.; Perkins, M. J.; Horsfield, A. *J. Am. Chem. Soc.* **1968**, *90*, 7141–7142. (d) Naydenov, B.; Richter, V.; Beck, J.; Steiner, M.;

Neumann, P.; Balasubramanian, G.; Achard, J.; Jelezko, F.; Wrachtrup, J.; Kalish, R. *Appl. Phys. Lett.* **2010**, *96*, 163108-1–163108-3. (e) Crook, N. P.; Hoon, S. R.; Taylor, K. G.; Perry, C. T. *Geophys. J. Int.* **2002**, *149*, 328–337.

191. (a) Buettner, G. R.; Mason, R. P. *Spin trapping methods for detecting superoxide and hydroxyl free radicals in vitro and in vivo.* In Cutler, R. G.; Rodriguez, H. ed., *Oxidative Stress and Aging, Critical Reviews*, World Scientific Publishing, River Edge, NJ, **2003**, Chapter 2, pp 27–38. (b) Dalton, H.; Wilkins, P. C.; Deighton, N.; Podmore, I. D.; Symons, M. C. R. *Faraday Discuss.* **1992**, *93*, 163–171. (c) Buettner, G. R. *Free Radic. Res. Commun.* **1993**, *19*, S79–S87. (d) Mitchell, D. G.; Rosen, G. M.; Tseitlin, M.; Symmes, B.; Eaton, S. S.; Eaton, G. R. *Biophys. J.* **2013**, *105*, 338–342.

192. Tsai, P.; Ichikawa, K.; Mailer, C.; Pou, S.; Halpern, H. J.; Robinson, B. H.; Nielsen, R.; Rosen, G. R. *J. Org. Chem.* **2003**, *68*, 7811–7817.

193. Liu, X.-H.; Chen, P.-Q.; Wang, B.-L.; Dong, W.-L.; Li, Y.-H.; Li, Z.-M.; Xie, X.-Q.; *Chem. Biol. Drug. Des.* **2010**, *75*, 228–232.

194. Chatterjee, S.; Ye, G.; Pittman, Jr., C. U. *Tetrahedron Lett.* **2010**, *51*, 1139–1144.

195. Porcheddu, A.; De Luca, L.; Giacomelli, G. *Synlett* **2009**, *13*, 2149–2153.

196. Oae, S.; Shinhama, K.; Fujimori, K.; Kim, Y. H. *Bull. Chem. Soc. Jpn.* **1980**, *53*, 775–784.

197. Chang, X.-W.; Han, Q.-C.; Jiao, Z.-G.; Weng, L.-H.; Zhang, D.-W. *Tetrahedron* **2010**, *66*, 9733–9737.

198. Jahani, F.; Tajbakhsh, M.; Golchoubian, H.; Khaksar, S. *Tetrahedron Lett.* **2011**, *52*, 1260–1264.

199. Babu, K. S.; Rao, V. R. S.; Rao, R. R.; Babu, S. S.; Sakhamuri, S.; Rao, J. M. *Can. J. Chem.* **2009**, *87*, 393–396.

200. Shintani, R.; Murakami, M.; Tsuji, T.; Tanno, H.; Hayashi, T. *Org. Lett.* **2009**, *11*, 5642–5645.

201. Stewart, J. M.; Westberg, H. H. *J. Org. Chem.* **1965**, *30*, 1951–1955.

202. Robinson, M. W. C.; Davies, M. A.; Buckle, R.; Mabbett, I.; Taylor, S. H.; Graham, A. E. *Org. Biomol. Chem.* **2009**, *7*, 2559–2564.

203. (a) Tilvawala, R.; Pratt, R. F. *Biochemistry* **2013**, *52*, 7060–7070. (b) Zinner, G.; Ruthe, V.; Hitze, M.; Vollrath, R. *Synthesis* **1971**, *1971*, 148–149.

204. Izydore, R. A.; Jones, J. T.; Mogesa, B.; Swain, I. N.; Davis-Ward, R. G.; Daniels, D. L.; Frazier Kpakima, F.; Spaulding-Phifer, II, S. T. *J. Org. Chem.* **2014**, *79*, 2874–2882.

205. Kim, J. K.; Kim, K. M.; Ryu, E. K. *Synth. Commun.* **1992**, *22*, 1427–1432.

206. Kaupp, G.; Schmeyers, J.; Boy, J. *Tetrahedron* **2000**, *56*, 6899–6911.

207. Marell, D. J.; Emond, S. J.; Kulshrestha, A.; Hoye, T. R. *J. Org. Chem.* **2014**, *79*, 752–758.

208. Shioji, K.; Matsuo, A.; Okuma, K.; Nakamura, K.; Ohno, A. *Tetrahedron Lett.* **2000**, *41*, 8799–8802.

209. Rothenberg, G.; Downie, A. P.; Raston, C. L.; Scott, J. L. *J. Am. Chem. Soc.* **2001**, *123*, 8701–8708.

210. Yato, M.; Homma, K.; Ishida, A. *Tetrahedron* **2001**, *57*, 5353–5359.

211. van Buijtenen, J; van As, B. A. C.; Meuldijk, J.; Palmans, A. R. A.; Vekemans, J. A. J. M.; Hulshof, L. A.; Meijer, E. W. *Chem. Commun* **2006**, 3169–3171.

212. Zhang, B.; Han, L.; Li, T.; Yan, J.; Yang, Z. *Synth. Commun.* **2014**, *44*, 1608–1613.

213. Xie, X.; Stahl, S. S. *J. Am. Chem. Soc.* **2015**, *137*, 3767–3770.

214. Banister, S. D.; Yoo, D. T.; Chua, S. W.; Cui, J.; Mach, R. H.; Kassiou, M. *Bioorg. Med. Chem. Lett.* **2011**, *21*, 5289–5292.

215. Sigma-Aldrich website, http://www.sigmaaldrich.com/ (accessed February 3, 2016)

216. Miller, A. D.; Tannaci, J. F.; Johnson, S. A.; Lee, H.; McBee, J. L.; Tilley, T. D. *J. Am. Chem. Soc.* **2009**, *131*, 4917–4927.

217. Janzen, E. G.; Jandrisits, L. T.; Shetty, R. V.; Haire, D. L.; Hilborn, J. W. *Chem.-Biol. Interactions* **1989**, *70*, 167–172.

218. Lee, C.; Yang W.; Parr, R. G. *Physical Review B* **1988**, *37*, 785–789.

219. Cossi, M.; Rega, N.; Scalmani, G.; Barone, V. *J. Comput. Chem.* **2003**, *24*, 669–681.